Freie Universität Berlin

Design, Synthesis, and Evaluation of Bivalent Estrogen Ligands

DISSERTATION

zur Erlangung des akademischen Grades des Doktors der Naturwissenschaften (Dr. rer. Nat.)

eingereicht im Fachbereich Biologie, Chemie, Pharmazie
der Freien Universität Berlin

vorgelegt von

Min Shan

aus Suzhou, China

November 2011

The work presented herein was carried out in the research group of Prof. Dr. Rainer Haag from October 2006 until November 2011 at Institute of Chemistry and Biochemistry of Freie Universität Berlin (Berlin, Germany).

1st Reviewer: Prof. Dr. Rainer Haag, Freie Universität Berlin

2nd Reviewer: Prof. Dr. Christoph A. Schalley, Freie Universität Berlin

Disputation on Dec 12, 2011

“When you have eliminated the impossible, whatever remains, however improbable, must be the truth”.

- *Sherlock Holmes*, by Sir Arthur Conan Doyle (1859-1930, Scotland).

Acknowledgements

First I would like to thank my supervisor Prof. Dr. Rainer Haag for offering me the opportunity to accomplish my doctor thesis in his group, giving me the scientific and personal supports to manage my work, as well as helping me to understand the science and establish the goal for my future development.

I would like to thank Prof. Dr. Christoph A. Schalley for spending his valuable time to take over the second reviewer of my thesis.

I would like to acknowledge Prof. Dr. John A. Katzenellenbogen (University of Illinois) for his advices and the nice collaboration with his group. I learned so much by discussing with him and cannot have so many fruitful results without his help.

I would like to acknowledge Dr. Markus Weber (Zuse Institut Berlin) for the great collaboration with his group.

I would like to acknowledge Prof. Dr. Oliver Seitz (Humboldt-Universität zu Berlin) for the collaboration with his group, which supported the first success in my work.

I am grateful to my collaborators Kathy Carlson, Alexander Bujotzek, and Frank Abendroth for their hard work over the past years.

I am grateful to Dr. Pamela Winchester, Dr. Christopher Popeney, Wiebke Fischer, and my wife Ying Luo for proofreading and correcting my dissertation as well as my manuscript.

I am grateful to the former and present members of the Haag group and the multivalent subgroup for their great help and many pleasant moments over the past years. Especially, I would like to thank my former and present partners in the labor and office, Dr. Ewelina Burakowska, Dr. Stefan Kamlage, Dr. Adam Sisson, Dr. Christopher Popeney, Dr. Ilona Papp, Wiebke Fischer, Haixia Zhou, Dirk Steinhilber, Andrea Schulz, Indah Nurita Kurniasih, Florian Mummy, and Christian Kördel.

I would like to thank Prof. Dr. Carl Christoph Tzschucke, Dr. Christopher Popeney, Dr. Carlo Fasting, Dr. Shangjie Xu, Dr. Juliane Keilitz, Dr. Mohiuddin Abdul Quadir, and Timm Heck for the discussion of chemistry problems. I am grateful to Winfried Münch and Marleen Selent for their kind assistance and helpful advices on HPLC. I also need to thank Gabriela Hertel, Jutta Hass, Katharina Tebel, and Katrin Wittig for taking care of the chemical ordering, labor equipment, and

complicated paperwork.

I appreciate all the research facilities in the Institute of Chemistry and Biochemistry, in particularly Dr. Andreas Schäffer, Dr. Andreas Springer, and their colleagues for their numerous assistances of NMR and MS measurements.

I appreciate the financial support afforded by Deutsche Forschungsgemeinschaft (SFB765) during the past years and various valuable interdisciplinary literatures provided by SFB765 and Dahlem Research School.

Finally I would like to thank my family and friend for their love and support, and especially my wife Ying Luo for her understanding, patience, and encouragement.

Table of contents

1. Introduction

1.1. Multivalency as a binding strategy for natural and artificial applications

Protein complexes, antibodies, viruses and cells are multivalent entities that possess a number of structurally separate binding moieties or recognition units that are able to interact with another multivalent entity. Thus, a multivalent or polyvalent interaction is defined as simultaneous bindings between such multifunctional entities.[1] The most notable feature of the multivalent interaction is that the binding affinity (avidity) of a multivalent species could be collectively much stronger than its monovalent counterparts. From a thermodynamic point of view, this enhancement could be attributed to the increased Gibbs free energy of the interaction. Therefore, multivalency is frequently utilized by nature to achieve a tight binding. For instance, the influenza virus binds to a bronchial epithelial cell surface (Figure 1 left) by interacting multiple trimers of the hemagglutinin HA3, a lectin, which is distributed approximately 2-4 per 100 nm^2 on the surface of the virus with multiple sialic acid SA, a terminal sugar on many glycoproteins, which is distributed approximately 50-200 per 100 nm^2 on the cell membrane and results in infectious diseases.[1] To prevent such undesired multivalent biological interactions, several mucins (glycosylated proteins) contained in the fluid coating the interior of the lungs of most mammals presenting oligosaccharides terminated in sialic acid can be used to interact with influenza viruses and thereby inhibit such attachments.[2] Similarly to this natural multivalent inhibition of the influenza virus, a comparison between the mono- and multivalent inhibition has been investigated by Whitesides and co-workers (Figure 1 right).[3,4] The authors demonstrated an active polymeric inhibitor of the influenza virus containing 20% sialic acid on a polyacrylamide backbone with a low value of the inhibition constant 600 pM. By contrast, the inhibition constant of the monomeric inhibitor was 2 mM.

One of the most common artificial multivalent applications is the carbohydrate-protein interaction. In this case, the term “multivalent effect” has also been called the “cluster glycoside effect”.[5] It is known that binding constants (association constant, K or K_a) of mono- and oligosaccharides to most proteins are not effective enough for drug design ($K_a \approx 10^3$ - 10^6 M^{-1}).[6] In order to obtain a high-affinity binding to the target protein receptors, many multivalent or

"clustered" carbohydrate analogs have been prepared.[5-7] An good example reported by Kitov et al. has demonstrated that a water-soluble, pentavalent carbohydrate ligand has a subnanomolar inhibitory activity (half maximal inhibitory concentration, IC_{50} = 0.24 nM) which is 10 million-fold higher than that of monovalent carbohydrate (IC_{50} = 2.1 mM).[7] More recently, Schwefel et al. investigated the binding potency of multivalent ligands for the inhibition of wheat germ agglutinin (WGA) and found that a tetravalent carbohydrate ligand tethered on a cyclopeptide backbone is up to 6400 times more potential than the corresponding monovalent analogs.[8]

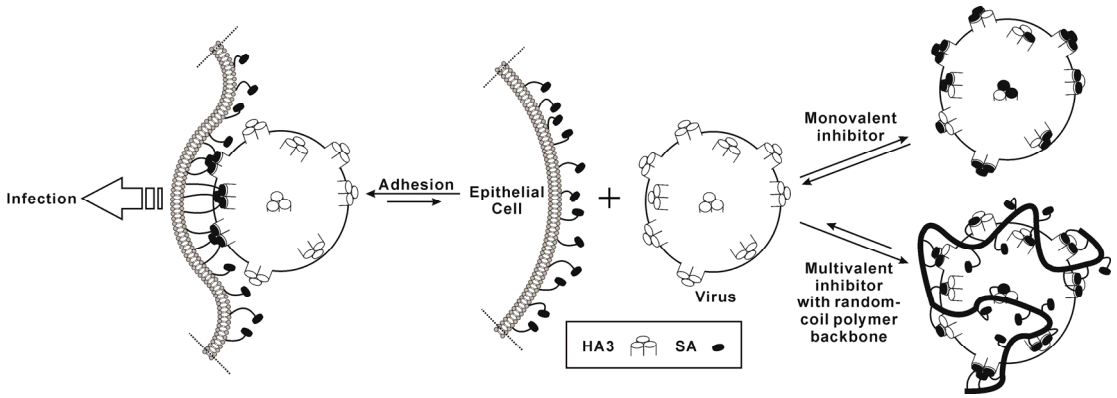

Figure 1. The adhesion of an influenza virus to the surface of an epithelial cell (left) and its inhibition by mono- and multivalent sialic acid inhibitors (right). HA3 and SA are represented as trimers of the hemagglutinin of the virus and sialic acid of the cell, respectively.[1,3,4]

Nowadays, more and more scientists have taken advantage of multivalency as a central strategy to achieve strong interactions in other fields, such as the aggregation of a synthetic trivalent hapten with anti-2,4-DNP IgG into bicyclic trimers,[9] gradient-driven motions of multivalent ligands molecule on a multiple receptor-functionalized surface,[10] and the bivalent interaction between covalent dimers of human carbonic anhydrase II and ligands presented at the surface of mixed self-assembled monolayer (SAM).[11]

1.1.1. Structure of a multivalent ligand

Unlike a monovalent ligand, a multivalent ligand often consists of three parts: the tethered binding moiety (ligand), spacer (linker), and scaffold (architecture).

1.1.1.1. Binding moiety

The binding moiety of the multivalent ligand is essential for the multivalent interaction. However, a successful multivalent interaction depends more on how these binding moieties are presented, rather than the binding moieties themselves. Thus, a rational design of the multivalent ligand does not only include the ligand design such as the tethered position and the linkage group but also other physical factors like the density and spacing of binding moieties.[3,12] Recently, it has been demonstrated by Haag and co-workers that multivalent saccharides presented on hyperbranched polyglycerol (hPG) had a much higher binding affinity (1-70 nM) than a low valency control presented by a pentaerythritol (60 μM). This indicated that the density of the multivalent saccharides has a large influence on the multivalent carbohydrate-protein interaction.[13]

1.1.1.2. Bivalent spacers

A spacer can be understood as a synthetic covalent linker between the tethered binding moieties in the case of bivalent ligands. Meanwhile it provides certain information such as the distance between binding moieties, flexibility, and rigidity of the bivalent ligand so that a tight bivalent receptor-ligand interaction can occur without steric hindrance. Although such information can be predicted and estimated by computer modeling, the most optimal spacer will usually be found only after a systemic spacer screening.[8,14,15]

Unlike chemically or enzymatically labile linkers applied in drug delivery applications, the spacer in a multivalent ligand has to be stable so that the tethered binding moieties are capable of interacting with the multivalent receptor under various chemical and biological conditions.[16,17] Meanwhile, the spacer should be at least a neutral contributor to the binding event. In other words, the spacer should not interact with the receptor, such as the absorption on the surface of a protein, so that any enhanced activity can be readily distinguished and attributed to the multivalent effect. For example, it has been reported that polyethylene glycol (PEG) is resistant to the nonspecific adsorption of proteins and allows the multivalent ligand to only process desired interactions between tethered binding moieties and the protein.[18]

In order to achieve a multivalent binding under certain geometric requirements, several essential factors such as the spacer length and conformational property (flexibility versus rigidity) need to be considered. The spacer length should match the spacing between the multiple binding

sites of a multivalent receptor, which is easily sufficed by chemical synthesis such as polymerization. Because the latter factor is difficult to predict even by using the computer modeling, the majority of effort for the multivalent ligand design should be spent on it. Mammen et al. investigated the entropic costs of flexible and rigid spacers, and found that entropic costs are related to the initial number of spacer conformations including bound and unbound states. The lower the number, the less entropic cost that the ligand-receptor interaction needs to overcome.[1,19] Therefore, they suggested that flexible spacers could not work effectively as spacers in the multivalent interaction due to the severe loss in conformational entropy (approximately 0.7 kcal·mol^{-1} per freely rotating single bond) during the binding.[20] In the case of a bivalent ligand, the loss of conformational entropy becomes much more severe in the whole binding event. Moreover, Whitesides and co-workers summarized the choice of a spacer for the multivalent ligand (Figure 2). A common approach is to use a spacer with a rigid central element so that the loss in conformational entropy can be minimized.[19] Using a rigid central element, however, is challenging since a small geometric mismatch in the structure with their targets will result in a steric repulsion between the ligand and receptor and consequently impact their binding avidity.

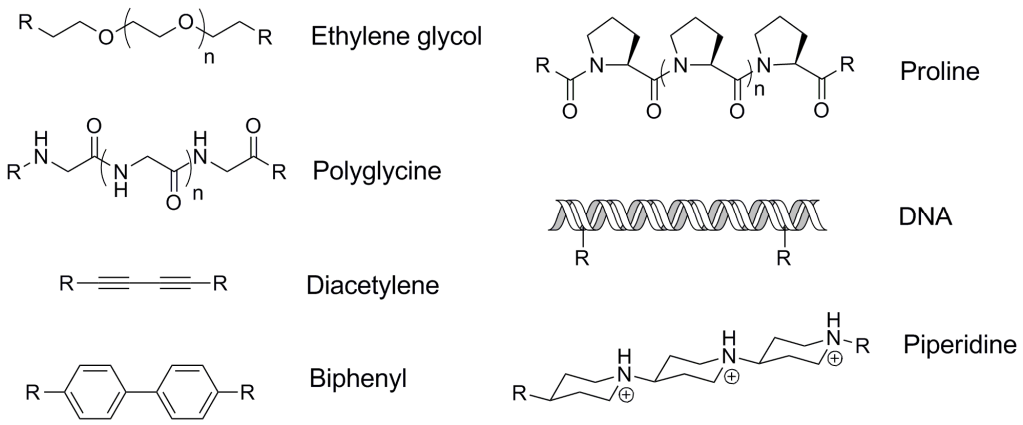

Figure 2. Representative examples of spacers that have been used in bivalent ligands: ethylene glycol,[7,21] polyglycine,[22] diacetylene,[23] biphenyl,[24] proline,[25,26] DNA,[27] and piperidine.[28]

More detail about additional thermodynamic issues will be discussed in Section 1.1.2. Recently, in a computational study and a NMR study of bivalent estrogen ligand it was found that not only the undesired conformation of the spacer gives a entropic penalty, but also the interaction between the functionalized group such as aryl in the spacer and binding moieties can result in a enthalpic loss.[29,30]

1.1.1.3. Multivalent scaffolds

A multivalent scaffold is not only a tethering system where binding moieties can attach, but also presents its binding moieties with certain structural and dimension information, such as valency, size, and shape, which could significantly influence the binding ability of multivalent ligands. The most common scaffolds applied for multivalent ligands are linear, random-coil polymer like polyacryamide,[2,3] and approximately spherical polymers such as dendrimer (poly(amido)amine, PAMAM),[31,32] and hyperbranched dendrimer (hPG).[13,33,34] In general, the scaffold of a multivalent ligand needs to match the spacing and the symmetry of its corresponding multivalent receptor to achieve a maximum tight binding. Compared to spherical dendrimers, hyperbranched dendrimers such as hPG have the advantage that they can interact with a number of cell surface receptors.[19]

The multivalent ligand can be classified by the number of its repeating binding moieties on its scaffold, denoted as "structural valency," e.g., bivalent for two repeating moieties, trivalent for three repeating moieties, and so on. Generally, to bind to a certain type of multivalent receptor with *N* binding sites, the corresponding multivalent ligand with *N* binding moieties should be developed. In practice, however, not all the binding moieties of a multivalent entity are involved in multivalent interactions with another entity due to steric reasons, for example, the multivalent binding between the influenza virus and the cell surface (Figure 1). Thus, these unbound binding moieties seem to be functionally "inactive" for the binding. Therefore, the concept "functional valency" was introduced to distinguish this phenomenon from the structural valency.[6]

Since a multivalent ligand has a greater structural complexity than a monovalent ligand, it is not surprising to observe a biological activity change by altering a single structural feature of a multivalent ligand. For instance, Kiessling and co-workers investigated the influence on the multivalent ligand-receptor binding mechanism by varying the multivalent ligand architecture, including scaffold shape, size, valency, and density of binding moieties.[35-37] They found that ligands with polydisperse polyvalent scaffolds are effective inhibitors for the lectin concanavalin A (Con A), while other linear oligomeric scaffolds mediate receptor clustering. More recently, Haag and co-workers investigated the structure-activity relationship (SAR) of dendritic polyglycerol sulfate (dPGS, a polyanionic polymer) binding to L-selectin in correlation with the

size and the surface charge density based on the dPGS ranging from approximately 4 to 2000 kDa in molecular weight.[38,39] In this study they demonstrated that the strong inhibitory potential of dPGS was dependent on not only the strong electrostatic interaction with cationic surface potential on L-selectin but also the steric shielding of the carbohydrate binding site by its scaffold, i.e., flexible dPGS particles in this case.

1.1.2. Thermodynamics of multivalent interactions

For a multivalent ligand design, it is necessary to survey and understand the origin of greatly enhanced multivalent interactions. So far, the notion of a multivalent ligand binding to a multivalent receptor with an affinity greater than that of the monovalent counterpart has been attributed to a thermodynamic gain. The difference between the thermodynamics of such multivalent and monovalent interactions can be demonstrated in a thermodynamic model (Scheme 1).[1]

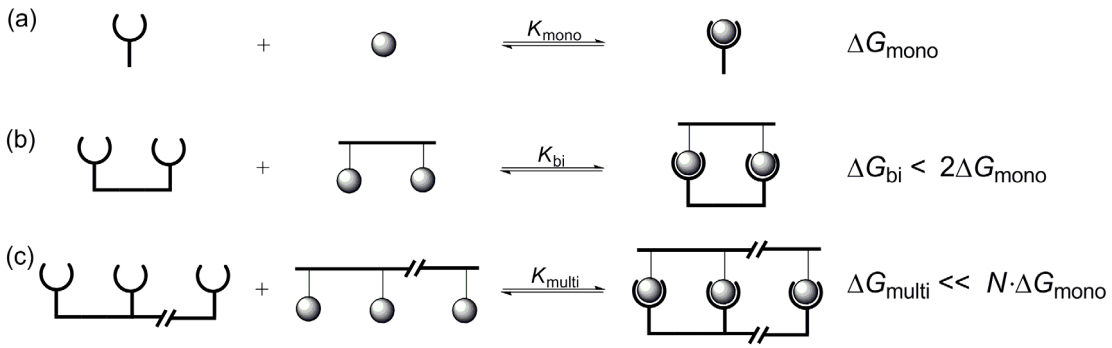

Scheme 1. Comparison of thermodynamic parameters of association in (a) mono-, (b) bi-, and (c) multivalent interactions.[1]

Once a monovalent interaction between a receptor and a ligand takes place, a free energy change ΔG_{mono} will occur. Therefore, for N independent monovalent interactions there is a total free energy of $N \cdot \Delta G_{mono}$. In the case of a multivalent interaction, however, a multivalent receptor (an influenza virus) with N binding sites interacts more strongly with a multivalent ligand (a multivalent inhibitor with the random-coil polymer backbone) with N binding moieties than with N times of monovalent inhibitors (Figure 1 right), where $K_{multi} >> (K_{mono})^N$. Since the enhancement of its binding constant K_{multi} is related to the Gibbs free energy ΔG_{multi} by the van't Hoff equation (Equation 1),

$$\Delta G^{\circ} = - RT \cdot \ln K^{\circ} \quad (1)$$

the free energy ΔG_{multi} of a multivalent interaction is more favorable (negative) than the total free energy $N \cdot \Delta G_{mono}$ of N independent monovalent interactions, $\Delta G_{multi} << N \cdot \Delta G_{mono}$.

Furthermore, it is known that free energy ΔG_{multi} of a multivalent interaction is made up of enthalpic (ΔH_{multi}) and entropic ($T \cdot \Delta S_{multi}$) components (Gibbs equation, Equation 2).

$$\Delta G^{\circ} = \Delta H^{\circ} - T \cdot \Delta S^{\circ} \quad (2)$$

Thus, it is possible to survey the origin of the multivalent effect and find out which component contributes most prominently to the free energy in multivalent interactions.

1.1.2.1. The role of enthalpy in multivalent interactions

The enthalpy change ΔH° is a parameter of the total energy generated by a chemical or enzymatic reaction and only depends on the final as well as initial states of the system. Although the enthalpy largely depends on the nature of the ligand and the binding site of the receptor, the enthalpy change in multivalent interactions could be either enhanced by certain conformational change of the binding site[40] or diminished by a undesired interaction such as steric repulsion around the active binding sites of the multivalent receptor.[1]

In enthalpically enhanced multivalent interactions, the value of ΔH_{multi} is more negative than the total value of $N \cdot \Delta H_{mono}$. In such cases, the first ligand-receptor binding results in a conformational change of the unbound adjacent binding sites which promotes the next ligand-receptor binding. Besides the best studied interaction between four oxygen molecules and the tetrameric hemoglobin,[40] a similar observation has been found in the case of a pentameric binding of cholera toxin B5 to five oligosaccharide portion ganglioside GM_1 molecules on the surface of a cell by Schön et al.[41] The authors studied the binding of pentameric B5 to five GM_1 units in solution via calorimetric method and found the binding of cholera toxin to the first GM_1 unit enhances the favorable enthalpy of adjacent binding to the next GM_1. For instance, the intrinsic binding constant for GM_1 to the pentameric B5 at 37°C was 1.05×10^6 M^{-1}, which was increased by a factor of 4 when an adjacent binding site had been occupied. The additional enthalpy from interactions between subunits of B5 is -11 kcal·mol^{-1}, which is 10% of the total folding enthalpy for each subunit. It suggested that a relatively small protein conformational

change takes place once the first GM_1 binds to pentameric B5 so that the subsequent binding will be more enthalpically favorable. Moreover, it was found that the states with nonadjacent bound oligo-GM_1 never became significantly populated (less than 2% of the total population).

These two enthalpically enhanced examples in biology do not involve multivalent interactions and their enhanced enthalpies are often called cooperative enthalpy (Section 1.1.3.1). By contrast, in the case of multivalent interactions, the structural influence of a multivalent ligand on the binding event cannot be ignored. This structural or steric influence is reflected in energetically unfavorable conformational changes either at the ligand or at the receptor. The more conformationally rigid the multivalent entity is, the more unfavorable contribution to the whole binding it has. For a better understanding, a theoretically binding mode was built up to explain these circumstances (Scheme 2).[1] Considering a monovalent interaction (Scheme 2a), if the two binding sites are independent and not interfered by a previous binding event, the binding of two monovalent ligands to the bivalent receptor occurs with twice the enthalpy $2 \cdot \Delta H_{mono}$ ($N = 2$). A bivalent ligand, whose two binding moieties are tethered by a certain rigid spacer, can exactly match the geometry of the bivalent receptor (unstrained status) and this binding will occur with exactly twice enthalpy of a monovalent ligand, i.e., $\Delta H_{bi} = 2 \cdot \Delta H_{mono}$. Such a bivalent interaction, however, is rare. In practice, the spacer of the bivalent ligand often does not match the geometry of the bivalent receptor but the two entities can still bind. To accommodate the binding, either the conformation of the receptor or the ligand, even both species must be distorted from their equilibrium conformation (strained status, Scheme 2b). As a consequence, the second ligand-receptor binding in a bivalent interaction is interfered by the first binding event so that the enthalpy ΔH_{bi} is less favorable than the total enthalpy $2 \cdot \Delta H_{mono}$. Such interactions are described as enthalpically diminished.[1]

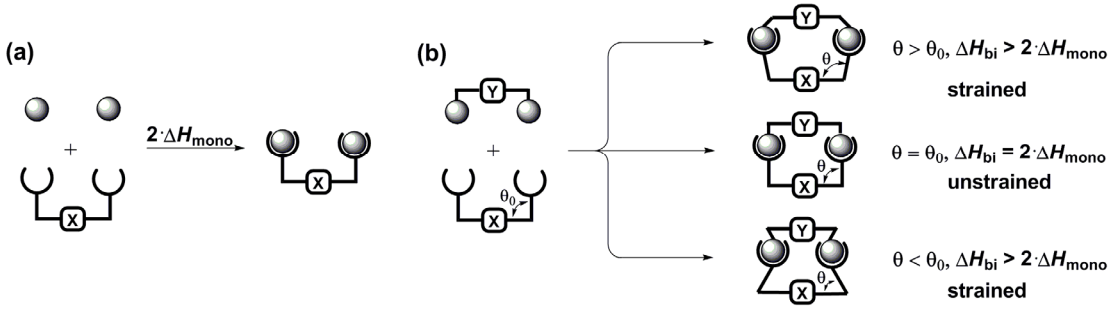

Scheme 2. The enthalpic change of (a) mono- and (b) bivalent interactions due to steric

repulsions.[1]

1.1.2.2. The role of entropy in multivalent interactions

The enhancement of the free energy in a multivalent interaction is traditionally considered from entropic terms, i.e., $T{\cdot}\Delta S$.[1] ΔS°, the difference between the final and initial entropic states of all particles in a reaction, is a parameter representing the change in disorder of the system. It is stated by the Second Law of Thermodynamics that "in a spontaneous process, the entropy of the universe increases" (an overall increase in disorder). This is in consideration of the fact that a spontaneous process is determinated by the free energy, rather than by enthalpy or entropy. Any spontaneous interaction taking place between two entities such as ligand and protein in highly ordered organisms will result in less disorder in the product of two entities, i.e., $\Delta S^{\circ} < 0$, and a greater increased disorder for the surroundings of this organism.[42] Towards a thermodynamically favorable multivalent interaction, a multivalent ligand should have a small decrease in entropy from its initial state to the finial state than N times of entropic decrease in the case of the independent monovalent ligand.

Unlike the enthalpy, the overall entropy of a particle can be comprised of four components: the translational, rotational, conformational, and solvation associated entropies (Equation 3).[1,43]

$$\Delta S^{\circ} = \Delta S^{\circ}_{trans} + \Delta S^{\circ}_{rot} + \Delta S^{\circ}_{conf} + \Delta S^{\circ}_{sol} \quad (3)$$

Before the multivalent interaction takes place, both ligand and receptor are free to translocate in three dimensions and to rotate on three principal axes.[43] Following the binding event, the translational and rotational freedom of the individual entity is lost. Generally, translational and rotational entropies are considered as a single term, i.e., $\Delta S^{\circ}_{trans} + \Delta S^{\circ}_{rot}$. The translational entropy ΔS°_{trans} of a entity is related to the logarithm of its molecular weight (ln(M)) as well as inversely to the logarithm of its concentration ($\ln([C])^{-1}$) according to the Sackur-Tetrode equation in the gas phase.[1,43] Similarly, the rotational entropy ΔS°_{rot} has a logarithmic relationship to the product of its three principle moments of inertia I_x, I_y, and I_z ($\ln(I_x, I_y, I_z)$).[1] Thus, the value of their sum ($\Delta S^{\circ}_{trans} + \Delta S^{\circ}_{rot}$) for a entity is only weakly dependent on their mass and dimensions. Thereby, it can be assumed that the translational and rotational entropies of all entities are equal, if they are at the same concentration.[1] This assumption implies that a multivalent ligand has approximately the same value for the translational and rotational entropies as a monovalent ligand. Consequently, the

interaction between a multivalent ligand with *N* binding moieties with a multivalent receptor results in far less translational and rotational entropies than *N* times of independent monovalent interactions, since only the translational and rotational entropy of one multivalent ligand is lost instead of *N* times of monovalent ligands.

Moreover, Lundquist et al. compared translational and rational entropies in the gas phase to those in aqueous solution.[43] They found that the ability of a particle to move in three dimensions is greatly diminished in aqueous solution than in the gas phase due to the localizing effect of nearby water molecules. Furthermore, the value of the translational and rational entropies is crucial, since these two components are a large fraction of the whole interaction entropy and the free energy.

As mentioned in the Section 1.1.1, a multivalent ligand is composed of scaffold, spacer, and binding moieties, which makes its conformation more uncertain than that of a single monovalent ligand. Thus, the multivalent ligand has clearly higher comformational entropy caused by its higher disorder to overcome before the achievement of the multivalent binding than a monovalent ligand. Here, a simple bivalent interaction was demonstrated as a mode for the discussion about the role of the conformational entropy in multivalent interaction (Scheme 3).

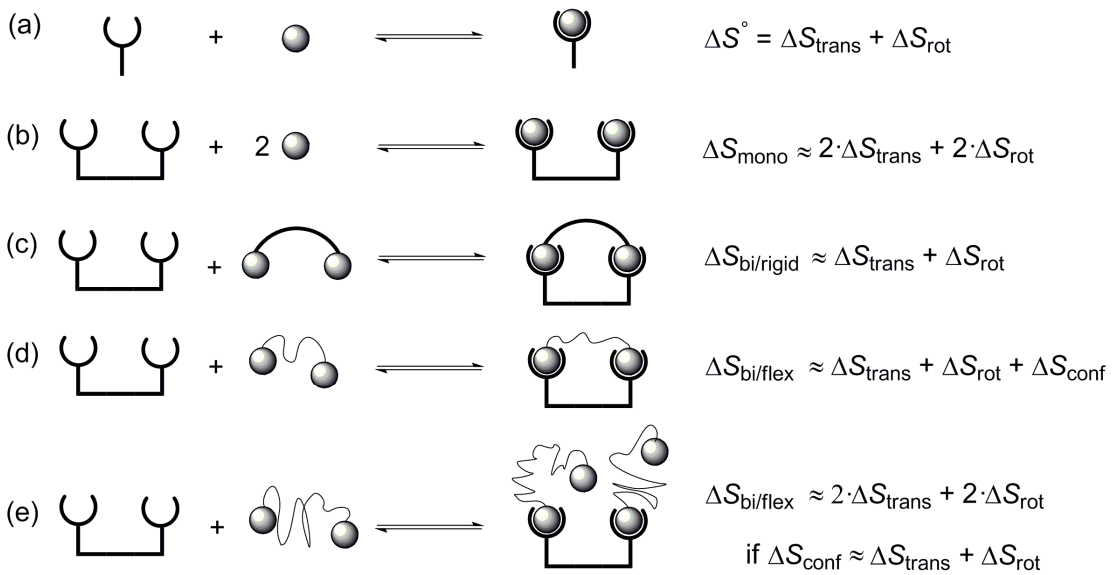

Scheme 3. The entropic cost of an interaction between (a) a monovalent ligand and a monovalent receptor, (b) two monovalent ligands and a bivalent receptor, (c) a bivalent ligand tethered by a suitable rigid spacer and a bivalent receptor, (d) a bivalent ligand tethered by a suitable flexible spacer and a bivalent receptor, and (e) a bivalent ligand tethered by a long flexible spacer and a bivalent receptor.

In the case of an association of a bivalent receptor with two monovalent ligands, the total entropic cost ΔS_{mono} is double the sum of the translational and rotational entropies (Equation 4 and Scheme 3b).

$$\Delta S_{mono} \approx 2 \cdot \Delta S_{trans} + 2 \cdot \Delta S_{rot} \quad (4)$$

This equation only represents a qualitative summation, in which the translational and rotational entropies were assumed to have the greatest contribution and other possible contributions, such as from conformational, vibrational, and solvation entropies, are relatively insignificant,[16] e.g., the translational entropy of a water molecule is roughly 3000-fold larger than the vibrational entropy.

In the case of an association of a bivalent receptor with a bivalent ligand tethered by a suitable rigid spacer, if the bivalent ligand only retains one conformation and the spacing of the bivalent ligand matches that of the bivalent receptor, a single ligand-receptor interaction can be followed by a subsequent intramolecular interaction between the second binding moiety and the second binding site without any additional translational and rotational entropic cost. Thus, the total entropic cost $\Delta S_{bi/rigid}$ of the whole bivalent interaction is approximately the sum of translational and rotational entropy which is only half the entropic cost of the association of a bivalent receptor with two monovalent ligands (Equation 5 and Scheme 3c).

$$\Delta S_{bi/rigid} = \Delta S_{trans} + \Delta S_{rot} \quad (5)$$

Such an estimation, however, is based on certain limited considerations: (1) There is only one conformation for this bivalent ligand ($\Delta S_{conf} = 0$), and no torsional rotation around bonds takes place. (2) As mentioned in the last section, the translational and rotational entropies are equal due to their weakly logarithmical relationship to molecular weight. (3) The interaction of two particles, either bivalent or monovalent, become one particle, the ligand-receptor complex, which results in the net loss of the free translation and rotation of a single particle.[1,43] In other words, this bivalent interaction is maximally entropically enhanced by using this rigid spacer.

The structural parameters, length, angle, and curvature, of the necessarily rigid spacer, however, are difficult to predict. A small structural mismatch will lead to a weak binding due to some unfavorable steric interactions or a reduction in complexation strength. Therefore, such bivalent ligands are unrealistic to develop. In practice, the bivalent ligand with a flexible spacer is more attractive, although the total entropic cost $\Delta S_{bi/flex}$ for an association between a bivalent receptor and a bivalent ligand tethered by a suitable flexible spacer becomes less favorable due to

additional conformational entropy ΔS_{conf} (Equation 6 and Scheme 3d).

$$\Delta S_{bi/flex} = \Delta S_{trans} + \Delta S_{rot} + \Delta S_{conf} \quad (6)$$

A multivalent ligand tethered by a flexible spacer exists as a number of available conformations before the achievement of the multivalent binding with multivalent receptor, and therefore has higher conformational entropy than the multivalent ligand-receptor complex. The more flexible the spacer is, the more disorder it has due to its access to more conformational states. In general, a flexible spacer will always lead to an unfavorable entropic contribution to the whole free energy.[1] If the conformational entropy is less than the sum of its translational and rotational entropies, this bivalent interaction is still more entropically enhanced than two independent monovalent interactions (Scheme 3d). However, once the conformational entropy is equal to the sum of the translational and rotational entropies, the entropic enhancement for a bivalent interaction becomes negligible or even vanishes. This means, the gained translational and rotational entropies can not compensate the loss of the conformational entropy. As a consequence, this bivalent interaction is entropically neutral (Equation 7) so that the remaining unbound binding site of the bivalent receptor may bind either to the second binding moiety of the bound bivalent ligand or to another unbound bivalent ligand (Scheme 3e).

$$\Delta S_{bi/flex} \leq (2\Delta S_{trans} + 2\Delta S_{rot}), \text{ if } \Delta S_{conf} \leq (\Delta S_{trans} + \Delta S_{rot}) \quad (7)$$

Moreover, the conformation entropy of the intramolecular interaction can also exceed the sum of the translational and rotational entropies, meaning that the bivalent interaction is made entropically less favorable and unachievable.[1]

Although it is difficult to quantify the loss of conformational entropy in a multivalent interaction, an estimation of the conformational entropy associated with freezing a single rotating carbon-carbon bond is approximately 0.5 kcal·mol^{-1} at 298 K.[1,20] Therefore, Mammen et al. concluded that the conformational entropy could be large for a long flexible chain. For example, for a triethylene glycol spacer the unfavorable loss could be 10 kcal·mol^{-1}.[1] It was also argued that the bivalent ligand tethered with a flexible oligoethylene glycol (OEG) spacer could be expected to fail due to this entropic reason.

Several groups have synthesized a variety of conformationally “locked” oligosaccharides in order to avoid losses in conformational entropy during ligand binding but they found that such “locked” ligands did not offer any significant entropic improvement than other “flexible”

ligands.[44,45] This was because such a structural change can also lead to enthalpic reduction in the free energy, as estimated by Lundquist et al. in their work.[43,46] Interestingly, in NMR studies of overall protein conformational flexibility during ligation, it was found that a range of conformational changes take place in the protein during the ligand-protein interaction and that this conformational flexibility can compensate the loss of the free energy at the actual binding site.[47,48] Remarkably, although the flexibility suffers from the conformational entropy, it can increase the possibility that all ligand-receptor interactions could occur without energetic strain. This enthalpy-entropy compensation will be discussed in the next section.[1,42,49]

Although it was argued that the flexible spacer, such as OEG, should not function effectively as the spacer in multivalent ligands due to their severe loss in conformational entropy, Kramer et al. successfully applied such flexible spacers in a bivalent study with cyclic-nucleotide-gated (CNG) channels and found the polymer-linked (PEG) bivalent ligand containing two cyclic GMP (cGMP) moieties up to a thousand times more potent than the monovalent cGMP in activating CNG channels and cGMP-dependent protein kinase.[50] This observation indicated that the conformation entropy during the ligand binding might be smaller than the prediction mentioned above. The authors attributed such an enhancement to the decrease in the dissociation rate caused by the highly effective concentration (C_{eff}) of bivalent cGMP (more detail in Section 1.1.4).

In 2004, Reinhoudt and co-workers reported that the bivalent binding constant of a bis(adamantyl)-functionalized calyx[4]arene to β-cyclodextrin (CD) SAMs on gold surface ($K \approx 10^{10}$ M^{-1}) was 3 orders of magnitude stronger than that of a bis(adamantyl)-functionalized calyx[4]arene to an EDTA-tethered β-CD dimer in solution ($K = 1.2\times10^{7}$ M^{-1}).[51] The authors rationalized this result by using a theoretical model, in which a bivalent binding of a bivalent ligand to a bivalent receptor was assumed to be two consecutive monovalent binding events, rather than a "simultaneous" binding event. In this interpretation, a bivalent binding starts with an intermolecular interaction followed by an intramolecular interaction, and the latter one is associated with the higher, more effective concentration term owing to the close proximity of two interacting species. Moreover, Reinhoudt et al. described a binding model for multivalent interactions in terms of intra- versus intermolecular binding (Scheme 4), in which the term "intramolecular" was used for the formation of an additional interaction between two multivalent entities with a previously existing interaction, while the term "intermolecular" indicated the

formation of a novel interaction between two unlinked multivalent entities.[52-54]

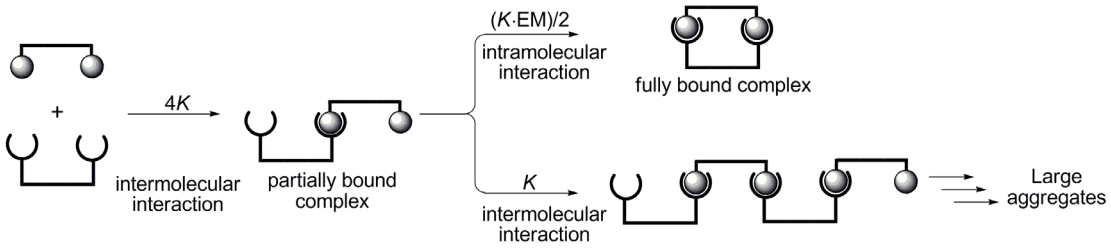

Scheme 4. Multivalent intra- versus intermolecular binding.[54-56]

Whether a multivalent binding occurs by intra- or intermolecular mode[54] is determinated first and foremost by the architecture of multivalent entities. For example, the four potential binding sites of concanavalin A are in four opposite directions and therefore, are intermolecularly bound by multivalent ligands.[6,57,58] In contrast, distances between binding domains in the small Shiga-like toxin are less than 10 Å so that the multivalent intramolecular mode can be adopted by multivalent ligands.[7,59] A second major factor is the thermodynamics of multivalent interactions. As mentioned above, a multivalent interaction is governed by entropy, especially conformational entropy. An intramolecular multivalent binding, however, becomes less favorable once the gained translational and rotational entropy cannot compensate for the conformational entropic penalty.[1]

To better identify whether a multivalent binding undergoes an intra- or intermolecular mode, Reinhoudt and co-workers recommended the use of the term "effective concentration."[54] If the effective concentration is higher than the actual ligand concentration in solution, an intramolecular multivalent binding is favored; otherwise an intermolecular multivalent binding will be adopted. In other words, the binding mode for the multivalent interaction adopts an intramolecular mode at low concentrations and an intermolecular mode at high concentrations. Unlike the effective concentration, which is calculated by physical geometries of multivalent entities, the term "effective molarity" (EM = K_d^{inter} / K_d^{intra}) can be experimentally estimated. Krishnamurthy et al. investigated the dependence of the EM on the spacer length for an intramolecular protein-ligand system and found that the EM reached a maximum once the flexible spacer length was the optimal length to allow the p-substituted benzenesulfonamides to bind to the active site in the human carbonic anhydrase II protein, and then, surprisingly, decreased slightly with the increasing spacer length.[18] The relationship between the spacer length and the binding affinity thus indicated that the conformational entropy for an intramolecular interaction did not strongly increase with the

increase in the flexible spacer length as previous described in reference 1, and implied that the most effective strategy for the design of multivalent ligands is to tether binding moieties with a flexible spacer which is significantly longer than the distance between binding sites of the multivalent target.

More recently, Hunter et al. proposed the "K·EM", i.e., the product of monovalent association constant multiplied by the effective molarity, which can determinate the population of multivalent binding mode (Scheme 4).[55,56] If the product of K·EM is less than 1, the intermolecular binding mode will be adopted and the partially bound complex will be more stable than a fully bound complex. In contrast, if the product of K·EM is greater than 1, the major species will be the fully bound complex and the intramolecular binding mode will become favorable.

Finally, the solvation entropy is defined as the entropic change of the surrounding molecules.[1] In biology, this entropy is caused by intermolecular interactions between water molecules and the ligand via hydrogen bond or other hydrophobic interactions. In a quantitative study about such hydrophobic interactions,[60] it was reported that this entropic change in either a monovalent or multivalent system has similar values, unless the tethered spacer or the scaffold has additional interactions with the binding moieties or the surface of the multivalent protein. Therefore, the discrimination between monovalent and multivalent ligands in unfavorable contributions of the solvation entropy could be ignored,[1] such that

$$\Delta S_{\text{multi,sol}} \approx \Delta S_{\text{mono,sol}} = \Delta S_{\text{sol}}.$$

1.1.2.3. The thermodynamic origin of multivalent interactions

Based on the above interpretation of the roles of enthalpy and entropy in multivalent interactions, a multivalent interaction with N binding sites is used as a mode to survey the thermodynamic origin of multivalent interaction. According to a review by Mammen et al.,[1] thermodynamic comparison between a monovalent and a multivalent interaction with the three thermodynamic parameters (ΔG°, ΔH°, and ΔS°) could be expressed as follows:

$$\Delta G_{\text{mono}} = \Delta H_{\text{mono}} - T\cdot\Delta S_{\text{mono}},\ \Delta S_{\text{mono}} \approx \Delta S_{\text{trans}} + \Delta S_{\text{rot}} + \Delta S_{\text{sol}}$$

$$\Delta G_{\text{multi}} = \Delta H_{\text{multi}} - T\cdot\Delta S_{\text{multi}},\ \Delta H_{\text{multi}} \approx N\cdot\Delta H_{\text{mono}},\ \Delta S_{\text{multi}} \approx \Delta S_{\text{trans}} + \Delta S_{\text{rot}} + \Delta S_{\text{conf}} + \Delta S_{\text{sol}}.$$

Therefore, a free energy difference ($\Delta\Delta G$) between N independent monovalent interactions and a

multivalent interaction could be obtained as Equation 8:

$$\Delta\Delta G = \Delta G_{multi} - N\cdot\Delta G_{mono} = (\Delta H_{multi} - N\cdot\Delta H_{mono}) - T\cdot(\Delta S_{multi} - N\cdot\Delta S_{mono})$$
$$= T\cdot(N - 1)\,\Delta S_{mono} - T\cdot\Delta S_{conf} \quad (8)$$

From Equation 8, it was found that a tight multivalent binding needs a negative value of the free energy difference ($\Delta\Delta G < 0$). Therefore, the conformational entropy of the multivalent ligand could be a crucial factor.

In a well-studied calorimetric measurement preformed by Rao et al.,[61,62] a trivalent D-Ala-D-Ala molecule bound to a trivalent vancomycin molecule with a very high affinity shown by a low dissociation constant (K_d) of approximately 4×10^{-17} M and a free energy -22 kcal·mol^{-1}. Interestingly, it was found that the enthalpic contribution ΔH_{tri} of the association was -40 kcal·mol^{-1} and the entropic term was $T\cdot\Delta S_{tri}$ = -18 kcal·mol^{-1}, which are roughly three and 4.5 times those of their monovalent counterparts, respectively ($\Delta H_{mono} \approx$ -12.0 kcal·mol^{-1}, $T\cdot\Delta S_{mono} \approx$ -4.1 kcal·mol^{-1}). The authors concluded that the enthalpic contribution ΔH_{tri} primarily originates from the enthalpy of three associations between three binding moieties and three binding sites, which, however, was slightly more negative than the assumed result, i.e., $\Delta H_{tri} < 3\cdot\Delta H_{mono}$. The entropic contribution ($T\cdot\Delta S_{tri1}$) for the first binding step of the trivalent interaction was assumed as -4.7 kcal·mol^{-1}, which was similar to that of monovalent counterparts and indicated that the total entropic contribution for the last two intramolecular steps ($T\cdot\Delta S_{tri2} + T\cdot\Delta S_{tri3}$) was much more negative (-13.3 kcal·mol^{-1}) than expected. To address this question, Rao et al. further analyzed this entropic contribution $T\cdot\Delta S_{tri2} + T\cdot\Delta S_{tri3}$ in light of Williams's previous work,[63] and estimated the additional conformational entropy $T\cdot\Delta S_{tri2,conf} + T\cdot\Delta S_{tri3,conf}$ in the last two intramolecular binding steps to be approximately -41 kcal·mol^{-1}. This means that the conformational entropy is the largest fraction of the total entropic contribution in this trivalent interaction and that $T\cdot\Delta S_{tri}$ becomes much less favorable than in the monovalent interaction. Therefore, this tight trivalent interaction can be attributed to the favorable enthalpy, rather than to the entropy.

Similarly, Dam et al. investigated the binding of a series of mono-, bi-, tri-, and tetravalent carbohydrates to concanavalin A (CoA) and *dioclea grandiflora* lectin (DGL) *via* isothermal titration calorimetry (ITC).[6] They found that in all multivalent binding systems the enthalpic term increased proportionally with the valency compared to monovalent cases. For example, ΔH_{tetra} with a value of -53 kcal·mol^{-1} for tetravalent ligand was almost four times greater for the

monovalent ligand (ΔH_{mono} = -14.7 kcal·mol^{-1}). By contrast, the entropic term in multivalent cases was not proportional and much more negative, e.g., $T\cdot\Delta S_{tetra}$ = -43.3 kcal·mol^{-1} and $T\cdot\Delta S_{mono}$ = -7.1 kcal·mol^{-1}. Although the authors did not further discuss this entropic term like in the last example, the origin of this enhanced entropic term may be attributed to the conformational entropy.

From these two studies evidence for enthalpy-entropy compensation was found, which was also noticed by Williams et al. in their previous work.[42,63] They noted a tighter binding and a more negative enthalpy accompanied by a loss in conformational mobility and a greater entropic loss. Moreover, Krishnamurthy et al. investigated the associated thermodynamics of bovine carbonic anhydrase II (BCA) and para-substituted benzenesulfonamides tethered by side chains of varying lengths.[49] They found that the increased chain length resulted in a less favorable enthalpy but a less unfavorable entropy of binding. As a consequence, the dependence of the enthalpy on chain length was almost perfectly compensated by that of the entropy, which resulted in the independence of dissociation constant on the chain length. Additionally, a similar observation was also found by de Mol et al. in a thermodynamic study of immunoreceptor tyrosine-based activation motif (ITAM) based ligand binding to Syk Tandem SH2,[64,65] in which they connected two SH2 binding motifs either with a flexible peptide or with a rigid spacer of comparable length. In principle, the rigid spacer is probably more promising for reducing the conformational entropy. This expected entropy advantage, however, was not realized. They found that the bivalent ligand tethered by the rigid spacer was bound with a considerably higher entropic loss (-9.3 kcal·mol^{-1}) than the flexible-tethered ligand, although the enthalpic enhancement of this rigidity was only -8.9 kcal·mol^{-1}. Consequently, the association constants of both bivalent ligands were within the same order of magnitude due to the enthalpy-entropy compensation. This observation was attributed to a further decrease in protein flexibility upon binding to this rigid ligand. Furthermore, such enthalpy-entropy compensation was also observed in the research of non-covalent macromolecular interaction,[66] which is not discussed here.

1.1.3. Cooperativity and enhancement factor

The interpretation that the thermodynamic origin of multivalent interactions is attributed to their

entropic contribution is often poor due to complications arising from the influence of binding at one site on binding at the other site, i.e., the cooperativity between binding sites. Therefore, to better understand the multivalent interactions, it is necessary to further discuss the role of the cooperativity in this process.

1.1.3.1. Cooperativity in multivalent interactions

Cooperativity is a phenomenon in nature which arises from the interplay between a binding of one ligand to one binding site of a multiple receptor and the subsequent binding, for example, in the transport of oxygen molecules by hemoglobin.[67] In this case, the binding of the first oxygen molecule to hemoglobin results in a conformational change of the protein such that the subsequent binding is much more favorable than the first one and a greater free energy will be released. The stoichiometric binding constants are defined in the following equation (Equation 9):[55]

$$K_{a1}=\frac{[RL]}{[R][L]},\ K_{a2}=\frac{[RL_2]}{[RL][L]},\ \ldots,\ K_{aN}=\frac{[RL_N]}{[RL_{N-1}][L]}, \tag{9}$$

where N represents the amount of the binding sites of a multivalent receptor R, and L the ligand. Hunter and Anderson defined an interaction parameter α_H to describe the degree of the cooperativity in the case of bivalent interactions[55] (Equation 10):

$$\alpha_H = K_{a2} / K_{a1} \tag{10}$$

$\alpha_H > 1$: Positive cooperativity, the subsequent binding is more favorable than the first one.

$\alpha_H = 1$: No cooperativity, the subsequent binding is as favorable as the first one.

$\alpha_H < 1$: Negative cooperativity, the subsequent binding is less favorable than the first one.

In a similar definition, Whitesides and co-workers also compared the free energy change in a multivalent interaction with a monovalent interaction.[1] They used the term $\Delta G_{avg,multi}$ to describe the average free energy of a interaction between a binding moiety and a binding site of two multivalent entities, which can be greater than, equal to, or less than the free energy ΔG_{mono} in an analogous monovalent interaction (Equation 11).

$$\alpha_w=\frac{\Delta G_{avg,multi}}{\Delta G_{mono}}=\frac{\Delta G_{multi}}{N\cdot\Delta G_{mono}}=\frac{\lg(K_{multi})}{\lg(K_{mono})^N} \tag{11}$$

The authors classified the multivalent interaction as synergistic ($\alpha_w > 1$), additive ($\alpha_w = 1$),

and interfering ($\alpha_w < 1$). Since the binding of second oxygen molecule to hemoglobin occurs with a more favorable free energy than the first binding, the binding of four oxygen molecules to tetrameric hemoglobin is a positive (synergistic) cooperativity. However, this example does not involve multivalency.

Compared to the rare example[68] of positive cooperativity in multivalent interactions, there are several examples for the negative cooperativity. One example is the multivalent carbohydrate-lectin interactions investigated by Brewer and co-workers,[69] in which the binding affinities of the di-, tri-, and tetravalent trimannoside to two lectins were enhanced by the greater positive entropy of binding contributions compared to monovalent analogues. Hill plots analysis for these interactions, however, indicated that tri- and tetravalent trimannoside have greater negative cooperativity than bivalent trimannoside. In other words, the negative cooperativity increased with the increase of functional valency. Additionally, the negative cooperativity was also found by using the ITC measurement in the case of the binding of asialofetuin (a glycoprotein with nine epitopes) to galection[70] and lectins to mucins, [71,72] respectively.

1.1.3.2. Enhancement factor as an evaluation index

Although most multivalent interactions exhibit negative cooperativity, their multivalent binding affinities are still much higher than the monovalent counterparts. Therefore, in order to better demonstrate the difference between a multivalent and monovalent interaction, Whitesides and co-workers proposed an enhancement factor β,[1,19] which reflects the strength of a multivalent association relative to the corresponding monovalent association and was defined as the ratio of the multivalent binding constant to the monovalent binding constant (Equation 12):

$$\Delta G_{multi} = \Delta G_{mono} - RT\ln(\beta)$$
$$\beta = K_{a,multi} / K_{a,mono} \quad (12)$$

For instance, in the case of a trivalent D-Ala-D-Ala molecule binding to a trivalent vancomycin molecule studied by Rao et al.,[61,62] the average free energy of the trivalent interaction ($\Delta G_{avg,tri}=\Delta G_{tri}/3$=-22/3 kcal·mol^{-1}) and the free energy of its corresponding monovalent interaction (ΔG_{mono}) were -7.3 and -7.9 kcal·mol^{-1}, respectively. According to Equation 11, this high affinity trivalent interaction had a negative cooperativity ($\alpha_W < 1$), although

it had a 6.1×10^{10} greater activity ($\beta = K_{d,mono}/K_{d,tri} = [(2.7\times10^{-6}\ M)/(4\times10^{-17}\ M)]$) than the monovalent interaction in terms of the enhancement factor β. Moreover, the term β will be a useful parameter in the case of the unknown binding number N.

In order to demonstrate the binding enhancement of the multivalent interaction, Gargano et al. illustrated a theoretical mode, in which the simplest multivalent system, namely bivalent interaction, was chosen (Scheme 5).[73] To address the equilibrium constant K_{bi} of this bivalent interaction from completely unbound state to fully bound state though steps 1, 2, and 3, the association of the bivalent ligand with the bivalent receptor could be viewed as a sum of three other equilibriums, i.e., $K_1 \cdot K_2 \cdot K_3$. These three association constants were solved in terms of the association constant of a monovalent ligand K_{mono} and a statistical factor for each association. Therefore, $K_1=4K_{mono}$, $K_2=K_{mono}$. Since the equilibrium of step 3 represented a competition between an intra- and intermolecular interaction, its association constant was equal to the effective concentration, i.e., $K_3 = C_{eff}$. Moreover, the authors estimated that the effective concentration C_{eff} for a bivalent ligand tethered by a 30 Å spacer was $10^{-2}/2$ M. Thereby, the bivalent association constant K_{bi} of this bivalent interaction was $0.02(K_{mono})^2\ M^{-1}$. From this theoretical bivalent mode, it was concluded that the design of a nanomolar active bivalent ligand ($K_{bi}=10^9\ M^{-1}$) should be based on a monovalent ligand with the micromolar activity ($K_{mono}= 2.2 \times 10^5\ M^{-1}$).

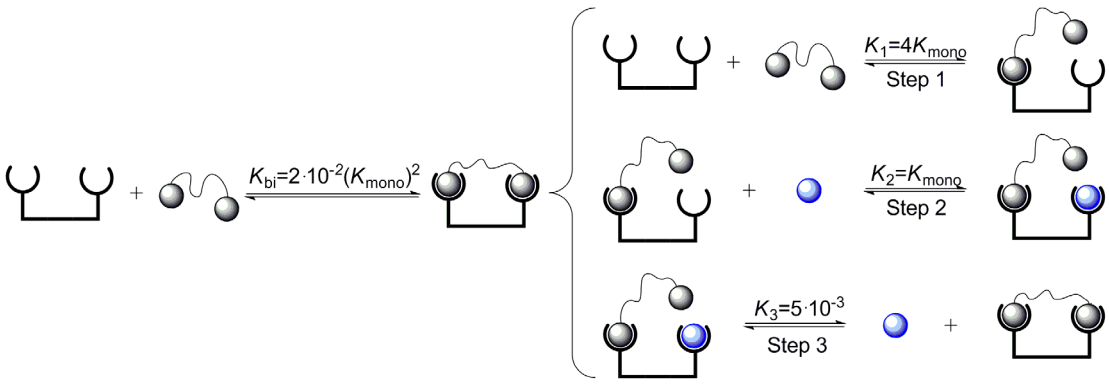

Scheme 5. Theoretical model for a bivalent interaction.[73]

1.1.4. Kinetics of multivalent interactions

The thermodynamic aspects of multivalent interactions are often highlighted due to the relationship between the Gibbs free energy ΔG° and the binding constant K (Equation 1). By

contrast, the role of the kinetics has been rarely surveyed. Moreover, the kinetics in multivalent interactions is fundamentally different from its monovalent counterpart and involves a sequence of association and dissociation steps.[61] Although the rate constants for each kinetic step cannot be measured so far, a mono- and a bivalent interaction were applied here as modes for discussing the kinetic role in multivalent interactions, in particularly regarding rates of association and dissociation (Scheme 6).

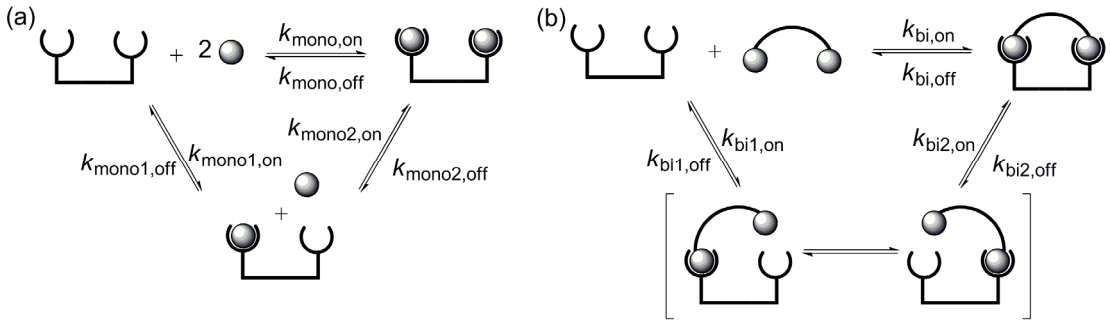

Scheme 6. Kinetic schemes describing the association and dissociation of (a) a mono- and (b) bivalent ligand with a bivalent receptor.

At equilibrium, the concentration of each species in Scheme 6 does not change with time, and the rate at which the mono- or bivalent ligand associates with the bivalent receptor equals the rate at which the ligand-receptor complex dissociates to form unbound ligand and receptor. Therefore, the dissociation constant K_d for the mono- and bivalent interaction can be expressed by rates of dissociation k_{on} and association k_{off} as following, respectively:

$$K_{d,mono} = \frac{k_{mono,off}}{k_{mono,on}}, \text{ where } k_{mono,off} = k_{mono1,off} \cdot k_{mono2,off}, \text{ and } k_{mono,on} = k_{mono1,on} \cdot k_{mono2,on}; \quad (13)$$

$$K_{d,bi} = \frac{k_{bi,off}}{k_{bi,on}}, \text{ where } k_{bi,off} = k_{bi1,off} \cdot k_{bi2,off}, \text{ and } k_{bi,on} = k_{bi1,on} \cdot k_{bi2,on}; \quad (14)$$

$$K_{d,bi} < K_{d,mono}, \text{ i.e., } \frac{k_{bi,off}}{k_{bi,on}} < \frac{k_{mono,off}}{k_{mono,on}}. \quad (15)$$

1.1.4.1. The kinetics during the multivalent association and dissociation

As Equation 15 showed that a tight binding (with a small dissociation constant K_d) of bivalent interaction can be achieved either by a increased association rate $k_{bi,on}$ or by a decreased

dissociation rate $k_{bi,off}$ compared to those of monovalent interaction, it is necessary to separately discuss these two terms.

Since the diffusion mechanism of the interacting species and the thermodynamic cost (the activation energy $\Delta G^{\neq}_{on}$) of the first ligand-receptor interaction between two multivalent entities are approximately same as those in monovalent interactions, the first association rate $k_{bi1,on}$ of bivalent interactions has a similar value as the first association rate $k_{mono1,on}$ in analogous monovalent interactions.[1,54,74] Thus, the first association of bivalent interactions is often rate-determining step. By contrast, the subsequent intramolecular interaction is related to the effective concentration and has a much higher association rate than that in the monovalent interaction ($k_{bi2,on} > k_{mono2,on}$). Remarkably, such an interpretation is poor in the case of a multivalent ligand containing rigid element or spacer. For instance, Badjic et al. studied the self-assembly of a two-component triply threaded superbundle via ^{1}H NMR spectroscopy.[75] They found that the formation of a doubly threaded superbundle intermediate was relatively fast and this intermediate was kinetically stable on the NMR timescale. Conversely, the last intramolecular threaded was hampered by its rigid spacer, and consequently, the association constant K_a for the last threaded was only 4.

Unlike the association rate mentioned above, a dissociation process of multivalent interactions requires breaking N times ligand-receptor interaction, and the overall dissociation rate is determinated by the last dissociation of the monovalently bound ligand-receptor complex to form the unbound multivalent ligand and receptor.[1,54,74] In other words, this dissociation rate ($k_{di1,off}$) of monovalently bound ligand-receptor in bivalent interactions is equal to the dissociation rate ($k_{mono1,off}$) of the monovalent counterpart. Moreover, in a well-studied kinetic example about the bivalent cGMP reported by Kramer et al. it has been demonstrated that the decrease in the dissociation rate was more likely the origin of the enhanced binding affinity (the decreased dissociation constant K_d).[50] Based on the kinetic experiment results, the authors proposed that the overall dissociation rate ($k_{di,off}$) of the fully bound ligand-receptor to completely unbound ligand and receptor is equal to twice the intrinsic dissociation rate of monovalent cGMP ($k_{mono,off}$) times the probability that the second site is not occupied, i.e.,

$$k_{di,off} = \frac{2k_{mono,off} \cdot K_d}{C_{eff} + K_d}, \tag{16}$$

where C_{eff} refers to the effective concentration of the bivalent ligand and K_d the dissociation constant. In the case of the dissociation of the bivalent cGMP tethered by a spacer of 39 Å (PEG2000), the effective concentration C_{eff} was 13.4 mM and the dissociation constant K_d for the monovalent cGMP was 4 μM, this gave a 3400-fold slower bivalent dissociation rate than for the monovalent cGMP ($3400k_{bi,off} = k_{mono,off}$). In contrast, the bivalent cGMP tethered by a spacer of PEG20000, which was much longer than the space separation between two binding sites, had a smaller C_{eff} value and dissociated more easily due to the lower probability of rebinding for each cGMP moiety.

Similar observation of trivalent interaction reported by Rao et al. also indicated that a fast intramolecular rebinding of partially bound ligand-receptor complexes was the kinetic origin of the high stability of this trivalent complex.[61] Moreover, a stepwise association and dissociation mechanism was also proposed. Recently, in a kinetic study of bivalent ITAM ligand binding to Syk Tandem SH2 receptor it was found the association and dissociation of the fully bound ligand-receptor complex were extremely rapid and had a short lifetime of approximately 4 s.[64] More recently, Lata et al. investigated the switchable recognition of histidine-tagged proteins,[76] in which fluorescence dequenching method was applied to measure the dissociation between multivalent chelator heads supramolecules (containing two, three, or four nitrilotriacetic acid (NTA) moieties, respectively) and oligohistidine. Interestingly, the trivalent NTA had the subnanomolar affinity and showed an increase in stability by four orders of magnitude compared to that of monovalent NTA. It is notably that the difference of the association rate between the tri- and monovalent NTA was only 1.3 times. Therefore, the tight binding between the trivalent NTA and oligohistidine was due to the decreased dissociation rate $k_{tri,off}$, rather than the association rate $k_{tri,on}$.

More interestingly, by using NMR spectroscopy method Jiang et al. investigated the thermodynamic and kinetic behavior of hetero bivalent interactions in which it was found that the hetero bivalent guest tethered by a shorter spacer (one methylene unit less, GuestC2, Scheme 7) forms a more stable fully bound complex ($\Delta G_{GuestC2}$-$\Delta G_{GuestC3}$ = -4.9 kJ·mol^{-1}) than that tethered by a long spacer.[77] Moreover, the authors also measured the association rates (k_{on4}) of last intramolecular threading step (21-crown-7) and found that the association rate ($k_{on4,GuestC2}$) for the thermodynamic more stable complex (GuestC2+Host) was 7.54×10^{-4} s^{-1} with a half life of 15.3

min and for the other complex (GuestC3+Host, $k_{on4,GuestC3}$) was 4.37×10^{-3} s^{-1} with a half life of 2.6 min. Furthermore, the activation energies for the formations of both fully bound complexes were estimated: 91.8 and 86.6 kJ·mol^{-1}, respectively. This finding implied that a minor structural change of the multivalent ligand (one methylene unit) could result in a large difference in thermodynamics and kinetics. Additionally, based on their previous study about the association constant ($K_4 \geq 10^4$ M^{-1}),[77] the dissociation rate k_{off4} of these fully bound complexes can be neglected when compared to the association rate k_{on4}.

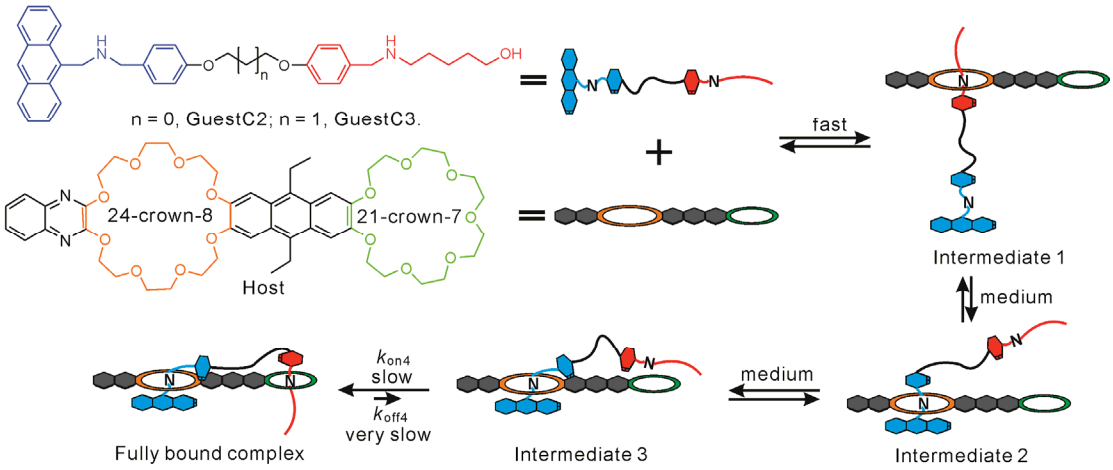

Scheme 7. A hetero bivalent guests-host interaction and the possible formation pathway in which different association and dissociation rates were estimated by using ^{1}H NMR spectroscopy.[77]

1.1.4.2. Impact on the dissociation rate and the rebinding effect

A kinetic stabile multivalent interaction is most likely due to the decreased dissociation rate k_{off} and the rebinding effect. These two terms can be influenced by two factors, i.e., the effective concentration C_{eff} and the presence of a monovalent competitor. The former one has been discussed above in the case of the bivalent cGMP tethered by the spacer of PEG20000, while the latter one has been often applied in the dissociation phase of SPR measurement to prevent the association (rebinding) of multivalent ligand (or receptor) with the functionalized surface. In the study of using bivalent carbonic anhydrase II to the SAM presenting benzenesulfonamide ligand, Mack et al. found that the dissociation rate $k_{di,off}$ of bivalent BCA increased with the high concentration of free monovalent ethoxzolamide ligand in buffer and this rate approached an asymptotic value at the highest concentrations of free ligand.[11] In a stepwise dissociation, the

concentration of the partially bound species is dependent on the concentration of the monovalent competitor, which can prevent rebinding of this partially bound multivalent ligand-receptor complex. Moreover, an increase in the dissociation rate caused by competition with the monovalent ligand also indicates a successful formation of multivalent interactions and implies that a high-affinity multivalent ligand-receptor complex can be achieved by the kinetic control and reversibility.[54]

1.2. Estrogen receptor as a bivalent target

In the late 1950s, Jensen and Jacobsen first demonstrated that certain proteins were only found in the estrogen target tissues and selectively bound to the tritium labeled estrogen, 17β-estradiol ([^{3}H]-E_2).[78] Subsequently, more and more experimental evidence was found to establish the correlation between these estrogen bound proteins and certain tumor tissues such as breast cancer tissue. Nowadays, it is known that there are two types of proteins which bind to estrogen and regulate various biological activities in the human body via transcription functions. One is a member of intracellular nuclear receptor, and another is a G protein-coupled receptor (GRCR), i.e., GPR30, which is located on the cell membrane. The estrogen receptor (ER) in this thesis refers to the former. In addition to its role in the female reproductive system, the human ER is capable of regulating the growth and differentiation of tissues such as skeletal, neural, and cardiovascular in both males and females.[79-81]

1.2.1. Estrogen receptor

In 1966 the ER was isolated as an extractable protein from rat uterus and two decades later the first ER was cloned by Green and Greene.[82,83] This receptor had been regarded as the only human ER until Kuiper et al. demonstrated a second ER in 1996.[84] These two receptors are known as ERα and ERβ, respectively, and distributed in different tissues at different levels, e.g., ERα in endometrium and breast cancer cells, while ERβ in brain and bone.[85] Both ER subtypes are composed of five domains and have a significant overall sequence homology (Figure 3). The gene of ER is regulated by two active functions. In the absence of human estrogen the gene transcription is activated by the N-terminal domain neighboring with DNA binding domain (DBD),

and this active function, denoted as the active function 1 (AF-1), is much weaker than the ligand-dependent active function 2 (AF-2) in the ligand-binding domain (LBD), which is located in the C-terminal domain of the receptor.[86,87] The finding of ERα-overexpression in breast cancer tissue established the correlation between the tumor tissue proliferation and estrogen. Although various antiestrogen ligands which bind to the ERα and down-regulate the gene expression in the tumor cells have been developed over the last 50 years,[79-81] it is particularly challenging to develop a high ER subtype selective ligand due to the high homology.[88,89]

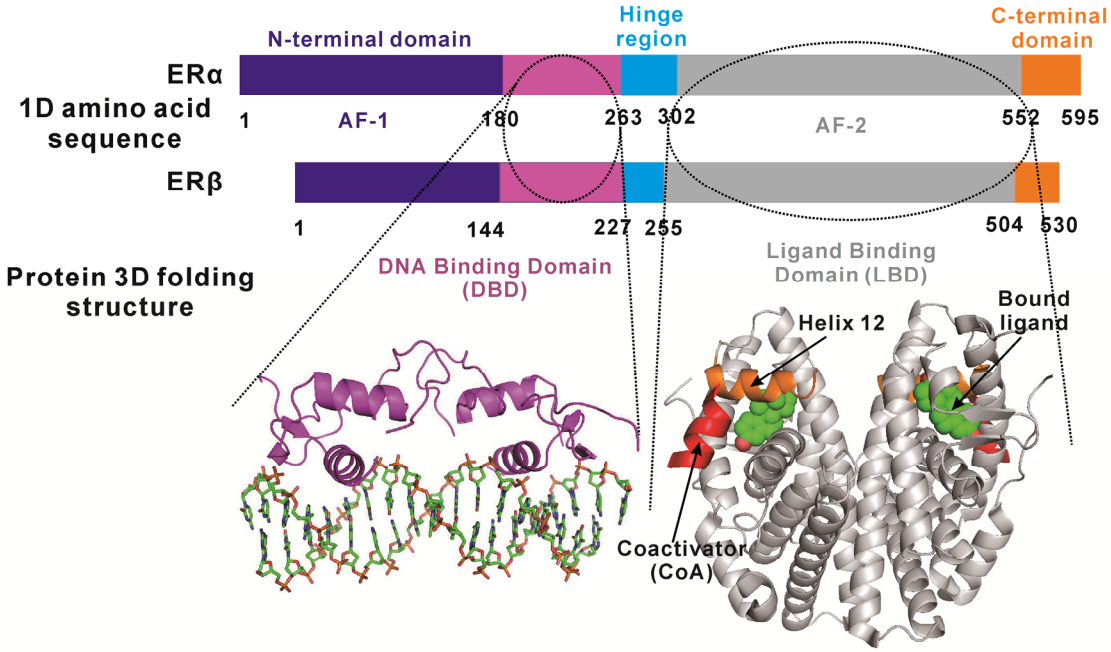

Figure 3. The 1D and 3D structure of two estrogen receptor (ER) subtypes. Top: 1D amino acid sequence of two ER subtypes. Below left: Dimeric 3D protein structure of DNA binding domain (DBD, ribbons in violet, PDB 1HCQ) of ER binds to an estrogen response element (ERE, sticks) of DNA. Below right: Dimeric 3D protein structure of ER ligand-binding domain (LBD, ribbons in gray, PDB 1GWR), a bound coactivator (CoA) peptide (ribbon in red), and a bound ligand (spheres).

1.2.2. Mechanism of transcriptional activation

Similarly to the other nuclear receptors, an estrogen molecule such as endocrine 17β-estradiol (E_2) binding to the ER results in the ER-dissociation of heat shock protein (HSP) and corepressor. Subsequently, a conformational change in the ER LBD takes place so that two ER-ligand complexes can dimerize and recruit coactivator (CoA) proteins, e.g., steroidal coactivator 3 (SC3), to form an active ER-ligand-CoA complex. Then, this dimeric complex translocates from the

cytoplasm into the cell nucleus, where its DBD can bind to the estrogen response element (ERE, Figure 3), a specific sequence of DNA, and interact with other factors such as RNA polymerase. Consequently, mRNA is expressed and the transcription occurs followed by the proliferation of the cell (Figure 4).[79,90-93]

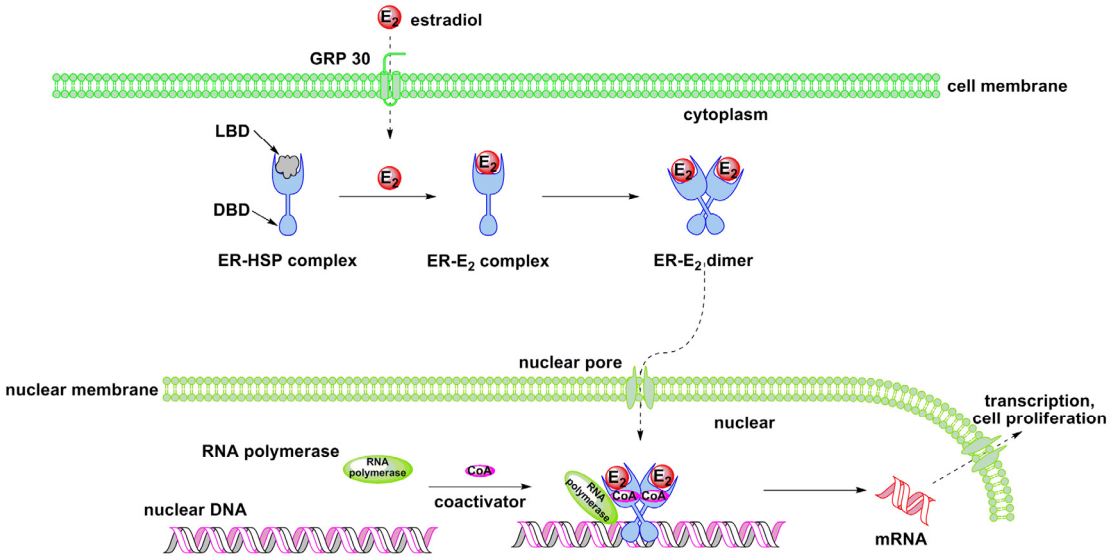

Figure 4. Schematic representation of transcriptional mechanism of ER with estrogen in a cell.[79]

The ligands involved in ER-binding not only have different binding affinities to ER due to individual chemical structure but also dramatically affect the ability of ER to display diverse functions such as agonism, partial antagonism, or antagonism. In the case of agonist E_2, the ER-E_2 binding triggers a conformational change of the C-terminal helix of the ER LBD, helix 12 (H12), such that E_2 can be fully buried within a hydrophobic ligand-binding pocket (LBP) and two monomeric ER-E_2 complexes can form a stable homodimer. Meanwhile, the repositioning of H12 exposes a hydrophobic groove on the ER LBD surface, which is an essential prerequisite for a subsequent ER-CoA binding (Figure 3).[79] Additionally, Katzenellenbogen and co-workers investigated conformations and dynamics of the ER LBD and found that the ER LBP has more flexibility than the rest portion of the ER LBD. This flexible region, however, becomes more stabile and rigid, once a ligand binds to the ER.[94,95]

Moreover, some exogenous ligands have been synthesized. Among them, diethylstilbestrol (DES) has a similar transcription ability as E_2 (Scheme 8a and Figure 5 left), while *cis*-4-OH tamoxifen (OHT) leads to an antagonist in the breast tissue (Scheme 8b and Figure 5 right).[79,96-98]

The bulky and basic side chain of OHT prevents the reposition of H12, with the result that the ER-OHT complex has a different conformation than in the above mentioned E_2 example. Therefore, the hydrophobic CoA binding groove is not exposed and this ER-OHT complex dimer interacts with other proteins such as corepressor instead of CoA. This leads to an inhibition of the gene transcription process of the tumor tissue. Remarkably, in other tissue such as bone, the ER-OHT complex dimer still can recruit the other CoA protein to mime the transcription effect of the estrogen and prevent osteoporosis. Thus, OHT is regarded as a partial antagonist or a selective estrogen receptor modulator (SERM). By contrast, fulvestrant (FUL) does not have any agonistic effect, and its bulking side chain can destabilize the helix folding of ER and accelerate the receptor degradation (Scheme 8c).[79,99]

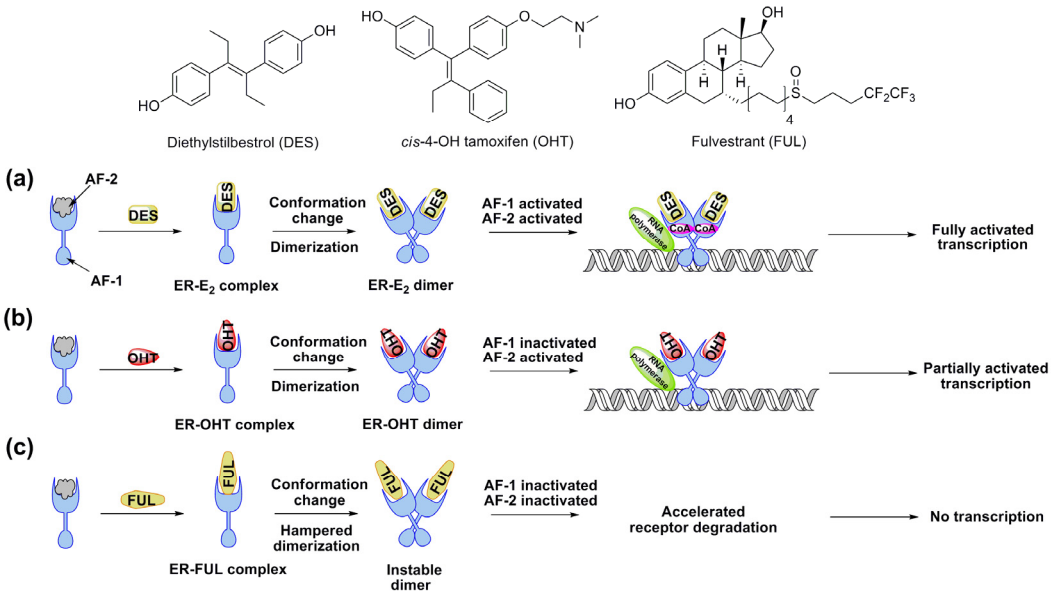

Scheme 8. Three different transcriptional consequences following the binding of the ER with (a) an agonist *trans*-diethylstilbestrol (DES), (b) a partial antagonist *cis*-4-OH tamoxifen (OHT), and (c) an antagonist fulvestrant (FUL) in the breast tissue.[79]

In the current chemotherapy of breast cancer, a number of drugs including the above examples have been developed to up- or down-regulate estrogen gene expressions.[80,100] Unfortunately, such treatments have side effects like other chemotherapies. For instance, OHT causes hot flashes and increases the risk of endometrial cancer.[81] Therefore, it is necessary to develop a new strategy such as multivalency to develop novel drugs with highly selective in vitro/vivo properties.

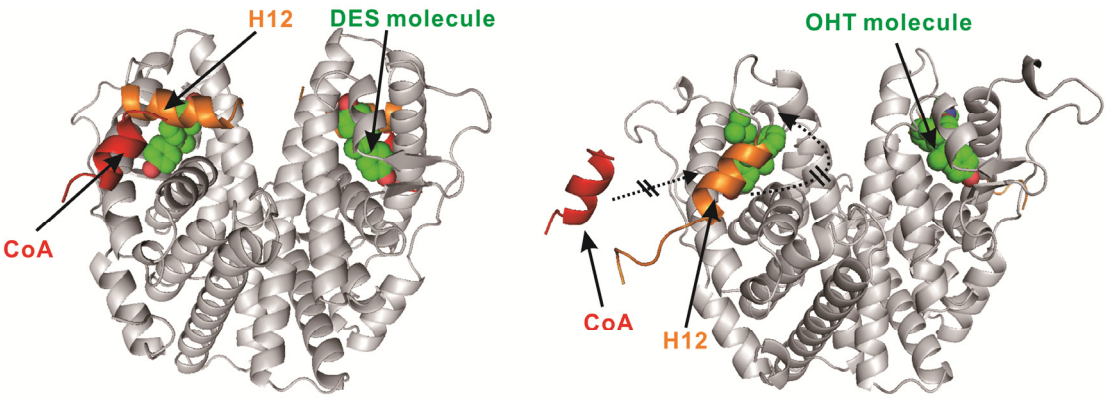

Figure 5. Left: Crystal structure of the agonistic mechanism of dimeric ERα LBD (PDB 3ERD, ribbons in gray, the ribbon of H12 in orange) with two DES molecules (spheres) and two CoA proteins (ribbon in red). Right: Structural basis for the antagonistic mechanism of dimeric ERα LBD (PDB 3ERT, ribbons in gray) with two OHT molecules (spheres). The binding region of the CoA protein (ribbon in red) is occupied by H12.

1.2.3. Estrogen receptor ligand-binding domain exists as dimer

In 1977 Weichman et al. found that the dissociation of [^{3}H]-E_2 from calf uterus ER have two different dissociation rates, a fast and a slow rate, which were purported to correspond to [^{3}H]-E_2 dissociation from the nonactive monomeric ER and active dimeric ER, respectively.[101] After two decades Salomonsson et al. demonstrated in a kinetic study that the spontaneous dimerization of active human ER LBD does not depend on the presence of DBD, estrogen ligand, and elevated temperature.[102] In this case, only one dissociation rate for E_2 was found, which suggested that the human ER LBD exists as a dimer which possesses two estrogen binding sites, rather than a monomer. In 1997 Brzozowski et al. crystallized two dimeric ER-ligand complexes.[103] This breakthrough provided not only an intuitive understanding of the agonistic and antagonistic mechanisms in ER-estrogen interactions but also comprehensive structural parameters of the ER such as the C_2-symmerty and a 1703 Å^2 dimer interface (15% of the total surface area of each monomer, Figure 6).

Brandt et al. studied the correlation between the ER ligand-binding and the stability of the ER dimer in vitro by using indirect methods such as size-exclusion chromatography.[104] The authors examined the dissociation rate of the ER LBD dimer and found that the half-life time of the ER homodimer significantly increased by a factor of 3 in the presence of E_2 compared to it in the absence of E_2. This enhancement indicated that ER-ligand binding results in a conformational

change in the ER LBD that affects the dimer interface. Additionally, the equilibrium dissociation constant (K_d) of this ER dimer has been estimated and is about 2-3 nM.

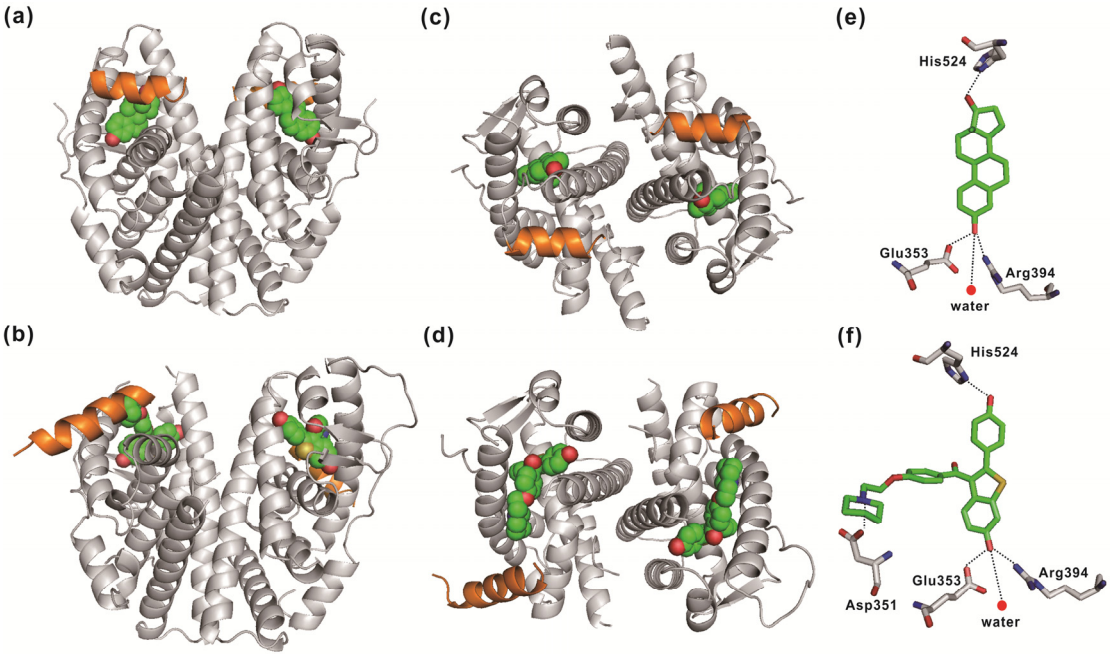

Figure 6. Ribbon representations of dimeric ERα LBD-ligand complexes. 1. The dimer viewed perpendicular to the dimer axis: The crystal structure of ERα LBD dimer (ribbons in gray, the ribbon of H12 in orange) complex with (a) two E_2 molecules (spheres, PDB ID code 1ERE); and (b) two raloxifene (RAL) molecules (PDB ID code 1ERR). 2. The dimer viewed down the dimer axis: (c) ER-E_2 complex and (d) ER-RAL complex. 3. Hydrogen bond interactions between (e) an E_2 molecule and (f) a RAL molecule in ERα LBD, hydrogen bonds are indicated by dashed lines and a highly ordered water molecule stabilized by a hydrogen bond network is indicated (red dot).

Although there are arguments that the ER dimerization is ligand-dependent,[104,105] new evidences has been found that ER can form a stabile dimer in vitro even without a ligand binding. Recently, Tamrazi et al. studied the in vitro thermodynamic and kinetic stability of dimeric ERα LBD with fluorescence resonance energy transfer (FRET) – based methods.[106] In this study, they found the dissociation constant K_d of the ERα LBD dimer was less than 0.1 nM under native conditions. Under a denaturant (2M urea) condition the ligand-unbound (apo) ERα LBD dimer had a K_d value of 1.0 nM, while the ligand-bound ERα LBD dimer in the presence of 1 μM E_2 or OHT even exhibited lower K_d values: 0.33 nM and 0.27 nM, respectively. In a following kinetic experiment (Scheme 9), the rate of a FRET signal development was governed not only by the dissociation rate of donor-donor and acceptor-acceptor homodimer into monomers but also by the re-association rate from monomers to donor-acceptor heterodimers. Remarkably, it was found that

dimer dissociation was the rate-determining step of this kinetic process, rather than the re-association of monomers. Similar to the above thermodynamic results, the rate of monomer exchange for apo ERα LBD was faster (a half-life time of 39±3 min at 28°C) than that for ligand-bound ERα LBD dimer in the presence of 1 μM E_2 or OHT by a factor of 3.8 or 6, respectively. Moreover, it was concluded, based on a series of ER-ligand comparisons, that a bound ligand could greatly enhance the stability of ERα LBD dimer and that this enhancement depended on the chemical structure and biologic activity of a ligand, rather than its ER-binding affinity.

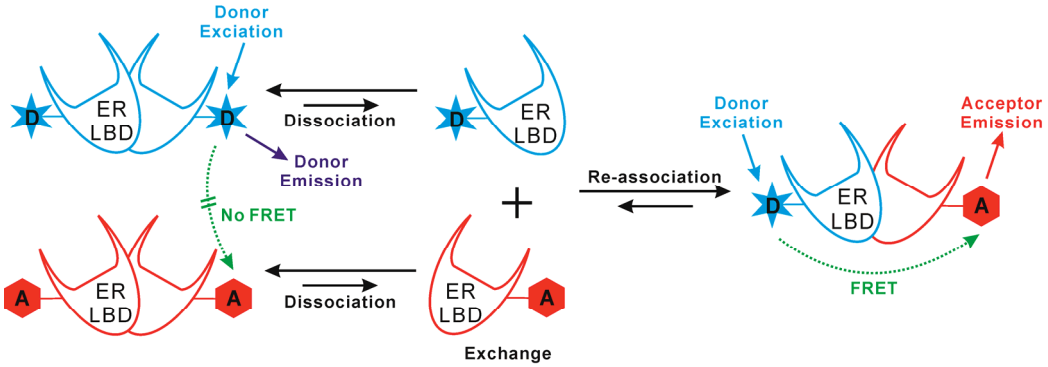

Scheme 9. Schematic presentation for the kinetics of an ER LBD monomer exchange: D denotes donor (fluorescein)-labeled ER LBD, A denotes acceptor (tetramethylrhodamine)-labeled ER LBD.[106]

1.2.4. Biological evaluation assay for the estrogen ligand

To evaluate the biological activities of the estrogen ligand, different in vitro protein- and cell-based assays have been established to determinate either the binding affinity to ER or the biological effect whether it is an agonist or antagonist after the uptake of ligand into an ER gene-cell.

1.2.4.1. Protein-based binding affinity assay

1.2.4.1.1. Competitive radiometric assay with [^{3}H]-E_2

In a competitive radiometric assay,[107-109] a constant amount of [^{3}H]-E_2 (2 nM, Figure 7, left) as tracer and increasing amounts of the competitor ligand are prepared and incubated with purified full-length human ER for 18-24 hours at 0°C. The formed ER-ligand complexes were then

absorbed onto hydroxyapatite and free unbound ligand was washed away. A liquid scintillation counting setup determinated the radioactivity (decays per minute, dpms) and the values were plotted against the concentration of the competitor ligand. Generally, sigmoidal dose response curves were observed and fitted by using GraphPad Prism software. The relative binding affinity (RBA) value of E_2 was normalized to 100%, whereby a binding curve that had shifted to the left indicated a ligand (**X** in Figure 7 right) that was bound to ER with a higher affinity than E_2. Conversely, a right-shifted curve represented a lower affinity (**Y** in Figure 7 right). From these dose response curves, the half maximal inhibitory concentration (IC_{50}) of the individual estrogen ligand can be calculated and converted to the RBA value via Equation 17.

$$\text{RBA (\%)} = \frac{IC_{50}(E_2)}{IC_{50}(Competitor)} \cdot 100\% \qquad (17)$$

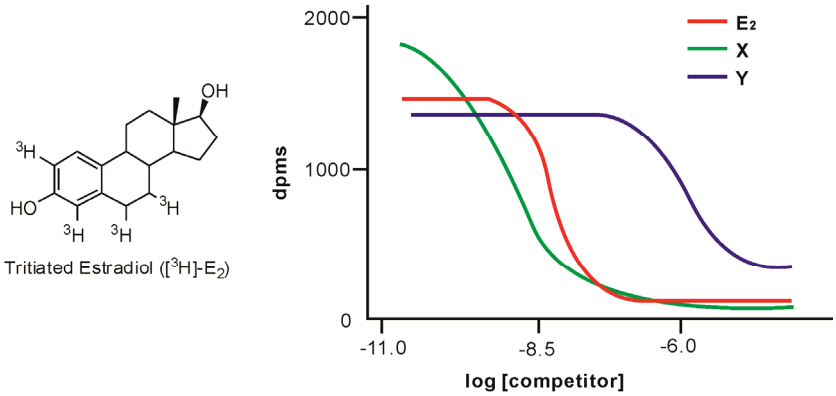

Figure 7. Left: The chemical structure of tritiated-estradiol ([^{3}H]-E_2). Right: representative plot of the relative binding affinity (RBA) value for E_2, a stronger ER-binding ligand X, and a weaker ER-binding ligand Y (dpms: decays per minute).

1.2.4.1.2. Enzyme fragment complementation binding affinity assay

Since the competitive radiometric assay mentioned above has several disadvantages such as radioactivity, non homogenous, and a filtration step, DiscoveRx offers a homogenous high-throughput cAMP assay kit called HitHunter^{TM} based on a patented enzyme (β-galactosidase) complementation technology using either chemiluminescent or fluorescent substrates.[110-113] Similar to the competitive radiometric assay, a constant amount of a genetically engineered inactive fragment, enzyme donor (ED) of *E. coli* β-galactosidase, is applied as tracer to compete with increasing amounts of an evaluated estrogen ligand. After 90 minutes incubation with the ER

at room temperature, another inactive fragment, enzyme acceptor (EA), which can spontaneously recombine with the unbound ED to form an active tetrameric β-galactosidase, was added. The amount of the formed tetramer can be measured by hydrolysis of chromogenic, chemiluminescent or fluorogenic substrates and is proportional to the amount of ER bound by the estrogen ligand. A sigmoidal dose response curve (the quantity of the chemiluminescence or fluorescence against the concentration of the estrogen ligand) and the IC_{50} value were then obtained so that the RBA value of the individual ligand could be converted by Equation 17.

1.2.4.2. Cell-based assay

Compared to the above-mentioned binding affinity assays, cell-based assays are more complicated because they are conducted in a living tissue cell like estrogen receptor positive breast cancer cell (MCF-7). Many factors need to be accounted for, such as membrane penetration, cytotoxicity, metabolism, and nonspecific binding to other cellular components.[109,114]

In order to monitor gene transcription activity in the cell, reporter gene assays such as luciferase assay in MCF-7-2a cells have been established. These cells have been stably transfected with a reporter plasmid ERE_{wtc}luc. Once a dimeric ER-ligand complex is formed and interacts with the ERE of plasmid, the luciferase gene is activated and light is produced by the oxidation of a luciferin. A quantification of the luciferase expression can evaluate the agonistic or antagonistic potency of a estrogen ligand.[115,116]

1.3. Previously reported bivalent estrogen receptor ligands

Since the homodimer of two ER LBD subunits are essential for the binding of ER to DNA, it is very necessary to develop a novel bivalent estrogen ligand targeting the homodimer of the ER LBD. Once such a bivalent ligand bridges between two ER LBDs, increasing ligand binding affinity, enhanced dimer stabilization, and unusual bioactivity are anticipated.[117] Moreover, it has been demonstrated that this homodimer of the ER LBD has a high in vitro stability through thermodynamic and kinetic experiments, in particular in the presence of the estrogen ligand.[106] Additionally, the crystal structures of dimeric ER-ligand complexes have confirmed that two ER LBD subunits bind to each other in a head-to-head mode and possess a C_2-symmetry, which

facilitate the design and preparation of a bivalent ligand with the same symmetry. During the last two decades several groups have independently prepared different bivalent estrogen ligands and evaluated their ER-binding affinities in vitro.[117-121]

In 1994 Bergmann et al. first investigated the effects of bivalent ligands on ER by tethering two hexestrol molecules (HEX, a non-steroidal ER agonist) with varying lengths of carbon-carbon or PEG spacers.[117] The highest binding affinity was 6.92% of E_2 and achieved by tethering two HEX molecules with 8 carbon atoms ($(CH_2)_8$, C8) spacer (maximum length approximately 8.8 Å, Figure 8a). However, it is still weaker than that of monovalent counterparts. Remarkably, a unique biphasic interaction of this C8-tethered bivalent ligand to ER was observed. This suggested that a possible structure-specific negative site-site interaction occurs during the ER-ligand interaction. Three years later, Osella et al. prepared a bivalent estrogen ligand by tethering two E_2 molecules with an iron carbonyl system (Figure 8b).[118] Unfortunately, only poor results were obtained in ER-binding assays.

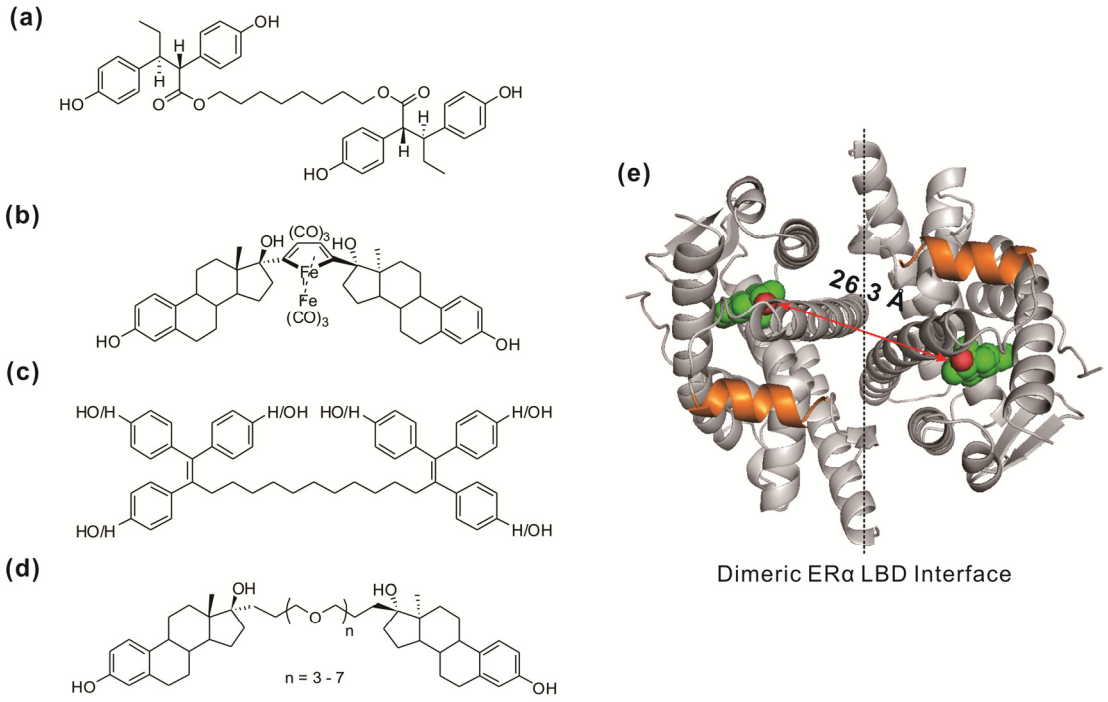

Figure 8. Some previously reported bivalent estrogen ligands prepared by: (a) Bergman et al.,[117] (b) Osella et al.,[118] (c) Groleau et al.,[119] (d) Berube and co-workers,[120,121] and (e) the distance between two E_2 molecules at the 17 position (spheres) in the ERα LBD homodimer (ribbons in gray, H12 in orange, PDB ID code 1ERE) is 26.3 Å and viewed down the dimer axis.

These two above studies were published before the breakthrough of the dimeric ER LBD

crystal structure reported by Brzozowski et al. in 1997.[103] Thus, the low ER-binding affinities of these bivalent ligands are mostly due to the insufficient length of spacers which did not allow two estrogen moieties to bridge the space separation between the ER LBD dimer. According to the distance measurement of the ER LBD dimer (PDB ID code 1ERE) by using the modeling software PyMOL, the closest distance between two E_2 molecules is 26.3 Å at the 17-position of the steroidal structure (Figure 8e). This estimation explains why the bivalent tamoxifen (TAM) ligands tethered with a $(CH_2)_{11}$ spacer (maximum length ca. 12.4 Å, Figure 8c) prepared by Groleau et al. only possessed less activity than the monovalent TAM.[119]

In the last decade, Berube and co-workers prepared several bivalent E_2 ligands of varying PEG spacer lengths and evaluated their ER binding affinities and cytocidal activities on breast and skin cancer cell lines in vitro.[120,121] Although their spacer lengths (e.g., n = 7, maximum length 31.2 Å, Figure 8d) were sufficient enough to bridge the space separation between two ER LBDs, these bivalent ligands still gave low binding affinities for ERα and no affinity for ERβ. The authors concluded that the introduction of the PEG spacer at 17α position of E_2 greatly reduced the ability of the estrogenic potion to bind to the ER. However, they did not mention whether they used the ER crystal structure to rationally design their bivalent ligands and why they tethered two E_2 molecules at the 17α position. On the basis of published agonistic ER LBD crystal structures, e.g., PDB ID code 1ERE, the repositioning of H12 of the ER-ligand binding resulted in a full encapsulation of the E_2 molecule within a three-layer helical "sandwich" folding ER LBD (denoted as "mouse-trap" model, Figure 9a). In other words, it seems that no obvious entrance or exit routes exists for the spacer tethered at 17α position of E_2.[103] This could be used to explain why these bivalent ligands have low binding affinities.

Recently, Nettels et al. demonstrated the flexibility and plasticity of the ER LBD in X-ray studies.[122] A large substituent such as a phenyl vinyl group at the 17α-position of an E_2 molecule can lead to a unusual distortion of ERα LBD conformation and an overall binding affinity enhancement. In the crystal structure of this dimeric ER-ligand complex (PDB ID code 2P15, Figure 9b), two short helices of the ER LBD, helices 7 and 8 (H7 and H8), unwind to generate a large pocket to accommodate this bulky substituent group and thus to provide an additional access to the exterior of the protein. This finding indicated that not only H12 but also other helical and loop elements of the hydrophobic ER LBP adopted different conformations with different ER

ligand-binding modes. More recently, Li et al. studied a crystal structure of ERα LBD bound with a novel E_2-derived metal complex, estradiol-pyridine tetra acetate europium (III), and demonstrated that the Eu-tagged side chain at 17α position of E_2 molecule pointed to an open space toward H8 (Figure 9c).[123]

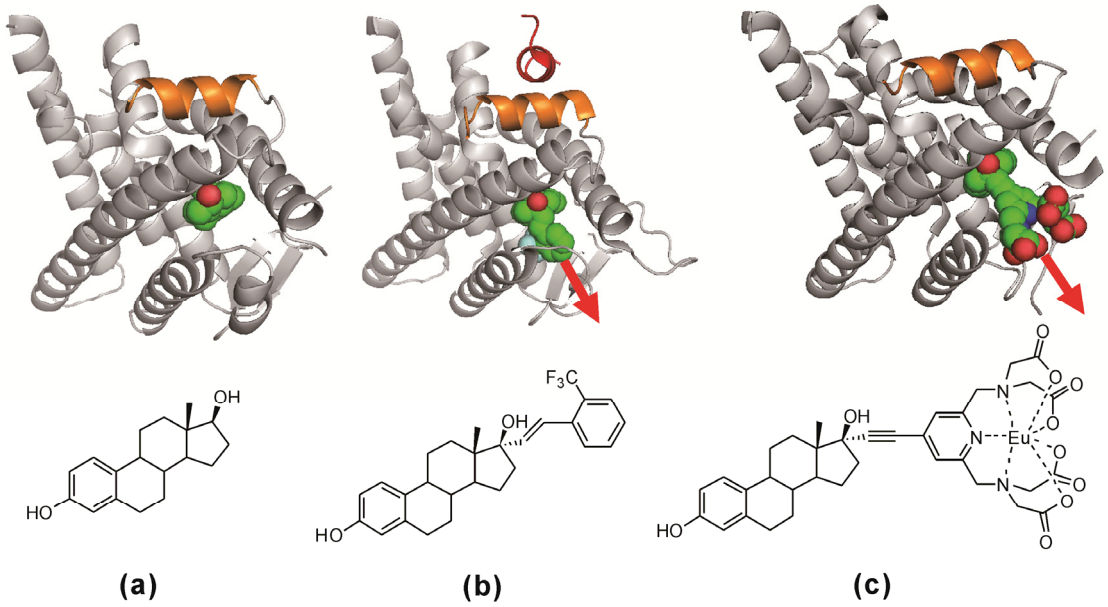

Figure 9. Three conformations of ER LBD adopted by individual ER-ligand binding: (a) E_2 (PDB ID code 1ERE), (b) 17α-o-trifluoromethyl phenyl vinyl E_2 (PDB ID code 2P15), and (c) 17α-Pyridine tetra acetate europium (III) E_2 (PDB ID code 2YAT). ER LBD is presented as ribbons in gray, H12 as a ribbon in orange, CoA peptide as a ribbon in red, bound ligands as spheres and the orientation pointed by a large substituent at 17α position is indicated as a red arrow.

Based on this finding, LaFrate et al. prepared two series of bivalent steroidal ligands by tethering two ethynylestradiol (EE_2) molecules at 17α position either with oligopropylene glycol (OPG) or oligobutylene glycol (OBG) spacer of varying lengths (24.2-45.3 Å, Figure 10 left) which were sufficiently long enough to bridge the space separation between two ER LBDs.[124] In this study, the ERα binding affinity reached a maximum binding affinity (RBA = 6.9%) in the case of the bivalent steroidal ligand tethered by 34-35 Å spacers (Figure 10 right) for ERα. This spacer length was considerably longer than the closest distance (26.3 Å) between two E_2 molecules at 17α position (Figure 8e) which was attributed to the fact that a realistic spacer had to adopt a different conformation from the all-extended distance estimated in the ER crystal structure (Figure 8).

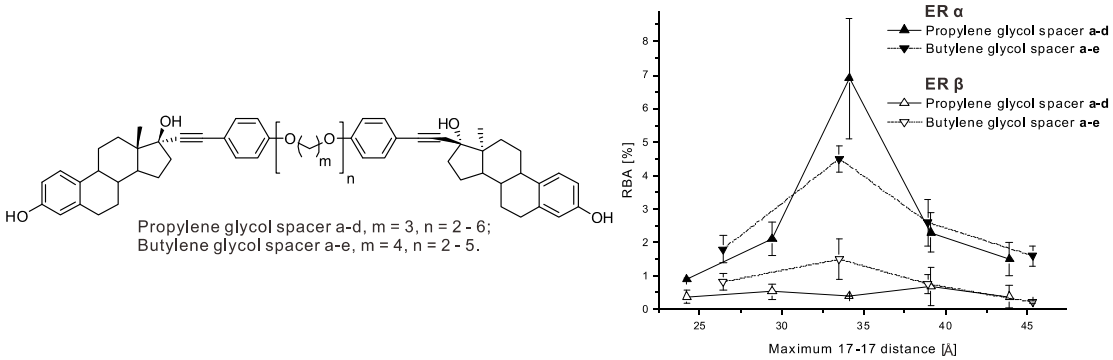

Figure 10. Left: Bivalent steroidal ligands prepared by LaFrate et al.; Right: a plot of relative binding affinity (RBA) against the maximum spacer length between the 17-position of ethynylestradiol for oligopropylene glycol (OPG) and oligobutylene glycol (OBG) ether-tethering bivalent steroidal ligands.[124]

More recently, two additional studies of bivalent ligands in the field of ER were independently investigated by Wendlandt et al. and Scutaru et al. (Figure 11).[125,126] Although the authors did not report the ER-ligand binding affinities, these compounds showed relatively high intracellular activities in the MCF-7 cell line.

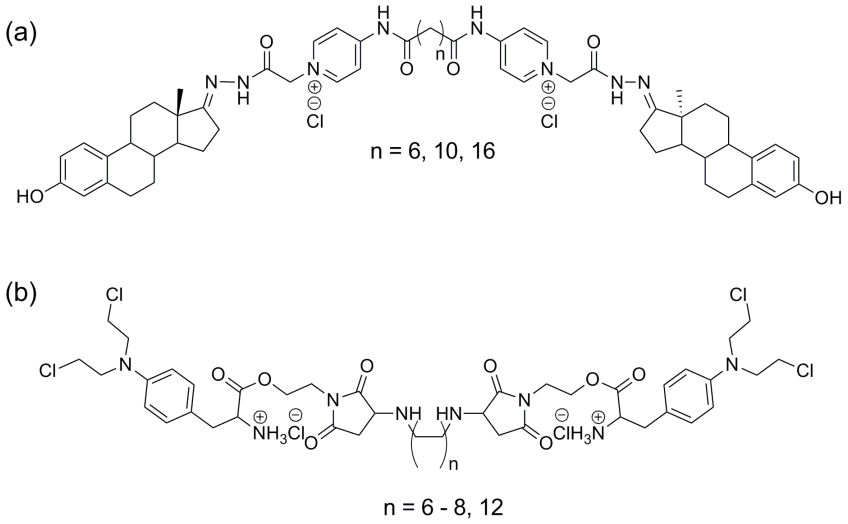

Figure 11. Bivalent ligands investigated by (a) Wendlandt et al.[125] and (b) Scutaru et al..[126]

Interestingly, besides these bivalent estrogen ligands, two multivalent estrogen-polymer conjugates have been investigated as well for their ER binding potency in vitro. Compared to these bivalent estrogen ligands, the ER transcription of multivalent estrogen-polymer conjugates constructed on a linear poly(methacrylic acid) polymer or linear, sequence-specific peptoid oligomers depends on their structure and valence.[127,128]

All the bi- and multivalent estrogen ligands mentioned above were proposed for binding to

the intracellular ER and to activate their estrogen action via a genomic pathway. Recently, E_2 has been reported to induce a rapid nongenomic actions of ER such as an activation of membrane-initiated kinase cascades which involved in the membrane localized GPR30.[129-134] In order to develop a selective estrogen ligand for the non-genomic pathway and keep this estrogen ligand outside the nucleus, Harrington et al. prepared estrogen-dendrimer conjugates (EDCs) based on a large, 6th-generation PAMAM dendrimer (Figure 12). The authors found that these EDC ligands were able to activate non-genomic activity and at the same time had an ineffectively nuclear gene expression (approximately 10,000-fold more ineffective than E_2 in genomic actions).[135] The authors also speculated that the multivalency of such an EDC ligand could contribute to its high potency in stimulating non-genomic signaling due to its avidity for clusters of membrane-associated ERs. In a further study, Kim et al. compared the ER binding access of EDC ligands connected by tethers of varying lengths (Figure 12) via NOESY, dynamic light scattering (DLS), and in vitro ER-binding assays. Most notably, the NOESY experiments in deuterium water showed that the tethered hydrophobic E_2 molecules were enwrapped by the long oilgoethylene glycol tether and buried in the PAMAM dendrimer. Consequently, the long-tethered EDC had a smaller radius in aqueous solvent than in organic solvent, so that its access to the ER was engendered due to the ligand shielding by the long and hydrophobic tethers.[136]

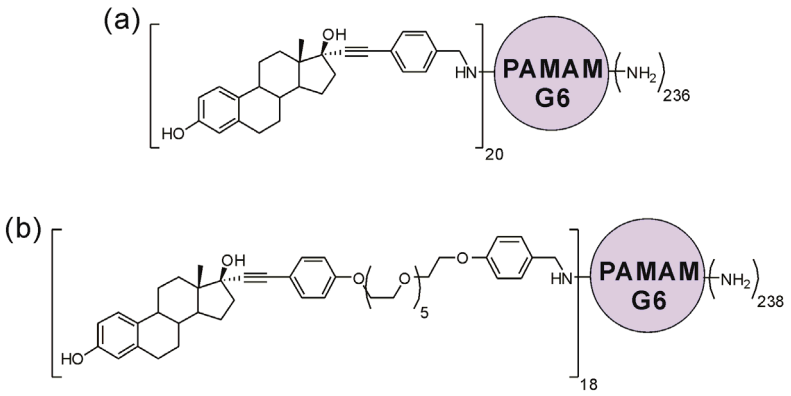

Figure 12. Chemical structures of (a) a short tethered estrogen dendrimer conjugate (EDC) and (b) a long tethered EDC.[129,130]

As mentioned above, multivalent strategy has been applied in the in vitro ER-binding studies to improve the bivalent ER-ligand interaction. However, there are several open questions, such as why the bivalent effect was low for bivalent estrogen ligands and how to prepare a high-affinity

bivalent ER ligand for both ER subtypes. To address these fundamental questions, the idea of designing, synthesizing, and evaluating of novel bivalent ER ligands will be discussed in this thesis.

2. Scientific goals

The goal of this thesis is to rationally design, chemically prepare, and biologically evaluate bivalent estrogen ligands tethered by flexible spacers so that a structure-activity relationship (SAR) for estrogen receptor (ER) and bivalent estrogen ligand could be established.

In many studies mentioned in Section 1.1, the multivalency has been successfully utilized to enhance the interactions between proteins with multiple binding sites and multivalent ligands. This concept has been further applied in the case of ER, since the ER-ligand binding and their subsequent dimeric complex play an essential role in the treatment of breast cancer (Section 1.2). Bivalency, the basic multivalent form, has been expected not only to enhance the binding affinities between the ER and the ER ligand but also manipulate the ER gene expression (Section 1.3).

In this thesis, different monovalent estrogen ligands should be chosen as the target molecules, such as *trans*-diethylstilbestrol (DES), raloxifene (RAL), and *cis*-4-OH tamoxifen (OHT), which not only have different ER-binding affinity but also various biological features caused by individual ER-binding modes. Firstly, for the rational ligand design, the crystal structure of ER ligand-binding domain (LBD) complex with individual monovalent ligand shall be modeled to obtain structural information about the dimeric receptor such as the distance between two binding sites and the binding mode. Secondly, a modular chemical preparation of selected bivalent estrogen ligands shall be carried out, which then would be evaluated in vitro to determinate their ER-binding affinities in the third step (Figure 13).

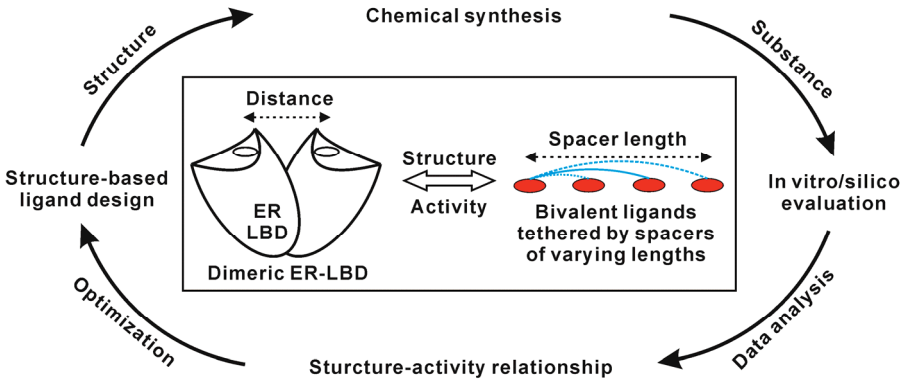

Figure 13. The progress of the design, synthesis, and evaluation of bivalent estrogen ligands tethered by flexible spacers of varying lengths to establish their structure-activity relationship to the dimeric estrogen receptor ligand binding domain (ER LBD).

Moreover, these bivalent ligands shall also be investigated by 2D NMR spectroscopy, the computer modeling, and the computer simulation to further explain their biological activities and establish the SAR. An optimization based on this new understanding of the SAR will be valuable for the design of a new generation of bivalent estrogen ligands that will make further progress towards high-affinity bivalent estrogen ligands (Figure 13).

Additionally, since the chemical preparation of bivalent estrogen ligands is the crucial step in this work, individually prepared bi-functionalized flexible spacers and monovalent ligand precursors were convergently brought together to obtain the bivalent ligands.

This thesis has the following objectives:

(1) To develop a structure-based bivalent estrogen ligand design by using the crystal structure of the receptor-ligand complex.

(2) To prepare a series of bi-functionalized flexible spacers with different linkage groups and varying lengths via a modular synthetic route.

(3) To prepare several different bivalent estrogen ligands according to their individual ER-binding modes.

(4) By using different analytic methods such as in vitro ER competition binding assays, spectroscopic methods (NMR and UV), and computer modeling to evaluate the ER-binding abilities of bivalent estrogen ligands, explain their ER-binding mechanisms, and establish their SAR.

3. Results and discussion

3.1. Bi-functionalized oligoethylene glycols as spacers

3.1.1. Synthetic route of oligoethylene glycol

Since a bivalent ligand is composed of two binding moieties and a spacer, a bi-functionalized spacer is essential for the whole chemical preparation. For our purpose, bi-functionalized oligoethylene glycols (OEGs) was chosen to tether two estrogen moieties due to its peculiar biological, chemical, and physical properties such as non-toxicity, biocompatibility (non-immunogenic, non-antigenic), and strong hydrophilicity (good solubility in an aqueous environment).[137] In addition, it has been reported that OEGs are resistant to nonspecific adsorption of proteins.[18] Therefore, there is no undesired interaction between the spacer and the protein surface except for the desirable interactions between the tethered binding moieties of bivalent ligand and the protein.

Although OEGs can be commercially obtained in a variety of molecular weights, only a limited number of exact-length (defined unit) OEGs are available with high purity (maximum length of six EG units, approximately 22.0 Å). Furthermore, the monodisperse OEGs with defined units cannot be synthesized by an anionic ring-opening polymerization of ethylene oxide (Scheme 10a), which is generally applied to prepare polyethylene glycols (PEGs).[138] Therefore, an alternative method is to use protective and leaving groups such as benzyl and tosyl, respectively, and combinations of linear OEG segments in an AB or ABA pattern via a nucleophilic substitution, where A represents a mono-protective OEG segment and B corresponds to a OEG segment with one or two leaving groups (Scheme 10b and c).[139-143] After the nucleophilic substitution, the protective group can be readily removed under a mild condition to obtain OEGs with two hydroxyl groups at both ends. To further tether two estrogen binding moieties, the terminal hydroxyl group need be converted into active groups like primary, secondary amine, or alkynyl.

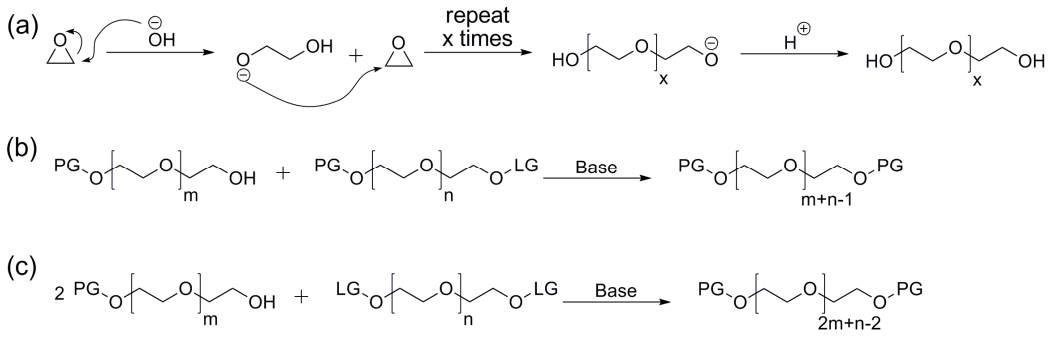

Scheme 10. (a) Anionic ring-opening polymerization of ethylene oxide initiated by hydroxide. Combinations of linear oligoethylene glycol (OEG) segments in (b) an AB or (c) an ABA pattern. PG denotes protective group and LG denotes leaving group.

3.1.2. Chemical preparation of bi-functionalized oligoethylene glycol

Following the synthetic route introduced above, the chemical preparation of bi-functionalized OEG was started with the synthesis of the ditosylates **1** by mixing the OEG of fewer repeating units with aqueous potassium hydroxide and tosyl chloride in THF (Scheme 11). Meanwhile, the monobenzylates **2** were synthesized by an addition of benzyl chloride into a mixture of OEG diol and sodium hydroxide via Williamson's ether synthesis. In order to simplify the purification and obtain good yields for this intermediate, the benzyl group was chosen as the protection group rather than the triyl ether,[144] and a large excess of OEG diol (five equivalents) was applied due to the following advantages: (1) The deprotection of benzyl group can be easily carried out under a mild hydrogenation condition with a quantitative yield. (2) The purification of monobenzylates **2** requires water extraction to wash away the large excess of OEG diol and a Kugelrohr distillation for removing the byproducts such as disubstituted product. Afterwards, by using the same procedure as for **1**, a monoprotective tosylate **3** was also prepared.

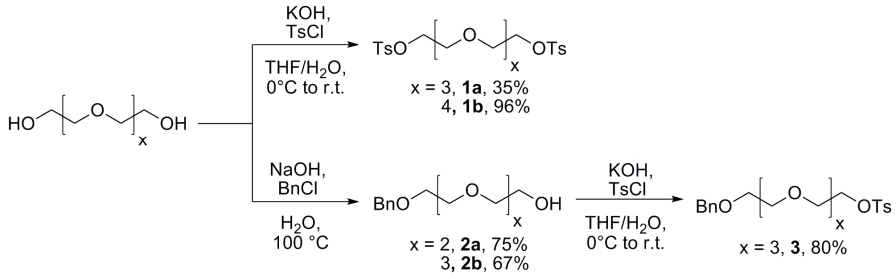

Scheme 11. Chemical preparation of the precursor OEG: ditosylates **1**, monobenzylates **2**, and monotosylate **3**.

To prepare dibenzylates **4**, the AB pattern was performed for the dibenzylates **4a-d** of short OEGs (y = 6-9, Scheme 12) by treating the appropriate glycol **2** with sodium hydride and monoprotective tosylate **3**, while the ABA pattern was carried out for the dibenzylates **4e-g** of long OEGs (y = 10-13). Afterwards, the benzyl group of **4** was removed by the palladium catalyzed hydrogenation in ethanol to give diol **5** without any further purification.

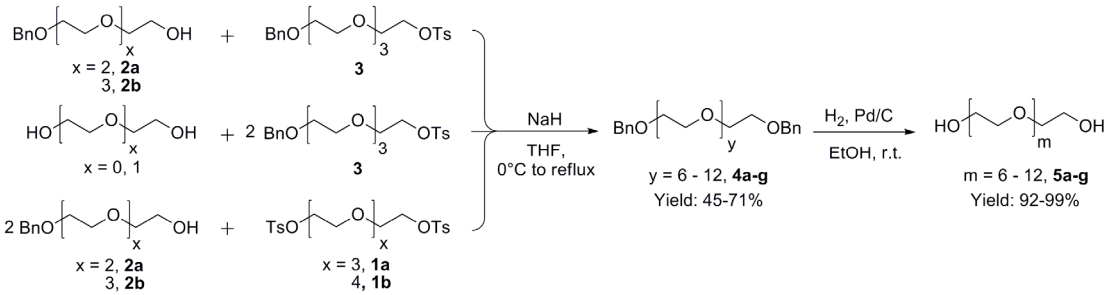

Scheme 12. Chemical preparation of dibenzylates **4** via an AB or ABA pattern and diol **5**.

Interestingly, predictions about the conformations of the OEG spacers can be made by considering the orbital interactions. It is known that an σ-σ* orbital interaction (π type) between a filled $\sigma_{C\text{-}H}$ bonding and an empty $\sigma^*_{C\text{-}O}$ antibonding occurs best if they are in the anti orientation (Figure 14a), so that a HOMO-LUMO delocalization of the filled C-H electron is possible (Figure 14b). Hence, the ethylene glycol adopts the gauche conformation in which each $\sigma_{C\text{-}O}$ bonding is anti to a $\sigma_{C\text{-}H}$ bonding (Figure 14c).[145-147]

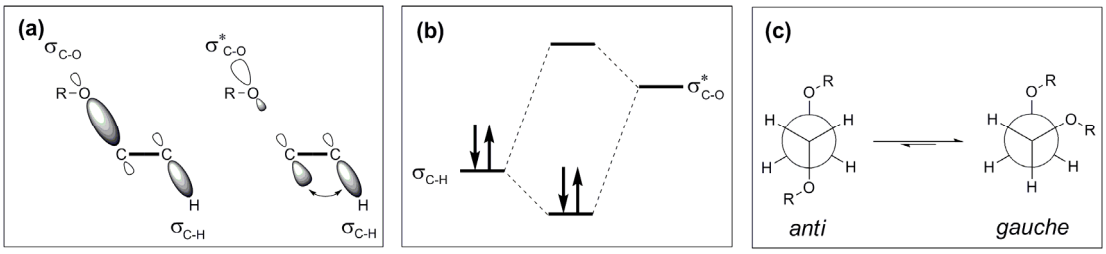

Figure 14. (a) Left: $\sigma_{C\text{-}O}$ bonding and σ C-H bonding; Right: $\sigma^*_{C\text{-}O}$ bonding and $\sigma_{C\text{-}H}$ bonding. (b) A HOMO-LUMO delocalization between a $\sigma_{C\text{-}H}$ bonding and an $\sigma^*_{C\text{-}O}$ antibonding. (c) The ethylene glycol prefers to adopt the gauche conformation than the anti conformation.

Consequently, such a gauche conformation has a shorter end to end distance than a staggered conformation. Moreover, each OEG repeating unit involves two to three water molecules in aqueous solvent due to the hydrogen bond interaction.[148] On the basis of these two factors, the

OEG prefers to form a helical or even a random coil conformation, rather than a linearly extended conformation (Figure 15).[29,149-152]

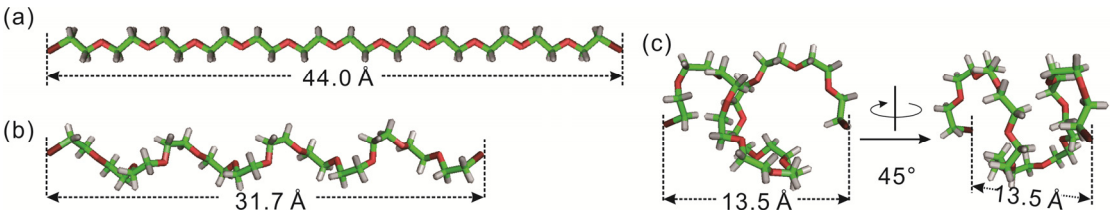

Figure 15. The distance measured by the modeling software PyMOL between two ends of a dibromide OEG spacer with 11 EG units (stick) in (a) a staggered linear conformation, (b) a helical conformation, and (c) a snapshot of a random coil conformation from an over 100 ns simulation time in water.[29]

As mentioned in Section 1.1.1, a spacer containing a rigid segment can be expected to minimize the loss in conformational entropy for a tighter binding.[19] For this purpose, either a hydrophobic carbon-carbon chain ($(CH_2)_4$ and $(CH_2)_8$, Scheme 13a) or a hydrophobic, rigid biphenyl group were introduced into the OEG structure. In the later case, a trityl ether protective group and acid-catalytic deprotection were used for the corresponding preparation (Scheme 13b).[144]

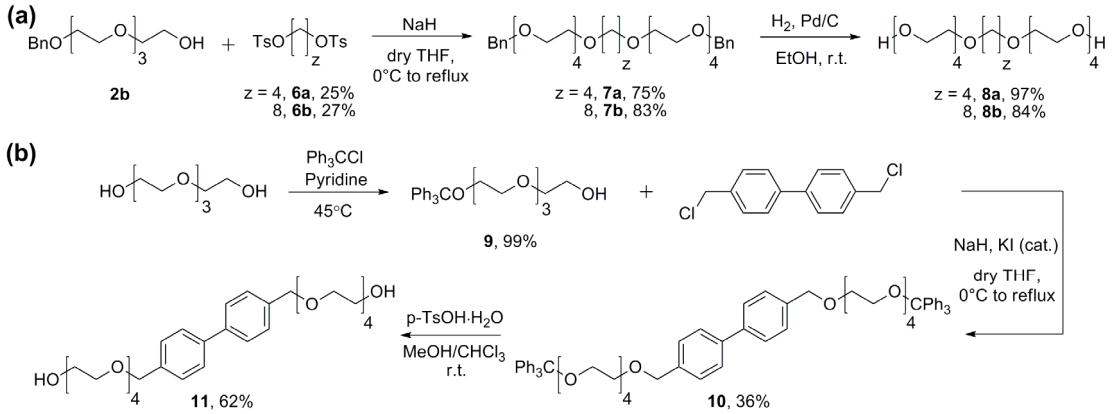

Scheme 13. Chemical preparation of (a) carbon-hybride OEG diol **8**, and (b) biphenyl-hybride OEG diol **11**.

3.1.3. Chemical modification of bi-functionalized oligoethylene glycol

In order to tether two bivalent estrogen moieties via different types of linkage groups, the hydroxyl group of OEG derivates (**5**, **8**, and **11**) should be converted into the following active terminal functionalized group.

3.1.3.1. Primary amine

As showed in Scheme 14, primary amine OEG **18**, **19**, and **20** can be straightforward obtained via a Staudinger reduction of the OEG azide **15**, **16**, and **17** with triphenylphosphine followed by hydrolysis.[153] An alterative method using a palladium catalyzed hydrogenation under neutral pH-condition was corroborated to be a failure, and a secondary amine was observed as a main product.[154,155] These corresponding OEG diamine spacers (**18**, **19**, and **20**) were applied to tether two *trans*-diethylstilbestrol (DES) ligands via a amide linkage group in the next step (Section 3.2.2).

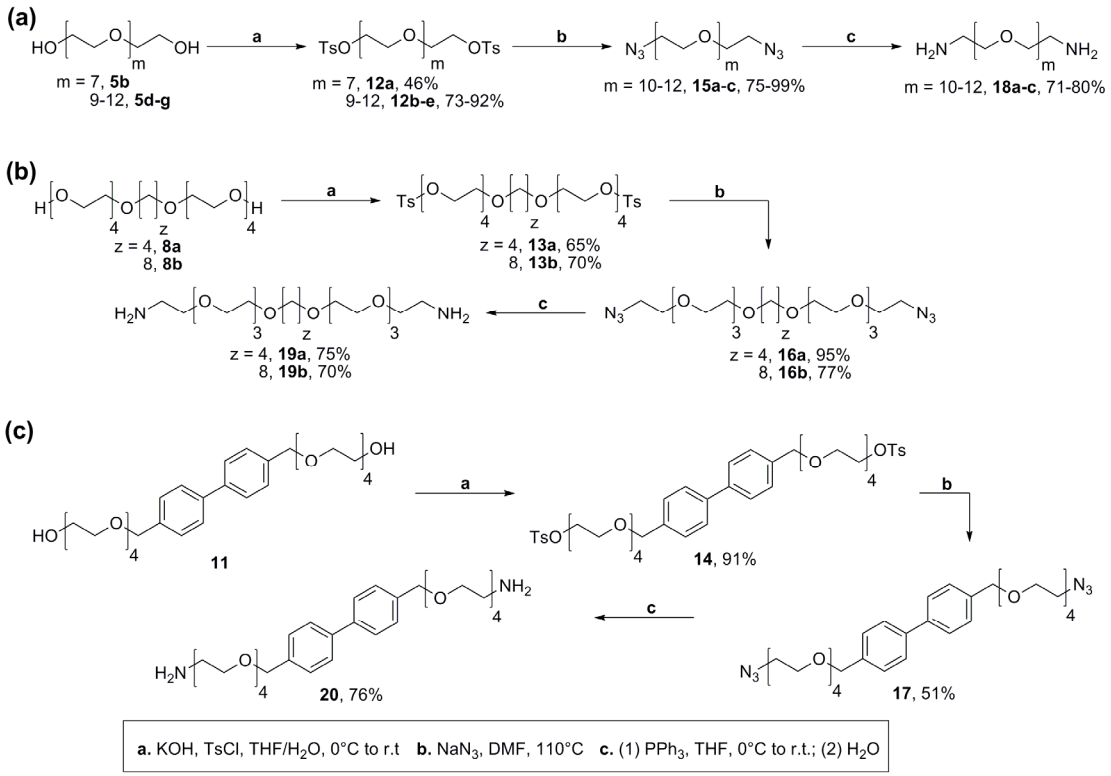

Scheme 14. Chemical preparations of (a) OEG diamine **18a-c**, (b) carbon-hybride OEG diamine **19a-b**, and (c) biphenyl-hybride OEG diamine **20**.

3.1.3.2. Alkynyl OEGs

The second type of active terminal group is alkynyl. These OEGs **21** can be readily obtained via a nucleophilic substitution of propargyl bromide with different OEGs (Scheme 15) and further applied to tether two raloxifene (RAL) ligands via a 1,3-dipolar cycloaddition (Section 3.3.2).[156-158]

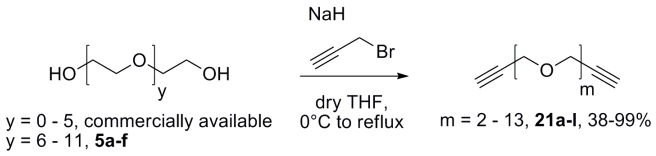

Scheme 15. Chemical preparations of dialkynyl OEG **21a-l**.

3.1.3.3. Bis(*N*-methylamine) OEG spacers

Secondary bis(*N*-methylamine) OEG derivates are difficult to synthesize and be purified due to over alkylation of primary amine in a nucleophilic substitution with the alkyl halide (Scheme 16a).[159] The most widely used procedure for the preparation of secondary amines is the reductive amination,[160-162] which requires aldehyde functionalized OEG precursors to form an imine intermediate with methyl amine. This intermediate can be simultaneously reduced in presence of a selective reduction agent like sodium cyanoborohydride (Scheme 16b). We first attempted this strategy but encountered difficulties in either oxidation of OEG diol or ozonolysis of diallyl OEG, which may have been due to a rapid hemiacetal formation.[163]

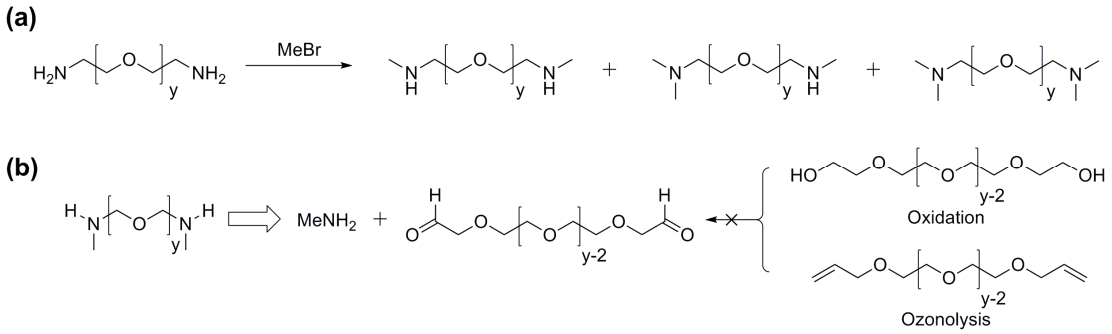

Scheme 16. (a) A over alkylation of primary amine with alkyl halide. (b) A reductive amination strategy based on a primary amine and a dialdehyde.

Alternatively, there are several other procedures for preparing a secondary amine,[164] such as the Eschweiler-Clark[165,166] and aza-Wittig reaction.[167-170] In order to circumvent the formation of the tertiary amine, a phosphonium diaza-diylides have been used as reagent to prepare primary or secondary amines.[171] Similarly, an iminophosphorane originating from the treatment of a azide with triphenylphosphine according to Staudinger reduction procedure has been reported to be alkylated in-situ by alkyl, allyl, or benzyl halides to afford the corresponding disubstituted aminophosphonium salt (Scheme 17), which can be eventually hydrolytically converted into a secondary amine with one equivalent of methanolic potassium hydroxide (KOH).[172]

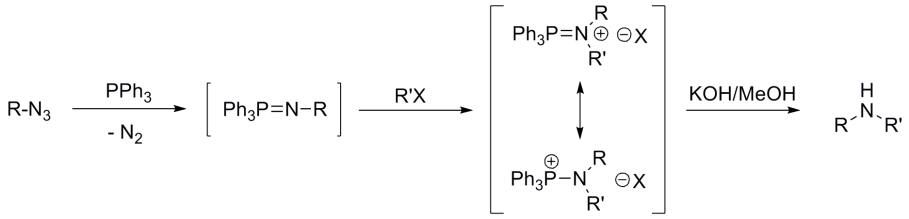

Scheme 17. The synthetic route of a secondary amine via an alkylation to an iminophosphorane intermediate followed by hydrolytic cleavage with methanolic potassium hydroxide (KOH).

According to this procedure, 2.2 equivalents of triphenylphosphine were added to a solution of diazide OEG **13a**[124] in anhydrous THF and stirred until TLC and ESI-TOF analysis indicated complete consumption of the azide. Subsequently, 2.1 equivalents of methyl iodide were added to this iminophosphorane intermediate, whereby a white precipitate (disubstituted amino-phosphonium salt) appeared. After 24 hours, ESI-TOF analysis showed the complete consumption of this intermediate, and the solvent including the excess of methyl iodide was removed under vacuum. Afterwards, two equivalents KOH (1% in methanol) were added to hydrolyze aminophosphonium salt to form the *N*-methyl diamine OEG **22a** (Scheme 18a).

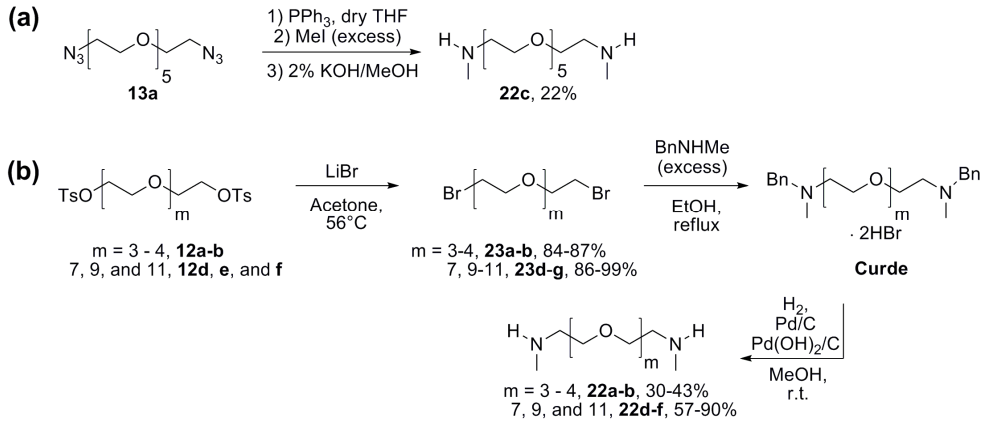

Scheme 18. (a) The synthetic route of a secondary amine via an alkylation to an iminophosphorane intermediate. (b) A novel synthetic route of a secondary amine via a nucleophilic substitution and a hydrogenation.

In order to remove the phosphine oxide, purification with column chromatography is required, which is one of drawbacks of the Staudinger reduction, especially for the hydrophilic OEGs, and results in a low yield (< 30%). Furthermore, this strategy was also applied for the other long OEGs derivates (m ≥ 7) but a problem of the incomplete formation of iminophosphorane was encountered. To overcome this synthetic problem, dibromide OEG **23** was first prepared based on

ditosylated OEG **12** (Scheme 18b). Afterwards, a nucleophilic substitution between a excess of *N*-benzyl methyl amine and dibromide **23** gave a benzyl protective tertiary amine which can be directly quantitatively converted into the desired *N*-methyl diamine OEG salt **22** under a palladium catalyzed hydrogenation (15 bar).[173] Before an imine condensation between this bis(*N*-methylamine) OEG and an aldehyde (Section 3.4.2), the secondary amine salts were neutralized with triethylamine by flash chromatography to obtain the secondary amine **22** with satisfactory yields.

In addition to the bi-functionalized OEG spacers mentioned above, similar strategies were applied for the preparations of several mono-functionalized OEG derivates, which formed different monovalent estrogen ligands tethered with a side-chain as a monovalent control (Scheme 19).

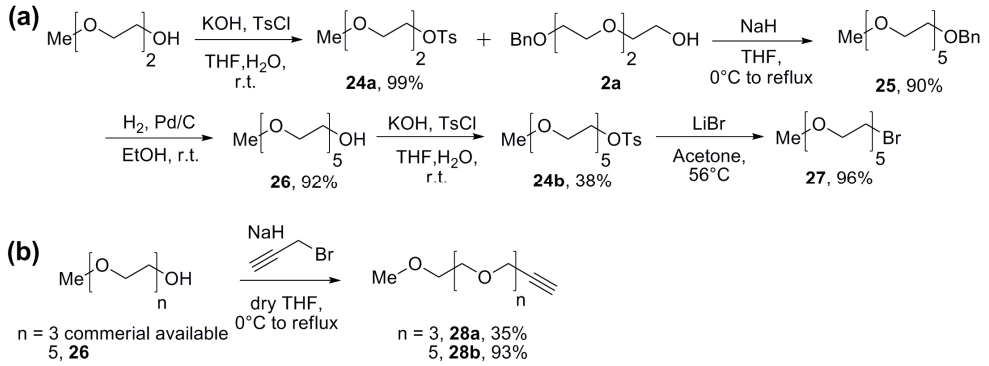

Scheme 19. Chemical preparation of mono-functionalized OEG derivates **27** (a) and **28** (b).

3.2. Bivalent *trans*-diethylstilbestrol ligand

3.2.1. Ligand design

As mentioned in Section 1.2, *trans*-diethylstilbestrol (DES) is an estrogen receptor (ER) agonist which binds deeply in the ER ligand-binding pocket (LBP) followed by repositioning the C-terminal helix 12 (H12). Consequently, the whole DES molecule is fully buried in the ER ligand-binding domain (LBD, Figure 16a-c). In order to find out the best linkage position and optimal spacer, the crystal structure of the ERα LBD bound with two *trans*-DES molecules (PDB ID code 3ERD)[96] was modeled by using the computer modeling software PyMOL. It was found that the closest distance (a straight line) between carbon 1 positions of two *trans*-DES molecules is 30.0 Å (Figure 16a and b). However, the actual spacer length should really be longer than 30.0

Å because it needs to adopt a non-linear pathway such that it can bypass the protein. Oligoethylene glycol (OEG) spacers of 39.5 to 46.7 Å lengths (EG10 to EG12, approximately 10 Å longer than the calculated distance) were chosen to tether two *trans*-DES moieties via an amide linkage group to achieve the intermolecular bivalent binding between two ER LBPs. Moreover, to interpret the folding of OEG spacer and minimize the loss of the conformational entropy, two carbon hybrid OEG spacers and one biphenyl hybrid OEG spacer, whose extended lengths were in the range of 34.8 to 39.8 Å, were also designed (Figure 16d, **32-34**). Furthermore, due to the facile geometric isomerization of the phenolic non-steroidal structure, a separation of the undesirable isomer from the desirable isomer still needs to be accounted for.

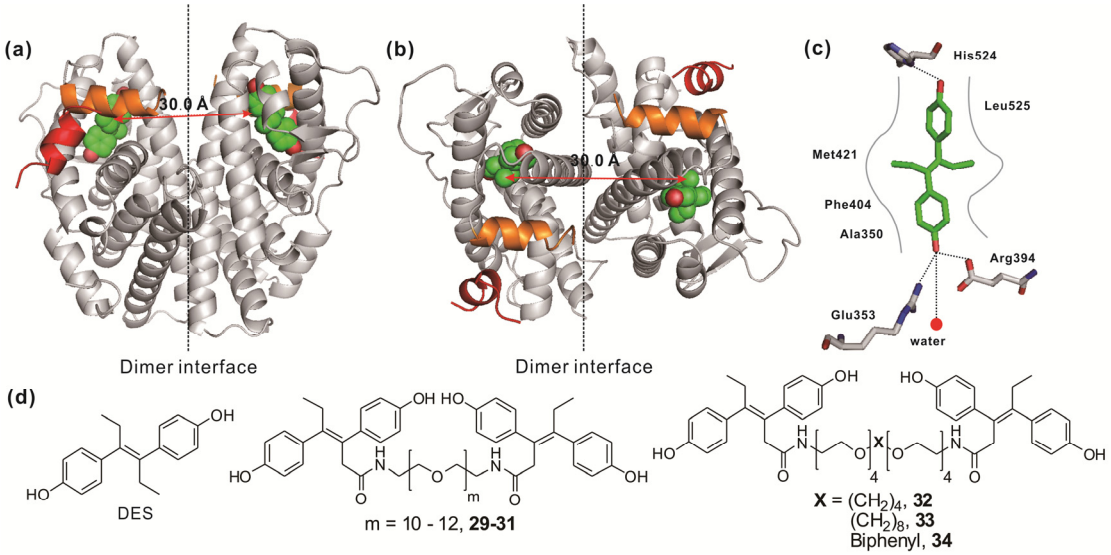

Figure 16. The distance between the carbons 1 of two *trans*-DES molecules (spheres) in the ERα LBD homodimer (ribbons in gray, ribbons of coactivator (CoA) and H12 in red and orange, respectively, PDB ID code 3ERD) is 30.0 Å. (a) The ER dimer viewed perpendicular to the dimer axis. (b) The dimer viewed down the dimer axis. (c) Hydrogen bond and hydrophobic interactions between a *trans*-DES molecule and ERα LBD: hydrogen bonds are indicated by dashed lines and a highly ordered water molecule (red dot) stabilized by a hydrogen bond network is indicated. (d) Chemical structures of *trans*-DES and bivalent *trans*-DES ligands (**29-34**).

3.2.2. Chemical preparation

To obtain these bivalent *trans*-DES ligands, a carboxylic acid *trans*-DES derivative **39** (Scheme 20a) needed to be prepared, which has a different structure than the symmetrical *trans*-DES molecule.[174,175] In 1980, Goswami et al. developed a synthetic route of a asymmetrical DES derivative to study the ER-binding properties of a series of side-chain halogenated hexestrol

derivatives.[176] According to their procedure, the synthesis of bivalent DES ligand was started with a alkylation of commercial available deoxyanisoin with sodium hydride and ethyl iodide to give α-ethyldeoxyanisoin **35** with a yield of 67%. An ester-functionalized side-chain could be subsequently introduced by the Reformatsky reaction with ethyl bromoacetate and zinc in benzene, and a mixture of diastereomeric β-hydroxyl esters **36** was obtained with a yield of 82%. Initially, these two diastereomers were separated by HPLC and characterized individually. This diastereomeric separation, however, was not necessary, since the β-hydroxyl group in **36** was eliminated by treatment with thionyl chloride in pyridine to give a mixture of *cis/trans*-isomers of α,β-unsaturated ester **37** with a yield of 98%.

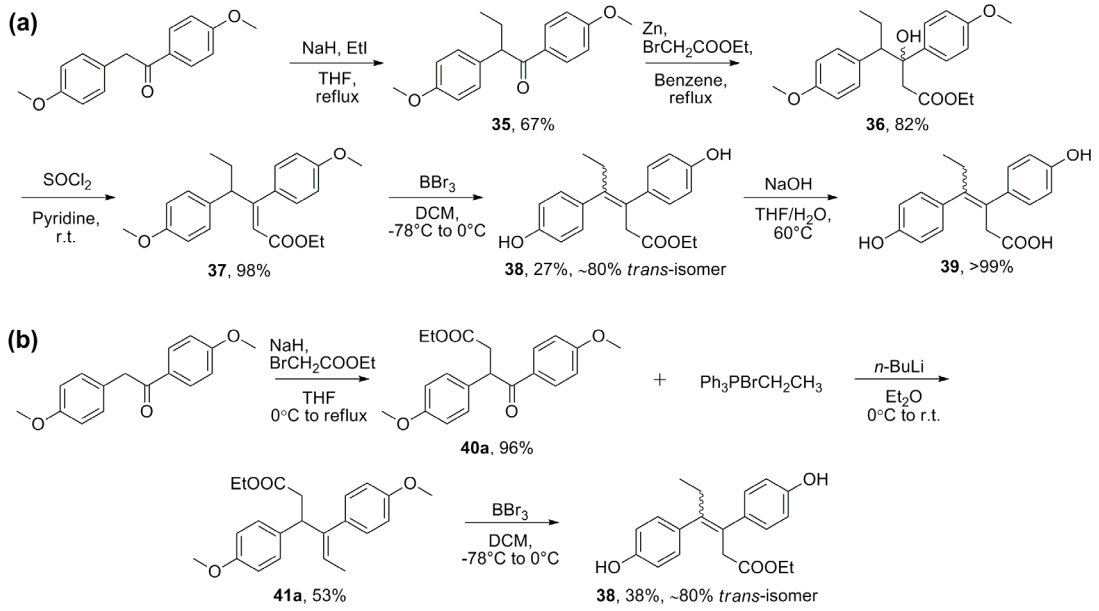

Scheme 20. Two synthetic routes of a carboxylic acid DES derivate **38** and **39** via two synthetic pathways.

Since the double bond in α,β-unsaturated ester **37** finally needed to migrate to the β,γ-position, a separation of *cis/trans*-isomers of **37** did not have to be performed. During the removal of the methyl ether group with boron tribromide in dichloromethane, the migration of the double bond took place spontaneously to form the stilbene ester **38** with a yield of 27% as a mixture of *cis*:*trans* = 1:4 isomer, and a styrene ester with a yield of 72%.[177] In addition to this procedure, it has been reported that the migration of α,β-double bond could be carried out by treating the α,β-unsaturated ester isomer **37** with potassium *tert*-butoxide in anhydrous DMSO to give a methyl ether protected β,γ-unsaturated stilbene ester,[178] which, however, underwent a

mixture of stilbene and styrene ester during the deprotection of methyl ether with boron tribromide. Finally, a hydrolysis of the mixture stilbene ester isomers **38** with aqueous sodium hydroxide gave the desired carboxylic acid **39** as a isomer mixture (*cis*:*trans* = 1:4) with a quantitative yield.

In order to have a sufficient chemical precursor for the synthesis of bivalent DES ligands, another synthetic route with a higher total yield was applied (Scheme 20b), in which a γ-keto ester **40a** was first prepared by treating deoxyanisoin with sodium hydride and ethyl bromoacetate with a yield of 96%. Then, the Wittig reaction between the ketone ester **40a** and ethyltriphenyl-phosphonium bromide was performed and gave the olefin **41a** as a mixture of *cis*- and *trans*-isomers with a yield of 53%.[179] By using the same deprotection procedure for the methyl ether group with boron tribromide, the stilbene ester **38** was obtained with a yield of 38%, in which the ratio of *cis*- to *trans*-isomer was 1:4. Finally, the stilbene ester **38** was further converted into the carboxylic acid **39** under the same basic hydrolysis condition.

Additionally, this kind of *cis*-stilbene structure readily underwent an isomerization to *trans*-isomer via a second order reaction in organic solvents of low dielectric constants. The corresponding mechanism was shown in Scheme 21.[180,184] Thus, the mixture of carboxylic acid **39** isomers was first applied to form mono- and bivalent DES ligands **42** and **43** via an amide formation with ethylamine or 1,2-bis(2-aminoethoxy)ethane in the presence of EDC and HOBT in THF with yields of 16-23%,[182] which could be improved up to 70% for bivalent DES ligands **29-34** by using PyBOP as the amide coupling reagent in a solvent mixture of DMF/DCM (Scheme 22).[183] It has been reported that the *trans*-isomer of DES had a much higher biological potency such as in vitro ER-binding affinity than the *cis*-isomer.[180,184] Moreover, Katzenellenbogen and co-workers investigated the isomerization from *trans*-isomer to *cis*-isomer and monitored by analytic RP-HPLC. They found that this isomerization not only spontaneously took place in cultures of ER positive MCF-7 human breast cancer cells but also in the cell-free medium.[185] Therefore, a geometrical separation of *cis*-*cis*, *cis*-*trans*, and *trans*-*trans* isomer of bivalent DES ligand was performed by reversed phase high-performance liquid chromatography (RP-HPLC) to give three pure isomers for bivalent DES ligands **29-34**. Among these isomers, the *cis*-*cis* isomer was found to be stable in polar solvent such as DMSO and water even after 48 hours.

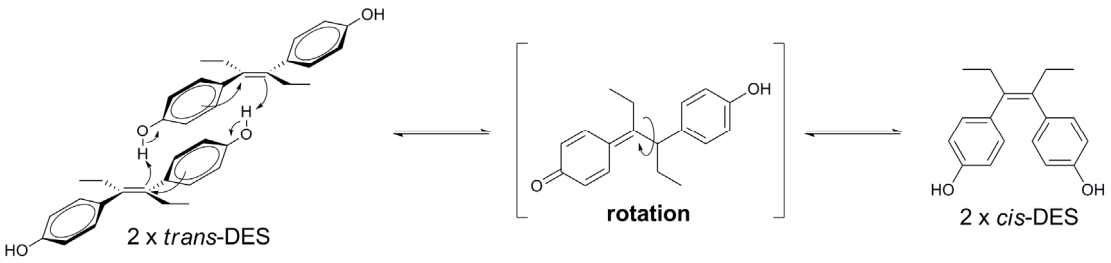

Scheme 21. A proposed mechanism for *cis*- and *trans*- isomerization of DES molecules.[181]

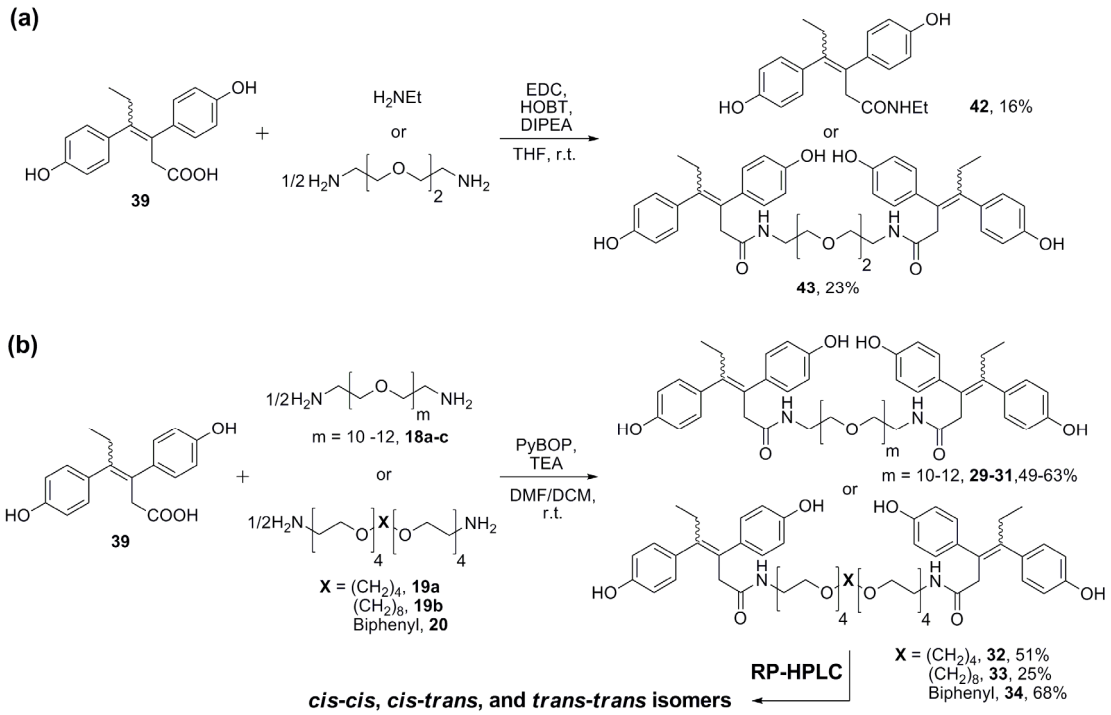

Scheme 22. (A) Chemical preparation of mono- and bivalent DES ligands **42** and **43**; (B) Chemical preparation of bivalent DES ligands **29**-**34**.

3.2.3. Biological evaluation

In order to evaluate the binding properties of these mono- and bivalent DES ligands, competitive radiometric assays with tritiated-estradiol ($[^3H]$-E_2)[107-109] for both ER subtypes, i.e., ERα and ERβ, were carried out in the group of Prof. Dr. John A. Katzenellenbogen (Department of Chemistry, University of Illinois at Urbana-Champaign). In the binding assays, $[^3H]$-E_2 was used as a tracer and estradiol (E_2) as a standard.[107,108] For six bivalent ligands **29**-**34**, the evaluated bivalent ligands were of two types: (1) homo bivalent ligands, in which both of DES molecules were *trans*-isomer, and were expected to have higher affinities than (2) hetero bivalent ligands, in which one *trans*-DES molecule was tethered to one *cis*-DES molecule. Whereas hetero bivalent

ligands (*trans*-*cis* isomer) had similar lipophilicity as homo bivalent (*trans*-*trans* isomer) in the aqueous environment, their binding behaviors could be considered as a monovalent control for homo bivalent ligands. In addition, a mixture of 80% *trans*-isomer was used in binding assays for three monovalent controls **38**, **39**, and **42** as well as one bivalent ligand **43**. Binding affinities expressed as relative binding affinity (RBA) values, i.e., relative to the binding affinity of E_2 (RBA = 100%, Section 1.2.4, Equation 17), are shown in Table 1 and Figure 17. In general, binding affinities of mono- and bivalent DES ligands were lower than that of E_2. Among bivalent DES ligand **29**-**34**, bivalent *trans*-DES ligand **30** tethered by a OEG spacer of 43.1 Å length had a relative high affinity which, however, was lower than the binding affinity of bivalent ligand **43** tethered by a spacer of 10.8 Å length for both ER subtypes.

Table 1. ERα and ERβ binding affinities of mono- and bivalent ligands.

Ligand	Maximum spacer length [Å][a]	*trans*- / *trans*-*trans* isomer		*trans*-*cis* isomer	
		ERα	ERβ	ERα	ERβ
38	-	7.87 ± 1.9	41.98 ± 6.7	-	-
39	-	0.011 ± 0.002	0.051 ± 0.011	-	-
42	-	0.067 ± 0.004	0.159 ± 0.004	-	-
43	10.8	0.230 ± 0.005	0.247 ± 0.026	-	-
29	39.5	0.012 ± 0.001	0.039 ± 0.011	0.015 ± 0.004	0.029 ± 0.006
30	43.1	0.021 ± 0.005	0.048 ± 0.004	0.126 ± 0.014	0.236 ± 0.052
31	46.7	0.012 ± 0.003	0.023 ± 0.006	0.007 ± 0.001	0.019 ± 0.001
32	34.8	0.006 ± 0.001	0.013 ± 0.004	0.007 ± 0.001	0.006 ± 0
33	39.8	0.013 ± 0.002	0.022 ± 0.002	0.012 ± 0.001	0.016 ± 0.002
34	39.0	0.008 ± 0.002	0.020 ± 0.006	0.003 ± 0.001	0.008 ± 0

a. The maximum spacer length, between two amide groups in an extended conformation, was measured by the modeling software PyMOL.

It has been reported that the ER-binding affinity of monovalent *trans*-DES was 372% and 278%, for ERα and ERβ, respectively.[186] These results strongly indicate that the introduction of a hydrophilic group, such as carboxylic acid, ester, or amide, on the hydrophobic core of *trans*-DES can dramatically reduce the ER-binding affinity due to the hydrophobic character of the ER LBP compared to the *trans*-DES.[181] On the other hand, in the agonistic ER-ligand binding mode, the bound ligand like E_2 or *trans*-DES is fully encapsulated within a three-layer helical "sandwich" folding ER LBD where there is no obvious access to the exterior of the ER LBD unless through a large substituent such as a phenyl vinyl group at the 17α-position of E_2 molecule (Section 1.3).

Therefore, weak binding affinities of these bivalent *trans*-DES ligands could also be attributed to this agonistic ER-binding mode.

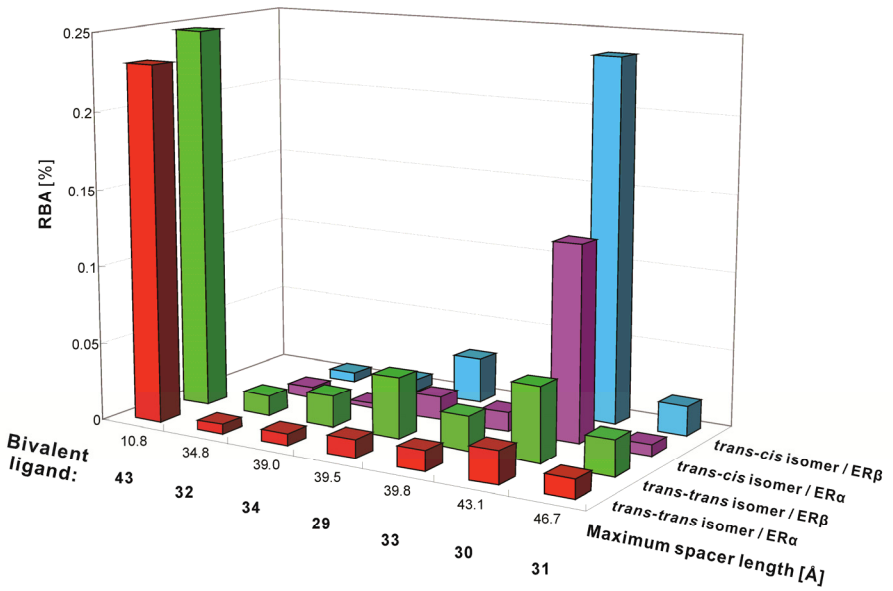

Figure 17. The relationship between relative binding affinity (RBA) and maximum spacer length. Bivalent ligands (**29-34**) were evaluated separately for *trans-trans* isomer (columns in red and green, for ERα and ERβ, respectively) and *trans-cis* isomer (columns in violet and blue, for ERα and ERβ, respectively), while **43** for 80% *trans*-isomer. Error bars are not shown in this figure.

Nevertheless, there are several findings in these binding affinity results:

(1) Bivalent ligand **43** with a diethylene glycol spacer has a much higher RBA value than other bivalent ligands, although it is not capable of forming a simultaneous binding to two ER LBPs due to its short spacer length (10.8 Å versus 30.0 Å). It was speculated that its high binding affinity must be attributed to either an enhanced rebinding (a decreased dissociation rate k_{off}) caused by a high effective concentration of the second DES molecule[50] or an additional interaction between the second DES molecule and the ER surface.[188,189]

(2) Among bivalent DES ligands with the maximum spacer length from 34.8 to 46.7 Å, bivalent ligand **30** tethered by a 43.1 Å OEG spacer has the highest binding affinities in both ER subtypes for each isomer. This length, 43.1 Å, is much longer than the calculated distance and it is still not clear why the *trans-cis* isomer of **30** has a higher binding affinity than its corresponding *trans-trans* isomer.

(3) It is surprising that bivalent ligands **32-34** tethered by hybrid OEG spacers does not have any higher ER-binding potencies compared to **29-31** tethered by OEG spacers, which indicates

that a hydrophobic, rigid segment cannot enhance the ER-binding affinity. In order to further understand the reason behind, a computational calculation study was carried out (Section 3.2.4).

Additionally, to better understand structure-activity relationship (SAR) of bivalent estrogen ligand and achieve the bivalent ER-ligand binding, two new strategies were developed. Firstly, a new DES derivative with the linkage group that is located far away from the hydrophobic core will be prepared, since it has been reported that the introduction of a pentamethylene side-chain ($(CH_2)_5$, Scheme 23) can avoid the hydrophobic ER LBP, and thus, enhance the ER-binding affinity.[190,191] However, due to time limitation, this chemical preparation was not able to be finished. Secondly, it was found that by using an antagonistic ligand such as raloxifene it is possible to avoid the undesirable impact caused by a completely buried agonistic ER-binding mode. Based on this consideration, we prepared a new series of bivalent raloxifene ligands (Section 3.3).

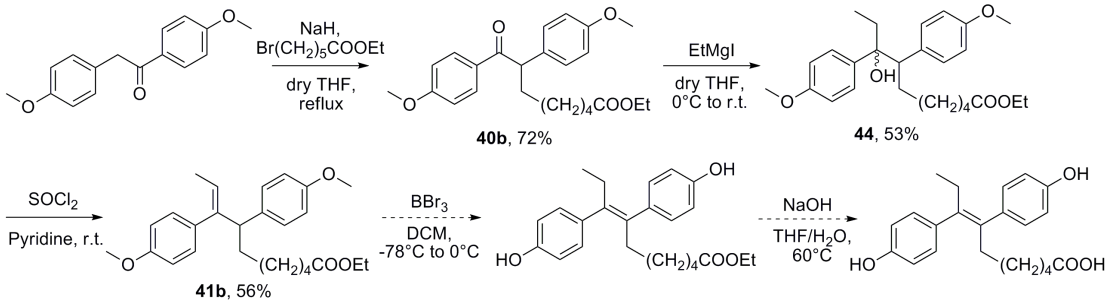

Scheme 23. The synthetic route for a pentamethylene side-chain DES derivate.

3.2.4. Computational study

Computational studies were carried out in the group of Dr. Markus Weber (Zuse Institute Berlin) to investigate end-to-end distances of OEG and hybrid OEG spacers in water, estimate conformational entropy, and describe their thermodynamic contribution during the ligand binding process.[29]

3.2.4.1. End-to-end distances of bivalent DES ligands tethered by a OEG spacer

It was found that end-to-end distances of OEG spacer over 100 ns simulation time in water were

less than half of those measured in extended conformations, which indicated that a folded conformation was favored over a linear extended conformation. For example, the end-to-end distance of OEG spacer **23f** in a fully extended conformation and in water is 34.1 and 15.0 Å, respectively. Furthermore, the end-to-end distance further decreased below 10 Å, once two hydrophobic DES moieties were tethered by OEG spacer **23f** to form bivalent ligand **29**. Additionally, such a end-to-end distance decrease was observed not only in the case of bivalent DES ligands but also in other bivalent steroidal ligands,[29,124] which suggests that folded conformations are the dominate conformation in the aqueous environment.

3.2.4.2. Conformational entropy estimation

In this computational study, it was also observed that the ligand-attachment on the spacer resulted in a lower conformational entropy than the no-ligand spacer, which means a decreased conformational freedom of bivalent ligands. Remarkably, bivalent ligand tethered by biphenyl hybrid OEG spacer such as **34** had a significant decrease in the entropy compared to those tethered by OEG or carbon-carbon hybrid OEG spacers. This decrease can be attributed to a stable hydrophobic-hydrophobic interaction between two DES moieties and biphenyl segment that caused bivalent ligand **34** to adopt a stacked conformation. Consequently, this stacked conformation not only neutralized the distance spanned by the linear elements but also punished bivalent ligand **34** with more energy penalty for the ER-ligand binding, which in turn reduced its ER-binding affinity compared to other bivalent ligands such as **29-31** tethered by OEG spacers.

3.3. Bivalent raloxifene ligands

3.3.1. Ligand design

As mentioned in Section 1.2.2, individually bound ER ligand resulted in a different conformation change of the ER LBD, in particular for the C-terminal helix, H12. In the agonistic ER-ligand binding mode, the bound ligand like E_2 or *trans*-DES is fully encapsulated within a three-layer helical "sandwich" folding ER LBD and there is no obvious access to the exterior of the ER LBD unless through a large substituent such as a phenyl vinyl group at the 17α-position of E_2 molecule

(Section 1.3). By contrast, although raloxifene (RAL) binds into the same hydrophobic pocket of the ERα LBD as E_2 and DES, its bulky side-chain stretches out of the hydrophobic ER LBP and has a hydrogen bond interaction with the surface aspartic acid (Asp351) of the ERα LBD (Figure 18a-c). This prevents the reorientation of helix 12 as well as the subsequent gene transcription. For our purpose, this bulky side-chain provided a way to tether two RAL moieties via a certain linkage so that the modification would only have a minor influence on the binding affinity.

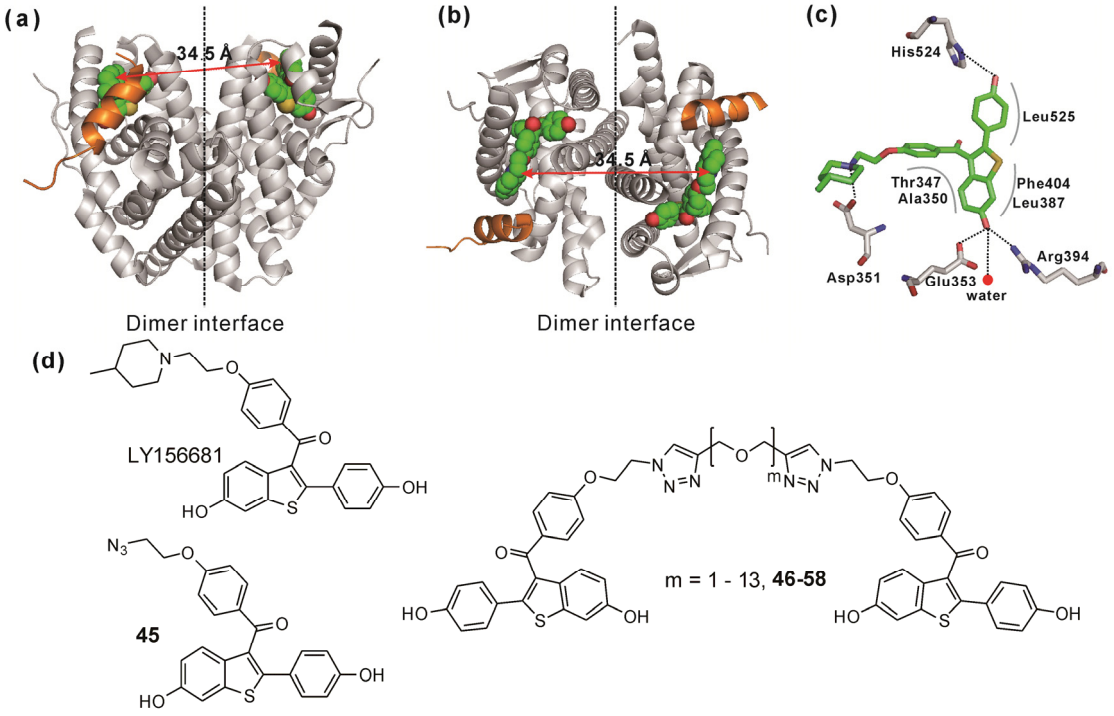

Figure 18. The distance between two nitrogen atoms of 4-methylpiperidin on LY156681 molecule (spheres) in the ERα LBD homodimer (ribbons in gray, the ribbon of H12 in orange, PDB ID code 2R6W) is 34.5 Å. (a) The ER dimer viewed perpendicular to the dimer axis. (b) The dimer viewed down the dimer axis. (c) Hydrogen bond and hydrophobic interactions between an LY156681 molecule and ERα LBD, hydrogen bonds are indicated by dashed lines and a highly ordered water molecule (red dot) stabilized by a hydrogen bond network is indicated. (d) Chemical structures of LY156681, the RAL azide derivate **45** and bivalent RAL ligands (**46-58**).

Dai et al. investigated ER binding affinities and activities of a series of RAL derivatives, which had binding constants of < 10 nM.[192] For instance, one of the derivatives, LY156681, was crystallized with the dimeric ERα LBD (PDB ID code 2R6W, Figures 18). This crystal structure was modeled by using the computer modeling software PyMOL. It was found that the closest distance between two nitrogen atoms of piperidins at the side-chain of LY156681 was approximately 34.5 Å which was slight longer than the distance between two ER LBP in the

crystal structure of 1ERE (Figure 8). Although LaFrate et al. demonstrated that a maximum binding peak appeared when the bivalent EE_2 ligand was tethered by a 35.0 Å length spacer, it was still unclear why bivalent DES ligand **43** tethered by a flexible OEG spacer of 10.8 Å length had a higher affinity than other bivalent DES ligands. To address this question, a systematic OEG spacer length screening, namely from 4.7 to 47.7 Å, was carried out to investigate the SAR of bivalent RAL ligands and the impact of flexible OEG spacer length in the range of 5.0-50.0 Å.

"Click Chemistry," a 1,3-dipolar cycloaddition, was introduced by Sharpless and co-workers in 2001. This reaction provides a quick, reliably, region- and stereoselective method to join small units together via a 1,2,3-triazole linkage group.[157,158] Therefore, it takes advantages of this method to prepare a series of bivalent RAL ligands (Figure 18d, **46-58**) tethered by a exact-length OEG spacer (**21a-l**) based on a azide functionalized RAL derivative **45** developed in the group of Prof. Dr. Oliver Seitz (Department of Chemistry, Humboldt University Berlin).[193] Additionally, similar strategies were also applied to prepare three monovalent RAL ligands (**59-61**) which have an OEG monomethyl ether side-chain as a monovalent control.

3.3.2. Chemical preparation

13 bivalent RAL ligands (**46-58**) have been straightforwardly prepared by a copper (I) catalyzed cycloaddition based on the azide **45** and dipropargyl OEG ether **21a-l** in a mixture of water and *tert*-butyl alcohol (Scheme 24). Copper (II) sulfate pentahydrate was reduced by sodium ascorbate in-situ to provide the copper (I) source, with which the reaction is regiospecific and gives only 1,4-disubstituted 1,2,3-triazoles.[194] Extraction with a saturated ethylene diamine tetraacetic acid (EDTA) aqueous solution and a further column chromatography were applied to remove copper (I) and give the pure product with satisfied yields. With the same method, three monovalent RAL ligands (**59-61**) were prepared as well.

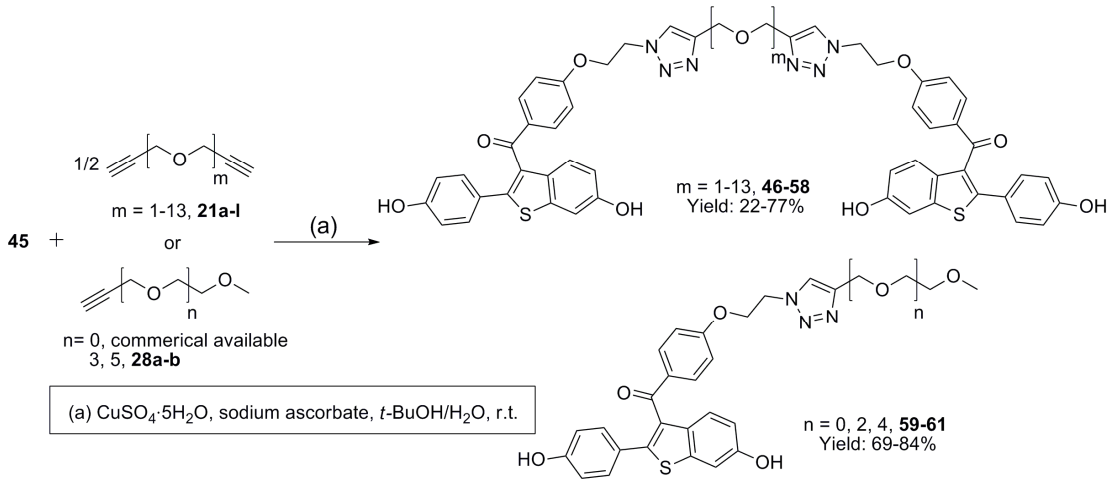

Scheme 24. Chemical preparation of mono- and bivalent RAL ligands **46-58** and **59-61** via Click Chemistry.

3.3.3. Biological evaluation

These 16 mono- and bivalent RAL ligands were biologically evaluated in the group of Prof. Dr. Oliver Seitz (Department of Chemistry, Humboldt University Berlin) by using HitHunter™ enzyme fragment complementation (EFC) estrogen chemiluminescent assay (DiscoveRx) according to the manufacturer's instructions to determinate their ER-binding affinities.[110,111] Recombinant human ERα, expressed in S. Frugiperda insect cells, binds to E_2 with a K_d of 0.300 nM. An enzyme-donor (ED) was used as tracer and E_2 as a standard. The binding affinities were expressed as RBA values, which are relative to the binding affinity of E_2 (RBA = 100%, Section 1.2.4, Equation 17), are showed in Table 2.

In general, all of the mono- and bivalent RAL ligands had lower binding affinities than E_2, and with increasing spacer length, binding affinities of bivalent ligands became weaker. Figure 19 shows the relationship between the RBA value and maximum spacer lengths of bivalent ligands. Whereas the closest distance measured between two LY156681 molecules at the nitrogen atom of 4-methyl piperidine in the crystal structure PDB ID code 2R6W is 34.5 Å, bivalent ligands tethered by shorter OEG spacers (less than 30 Å) are theoretically not capable of forming a simultaneous binding to two ER LBPs. Therefore, the binding affinity enhancement of a bivalent ligand, such as **46** over the monovalent ligand **60** or **61,** needs to be attributed to its second RAL moiety. It resulted in either a high effective concentration for rebinding[50] or an additional interaction with the ER LBD surface.[188,189] Compared to the significant decrease in effective

concentrations with increasing OEG spacer length (Table 2, column "C_{eff}"), binding affinities of bivalent ligands **47**-**50** were almost in the same range. Moreover, there are several reports about a secondary estrogen binding site close to or within the CoA binding groove of the ER LBD.[195-197] Thus, such binding affinity enhancement should be attributed to an additional binding, namely a non-specific binding of the second RAL moiety to the ER.

Table 2. Structures, maximum spacer lengths, relative binding affinities (RBA), and effective concentrations (C_{eff}) of mono- and bivalent RAL ligands **46**-**61**.

Compound	Structure	Maximum spacer length[a] [Å]	RBA[b] [%]	C_{eff}[c] [nM]
46	RAL2EG1	4.7	67.7 ± 27.5	7.59×10^{6}
47	RAL2EG2	8.4	18.6 ± 8.10	1.36×10^{6}
48	RAL2EG3	11.9	25.6 ± 11.1	4.73×10^{5}
49	RAL2EG4	15.5	14.2 ± 5.41	2.13×10^{5}
50	RAL2EG5	19.1	24.3 ± 9.28	1.15×10^{5}
51	RAL2EG6	22.7	3.73 ± 2.90	6.81×10^{4}
52	RAL2EG7	26.2	10.2 ± 2.15	4.40×10^{4}
53	RAL2EG8	29.8	4.51 ± 3.28	2.99×10^{4}
54	RAL2EG9	33.4	5.29 ± 1.47	2.13×10^{4}
55	RAL2EG10	37.0	4.68 ± 1.02	1.57×10^{4}
56	RAL2EG11	40.6	3.51 ± 0.66	1.19×10^{4}
57	RAL2EG12	44.2	4.41 ± 0.70	9.20×10^{3}
58	RAL2EG13	47.7	4.64 ± 0.63	7.29×10^{3}
59	RALEGMe	3.7	n. a.[d]	-
60	RALEG4Me	14.3	10.0 ± 6.58	-
61	RALEG6Me	21.5	3.42 ± 2.65	-

a. Distances between the carbons at 4-position of the 1,2,3-triazole were measured by the modeling software PyMOL and considered the maximum spacer length. b. Relative binding affinity (RBA) values were determined by competitive binding assays and were expressed as [$IC_{50}(E_2)$ / IC_{50}(compound)] × 100% (RBA for E_2 = 100%, $IC_{50}(E_2)$ = 3.11 nM). In these assays the K_d of E_2 is 0.300 nM for ERα. c. The effective concentration (C_{eff}) was calculated as the second RAL moiety in a hemisphere of radius equal to the spacer length of this bivalent ligand, once the first RAL moiety binds to the ER LBP.[50] d. not available.

Moreover, although the maximum spacer lengths of bivalent ligand **49** and **51** are very close to the maximum side-chain lengths of monovalent ligands **60** and **61**, respectively, bivalent ligand **49** had higher affinity than monovalent ligand **60**, while bivalent ligand **51** had almost the same affinity as monovalent ligand **61**. This observation suggested that the interaction between bivalent ligand **51** and the dimeric ER LBD was monovalent like monovalent ligand **61**, rather than bivalent, although bivalent ligand should be easily distinguishable from monovalent ligand due to

the number of RAL moieties. According to this finding and previous conclusions about the relationship between the multivalent ligand-receptor binding mechanism and the architecture of multivalent ligands in the literature (Section 1.1),[36,37,54] it is hypothesized that the spacer length of bivalent ligand **51** could be used to distinguish two types of ER-binding modes for bivalent RAL ligands: One is an intramolecular bivalent binding which simultaneously takes place between a ER LBP (steroidal site) and a secondary site (the subsite) on the same monomeric ER LBD, while the other is an intermolecular bivalent binding between two ER LBPs of dimeric ER LBD (Figure 20a).

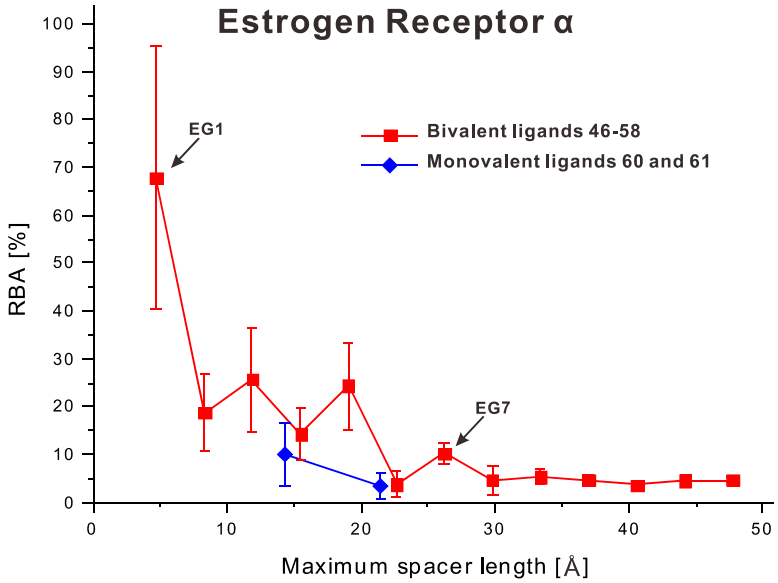

Figure 19. The relationship between relative binding affinity (RBA) and maximum spacer length. Bivalent RAL ligands (**46-58**) are in a red line and monovalent ligands (**60** and **61**) in a blue one.

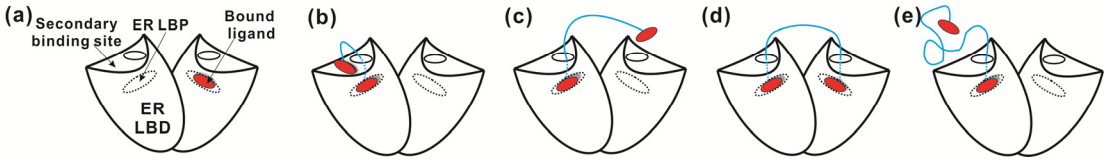

Figure 20. Schematic representation of (a) the construction of dimeric ER LBD in which each monomeric ER LBD has one LBP and one secondary binding site on the ER LBD surface and (b-e) four different binding behaviors for bivalent ligands with dimeric ER LBD to demonstrate the progress from an intramolecular to an intermolecular bivalent binding.

Such a hypothesis is represented in Figure 20b-e: (1) Bivalent ligands such as **46-50** tethered by short spacers formed an intramolecular bivalent binding (Figure 20b) on the same monomeric ER LBD[198] and their binding affinities decreased with the increasing spacer lengths and corresponding conformation entropies. Due to this reason, **46** with the shortest spacer reached the

highest binding affinity. (2) The spacer length of bivalent ligand **51** was so long that a secondary binding with the secondary site on the same ER LBD monomer was unfavorable, which was most likely due to entropy loss and defolding penalty (Figure 20c), while at the same time this spacer was still too short to bind to another ER LBP. As a consequence, its binding affinity was comparable to monovalent ligand **61**. (3) An intermolecular bivalent binding could be formed by those bivalent ligands tethered by long spacers. Therefore, their binding affinities should be higher than bivalent ligand **51** (Figure 20d); (4) This intermolecular bivalent binding mode became unfavorable for bivalent ligands such as **56**-**58** tethered by very long spacers due to their large loss of conformational entropies. As a consequence, their binding affinities were comparable to bivalent ligand **51** (Figure 20e). Moreover, in the applied competitive binding assays, the ER LBP (steroidal site) should always be occupied either by a tracer or an evaluated bivalent ligand.

As discussed above, it is proposed that the intermolecular bivalent binding could be achieved by bivalent ligand **52** whose spacer length was close to 30 Å and whose binding affinity was higher than that of bivalent ligand **51**. This speculation, however, poses two main questions in this study: (1) Why can an intermolecular bivalent binding be achieved by a 26.2 Å spacer which is much shorter than the predicated 34.5 Å and (2) why dose bivalent ligand **52** only have a relatively low binding affinity unlike the previously reported high-affinity bivalent WGA[8] and cGMP ligands[50] (Section 1.1)?

The first question can be addressed by computer modeling (Section 3.2.4), which demonstrates that bivalent ligand **52** has a different binding mode within the ER LBP as the LY156681 molecule in the crystal structure 2R6W. In order to solve the second question, Kim et al. have demonstrated that conformational and dynamic features of the estrogen tethered by poly(amido amine) PAMAM via a long, flexible tethered spacer could dramatically influence the ligand access to its target receptor, although the long spacer seemed to be more likely to bind to ER than a short one.[136] In the computer modeling for bivalent DES ligands (Section 3.3.4), it was speculated that not only folded conformations of bivalent ligands but also hydrophobic-hydrophobic interactions between two DES moieties can influence their ER-binding potencies.[29] To prove this speculation and solve the second question, a NMR and UV study of bivalent ligands tethered by different long OEG spacers has been carried out (Figure 21 and 22).

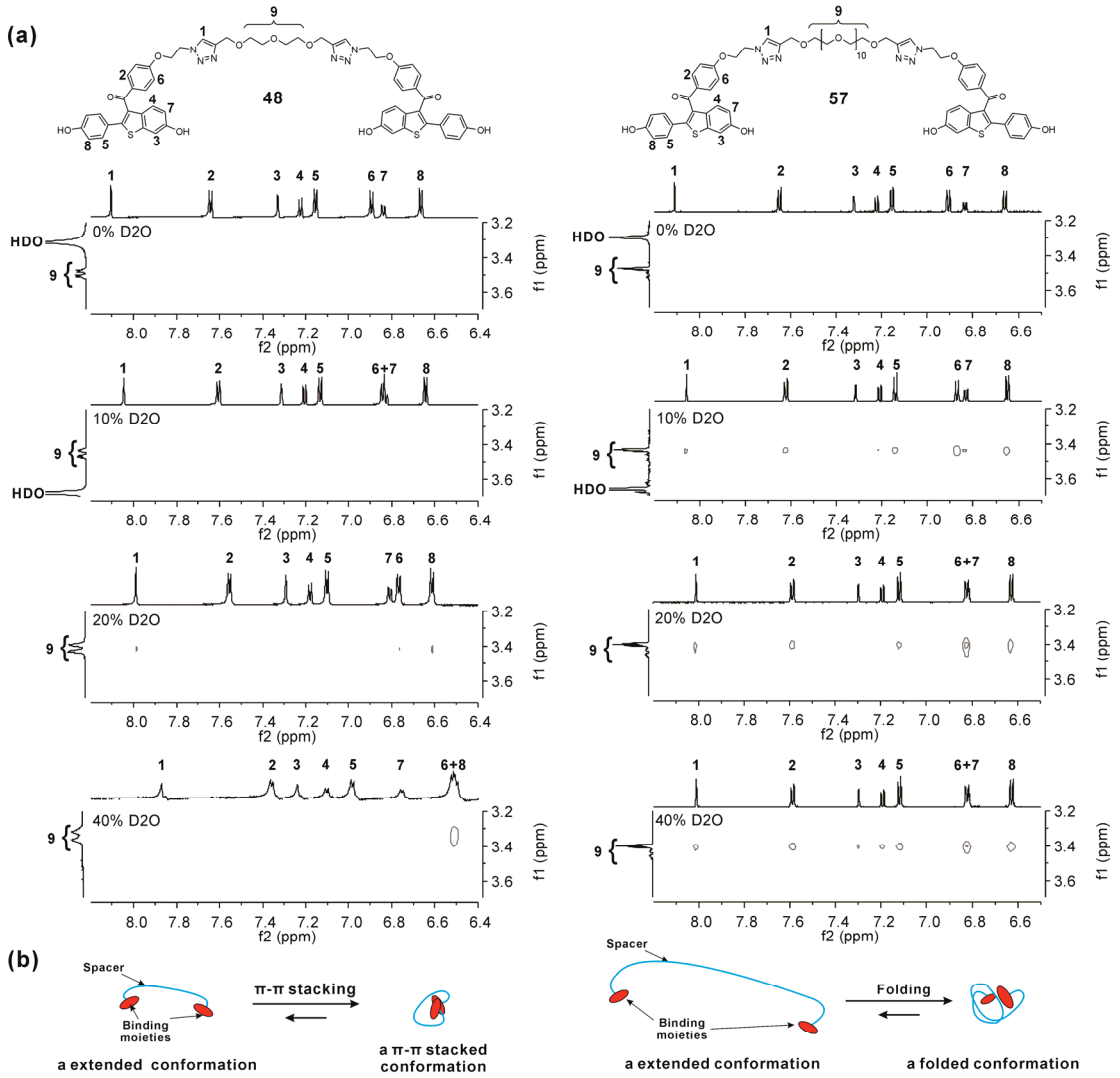

Figure 21. (a) Aromatic (proton 1-8) and OEG (proton 9) regions of the ^{1}H NMR and ROESY spectra of OEG tethering bivalent ligands **48** (left) and **57** (right) in a solution of DMSO-d6 with 0, 10, 20, and 40% D_2O (top to bottom). (b) Two proposed conformations of **48** (left) and **57** (right) in aqueous solution.

In the ROESY spectra (Figure 21), it was found that with the increasing proportion of deuterium water (from 0% to 40% D_2O), an intramolecular interaction between RAL molecules (aromatic proton 1-8) and the tethering OEG spacer (alkyl proton 9) became much stronger for bivalent ligand **57** than for bivalent ligand **48**. It is not surprising that the spacer of **57** was long enough to wrap the RAL binding moiety, while the spacer of **48** was not. Moreover, bivalent ligand **48** existed as a π-π stacked conformation as was evidenced by the significant upfield shift of the aromatic protons, especially the aromatic proton 6, which was caused by the large ring-current of such a stacked conformation. By contrast, the aromatic proton 6 of **57** only had a small upfield shift. This indicates that an intramolecular π-π stacking interaction between two

RAL molecules dominates in the case of short spacer tethering bivalent ligands such as **48**, rather than **57**. In other words, two RAL moieties of **57** were complexed with its OEG spacer and had a weak π-π stacking interaction in an aqueous environment, while two RAL molecules of **48** only stacked with each other and were more exposed to the receptor than those of **57**.

In the UV spectra (Figure 22), monovalent ligand **60** and bivalent ligands **46** and **58** have been investigated within different solvent systems (Figure 22 left). It was found the UV-absorption maximum for each bivalent ligand in aqueous solvent (3.85% DMSO/water, Figure 22 top left) had a bathochromic shift (λ_{max} = 290 and 293 nm, for **46** and **58**, respectively) compared to the monovalent ligand (λ_{max} = 287 nm for **60**). In contrast, no bathochromic shift was observed in organic solvent (3.85% DMSO/chloroform, Figure 22 lower left). Moreover, an intensity decrease was also observed in the aqueous solvent. This confirmed that an interaction between hydrophobic RAL molecules and the OEG spacer only dominated in aqueous solvent, not in organic solvent, which is consistent with the observation in the NMR spectra.

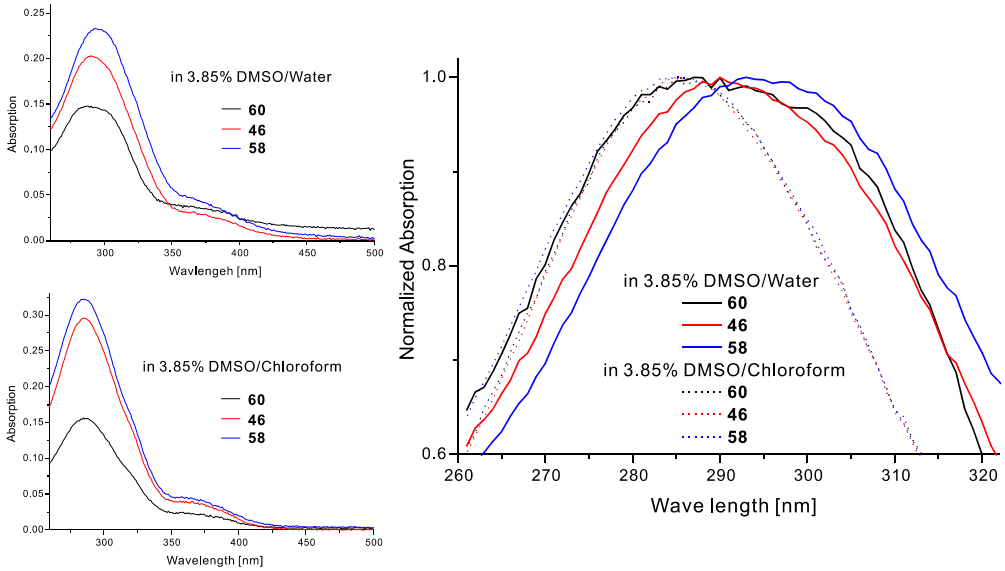

Figure 22. UV absorption spectra of 38.5 μM monovalent ligand **60**, bivalent ligands **46**, and **58** in 3.85% DMSO/chloroform (top left), 3.85% DMSO/water (lower left); the normalized absorption UV-spectra (right).

In the literature, similar hydrophobic-hydrophobic interaction has also been observed in a low temperature NMR and X-ray analysis,[199] in which two $GABA_A$-benzodiazepine receptor ligands linked by three and five atoms were demonstrated to adopt a stable, folded conformation either in solution or in the solid state. Thus, a low binding affinity was obtained. Similarly,

bivalent RAL ligands needed to overcome the energy penalty caused either by a π-π stacking or by a spacer folding, in order to gain access to the ER, which consequently resulted in a low in vitro receptor binding affinity. Furthermore, this finding is consistent with the previous report on the relationship between the ER-binding affinity and the tether structure of estrogen-PAMAM conjugate.[136]

3.3.4. Computer modeling and simulation

In order to evaluate the steric fit and thermodynamic properties, bivalent ligands **46**-**52** (covering spacer lengths from one EG unit to seven EG units in the extended conformation, i.e., from 4.7 to 26.2 Å, respectively) were modeled and parameterized for molecular dynamic (MD) simulations in the group of Dr. Markus Weber, in particular regarding the question: Could an intermolecular bivalent binding be achieved by bivalent RAL ligand **52** tethered by a 26.2 Å OEG spacer?[30]

Bivalent binding modes were modeled by first performing a monovalent alignment of the RAL moieties to the ligands from crystal structure with PDB ID code 2R6W, followed by energy minimization including protein structure and an explicit solvent in order to relax the OEG spacer portion of the bivalent ligand. In this study, it was found that an intermolecular bivalent binding to two ER LBPs was not possible for bivalent ligands **46**-**51** as the spacer length prohibited reaching both binding sites simultaneously. Bivalent ligand **52** could be accommodated in two ER LBPs of the crystal structure of ERα LBD 2R6W in an intermolecular bivalent binding mode (Figure 23). It was inferred that such an intermolecular bivalent binding to both ER LBPs was also possible for bivalent ligands **53**-**58** which feature longer OEG spacers.

Remarkably, the result from a 10 ns simulation of bivalent ligand **52** in the intermolecular bivalent bound state revealed some differences to the monovalent binding mode of LY156681. A hydrogen bond interaction between the 4-methyl piperidine at the side-chain of LY156681 and the residue Asp351 of ERα is characteristic for the monovalent ligand binding mode (Figure 18c).[103] Our bivalent ligands feature a 1,2,3-triazol ring structure at the same position, which is further connected to the OEG spacer. The simulation of bivalent ligand **52** show that the 1,2,3-trizol ring is hindered from interacting with the residue Asp351 because the tethered EG7 spacer forces the linkage groups to arrange towards each other and thereby serves as an elongation of the spacer

(Figure 23). In other words, the actual spacer of bivalent ligand **52** is composed by the OEG and the 1,2,3-triazol linkage parts, which suffices the required distance between two steroid binding sites.

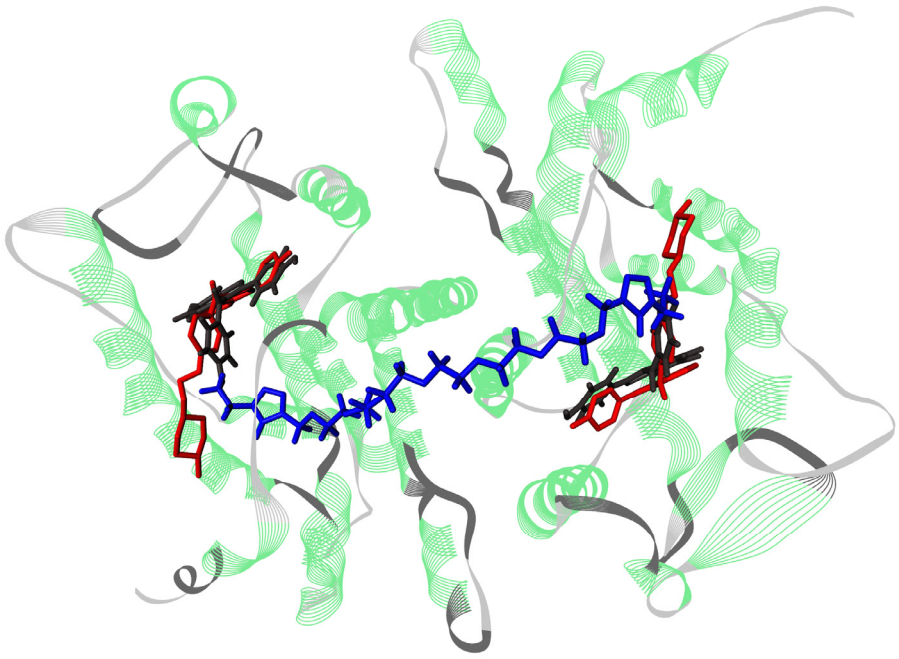

Figure 23. An overlay of bivalent ligand **52** (RAL moiety in black sticks, the 1,2,3-triazole and spacer in blue sticks) with LY156681 (in red sticks) bound to the ER LBP in the ERα LBD (green ribbons, PDB ID code 2R6W).

Thus, in this case, the spacer appears to have an undesirable impact on the enthalpy of the ligand-receptor interaction. The distance between two binding moieties of **52** in the ERα dimer obtained during the MD simulation was compared to the distance between two LY156681 molecules as can be found in the crystal structure (Figure 24). While the distances between the major parts of binding moieties (positions 1 to 4) of **52** changed only slightly (0.1 – 2.4 Å), the distances between the side-chains of LY156681 and the linkage groups of **52** (positions 5 to 7) showed a notable deviation (3.5 – 15 Å). In the latter case, a closer arrangement, especially for the 1,2,3-triazole parts, allowing for some relaxation of the attached spacer, was observed. Thus, it can be concluded that the bivalent RAL ligands have different ER-binding modes than the original RAL molecule, i.e., the absence of a hydrogen bond between bivalent ligand and Asp351 of the ERα. This feature can result in less ER-binding affinity.

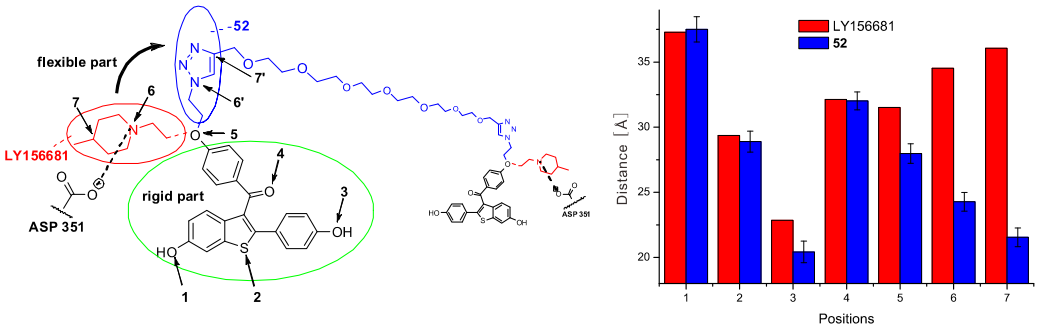

Figure 24. A distance comparison between two LY156681 molecules (in red) and two RAL moieties (in blue) of bivalent ligand **52** while bound to the ERα dimer (values obtained by 10 ns of MD simulation in water are plotted against values taken form the crystal structure of 2R6W).

3.4. Bivalent *cis*-4-OH tamoxifen ligand

3.4.1. Ligand design

Whereas the standard enthalpy $\Delta H°$ and entropy $\Delta S°$ of a ligand-receptor binding can be considered as the changes in intermolecular bond energy and the rearrangements undergone by the solvent molecules during the binding,[200] respectively, a high-affinity ER antagonoistic ligand like *cis*-4-OH tamoxifen (*cis*-OHT, Figure 25) can differently influence the enthalpic component via hydrogen bond and van der Waals interactions as raloxifene. On the basis of these considerations, new bivalent estrogen ligands tethered by same flexible spacers like bivalent RAL ligands were designed and prepared, so that both of them have a comparable conformational entropic cost caused by the spacer towards the ER-ligand binding. Meanwhile, *cis*-OHT was chosen as the estrogen binding moiety of bivalent estrogen ligands, because it was thought that this variation could be helpful to enhance the binding affinity of bivalent ER-ligand interaction.

The *cis*-isomer of OHT is an active metabolite of *cis*-tamoxifen (TAM, Figure 25) and has a high in vitro antagonistic potency for both ER subtypes.[201] In order to rationally design these bivalent *cis*-OHT ligands, a computer modeling of two crystal structures of the dimeric ER LBD bound to *cis*-OHT (PDB ID code 3ERT for ERα and 2FSZ for ERβ, Figure 25a and b) was performed by using the computer modeling software PyMOL. Compared to natural endogenous steroidal estrogen, e.g., E_2, the structures of ER bound to *cis*-OHT became in the 11β direction to accommodate the bulky and basic side-chain of *cis*-OHT by the reposition of H12.[96] Additionally,

this local remodeling of protein provided the bound *cis*-OHT molecule with an access to the exterior of the hydrophobic ER LBP so that a hydrogen bond could be formed between the surface aspartic acid (Asp351 of ERα and Asp303 of ERβ, respectively) and the basic amino group at the side-chain of *cis*-OHT molecule. Thus, to avoid any undesired impact on the ligand-receptor interaction caused by the structural modification, two *cis*-OHT moieties were tethered at this amino group via a carbon-nitrogen bond. It was found that the closest distance between these two nitrogen atoms in the dimeric ER LBD crystal structure was 33.2 and 34.3 Å, for ERα and ERβ, respectively. It is worth noting that there are four *cis*-OHT molecules in the crystal structure 2FSZ, two in the cognate binding sites (ER LPD) and other two in the hydrophobic CoA binding groove (subsite) of the protein surface. We found that the distance between the nitrogen atom of one *cis*-4-OHT molecule bound in the cognate binding site and another nitrogen atom of one *cis*-4-OHT molecule bound in the hydrophobic CoA binding groove of the same monomeric ER LBD was 16.7 Å.

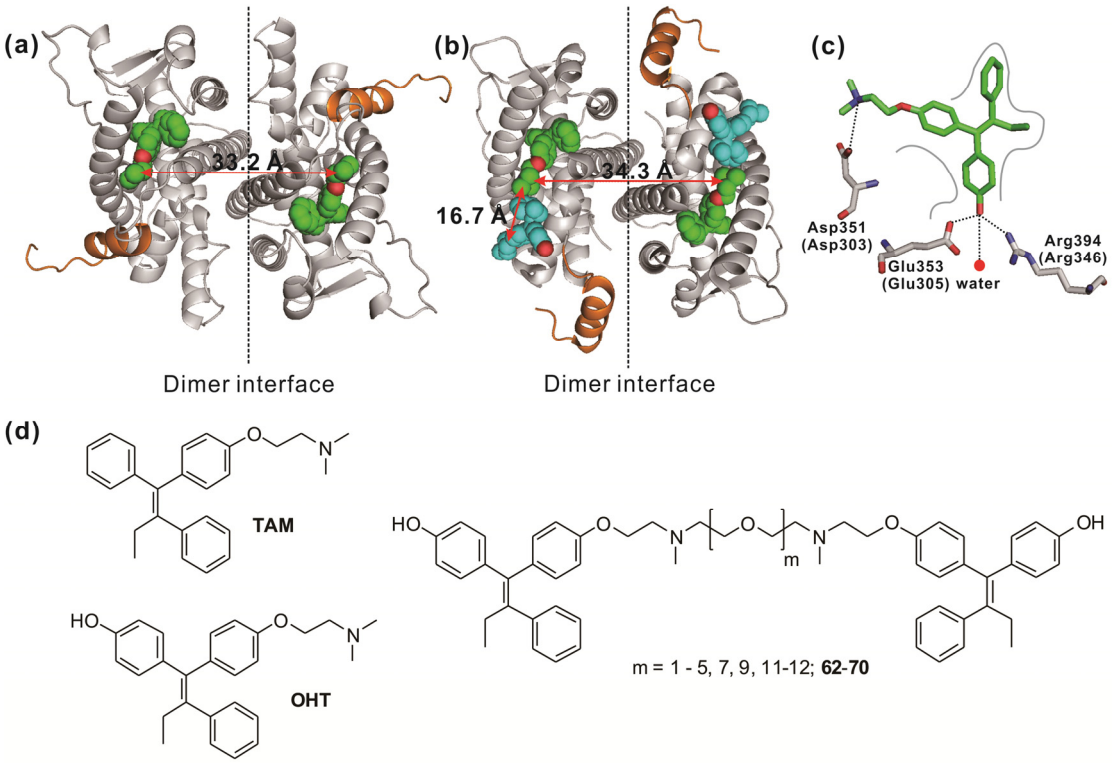

Figure 25. The distance between two nitrogen atoms of *cis*-4-OH tamoxifen (OHT) molecules (spheres) bound in the ER LBD homodimer (ribbons in gray, the ribbon of H12 in orange, PDB ID code 3ERT and 2FSZ) is 33.2 and 34.3 Å, for ERα and ERβ, respectively. (a) The crystal structure of the ERα dimer. (b) The crystal structure of the ERβ dimer. (c) Hydrogen bond interactions between an OHT molecule and ER LBD, hydrogen bonds are indicated by dashed

lines and a highly ordered water molecule (red dot) stabilized by a hydrogen bond network is indicated. (d) Chemical structures of *cis*-tamoxifen (TAM), *cis*-OHT, and bivalent *cis*-OHT ligands (**62**-**70**).

Like the previous study about bivalent RAL ligands, OEG was chosen as the spacer to tether two *cis*-OHT moieties. In order to further establish the intra- and intermolecular bivalent binding relationship for bivalent *cis*-OHT ligands, five short OEG spacers (EG1 to EG5) and four long OEG spacers (EG7, EG9 to EG11) were prepared as spacer to tether the binding moiety. The lengths of these OEG spacers varied from 7.2 to 43.1 Å, which were sufficient to span the space separating the between two cognate binding sites on dimeric ER LBD and between a cognate binding site and a CoA binding groove on the same monomeric ER LBD. Remarkably, the stereochemistry of OHT molecules played an important role in the ER-ligand binding and *cis*-OHT isomer had a stronger ER-binding affinity than E_2, approximately three times as much. By contrast, the *trans*-OHT isomer only had 2% RBA of E_2.[114,202]

3.4.2. Chemical preparation

According to previous reports, such a triarylethylene structure can be straightforwardly obtained, either by a nucleophilic substitution at deoxyanisoin with a Grignard reagent such as phenylmagnesium bromide or by a McMurry reaction between 4, 4'-dihydroxybenzophenone and propiophenone with low-valent titanium.[203-211] Thus, a McMurry reaction was applied to prepare dihydroxy triarylethylene **71** with a yield of 95%. Subsequently, the Mitsunobu reaction between one phenol group of **71** and benzyl carbamate protected 2-(methylamino) ethanol **72** in the presence of triphenylphosphine and diethylazodicarboxylate (DEAD) gave benzyl carbamate-protected endoxifen **73** as a mixture of *cis*:*trans* = 1:1 in a yield of 40%.[212] Under a mild hydrogenation condition, endoxifen **74** was obtained as a mixture of *cis*:*trans* = 1:1 isomers with a yield of 82% (Scheme 25).

Although the geometrical isomers of **74** can be separated by a RP-HPLC,[213] it was found the isomerization of *cis*-isomer of **74** to *trans*-isomer took place spontaneously during the subsequent nucleophilic substitution. Therefore, mono- and bivalent OHT ligands **69**, **70** and **75** were prepared based on both isomers of **74** with yields of 30-60%.[214] A geometrical isomer separation by RP-HPLC was not successful at first for bivalent ligands **69** and **70**, but was for monovalent

ligand **75** (Scheme 25).

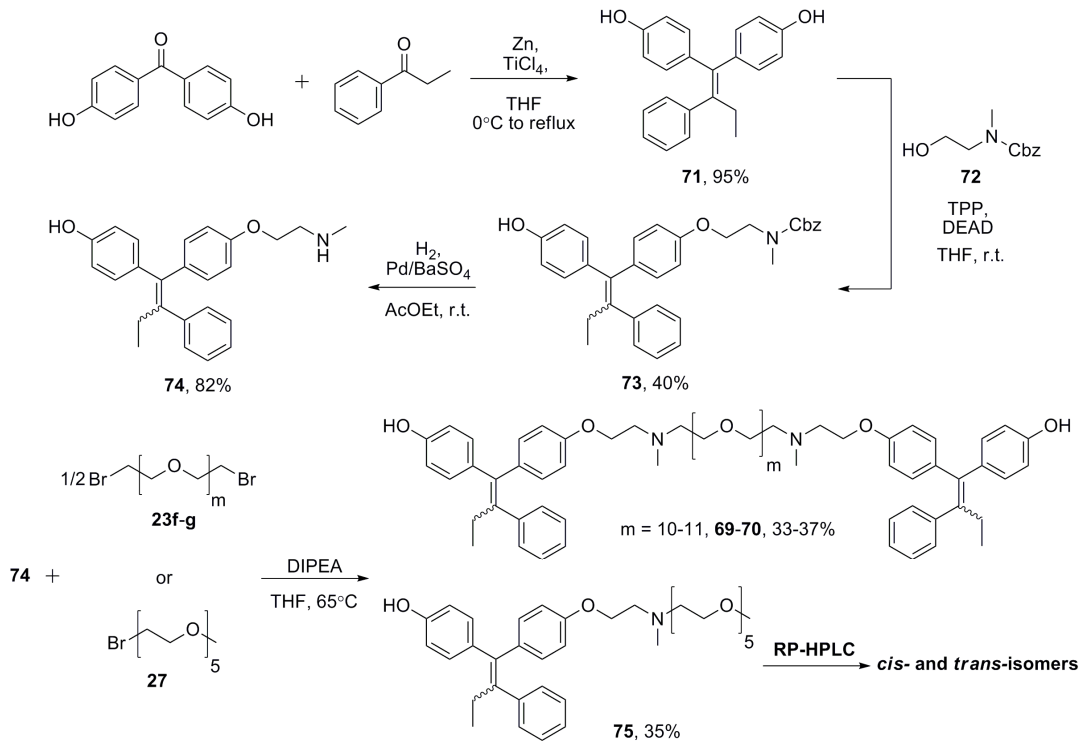

Scheme 25. Chemical preparation of mono- and bivalent OHT ligands (**69**, **70**, and **75**) via a nucleophilic substitution based on the amine **74**.

In order to obtain sufficient substance for the ER-binding assays, a novel synthetic partway was developed (Scheme 26), in which a nucleophilic substitution between dihydroxy triarylethylene **71** and bromoacetaldehyde diethyl acetal was performed to give the diethyl acetal **76** with a yield of 42%. After an acidic catalyzed hydrolysis, aldehyde **77** was obtained with a yield of 83% as a mixture of *cis*:*trans* = 1:1 isomers. Due to the facile isomerization of the triarylethylene structure, both isomers of **77** were applied for the reductive amination with bis(*N*-methylamine) OEG spacers **22** to obtain bivalent OHT ligands **62-69** with yields of 40-80%.[215-217] Subsequently, geometrical isomer separations by RP-HPLC were successful to give *cis*-*cis*, *cis*-*trans*, and *trans*-*trans* isomers for each bivalent ligand. To ensure the purity of these isomers,[179] after much effort it was found that only less than 3% *cis*-*cis* isomer underwent to *cis*-*trans* isomer, but no *trans*-*trans* isomer, after 48 hours in polar solvents such as methanol and water.

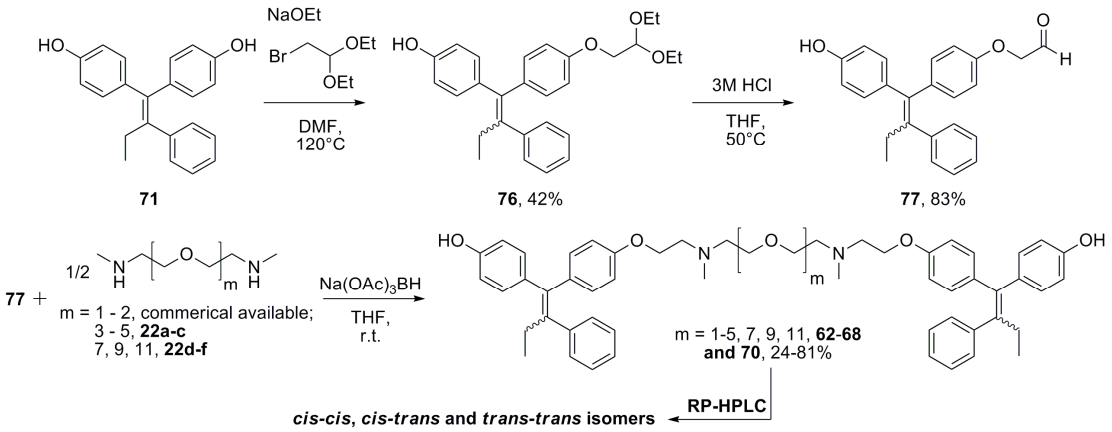

Scheme 26. Chemical preparation of bivalent OHT ligands **62-69** via a reductive amination.

3.4.3. Biological evaluation

In order to evaluate the binding affinities of mono- and bivalent OHT ligands prepared above, competitive radiometric assays with [^{3}H]-E_2[107,108] (Section 1.2.4) were carried out in the group of Prof. Dr. John A. Katzenellenbogen (Department of Chemistry, University of Illinois at Urbana-Champaign). For eight bivalent ligands (**62-69**), the evaluated bivalent ligands are of two types: (1) homo bivalent ligands, in which both of OHT molecules were *cis*-isomer, which were expected to have higher affinities than (2) hetero bivalent ligands, in which one *cis*-OHT molecule was tethered one *trans*-OHT molecule. Whereas hetero bivalent ligands, i.e., *cis-trans* isomer, had similar lipophilicity as homo bivalent, i.e., *cis-cis* isomer, in aqueous solvent, their binding behaviors could be considered as a monovalent control for homo bivalent ligands. Both isomers of the monovalent control **75** were evaluated separately for their ER-binding affinities. Additionally, two bivalent ligands **69** and **70** were also evaluated as a mixture of isomers, in which *cis-cis* : *cis-trans* : *trans-trans* = 1:2:1. These assays were performed for both ER subtypes, ERα and ERβ. [^{3}H]-E_2 was used as a tracer and E_2 as a standard. Binding affinities expressed as relative binding affinity (RBA) values, which is relative to the binding affinity of E_2 (RBA = 100%, Section 1.2.4, Equation 17), are showed in Table 3.

Table 3. Structure, maximum spacer lengths, and relative binding affinity (RBA) values of mono- and bivalent OHT ligands **62**-**70** and **75**.

Ligand	Structure, maximum spacer length [Å] [a]	*cis*- / *cis-cis* isomer		*trans*- / *cis-trans* isomer	
		ERα	ERβ	ERα	ERβ
62	OHT2EG1, 7.2	13.8 ± 4.3	6.11 ± 1.4	6.60 ± 0.5	3.44 ± 0.7
63	OHT2EG2, 10.8	16.4 ± 2.1	5.55 ± 1.3	23.5 ± 5.2	6.25 ± 0.6
64	OHT2EG3, 14.4	37.2 ± 2.3	13.9 ± 3.4	8.16 ± 2.0	9.57 ± 1.8
65	OHT2EG4, 18.0	14.9 ± 4.0	12.2 ± 2.1	13.6 ± 1.3	4.77 ± 1.5
66	OHT2EG5, 21.6	20.8 ± 5.5	12.8 ± 2.0	10.9 ± 2.3	3.20 ± 1.0
67	OHT2EG7, 28.8	30.7 ± 2.8	20.7 ± 1.6	32.3 ± 8.1	9.48 ± 1.4
68	OHT2EG9, 35.9	28.1 ± 3.7	7.92 ± 1.5	23.9 ± 6.9	7.85 ± 2.0
70	OHT2EG11, 43.1	27.9 ± 4.0	7.17 ± 1.4	18.0 ± 5.0	7.60 ± 2.2
75	OHTEG5Me, 19.2	78.1 ± 12	34.2 ± 1.7	12.4 ± 2.2	8.03 ± 0.0070
69 [b]	OHT2EG10, 39.5	17.2 ± 2.0	9.53 ± 2.4	-	-
70 [b]	OHT2EG11, 43.1	21.8 ± 3.1	9.75 ± 0.57	-	-

a. The maximum spacer length, between two nitrogen atoms in a extend conformation, was measured by the modeling software PyMOL. b. For bivalent OHT ligands **69** and **70**, their ER-binding affinities were also evaluated based on a mixture of *cis-cis* : *cis-trans* : *trans-trans* = 1:2:1 isomers.

In general, binding affinities of bivalent OHT ligands were lower than that of E_2 and the RBA values in ERα are higher than in ERβ. Figure 26 shows the relationship between the RBA values and maximum spacer lengths of bivalent OHT ligands, in which the binding affinities of bivalent OHT ligands were related to the maximum spacer length and peaked at 14.4 and 28.8 Å (EG3 and EG7, respectively) in both ER subtypes. These results are not only consistent with our previous interpretation about the intra- and intermolecular ER-binding (Section 3.3.3) but also more precisely provide information about the spacer length for each mode on the ER (Figure 20). Moreover, *cis-cis* isomers of **64**-**67** had overall stronger ER-binding affinities than the *cis-trans* isomers on the ERβ, but not on the ERα. In addition, the *cis*-isomer of monovalent ligand **75** had a much higher binding affinity in both ER subtypes than its *trans*-isomer and bivalent OHT ligand **65** which was tethered by a comparable long spacer. This indicated that the stereochemistry did play an important role in the ER-binding event and suggested that the *trans-trans* isomer of bivalent OHT ligand could have much weaker binding affinity compared to the other isomers. On the other hand, certain intramolecular interactions, e.g., a π-π stacking between two OHT moieties or a spacer folding, took place within the bivalent OHT ligands and led to an unfavorable conformation towards the ER-binding. As a consequence, the binding affinities of bivalent OHT

ligands were significantly reduced due to the energy penalty of the deconstruction of such conformations. Remarkably, it was suspected that an isomerization of high-affinity *cis*-isomer to low-affinity *trans*-isomer also occurred in the case of bivalent OHT ligand based on the approximate RBA values of pure *cis-cis* isomer of **70** and its isomer mixture (Table 3, line 8 and 11).

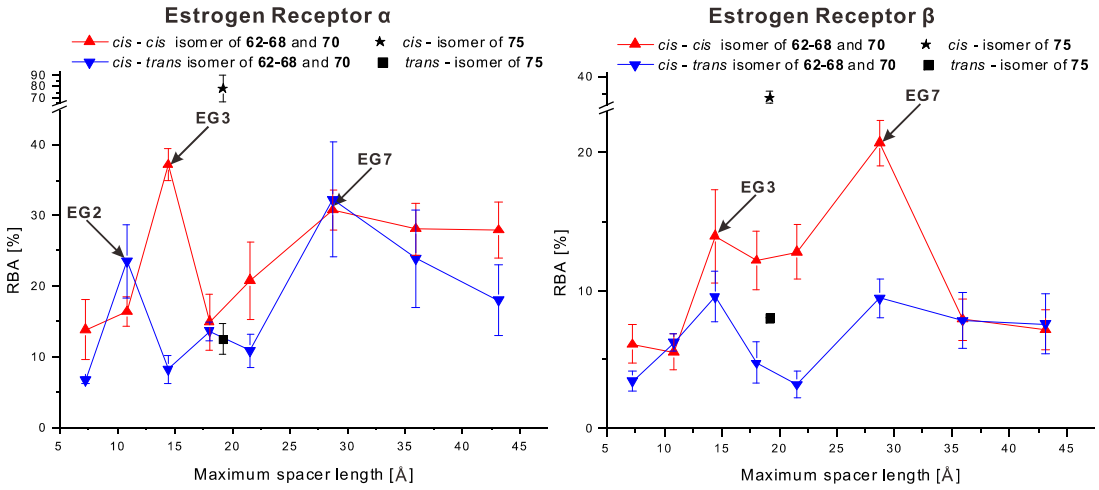

Figure 26. The relationship between relative binding affinity (RBA) for both ER subtypes (left: ERα, right: ERβ) and maximum spacer length. A red line represents *cis-cis* isomers of bivalent OHT ligands (**62-68** and **70**), a blue line their *cis-trans* isomers, a black star the *cis*-isomer of monovalent ligand **75**, and a black square its *trans*-isomer.

Interestingly, bivalent OHT ligand **62** tethered by a 7.2 Å spacer (EG1) did not reach a maximum binding peak like in the case of bivalent RAL ligands, while bivalent OHT ligand **64** tethered by a 14.4 Å spacer (EG3) peaked on both ER subtypes. This difference implies that the *cis*-OHT moiety specifically bound to a different secondary site in the ERα as RAL moiety did. Therefore, an intramolecular bivalent binding could only be achieved by **64** rather than **62**. Moreover, the binding affinity difference between *cis-cis* and *cis-trans* isomers of **64** on the ERα (37.2% versus 8.16%) was higher than that on the ERβ (13.9% versus 9.57%). This suggested that the stereochemistry tolerance of this secondary site on the ERβ was lower than on the ERα. Additionally, the *cis-trans* isomer of bivalent OHT ligand **63** tethered by a 10.8 Å long spacer (EG2) also reached a maximum binding peak on the ERα, which indicated the *trans*-OHT moiety could additionally bind to a different secondary site, where the *cis*-OHT moiety did not.

The second maximum binding peak was reached by bivalent OHT ligand **67** tethered by a 28.8 Å long spacer (EG7) on both ER subtypes. It is inferred that this maximum binding peak is

achieved by an intermolecular bivalent binding between two ER LBPs. It cannot be rationalized why the difference between ER-binding affinities of *cis*-*cis* and *cis*-*trans* isomer of **67** on the ERα is nearly identical (30.7% versus 32.3%), although the *trans*-OHT only had 1.7% RBA of *cis*-OHT.[202] It has been expected that the binding affinity of the *cis*-*trans* isomer of **67** would be lower than that of the *cis*-*cis* isomer of **67**. Thus, it was speculated that the lipophilicity of the OHT moiety was so essential in the ER-binding that the *trans*-OHT moiety could also either bind to the ER LBP or interact somewhere on the ER surface. By contrast, the binding affinity difference between the *cis*-*cis* and *cis*-*trans* isomer of **67** on the ERβ (20.7% versus 9.48%) was much larger. This indicated that an intermolecular bivalent binding on the ERβ could be achieved by the *cis*-*cis* isomer of **67**. Remarkably, a slow decrease in the binding affinity with the increasing spacer length in the case of **67**, **68**, and **70** on the ERα, but not on the ERβ revealed that the intermolecular bivalent binding could still be achieve by spacers longer than 28.8 Å on the ERα, while on the ERβ it could only be formed by the spacer of 28.8 Å. This difference reflects the fact that the ERα LBP is slightly larger than the ERβ LBP and that these two ER subtypes have only 55% homology.

4. Summary and conclusion

In this thesis a convergent synthetic route was carried out to prepare three series of bivalent estrogen ligands tethered by flexible spacers of varying length according to the structure-based ligand design. These bivalent ligands were not only biologically evaluated with estrogen receptor (ER) to determinate their ER-binding affinities but also investigate via different methods to explain their ER-binding abilities.

In the first part of the work bivalent *trans*-diethylstilbestrol (DES) ligands tethered by oligoethylene glycol (OEG) or hybrid OEG spacers (e.g. containing a rigid biphenyl segment) with lengths in the range of 34.8-46.7 Å were studied. It was found that the polar amide linkage group of these bivalent ligands results in a dramatic decrease in the ER binding affinity compared to the original monovalent DES ligand and therefore, only weak binding affinities were observed. Among these bivalent DES ligands, bivalent DES ligand tethered by a OEG spacer of 43.1 Å gave the second best result which, however, was much lower than bivalent ligand tethered by a 10.8 Å OEG spacer. This finding indicated that there was an unexpected interaction between the second DES binding moiety and the receptor surface. Moreover, a computer calculation study demonstrated that there was not only an end-to-end distance decrease of bivalent ligand due to the folding conformation of the OEG spacer but also a stable hydrophobic-hydrophobic interaction between two DES moieties and the hybrid segment of the spacer.[29]

To further understand the structure-activity relationship (SAR) of bivalent estrogen ligand, in the second part bivalent raloxifene (RAL) ligands tethered by OEG spacers of lengths in the range of 4.7-47.7 Å were synthesized and a systematic investigation was carried out. Two bivalent binding modes, either intra- or intermolecular bivalent binding, were hypothesized to explain their different binding abilities (Figure 27a). It was found that 22.7 Å is the critical spacer length to distinguish the intra- from intermolecular bivalent binding on the dimeric ERα LBD. The maximum intermolecular bivalent binding affinity (10% RBA of estradiol (E_2)) was achieved when the spacer length is 26.2 Å. Remarkably, it was experimentally confirmed that bivalent ligands tethered by long spacers had weak ER binding affinities caused by ligand shielding due to folding of the OEG spacer. By contrast, those tethered by short spacers exposed their ligands to the receptor more readily. Consequently, they had more unimpeded access to the receptor and

stronger ER binding affinities (Figure 27b). Thus, not only the entropic (the folding of OEG spacer) but also the enthalpic (intramolecular interactions) difference between the initial and final conformation state of a bivalent ligand in the aqueous environment does have a major impact on the protein-ligand interaction. Moreover, the absence of hydrogen bond interaction between the linkage group (1,2,3-triazole) of bivalent RAL ligand and the protein residue (Asp351) had an undesirable impact on the enthalpic contribution of the ligand-receptor interaction.[30]

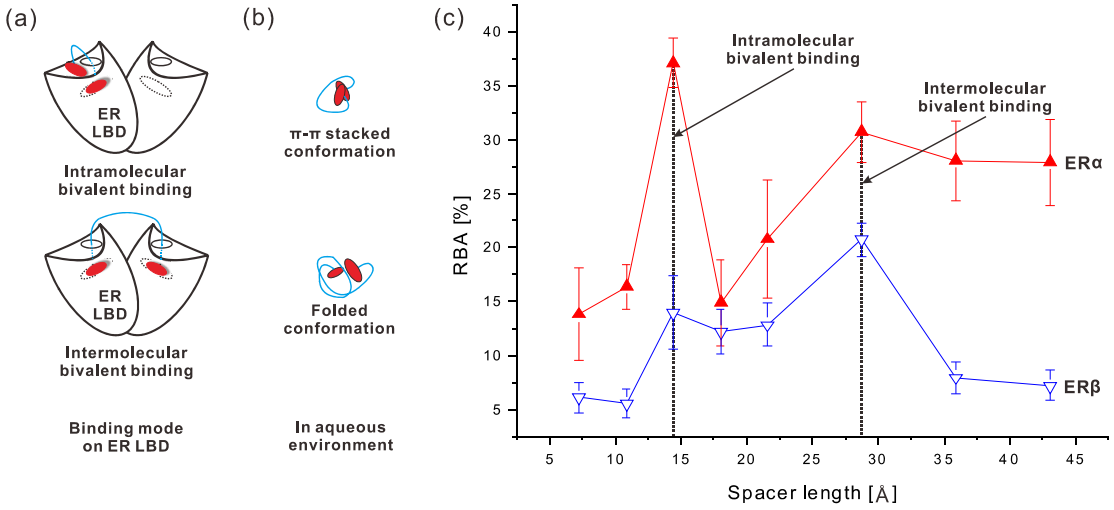

Figure 27. (a) Two bivalent binding modes on the dimeric estrogen receptor ligand binding domain (ER LBD). (b) The conformation of bivalent estrogen ligands tethered by flexible spacers of varying length in the aqueous environment. (c) Two maximum binding peaks (intra- and intermolecular) on both ER subtypes.

To avoid the undesirable decrease in ER binding affinity due to the modification of the ligand, it was necessary to design a bivalent estrogen ligand based on a high-affinity monovalent estrogen ligand with little modification. Therefore, in the third part bivalent *cis*-OH tamoxifen (OHT) ligands tethered by OEG spacers with lengths in the range of 7.2-43.1 Å were prepared based on the monovalent *cis*-OHT ligand and evaluated with two ER subtypes to determinate their ER binding affinities. Although their ER binding abilities were decreased by their undesirable conformation in the aqueous environment,[30] two maximum binding affinity peaks at the spacer lengths of 14.4 and 28.8 Å were found (up to 37% and 31% RBA of E_2, respectively, Figure 27c), which correspond to the intra- and intermolecular bivalent binding modes, respectively. These results were not only consistent with our previous hypothesis but they also provide an intuitive and precise understanding about the SAR of bivalent estrogen ligands for both ER subtypes, in

particular for ERβ.

Based on the ER binding affinities of the three bivalent estrogen ligands mentioned above and in previous reports, it has been sufficiently indicated that there are several factors needed to be considered for the bivalent estrogen ligand design. Firstly, an antagonistic estrogen binding moiety, e.g., RAL or *cis*-OHT, has a better access for the spacer to tether from the exterior of the receptor due to the antagonistic ER-binding mode. By contrast, an agonistic estrogen binding moiety has difficulty in getting such an access unless it has a large substitution at the 17α position of the steroidal structure which, however, can reduce the ER binding affinity of bivalent estrogen ligands. For instance, bivalent ethynyl estradiol (EE_2) ligands prepared by LaFrate et al.[124] showed much better ER binding affinity than bivalent E_2 ligands which did not have such an large substitute at the 17α position.[120,121] Secondly, the tethered position and the linkage group should be consistent with the environment of the individual bound estrogen ligand. In the case of bivalent *trans*-DES ligands, the introduction of a hydrophilic linkage group dramatically reduced its ER binding affinity. Conversely, the tertiary amine linkage group of bivalent *cis*-OHT ligands could maintain the hydrogen bond interaction with the protein residues, and consequently, bivalent *cis*-OHT ligands had much higher ER binding affinities. Thirdly, the use of a rigid central element as originally suggested by Whitesides et al.[1] can help to minimize the conformational entropy loss and enhance the binding affinity as long as there is no intramolecular interaction between this rigid element and the tethered estrogen binding moiety. A good example was demonstrated by bivalent estrogen ligands tethered by rigid DNA spacers.[198] In contrast, in the case of flexible spacers, it was found that there were intramolecular hydrophobic interactions between the biphenyl segment of the spacer and the tethered *trans*-DES moiety which could significantly reduce the ER binding affinity.[29] Finally, by using flexible spacers, some structural requirements such as the angle of ligand presentation and spacer length can be readily provided but not by rigid spacers. The flexibility of polyether spacers, however, also increased the structural uncertainty of the ligand due to its folded conformation and the hydrophobic-hydrophobic interaction of its tethered estrogen moieties.[30]

In conclusion, achieving high-affinity bivalent binding to the dimeric ER LBD is a daunting challenge. In this thesis, the SAR of bivalent estrogen ligands tethered by lengths of flexible spacers has been established. Two bivalent ER binding modes, intra- and intermolecular, that are

essential for the design of high-affinity bivalent estrogen ligand, have been proposed and confirmed based on two series of bivalent estrogen ligands, respectively. These results sufficiently indicate that the achievement of a bivalent binding to the ER dimer cannot simply be dissolved by a structure-based drug design, e.g., choosing a spacer to span the distance between two LBDs. Thus, a systemic understanding about the binding behavior of the bivalent ligands, in particular regarding the conformation of bivalent ligands in the aqueous environment, the intramolecular interaction caused by either the hydrophilic or hydrophobic parts of the bivalent ligand, and the character of the binding moiety, needs to be considered. Additionally, in the case of the ER, further investigation of intramolecular bivalent binding is warranted. Bivalent estrogen ligands tethered by flexible spacers of short length (approximately 10-14 Å) provide a new opportunity for the design of a high-affinity inhibitor of the ER-Coactivator interaction.

5. Outlook

Since the bivalent interaction between the dimeric estrogen receptor (ER) and bivalent estrogen ligand is strongly influenced by not only the spacer length of bivalent ligand but also its conformation in the aqueous environment, two different strategies could be carried out to improve the intra- and intermolecular bivalent interactions.

The first strategy is to develop a hetero bivalent ER inhibitor in which one estrogen ligand and one coactivator inhibitor are tethered by a flexible spacer of 10-15 Å. It was reported that a proportion of ER-positive tumors are intrinsically resistant to antihormonal therapy such as *cis*-4-OH tamoxifen. For example, in metastatic ER-positive breast cancer this proportion is approximately 80%.[218] On the other hand, the development of a coactivator inhibitor has also become more attractive in the recent years. The activity of the best coactivator inhibitor, however, is still just in the micromolar range.[219-221] Moreover, the hetero bivalent ligands have shown a potential application in different types of ligand-protein interaction as well as the chemical induced dimerization between two protein molecules.[222,223] Thus, a combination of the estrogen ligand and the coactivator inhibitor may overcome the drug resistance of ER-positive tumor and the low activity of the coactivator inhibitor.

Whereas the folded conformation of bivalent estrogen ligand caused by the gauche effect is the major drawback of the flexible spacer, Whitesides and co-workers proposed to use a rodlike oligopiperidine which is not only water soluble but also provides the bivalent ligand certain rigidity.[224] A similar concept has been applied in the case of bivalent estrogen ligands tethered by the biocompatible DNA spacer which gave more promising results than those with flexible spacers.[198] Therefore, tethering two estrogen ligands by a rigid spacer of approximately 30 Å is another way to improve the ER-binding affinity of the intermolecular bivalent interaction.

6. Experimental part

General. All chemical were purchased from Sigma-Aldrich, Acros, and Alfa Aesar, and were used without further purification. Anhydrous solvents were obtained from an anhydrous solvent purification system. For anhydrous reactions, all glasswares were oven-dried overnight and cooled under vacuum, then purged with argon; all such reactions were conducted under argon. ^{1}H and ^{13}C NMR spectra were recorded on a Joel EXC400 spectrometer or a Bruker AC250 spectrometer with probe temperatures of 25°C, ^{1}H NMR chemical shifts are reported in ppm (three significant digits) relative to the residual proton signal of the NMR solvent and coupling constants (*J*) are given in hertz (Hz). ^{13}C chemical shifts are reported in ppm (three significant digits) relative to the carbon signal of the NMR solvent. 2D NMR spectra were recorded on a Bruker AVANCE III 700 spectrometer with probe temperatures of 37°C. Thin layer chromatography (TLC) plates (Merck F254 silica gel on aluminum plates) were visualized by using 1.5 g $KMnO_4$, 10 g K_2CO_3, and 1.25 mL 10% NaOH in 200 mL water, with UV light (254 nm). High resolution mass spectra (HRMS) were obtained on an Agilent 6210 ESI-TOF spectrometer and UV-spectra were performed on a Varian Cary 100 UV/VIS spectrometer. GC/MS spectra were performed on a Varian Saturn 2100T spectrometer.

All final products were characterized with ^{1}H, ^{13}C NMR, and HRMS, except that those products which readily undergo a *cis-trans* isomerization, were characterized with ^{1}H NMR and HRMS.

6.1. Bi-functionalized oligoethylene glycol (OEG)

6.1.1. Chemical preparation of ditosylated OEG 1

(1) General procedure for chemical preparations of ditosylated OEG **1a-b**:

To a solution of the OEG diol (1.0 equivalent) in THF, 4-methylbenzene sulfonyl chloride (3.0 equivalents) was added at room temperature and then cooled to 0°C. To this mixture, potassium hydroxide (6.6 equivalents) in H_2O (0.9 g/mL) was added dropwise over 1 h. Then the reaction mixture was stirred at 0°C for 30 min and some white precipitation appeared. Afterwards this mixture was further stirred at room temperature until TLC analysis indicated complete consumption of the OEG diol. The reaction mixture was neutralized with a saturated ammonium

chloride solution and concentrated in vacuo. The residue was absorbed on the silica gel and further purified by column chromatography to obtain the pure ditosylate OEG **1**.

(2) Ditosylated OEG **1a**:

Tetraethylene glycol (17.4g, 89.6 mmol), 4-methylbenzene sulfonyl chloride (57.0 g, 299 mmol), potassium hydroxide (37.0 g, 660 mmol), 150 mL THF, and 40 mL H_2O were used and the crude product was purified by column chromatography (chloroform : MeOH = 10 : 1) to give the ditosylate **1a** as a light yellow oil (17.5g, 35%).

^{1}H-NMR ($CDCl_3$, 400 MHz) δ (ppm) = 7.79 (4H, d, J = 8.4 Hz, Ar-*H*), 7.33 (4H, d, J = 8.0 Hz, Ar-*H*), 4.17-4.14 (4H, m, $OCH_2CH_2OSO_2$), 3.69-3.67 (4H, m, $OCH_2CH_2OSO_2$), 3.58-3.55 (8H, m, OCH_2CH_2O), 2.44 (6H, s, CH_3).

^{13}C-NMR ($CDCl_3$, 100 MHz) δ (ppm) = 145, 133, 130, 128, 70.9, 70.8, 69.5, 68.9, 21.8.

(3) Ditosylated OEG **1b**:

Pentaethylene glycol (2.01 g, 8.45 mmol), 4-methylbenzene sulfonyl chloride (4.88 g, 25.4 mmol), potassium hydroxide (3.13 g, 55.8 mmol), 20 mL THF, and 3.5 mL H_2O were used and the crude product was purified by column chromatography (DCM : MeOH = 30 : 1) to give the ditosylate **1b** as a colorless oil (4.44 g, 96%).

^{1}H-NMR ($CDCl_3$, 400 MHz) δ (ppm) = 7.79 (4H, d, J = 8.4 Hz, Ar-*H*), 7.34 (4H, d, J = 8.5 Hz, Ar-*H*), 4.17-4.14 (4H, m, $OCH_2CH_2OSO_2$), 3.69-3.67 (4H, m, $OCH_2CH_2OSO_2$), 3.60-3.58 (12H, m, OCH_2CH_2O), 2.44 (6H, s, CH_3).

^{13}C-NMR ($CDCl_3$, 100 MHz) δ (ppm) = 145, 133, 130, 128, 70.9, 70.8, 70.7, 69.4, 68.9, 21.8.

6.1.2. Chemical preparation of monobenzylate OEG 2

(1) General procedure for chemical preparations of monobenzylate OEG **2a-b**:

To a solution of the OEG diol (4.0 equivalents) in 50% aqueous NaOH (4.0 equivalents), benzyl chloride (1.0 equivalent) was added and the reaction mixture was stirred and heated up to 100°C for 20 h. Then the mixture was cooled to 0°C and neutralized with a saturated ammonium chloride solution and concentrated in vacuo. The residue was distilled with a Kugel Rohr to obtain the pure monobenzylated OEG **2**.

(2) Monobenzylate OEG **2a**:

Triethylene glycol (31.8 g, 212 mmol), NaOH (8.48 g, 212 mmol), benzyl chloride (6.16 mL, 53.0

mmol), and 8.4 mL H_2O were used and the crude product was distilled with a Kugelrohr (140°C, 0.02 mbar) to give the monobenzylated **2a** a colorless oil (9.49 g, 75%).

^{1}H-NMR ($CDCl_3$, 400 MHz) δ (ppm) = 7.34-7.33 (4H, m, Ar-*H*), 7.29-7.26 (1H, m, Ar-*H*), 4.57 (2H, s, BnC*H*$_2$O), 3.72-3.59 (12H, m, OC*H*$_2$C*H*$_2$O), 2.60 (1H, s, CH$_2$O*H*).

^{13}C-NMR ($CDCl_3$, 100 MHz) δ (ppm) = 138, 128, 73.4, 72.7, 70.8, 70.6, 69.5, 61.9.

(3) Monobenzylate OEG **2b**:

Tetraethylene glycol (39.1 g, 201 mmol), NaOH (8.05 g, 201 mmol), benzyl chloride (5.84 mL, 50.0 mmol), and 8.0 mL H_2O were used and the crude product was distilled with a Kugelrohr (191-203°C, 0.27-0.31 mbar) to give the monobenzylated **2b** a colorless oil (9.51 g, 67%).

^{1}H-NMR ($CDCl_3$, 400 MHz) δ (ppm) = 7.34-7.33 (4H, m, Ar-*H*), 7.29-7.26 (1H, m, Ar-*H*), 4.56 (2H, s, BnC*H*$_2$O), 3.70-3.58 (16H, m, OC*H*$_2$C*H*$_2$O), 2.79 (1H, br s, CH$_2$O*H*).

^{13}C-NMR ($CDCl_3$, 100 MHz) δ (ppm) = 138, 129, 128, 73.4, 72.7, 70.8, 70.7, 70.4, 69.6.

6.1.3. Chemical preparation of monobenzylated, monotosylate OEG 3

To a solution of the monobenzylated **2b** (2.36 g, 8.31 mmol) in 20 mL THF, 4-methylbenzene sulfonyl chloride (2.40 g, 12.5 mmol) was added at room temperature and then cooled to 0°C. To this mixture, potassium hydroxide (1.54 g, 27.4 mmol) in 1.6 mL H_2O (0.9 g/mL) was added dropwise over 15 min. Then the reaction mixture was stirred at 0°C for 30 min and some white precipitation appeared. Afterwards this mixture was further stirred at room temperature until TLC analysis indicated complete consumption of **2b**. The reaction mixture was neutralized with a saturated ammonium chloride solution and concentrated in vacuo. The residue was absorbed on the silica gel and further purified by column chromatography (DCM : MeOH = 40 : 1) to give **3** as a colorless oil (2.91 g, 80%).

^{1}H-NMR ($CDCl_3$, 400 MHz) δ (ppm) = 7.79 (4H, d, J = 8.2 Hz, Ar-*H*), 7.34-7.32 (6H, m, Ar-*H*), 7.30-7.26 (1H, m, Ar-*H*), 4.56 (2H, s, BnC*H*$_2$O), 4.16-4.13 (2H, m, OCH$_2$C*H*$_2$OSO$_2$), 3.69-3.58 (14H, m, OC*H*$_2$CH$_2$OSO$_2$ and OC*H*$_2$C*H*$_2$O), 2.44 (3H, s, C*H*$_3$).

^{13}C-NMR ($CDCl_3$, 100 MHz) δ (ppm) = 145, 139, 133, 130, 129, 128, 73.4, 71.0, 70.8, 70.7, 69.6, 69.4, 68.9.

6.1.4. Chemical preparation of dibenzylate OEG 4

(1) General procedure for preparations of dibenzylate OEG **4a-f**:

To a solution of the hydroxyl functionalized OEG (monobenzylate alcohol or diol, 1.0 equivalent) in anhydrous THF at 0°C, sodium hydride (1.1 equivalents for monobenzylate alcohol or 2.2 equivalents for diol, respectively) was added portionwise and the reaction mixture was stirred at 0°C for an additional 30 min. Afterwards the mixture was heated up to reflux for 1 h and then cooled to 0°C again. To this mixture, the tosylated OEG (1.0 equivalent for monotosylated or 2.0 equivalents for ditosylated, respectively) in anhydrous THF was added dropwise though a dropping funnel over 30 min. Then the mixture was heated up to reflux for 20 h. The mixture was cooled to 0°C and neutralized with a saturated ammonium chloride solution, brine, and concentrated in vacuo. The residue was absorbed on the silica gel and further purified by column chromatography to obtain the pure dibenzylate OEG **4**.

(2) Dibenzylate OEG **4a**:

The monobenzylate OEG **2a** (500 mg, 2.08 mmol), sodium hydride (91.5 mg, 2.29 mmol), the monotosylated OEG **3** (95.9 mg, 2.18 mmol), and 30 mL anhydrous THF were used and the crude product was purified by column chromatography (DCM : MeOH = 40 : 1) to give the dibenzylate OEG **4a** as a colorless oil (653 mg, 62%).

^{1}H-NMR ($CDCl_3$, 400 MHz) δ (ppm) = 7.35-7.26 (10H, m, Ar-*H*), 4.56 (4H, s, BnCH_2O), 3.72-3.63 (28H, m, OCH_2CH_2O).

^{13}C-NMR ($CDCl_3$, 100 MHz) δ (ppm) = 139, 129, 128, 73.4, 70.8, 69.6.

(3) Dibenzylate OEG **4b**:

The monobenzylate OEG **2b** (610 mg, 2.14 mmol), sodium hydride (94.3 mg, 2.36 mmol), the monotosylated OEG **3** (987 mg, 2.14 mmol), and 30 mL anhydrous THF were used and the crude product was purified by column chromatography (DCM : MeOH = 40 : 1) to give the dibenzylate OEG **4b** as a colorless oil (583 mg, 50%).

^{1}H-NMR ($CDCl_3$, 400 MHz) δ (ppm) = 7.34-7.26 (10H, m, Ar-*H*), 4.57 (4H, s, BnCH_2O), 3.72-3.59 (32H, m, OCH_2CH_2O).

^{13}C-NMR ($CDCl_3$, 100 MHz) δ (ppm) = 139, 129, 128, 73.5, 70.9, 70.8, 70.6, 69.6.

(4) Dibenzylate OEG **4c**:

Ethylene glycol (84.4 mg, 1.36 mmol), sodium hydride (114 mg, 2.86 mmol), the monotosylated OEG **3** (1.25 g, 2.86 mmol), and 30 mL anhydrous THF were used and the crude product was

purified by column chromatography (chloroform : MeOH = 20 : 1) to give the dibenzylate OEG **4c** as a colorless oil (416 mg, 52%).

^{1}H-NMR ($CDCl_3$, 400 MHz) δ (ppm) = 7.34-7.27 (10H, m, Ar-*H*), 4.56 (4H, s, BnCH_2O), 3.68-3.63 (36H, m, OCH_2CH_2O).

^{13}C-NMR ($CDCl_3$, 100 MHz) δ (ppm) = 139, 129, 128, 73.4, 70.9, 70.8, 69.6.

(5) Dibenzylate OEG **4d**:

Diethylene glycol (147 μL, 1.52 mmol), sodium hydride (128 mg, 3.20 mmol), the monotosylated OEG **3** (1.47 g, 3.35 mmol), and 20 mL anhydrous THF were used and the crude product was purified by column chromatography (chloroform : MeOH = 20 : 1) to give the dibenzylate OEG **4d** as a colorless oil (455 mg, 47%).

^{1}H-NMR ($CDCl_3$, 400 MHz) δ (ppm) = 7.34-7.26 (10H, m, Ar-*H*), 4.56 (4H, s, BnCH_2O), 3.67-3.63 (40H, m, OCH_2CH_2O).

^{13}C-NMR ($CDCl_3$, 100 MHz) δ (ppm) = 139, 129, 128, 73.4, 70.9, 70.8, 69.6.

(6) Dibenzylate OEG **4e**:

The monobenzylated OEG **2a** (1.63 g, 6.76 mmol), sodium hydride (281 mg, 7.03 mmol), the ditosylated OEG **1b** (1.83 g, 3.35 mmol), and 75 mL anhydrous THF were used and the crude product was purified by column chromatography (DCM : MeOH = 20 : 1) to give the dibenzylate OEG **4e** as a colorless oil (1.61 g, 71%).

^{1}H-NMR (MeOD, 400 MHz) δ (ppm) = 7.35-7.25 (10H, m, Ar-*H*), 4.54 (4H, s, BnCH_2O), 3.67-3.64 (4H, m, OCH_2CH_2O), 3.64-3.60 (40H, m, OCH_2CH_2O).

^{13}C-NMR (MeOD, 100 MHz) δ (ppm) = 140, 130, 129, 74.3, 71.7, 70.8.

(7) Dibenzylate OEG **4f**:

The monobenzylated OEG **2b** (1.94 g, 6.84 mmol), sodium hydride (298 mg, 7.44 mmol), the ditosylated OEG **1a** (1.70 g, 3.35 mmol), and 40 mL anhydrous THF were used and the crude product was purified by column chromatography (DCM : MeOH = 30 : 1) to give the dibenzylate OEG **4f** as a colorless oil (1.11 g, 45%).

^{1}H-NMR ($CDCl_3$, 400 MHz) δ (ppm) = 7.34-7.28 (10H, m, Ar-*H*), 4.56 (4H, s, BnCH_2O), 3.66-3.64 (48H, m, OCH_2CH_2O).

^{13}C-NMR ($CDCl_3$, 100 MHz) δ (ppm) = 138, 128, 73.3, 70.8, 70.7, 69.6.

(8) Dibenzylate OEG **4g**:

The monobenzylated OEG **2b** (2.01 g, 7.08 mmol), sodium hydride (430 g, 10.6 mmol), the ditosylated OEG **1b** (1.93 g, 3.54 mmol), and 15 mL anhydrous THF were used and the crude product was purified by column chromatography (DCM : MeOH = 20 : 1) to give the dibenzylate OEG **4f** as a colorless oil (1.14 g, 41%).

^{1}H-NMR ($CDCl_3$, 400 MHz) δ (ppm) = 7.35-7.27 (10H, m, Ar-*H*), 4.57 (4H, s, BnCH_2O), 3.68-3.62 (52H, m, OCH_2CH_2O).

^{13}C-NMR ($CDCl_3$, 100 MHz) δ (ppm) = 138, 129, 128, 73.4, 70.8, 70.7, 69.6.

6.1.5. Chemical preparation of OEG diol 5

(1) General procedure for preparation of OEG diol **5a-g**:

To a solution of the dibenzylated OEG **4** (1.0 equivalent) in EtOH, palladium on carbon (0.1 equivalent) was added and the reaction mixture was hydrogenated under 1.0 bar H_2 and stirred at room temperature until TLC analysis indicated complete consumption of the dibenzylate. Afterwards the mixture was filtered over Celite and the filter cake was washed with MeOH three times. This solution was concentrated in vacuo and the pure OEG diol **5** was obtained without any further purification.

(2) OEG diol **5a**:

The dibenzylated OEG **4a** (639 mg, 1.26 mmol), palladium on carbon (134 mg, 0.13 mmol), and 10 mL EtOH were used and the OEG diol **5a** as a colorless oil (411 mg, 99%).

^{1}H-NMR (DMSO-d6, 400 MHz) δ (ppm) = 4.57 (2H, br s, -O*H*), 3.51-3.33 (28H, m, OCH_2CH_2O).

^{13}C-NMR (DMSO-d6, 100 MHz) δ (ppm) = 72.3, 69.8, 60.2.

(3) OEG diol **5b**:

The dibenzylated OEG **4b** (578 mg, 1.05 mmol), palladium on carbon (112 mg, 0.105 mmol), and 20 mL EtOH were used and the OEG diol **5b** as a colorless oil (394 mg, 99%).

^{1}H-NMR (DMSO-d6, 400 MHz) δ (ppm) = 4.57 (2H, dt, J = 1.5 Hz, 5.4 Hz, -O*H*), 3.51-3.33 (32H, m, OCH_2CH_2O).

^{13}C-NMR (DMSO-d6, 100 MHz) δ (ppm) = 72.3, 69.8, 60.2.

(4) OEG diol **5c**:

The dibenzylated OEG **4c** (408 mg, 0.690 mmol), palladium on carbon (73.0 mg, 0.0690 mmol),

and 20 mL EtOH were used and the OEG diol **5c** as a colorless oil (284 mg, 99%).

^{1}H-NMR (DMSO-d6, 400 MHz) δ (ppm) = 4.57 (2H, br s, -O*H*), 3.51-3.33 (36H, m, OCH_2CH_2O).

^{13}C-NMR (DMSO-d6, 100 MHz) δ (ppm) = 72.3, 69.8, 60.2.

(5) OEG diol **5d**:

The dibenzylated OEG **4d** (446 mg, 0.700 mmol), palladium on carbon (74.3 mg, 0.0700 mmol), and 20 mL EtOH were used and the OEG diol **5d** as a colorless oil (314 mg, 97%).

^{1}H-NMR (DMSO-d6, 400 MHz) δ (ppm) = 4.58 (2H, br s, -O*H*), 3.55-3.47 (36H, m, OCH_2CH_2O), 3.42 - 3.39 (4H, m, OCH_2CH_2O).

^{13}C-NMR (DMSO-d6, 100 MHz) δ (ppm) = 72.4, 69.8, 60.2.

(6) OEG diol **5e**:

The dibenzylated OEG **4e** (1.61 g, 2.36 mmol), palladium on carbon (252 mg, 0.236 mmol), and 20 mL EtOH were used and the OEG diol **5e** as a colorless oil (1.11 g, 93%).

^{1}H-NMR (DMSO-d6, 400 MHz) δ (ppm) = 4.57 (2H, t, J = 5.6 Hz, -O*H*), 3.55-3.39 (44H, m, OCH_2CH_2O).

^{13}C-NMR (DMSO-d6, 100 MHz) δ (ppm) = 72.3, 69.7, 60.2.

(7) OEG diol **5f**:

The dibenzylated OEG **4f** (1.11 g, 1.52 mmol), palladium on carbon (162 mg, 0.152 mmol), and 20 mL EtOH were used and the OEG diol **5f** as a colorless oil (770 mg, 92%).

^{1}H-NMR (DMSO-d6, 400 MHz) δ (ppm) = 4.57 (2H, t, J = 5.3 Hz, -O*H*), 3.51-3.46 (44H, m, OCH_2CH_2O), 3.42 - 3.40 (4H, m, OCH_2CH_2O).

^{13}C-NMR (DMSO-d6, 100 MHz) δ (ppm) = 72.3, 69.8, 60.2.

(8) OEG diol **5g**:

The dibenzylated OEG **4g** (1.12 g, 1.45 mmol), palladium on carbon (160 mg, 0.145 mmol), and 40 mL EtOH were used and the OEG diol **5g** as a colorless oil (860 mg, 99%).

^{1}H-NMR (DMSO-d6, 400 MHz) δ (ppm) = 4.58 (2H, t, J = 5.6 Hz, -O*H*), 3.54-3.45 (48H, m, OCH_2CH_2O), 3.42 - 3.40 (4H, m, OCH_2CH_2O).

^{13}C-NMR (DMSO-d6, 100 MHz) δ (ppm) = 72.3, 69.8, 60.2.

6.1.6. Chemical preparation of ditosylate 6

(1) General procedure for preparation of ditosylate **6a-b**:

To a solution of a diol (1.0 equivalent) in THF, 4-methylbenzene sulfonyl chloride (3.0 equivalents) was added at room temperature and then cooled to 0°C. To this mixture, potassium hydroxide (6.6 equivalents) in H_2O (0.9 g/mL) was added dropwise over 1 h. Then the reaction mixture was kept at 0°C for 30 min and some white precipitation appeared. Afterwards this mixture was further stirred at room temperature until TLC analysis indicated complete consumption of the diol. The reaction mixture was neutralized with a saturated ammonium chloride solution and concentrated in vacuo. The residue was purified either by recrystallization or by column chromatography to obtain the pure ditosylate **6**.

(2) Ditosylate **6a**:

1,4-butandiol (5.00 mL, 55.2 mmol), 4-methylbenzene sulfonyl chloride (31.9 g, 165 mol), potassium hydroxide (20.4 g, 364 mmol), 70 mL THF, and 20 mL H_2O were used and the crude product was purified two times recrystallization in $CHCl_3$ to give the ditosylate **6a** as a light crystal (5.47 g, 25%).

^{1}H-NMR ($CDCl_3$, 400 MHz) δ (ppm) = 7.75 (4H, d, J = 8.1 Hz, Ar-*H*), 7.35 (4H, d, J = 8.5 Hz, Ar-*H*), 3.99 (4H, t, J = 5.0 Hz, OC*H*$_2$CH$_2$), 2.46 (6H, s, C*H*$_3$), 1.70 (4H, p, J = 2.3 Hz, OCH$_2$C*H*$_2$).

^{13}C-NMR ($CDCl_3$, 100 MHz) δ (ppm) = 145, 133, 130, 128, 69.6, 25.2, 21.9.

(3) Ditosylate **6b**:

1,8-octanediol (7.08 g, 48.4 mmol), 4-methylbenzene sulfonyl chloride (28.0 g, 145 mol), potassium hydroxide (16.3 g, 291 mmol), 120 mL THF, and 16 mL H_2O were used and the crude product was purified by column chromatography (chloroform : MeOH = 40 : 1) to give the ditosylate **6b** as a light crystal (5.73 g, 27%).

^{1}H-NMR ($CDCl_3$, 400 MHz) δ (ppm) = 7.78 (4H, d, J = 8.2 Hz, Ar-*H*), 7.35 (4H, d, J = 8.1 Hz, Ar-*H*), 4.00 (4H, t, J = 6.4 Hz, OC*H*$_2$CH$_2$), 2.45 (6H, s, C*H*$_3$), 1.61 (4H, p, J = 6.6 Hz, OCH$_2$C*H*$_2$CH$_2$), 1.30-1.17 (8H, m, C*H*$_2$).

^{13}C-NMR ($CDCl_3$, 100 MHz) δ (ppm) = 145, 133, 130, 128, 70.7, 28.8, 25.4, 21.8.

6.1.7. Chemical preparation of dibenzylate 7

(1) General procedure for preparation of dibenzylate **7a-b**

To a solution of the monobenzylate OEG **2b** (2.05 equivalents) in anhydrous THF at 0°C, sodium

hydride (2.5 equivalents) was added portionwise at 0°C and the reaction mixture was stirred for an additional 30 min. Afterwards the mixture was heated up to reflux for 1 h and then cooled to 0°C again. To this mixture, the ditosylate **6** (1.0 equivalent) in anhydrous THF was added dropwise though a dropping funnel over 30 min. Then the mixture was heated up to reflux for 20 h. The mixture was cooled to 0°C and neutralized with a saturated ammonium chloride solution and concentrated in vacuo. The residue was absorbed on the silica gel and further purified by column chromatography to obtain the pure dibenzylate hybrid OEG **7**.

(2) Dibenzylate **7a**:

The monobenzylate OEG **2b** (2.39 g, 8.39 mmol), sodium hydride (409 mg, 10.2 mmol), the ditosylate **6a** (1.63 g, 4.09 mmol), and 40 mL anhydrous THF were used and the crude product was purified by column chromatography (chloroform : MeOH = 40 : 1) to give the dibenzylate hybrid OEG **7a** as a colorless oil (1.91 g, 75%).

^{1}H-NMR ($CDCl_3$, 400 MHz) δ (ppm) = 7.34-7.31 (8H, m, Ar-*H*), 7.29-7.26 (2H, m, Ar-*H*), 4.56 (4H, s, BnCH_2O), 3.72-3.55 (32H, m, OCH_2CH_2O), 3.45 (4H, m, CH_2), 1.63 (4H, m, CH_2).

^{13}C-NMR ($CDCl_3$, 100 MHz) δ (ppm) = 138, 128, 73.3, 72.6, 71.2, 70.7, 70.4, 70.2, 69.5, 61.8, 26.4.

(3) Dibenzylate **7b**:

The monobenzylate OEG **2b** (1.97 g, 6.92 mmol), sodium hydride (338 mg, 8.44 mmol), the ditosylate **6b** (1.54 g, 3.38 mmol), and 40 mL anhydrous THF were used and the crude product was purified by column chromatography (chloroform : MeOH = 40 : 1) to give the dibenzylate hybrid OEG **7b** as a colorless oil (1.91 g, 83%).

^{1}H-NMR ($CDCl_3$, 400 MHz) δ (ppm) = 7.34-7.26 (2H, m, Ar-*H*), 4.56 (4H, s, BnCH_2O), 3.68-3.54 (32H, m, OCH_2CH_2O), 3.43 (4H, t, *J* = 6.8 Hz, CH_2), 1.56 (4H, p, *J* = 6.7 Hz, CH_2), 1.35-1.25 (8H, m, CH_2).

^{13}C-NMR ($CDCl_3$, 100 MHz) δ (ppm) = 138, 128, 73.2, 71.5, 70.7, 70.6, 70.1, 69.4, 29.6, 29.4, 26.0.

6.1.8. Chemical preparation of hybrid OEG 8

(1) General procedure for preparation of hybrid OEG **8a**-**b**:

To a solution of the dibenzylated hybrid OEG **7** (1.0 equivalent) in EtOH, palladium on carbon

(0.1 equivalent) was added and the reaction mixture was hydrogenated under 1.0 bar H_2 and stirred at room temperature until TLC analysis indicated complete consumption of the dibenzylate. Afterwards the mixture was filtered over Celite and the filter cake was washed with MeOH three times. This solution was concentrated in vacuo and the pure OEG diol **8** was obtained without any further purification.

(2) Hybrid OEG **8a**:

The dibenzylated hybrid OEG **7a** (1.86 g, 2.98 mmol), palladium on carbon (317 mg, 0.298 mmol), and 20 mL EtOH were used and the OEG diol **8a** as a colorless oil (1.27 g, 97%).

^{1}H-NMR ($CDCl_3$, 400 MHz) δ (ppm) = 3.71-3.58 (32H, m, OCH_2CH_2), 3.47 (4H, br s, $HOCH_2CH_2$), 2.97 (2H, br s, O*H*), 1.64 (4H, br s, $OCH_2CH_2CH_2CH_2O$).

^{13}C-NMR ($CDCl_3$, 100 MHz) δ (ppm) = 73.1, 72.7, 71.3, 70.7, 70.5, 70.2, 70.1, 61.8, 61.7, 26.4.

(3) Hybrid OEG **8b**:

The dibenzylated hybrid OEG **7b** (1.88 g, 2.77 mmol), palladium on carbon (295 mg, 0.277 mmol), and 20 mL EtOH were used and the OEG diol **8b** as a colorless oil (1.15 g, 84%).

^{1}H-NMR (DMSO-d6, 400 MHz) δ (ppm) = 4.58-4.56 (2H, t, J = 5.3 Hz, O*H*), 3.51-3.34 (36H, m, OCH_2CH_2), 1.47 (4H, t, J = 6.4 Hz, $OCH_2CH_2CH_2CH_2$), 1.26 (8H, br s, $OCH_2CH_2CH_2CH_2$).

^{13}C-NMR (DMSO-d6, 100 MHz) δ (ppm) = 72.3, 70.3, 69.8, 69.5, 60.2, 29.2, 28.8, 25.6.

6.1.9. Chemical preparation of monotritylate OEG 9

To a mixture of tetraethylene glycol (20.0 mL, 0.115 mol) and pyridine (1.39 mL, 17.0 mmol), powdered trityl chloride (3.26 g, 11.0 mmol) were added portionwise at 45°C and this reaction mixture was further stirred at 45°C for 16 h. This reaction suspension was first separated and the solid was removed. The residue was dissolved in toluene and washed with water for three times to remove the excess of tetraethylene glycol. The organic layer was dried over $MgSO_4$ and concentrated in vacuo to obtain monotritylate OEG **9** as a light yellow liquid (4.99 g, 99%).

^{1}H-NMR (Acetone-d6, 250 MHz) δ (ppm) = 7.52-7.48 (5H, m, Ar-*H*), 7.36-7.24 (10H, m, Ar-*H*), 3.68-3.51 (14H, m, OCH_2CH_2), 3.18 (2H, t, J = 5.2 Hz, CH_2OH), 2.08 (1H, s, O*H*).

^{13}C-NMR (Acetone-d6, 62.5 MHz) δ (ppm) = 145, 130, 129, 128, 73.6, 71.6, 71.4, 71.2, 64.4, 62.1.

6.1.10. Chemical preparation of ditritylate hybrid OEG 10

To a mixture of **9** (4.36 g, 10.0 mmol) in anhydrous THF, sodium hydride (460 mg, 11.4 mmol) was added portionwise at 0°C. The mixture was first stirred at room temperature for 30 min and then heated up to reflux for 1 h. To this cooled reaction mixture, potassium iodide (160 mg, 0.952 mmol) and 4,4'-bis(chloromethyl)-1,1'-biphenyl (1.26 g, 4.76 mmol) was added at room temperature. The mixture was heated up to reflux for 18 h. The reaction was controlled until TLC analysis indicated complete consumption of 4,4'-bis(chloromethyl)-1,1'-biphenyl. The mixture was quenched with water and extracted with ether and brine. The organic layer was dried over $MgSO_4$ and concentrated in vacuo. The residue was purified by 2 times column chromatography (chloroform : AcOEt = 40:1 to 10:1) to obtain a light yellow oil **10** (1.81 g, 36%).

^{1}H-NMR ($CDCl_3$, 400 MHz) δ (ppm) = 7.53 (4H, d, J = 8.4 Hz, Ar-*H*), 7.45 (12H, m, Ar-*H*), 7.38 (4H, d, J = 8.4 Hz, Ar-H), 7.27 (12H, m, Ar-*H*), 7.21 (6H, m, Ar-*H*), 4.58 (4H, s, ArCH_2O), 3.68 (28H, m, OCH_2CH_2), 3.22 (4H, t, J = 5.2 Hz, ArCH$_2$OCH_2CH$_2$).

^{13}C-NMR ($CDCl_3$, 100 MHz) δ (ppm) = 144, 140, 138, 129, 128, 127, 73.2, 71.0, 70.9, 69.7, 63.5.

6.1.11. Chemical preparation of hybrid OEG 11

To a solution of ditriylate hybrid OEG **10** (2.65 g, 2.53 mmol) in a mixture of MeOH (12 ml) and chloroform (8 ml), catalytic amount of para-toluene-4-sulfonic acid monohydrate (30.0 mg, 0.127 mmol) and 2 drops water were added and then the reaction mixture was stirred at room temperature for 24 h. The reaction was controlled until TLC analysis indicated complete consumption of ditriylate **10**. Afterwards, a solution sodium carbonate (30.0 mg, 0.250 mmol) was added. The organic layer was dried over $MgSO_4$ and concentrated in vacuo. The residue purified by column chromatography (DCM : MeOH = 20:1) to obtain a yellow oil **11** (890 mg, 62%).

^{1}H-NMR ($CDCl_3$, 400 MHz) δ (ppm) = 7.55 (4H, d, J = 8.0 Hz, Ar-*H*), 7.40 (4H, d, J = 8.0 Hz, Ar-*H*), 4.59 (4H, s, ArCH_2O), 3.65 (28H, m, OCH_2CH_2), 3.58 (4H, t, J = 4.4 Hz, CH_2OH), 3.45 (2H, s, O*H*).

^{13}C-NMR ($CDCl_3$, 100 MHz) δ (ppm) = 141, 138, 129, 127, 73.2, 72.7, 70.8, 70.5, 69.7, 62.0.

6.1.12. Chemical preparation of ditosylate OEG 12-14

(1) General procedure for chemical preparations of ditosylate OEG **12-14**:

To a solution of the diol (1.0 equivalent) in THF, 4-methylbenzene sulfonyl chloride (3.0

equivalents) was added at room temperature and then cooled to 0°C. To this mixture, potassium hydroxide (6.6 equivalents) in H_2O (0.9 g/mL) was added dropwise over 1 h. Then the reaction mixture was kept at 0°C for 30 min and some white precipitation appeared. Afterwards this mixture was further stirred at room temperature until TLC analysis indicated complete consumption of the OEG diol. The reaction mixture was neutralized with a saturated ammonium chloride solution and concentrated in vacuo. The residue was absorbed on the silica gel and further purified by column chromatography to obtain the pure ditosylate OEG.

(2) Ditosylate OEG **12a**:

OEG diol **5b** (217 mg, 0.590 mmol), 4-methylbenzene sulfonyl chloride (339 mg, 1.76 mmol), potassium hydroxide (217 mg, 3.87 mmol), 5 mL THF, and 0.20 mL H_2O were used and the crude product was purified by column chromatography (chloroform : MeOH = 40 : 1) to give the ditosylate **12a** as a light yellow oil (184 mg, 46%).

^{1}H-NMR ($CDCl_3$, 400 MHz) δ (ppm) = 7.79 (4H, d, J = 8.4 Hz, Ar-*H*), 7.34 (4H, d, J = 8.0 Hz, Ar-*H*), 4.17-4.14 (4H, m, $OCH_2CH_2OSO_2$), 3.70-3.66 (4H, m, $OCH_2CH_2OSO_2$), 3.65-3.60 (16H, m, OCH_2CH_2O), 3.58 (8H, br s, OCH_2CH_2O), 2.45 (6H, s, CH_3).

^{13}C-NMR ($CDCl_3$, 100 MHz) δ (ppm) = 145, 133, 130, 128, 70.9, 70.7, 70.6, 69.4, 68.8, 21.8.

HRMS (ESI-TOF, positive): $[C_{30}H_{46}O_{13}S_2Na]^+$ cal. 701.2272, found 701.2250; $[C_{30}H_{46}O_{13}S_2K]^+$ cal. 717.2011, found 717.1992.

(3) Ditosylate OEG **12b**:

OEG diol **5d** (175 mg, 0.380 mmol), 4-methylbenzene sulfonyl chloride (221 mg, 1.15 mmol), potassium hydroxide (142 mg, 2.52 mmol), 5 mL THF, and 0.14 mL H_2O were used and the crude product was purified by column chromatography (chloroform : MeOH = 40 : 1) to give the ditosylate **12b** as a light yellow oil (211 mg, 73%).

^{1}H-NMR ($CDCl_3$, 400 MHz) δ (ppm) = 7.79 (4H, d, J = 8.3 Hz, Ar-*H*), 7.34 (4H, d, J = 8.0 Hz, Ar-*H*), 4.17-4.14 (4H, m, $OCH_2CH_2OSO_2$), 3.70-3.66 (4H, m, $OCH_2CH_2OSO_2$), 3.66-3.60 (24H, m, OCH_2CH_2O), 3.58 (8H, br s, OCH_2CH_2O), 2.45 (6H, s, CH_3).

^{13}C-NMR ($CDCl_3$, 100 MHz) δ (ppm) = 145, 133, 130, 128, 71.1, 71.0, 70.9, 69.6, 69.1, 22.0.

HRMS (ESI-TOF, positive): $[C_{34}H_{54}O_{15}S_2Na]^+$ cal. 789.2796, found 789.2772; $[C_{34}H_{54}O_{15}S_2K]^+$ cal. 805.2536, found 805.2511.

(4) Ditosylate OEG **12c**:

OEG diol **5e** (246 mg, 0.490 mmol), 4-methylbenzene sulfonyl chloride (278 mg, 1.45 mmol), potassium hydroxide (179 mg, 3.19 mmol), 10 mL THF, and 0.20 mL H_2O were used and the crude product was purified by column chromatography (DCM : MeOH = 10 : 1) to give the ditosylate **12c** as a light yellow oil (380 mg, 98%).

^{1}H-NMR ($CDCl_3$, 400 MHz) δ (ppm) = 7.79 (4H, d, J = 8.4 Hz, Ar-*H*), 7.34 (4H, d, J = 8.1 Hz, Ar-*H*), 4.17-4.15 (4H, m, $OCH_2CH_2OSO_2$), 3.70-3.67 (4H, m, $OCH_2CH_2OSO_2$), 3.65-3.61 (28H, m, OCH_2CH_2O), 3.58 (8H, br s, OCH_2CH_2O), 2.45 (6H, s, CH_3).

^{13}C-NMR ($CDCl_3$, 100 MHz) δ (ppm) = 145, 133, 130, 128, 70.9, 70.8, 70.7, 69.4, 68.9, 21.8.

(5) Ditosylate OEG **12d**:

OEG diol **5f** (302 mg, 0.552 mmol), 4-methylbenzene sulfonyl chloride (319 mg, 1.66 mmol), potassium hydroxide (205 mg, 3.65 mmol), 13 mL THF, and 0.23 mL H_2O were used and the crude product was purified by column chromatography (DCM : MeOH = 20 : 1 to 15 : 1) to give the ditosylate **12d** as a light yellow oil (434 mg, 92%).

^{1}H-NMR ($CDCl_3$, 400 MHz) δ (ppm) = 7.79 (4H, d, J = 8.2 Hz, Ar-*H*), 7.34 (4H, d, J = 8.0 Hz, Ar-*H*), 4.17-4.15 (4H, m, $OCH_2CH_2OSO_2$), 3.72-3.55 (44H, m, $OCH_2CH_2OSO_2$ and OCH_2CH_2), 2.45 (6H, s, CH_3).

^{13}C-NMR ($CDCl_3$, 100 MHz) δ (ppm) = 145, 133, 130, 128, 70.9, 70.7, 69.4, 68.9, 21.8.

HRMS (ESI-TOF, positive): $[C_{38}H_{62}S_2O_{17}Na]^+$ cal. 877.3321, found 877.3277; $[C_{38}H_{62}S_2O_{17}K]^+$ cal. 893.3060, found 893.3016.

(6) Ditosylate OEG **12e**:

OEG diol **5g** (1.29 g, 2.19 mmol), 4-methylbenzene sulfonyl chloride (0.92 g, 4.82 mmol), potassium hydroxide (490 mg, 8.76 mmol), 15 mL THF, and 1.0 mL H_2O were used and the crude product was purified by column chromatography (DCM : MeOH = 20 : 1) to give the ditosylate **12e** as a light yellow oil (1.76 g, 90%).

^{1}H-NMR ($CDCl_3$, 400 MHz) δ (ppm) = 7.79 (4H, d, J = 8.4 Hz, Ar-*H*), 7.34 (4H, d, J = 8.0 Hz, Ar-*H*), 4.17-4.15 (4H, m, $OCH_2CH_2OSO_2$), 3.70-3.57 (48H, m, $OCH_2CH_2OSO_2$ and OCH_2CH_2), 2.45 (6H, s, CH_3).

^{13}C-NMR ($CDCl_3$, 100 MHz) δ (ppm) = 145, 133, 130, 128, 71.0, 70.8, 69.5, 68.9, 21.9.

(7) Ditosylate OEG **13a**:

OEG diol **8a** (656 mg, 1.48 mmol), 4-methylbenzene sulfonyl chloride (856 mg, 4.45 mmol),

potassium hydroxide (549 mg, 9.78 mmol), 20 mL THF, and 0.5 mL H_2O were used and the crude product was purified by column chromatography (DCM : MeOH = 40 : 1) to give the ditosylate **13a** as a light yellow oil (718 mg, 65%).

^{1}H-NMR ($CDCl_3$, 400 MHz) δ (ppm) = 7.79 (4H, d, J = 8.2 Hz, Ar-*H*), 7.34 (4H, d, J = 8.0 Hz, Ar-*H*), 4.17-4.15 (4H, m, $OCH_2CH_2OSO_2$), 3.70-3.67 (4H, m, $OCH_2CH_2OSO_2$), 3.64-3.61 (12H, m, OCH_2CH_2), 3.59-5.54 (12H, m, OCH_2CH_2), 3.46 (4H, t, J = 5.3 Hz, $OCH_2CH_2CH_2CH_2O$), 2.45 (6H, s, CH_3), 1.63 (4H, p, J = 3.4 Hz, $OCH_2CH_2CH_2CH_2O$).

^{13}C-NMR ($CDCl_3$, 100 MHz) δ (ppm) = 145, 133, 130, 128, 71.3, 70.9, 70.8, 70.7, 70.3, 69.4, 68.9, 26.5, 21.9.

(8) Ditosylate OEG **13b**:

OEG diol **8b** (1.13 g, 2.27 mmol), 4-methylbenzene sulfonyl chloride (1.31 g, 6.82 mmol), potassium hydroxide (842 mg, 15.0 mmol), 10 mL THF, and 0.8 mL H_2O were used and the crude product was purified by column chromatography (chloroform : MeOH = 40 : 1) to give the ditosylate **13b** as a light yellow oil (1.29 g, 70%).

^{1}H-NMR ($CDCl_3$, 400 MHz) δ (ppm) = 7.79 (4H, d, J = 8.2 Hz, Ar-*H*), 7.34 (4H, d, J = 8.1 Hz, Ar-*H*), 4.17-4.15 (4H, m, $OCH_2CH_2OSO_2$), 3.70-3.67 (4H, m, $OCH_2CH_2OSO_2$), 3.64-3.61 (12H, m, OCH_2CH_2), 3.58-5.55 (12H, m, OCH_2CH_2), 3.43 (4H, t, J = 6.7 Hz, $OCH_2CH_2CH_2CH_2$) 2.45 (6H, s, CH_3), 1.58-1.52 (4H, m, $OCH_2CH_2CH_2CH_2$), 1.29 (8H, br s, $OCH_2CH_2CH_2CH_2$).

^{13}C-NMR ($CDCl_3$, 100 MHz) δ (ppm) = 145, 133, 130, 128, 71.7, 70.9, 70.8, 70.7, 70.2, 69.4, 68.9, 29.8, 29.6, 26.2, 21.8.

(9) Ditosylate OEG **14**:

OEG diol **11** (97.0 mg, 0.171 mmol), 4-methylbenzene sulfonyl chloride (72.0 mg, 0.376 mmol), potassium hydroxide (38.0 mg, 0.684 mmol), 10 mL THF, and 0.4 mL H_2O were used and the crude product was purified by column chromatography (chloroform : MeOH = 40 : 1) to give the ditosylate **14** as a light yellow oil (136 mg, 91%).

^{1}H-NMR ($CDCl_3$, 400 MHz) δ (ppm) = 7.76 (4H, d, J = 8.2 Hz, Ar-*H*), 7.34 (4H, d, J = 8.2 Hz, Ar-*H*), 7.38 (4H, d, J = 8.1 Hz, Ar-*H*), 7.30 (4H, d, J = 8.0 Hz, Ar-*H*), 4.58 (4H, s, $ArCH_2O$), 4.14-4.11 (4H, m, $OCH_2CH_2OSO_2$), 3.67-3.56 (28H, m, $OCH_2CH_2OSO_2$ and OCH_2CH_2O), 2.41 (6H, s, CH_3).

^{13}C-NMR ($CDCl_3$, 100 MHz) δ (ppm) = 145, 140, 138, 133, 130, 128, 127, 73.2, 71.0, 70.9, 70.8,

70.7, 69.7, 69.4, 68.9, 21.8.

6.1.13. Chemical preparation of diazide OEG 15-17

(1) General procedure for chemical preparations of diazide OEG **15-17**:

To a solution of the ditosylate OEG (1.0 equivalent) in anhydrous DMF, sodium azide (3.0 equivalents) was added at room temperature and then this mixture was stirred and heated up to 110°C for 12 h until TLC analysis indicated complete consumption of the ditosylate. The solvent was removed in vacuo and the residue was absorbed on the silica gel and further purified by column chromatography to obtain the pure diazide OEG.

(2) Diazide OEG **15a**:

Ditosylate OEG **12c** (177 mg, 0.218 mmol), sodium azide (43.0 mg, 0.654 mmol), and 10 mL anhydrous DMF were used and the crude product was purified by column chromatography (DCM : MeOH = 10 : 1) to give the ditosylate **15a** as a light yellow oil (122 mg, 99%).

^{1}H-NMR ($CDCl_3$, 400 MHz) δ (ppm) = 3.72-3.60 (40H, m, OCH_2CH_2O), 3.39 (4H, t, J = 5.1 Hz, N_3OCH_2).

^{13}C-NMR ($CDCl_3$, 100 MHz) δ (ppm) = 70.9, 70.8, 70.7, 70.2, 50.8.

(3) Diazide OEG **15b**:

Ditosylate OEG **12d** (195 mg, 0.228 mmol), sodium azide (45.0 mg, 0.685 mmol), and 6 mL anhydrous DMF were used and the crude product was purified by column chromatography (DCM : MeOH = 20 : 1) to give the ditosylate **15b** as a light yellow oil (103 mg, 75%).

^{1}H-NMR ($CDCl_3$, 400 MHz) δ (ppm) = 3.70-3.61 (44H, m, OCH_2CH_2O), 3.39 (4H, t, J = 5.2 Hz, N_3OCH_2).

^{13}C-NMR ($CDCl_3$, 100 MHz) δ (ppm) = 70.9, 70.8, 70.3, 50.9.

(4) Diazide OEG **15c**:

Ditosylate OEG **12e** (500 mg, 0.556 mmol), sodium azide (108 mg, 1.67 mmol), and 10 mL anhydrous DMF were used and the crude product was purified by column chromatography (DCM : MeOH = 20 : 1) to give the ditosylate **15c** as a light yellow oil (352 mg, 99%).

^{1}H-NMR ($CDCl_3$, 400 MHz) δ (ppm) = 3.68-3.61 (48H, m, OCH_2CH_2O), 3.36 (4H, t, J = 5.2 Hz, N_3OCH_2).

^{13}C-NMR ($CDCl_3$, 100 MHz) δ (ppm) = 70.9, 70.8, 70.7, 70.2, 50.9.

(5) Diazide OEG **16a**:

Ditosylate OEG **13a** (341 mg, 0.450 mmol), sodium azide (89.5 mg, 1.36 mmol), and 10 mL anhydrous DMF were used and the crude product was purified by column chromatography (DCM : MeOH = 40 : 1) to give the ditosylate **16a** as a light yellow oil (211 mg, 95%).

^{1}H-NMR ($CDCl_3$, 400 MHz) δ (ppm) = 3.70-3.62 (24H, m, OCH_2CH_2O), 3.58-3.56 (4H, m, $N_3OCH_2CH_2$), 3.47 (4H, t, J = 5.3 Hz, $OCH_2CH_2CH_2CH_2O$), 3.39 (4H, t, J = 5.2, $N_3OCH_2CH_2$), 1.64 (4H, p, J = 2.6 Hz, $OCH_2CH_2CH_2CH_2O$).

^{13}C-NMR ($CDCl_3$, 100 MHz) δ (ppm) = 71.3, 70.9, 70.8, 70.2, 50.9, 26.5.

(6) Diazide OEG **16b**:

Ditosylate OEG **13b** (367 mg, 0.450 mmol), sodium azide (89.5 mg, 1.36 mmol), and 15 mL anhydrous DMF were used and the crude product was purified by column chromatography (chloroform : MeOH = 40 : 1) to give the ditosylate **16b** as a light yellow oil (190 mg, 77%).

^{1}H-NMR ($CDCl_3$, 400 MHz) δ (ppm) = 3.70-3.63 (24H, m, OCH_2CH_2O), 3.59-3.57 (4H, m, $N_3OCH_2CH_2$), 3.44 (4H, t, J = 6.8 Hz, $OCH_2CH_2CH_2CH_2$), 3.39 (4H, t, J = 5.1, $N_3OCH_2CH_2$), 1.57 (4H, t, J = 6.7 Hz, $OCH_2CH_2CH_2CH_2$), 1.30 (8H, s, $OCH_2CH_2CH_2CH_2$).

^{13}C-NMR ($CDCl_3$, 100 MHz) δ (ppm) = 71.7, 70.9, 70.3, 50.9, 29.8, 29.7, 26.3.

(7) Diazide OEG **17**:

Ditosylate OEG **14** (501 mg, 0.570 mmol), sodium azide (113 mg, 1.72 mmol), and 10 mL anhydrous DMF were used and the crude product was purified by 2 times column chromatography (DCM : MeOH = 40 :1 and chloroform : MeOH = 40 : 1) to give the ditosylate **17** as a light yellow oil (179 mg, 51%).

^{1}H-NMR ($CDCl_3$, 400 MHz) δ (ppm) = 7.56 (4H, d, J = 8.1 Hz, Ar-*H*), 7.34 (4H, d, J = 8.1 Hz, Ar-*H*), 4.61 (4H, s, $ArCH_2O$), 3.71-3.62 (28H, m, OCH_2CH_2O), 3.37 (4H, t, J = 5.2 Hz, $N_3OCH_2CH_2$).

^{13}C-NMR ($CDCl_3$, 100 MHz) δ (ppm) = 140, 138, 128, 127, 73.2, 70.9, 70.2, 69.7, 50.9.

6.1.14. Chemical preparation of diamine OEG 18-20

(1) General procedure for chemical preparations of diamine OEG **18-20**

To a solution of diazide OEG (1.0 equivalent) in anhydrous THF, triphenylphosphine (2.1 equivalents) was added at 0°C and then the reaction mixture was stirred at room temperature for

10 h. Afterwards 0.05 mL water was added to hydrolyze the iminophosphoranes and the mixture was stirred at room temperature until TLC analysis indicated complete consumption of the diazide. The solvent was removed and the residue was absorbed on the silica gel and further purified by column chromatography to obtain the pure diamine OEG.

(2) Diamine OEG **18a**:

Diazide OEG **15a** (121 mg, 0.219 mmol), triphenylphosphine (122 mg, 0.459 mmol), and 10 mL anhydrous THF were used and the crude product was purified by column chromatography (MeOH : NH_4OH [25% in water] = 9 : 1) to give the ditosylate **18a** as a light yellow oil (78.6 mg, 71%).

^{1}H-NMR ($CDCl_3$, 400 MHz) δ (ppm) = 3.67-3.60 (36H, m, OCH_2CH_2O), 3.52 (4H, t, J = 5.1 Hz, H_2NOCH$_2$CH_2), 2.87 (4H, br s, H_2NOCH_2CH$_2$), 1.67 (4H, br s, H_2NOCH$_2$CH$_2$).

^{13}C-NMR ($CDCl_3$, 100 MHz) δ (ppm) = 73.5, 70.7, 70.5, 42.0.

HRMS (ESI-TOF, positive): $[C_{22}H_{49}N_2O_{10}]^+$ cal. 501.3382, found 501.3398.

(3) Diamine OEG **18b**:

Diazide OEG **15b** (97.8 mg, 0.164 mmol), triphenylphosphine (95.5 mg, 0.361 mmol), and 20 mL anhydrous THF were used and the crude product was purified by column chromatography (MeOH : NH_4OH [25% in water] = 9 : 1) to give the ditosylate **18b** as a light yellow oil (62.5 mg, 72%).

^{1}H-NMR ($CDCl_3$, 400 MHz) δ (ppm) = 3.68-3.61 (40H, m, OCH_2CH_2O), 3.53 (4H, t, J = 5.2 Hz, H_2NOCH$_2$CH_2), 2.89 (4H, t, J = 5.0 Hz, H_2NOCH_2CH$_2$), 1.99 (4H, br s, H_2NOCH$_2$CH$_2$).

^{13}C-NMR ($CDCl_3$, 100 MHz) δ (ppm) = 73.3, 70.7, 70.5, 41.9.

HRMS (ESI-TOF, positive): $[C_{24}H_{53}N_2O_{11}]^+$ cal. 545.3644, found 545.3629.

(4) Diamine OEG **18c**:

Diazide OEG **15c** (199 mg, 0.311 mmol), triphenylphosphine (180 mg, 0.685 mmol), and 20 mL anhydrous THF were used and the crude product was purified by column chromatography (MeOH : NH_4OH [25% in water] = 9 : 1) to give the ditosylate **18c** as a light yellow oil (146 mg, 80%).

^{1}H-NMR ($CDCl_3$, 400 MHz) δ (ppm) = 3.70-3.61 (44H, m, OCH_2CH_2O), 3.52 (4H, t, J = 5.2 Hz, H_2NOCH$_2$CH_2), 2.87 (4H, t, J = 5.0 Hz, H_2NOCH_2CH$_2$), 1.72 (4H, br s, H_2NOCH$_2$CH$_2$).

^{13}C-NMR ($CDCl_3$, 100 MHz) δ (ppm) = 73.5, 70.8, 70.5, 42.0.

HRMS (ESI-TOF, positive): $[C_{26}H_{57}N_2O_{12}]^+$ cal. 589.3906, found 589.3954.

(5) Diamine OEG **19a**:

Diazide OEG **16a** (206 mg, 0.419 mmol), triphenylphosphine (244 mg, 0.922 mmol), and 15 mL anhydrous THF were used and the crude product was purified by column chromatography (MeOH : NH_4OH [25% in water] = 9 : 1) to give the ditosylate **19a** as a light yellow oil (140 mg, 75%).

^{1}H-NMR (DCM-d2, 400 MHz) δ (ppm) = 3.61-3.52 (24H, m, OCH_2CH_2O), 3.46-3.43 (8H, m, OCH_2CH$_2$CH$_2$CH_2O and H$_2$NCH$_2$CH_2O), 2.80 (4H, t, J = 5.2 Hz, H$_2$NOCH_2CH$_2$), 1.61 (4H, t, J = 2.9 Hz, OCH$_2$CH_2CH_2CH$_2$O), 1.49 (4H, br s, H_2NOCH$_2$CH$_2$).

^{13}C-NMR (DCM-d2, 100 MHz) δ (ppm) = 73.9, 71.3, 70.9, 70.6, 70.4, 42.2, 26.8.

HRMS (ESI-TOF, positive): $[C_{20}H_{45}N_2O_8]^+$ cal. 441.3170, found 441.3198; $[C_{20}H_{46}N_2O_8]^{2+}$ cal. 221.1622, found 221.1625.

(6) Diamine OEG **19b**:

Diazide OEG **16b** (102 mg, 0.186 mmol), triphenylphosphine (103 mg, 0.390 mmol), and 10 mL anhydrous THF were used and the crude product was purified by column chromatography (MeOH : NH_4OH [25% in water] = 9 : 1) to give the ditosylate **19b** as a light yellow oil (64.5 mg, 70%).

^{1}H-NMR ($CDCl_3$, 400 MHz) δ (ppm) = 3.69-3.61 (20H, m, OCH_2CH_2O), 3.59-3.56 (4H, m, OCH_2CH_2O), 3.53 (4H, t, J = 5.0 Hz, H$_2$NCH$_2$CH_2O), 3.44 (4H, t, J = 6.8 Hz, OCH_2CH$_2$CH$_2$CH$_2$), 2.88 (4H, br s, H$_2$NOCH_2CH$_2$), 2.04 (4H, br s, H_2NCH$_2$CH$_2$O), 1.57 (4H, p, J = 6.6 Hz, OCH$_2$CH_2CH$_2$CH$_2$), 1.30 (8H, br s, OCH$_2$CH$_2$CH_2CH_2).

^{13}C-NMR ($CDCl_3$, 100 MHz) δ (ppm) = 73.2, 71.7, 70.7, 70.4, 70.2, 41.8, 29.8, 29.6, 26.2.

HRMS (ESI-TOF, positive): $[C_{24}H_{53}N_2O_8]^+$ cal. 497.3796, found 497.3805.

(7) Diamine OEG **20**:

Diazide OEG **17** (171 mg, 0.278 mmol), triphenylphosphine (170 mg, 0.611 mmol), and 15 mL anhydrous THF were used and the crude product was purified by column chromatography (MeOH : NH_4OH [25% in water] = 9 : 1) to give the ditosylate **20** as a light yellow oil (120 mg, 76%).

^{1}H-NMR (DCM-d2, 400 MHz) δ (ppm) = 7.59 (4H, d, J = 8.2 Hz, Ar-*H*), 7.42 (4H, d, J = 8.2 Hz, Ar-*H*), 4.58 (4H, s, ArCH_2O), 3.65-3.56 (24H, m, OCH_2CH_2O), 3.44 (4H, t, J = 5.2 Hz,

$H_2NCH_2CH_2O$), 2.79 (4H, t, J = 5.3 Hz, $H_2NOCH_2CH_2$), 1.46 (4H, br s, $H_2NCH_2CH_2O$).

^{13}C-NMR (DCM-d2, 100 MHz) δ (ppm) = 140, 138, 129, 127, 74.0, 73.1, 70.9, 70.6, 70.1, 42.2.

HRMS (ESI-TOF, positive): $[C_{30}H_{49}N_2O_8]^+$ cal. 565.3483, found 565.3472; $[C_{30}H_{50}N_2O_8]^{2+}$ cal. 283.1778, found 283.1773.

6.1.15. Chemical preparation of dialkynyl OEG 21

(1) General procedure for preparation of dialkynyl OEG **21a-l**:

To a solution of the OEG diol **5** (1.0 equivalent) in anhydrous THF at 0°C, sodium hydride (2.2 equivalents) was added portionwise and the reaction mixture was stirred at 0°C for an additional 30 min. Afterwards the mixture was heated up to reflux for 1h and then cooled to 0°C again. To this mixture, propargyl bromide (2.2 equivalents, 80% in toluene) was added dropwise though a dropping funnel over 30 min. Then the mixture was heated up to reflux for 20 h. The mixture was cooled to 0°C and neutralized with a saturated ammonium chloride solution and concentrated in vacuo. The residue was absorbed on the silica gel and further purified by column chromatography to obtain the pure dialkynyl OEG **21**.

(2) Dialkynyl OEG **21a**:

Ethylene glycol (666 mg, 10.7 mmol), sodium hydride (945 mg, 23.6 mmol), propargyl bromide (2.55 mL, 23.6 mmol) and 40 mL anhydrous THF were used and the crude product was purified by column chromatography (hexane : AcOEt = 5 : 1) to give the dialkynyl OEG **21a** as a colorless oil (608 mg, 41%).

^{1}H-NMR ($CDCl_3$, 400 MHz) δ (ppm) = 4.21 (4H, d, J = 2.4 Hz, OCH_2CCH), 3.72 (4H, s, OCH_2CH_2O), 2.43 (2H, t, J = 2.3 Hz, OCH_2CCH).

^{13}C-NMR ($CDCl_3$, 100 MHz) δ (ppm) = 79.7, 74.8, 69.0, 58.6.

GC-MS (70 eV), m/e (relative intensity): 98.8 (73.6, $[M\text{-}C_3H_3]^{+\bullet}$), 83.0 (21.4), 81.0 (22.5), 67.0 (27.7), 53.1 (20.2), 43.1 (56.0), 39.1 (99.9, $[C_3H_3]^{+\bullet}$).

(3) Dialkynyl OEG **21b**:

Diethylene glycol (739 mg, 6.89 mmol), sodium hydride (606 mg, 15.2 mmol), propargyl bromide (1.56 mL, 14.5 mmol) and 20 mL anhydrous THF were used and the crude product was purified by column chromatography (hexane : AcOEt = 4 : 1) to give the dialkynyl OEG **21b** as a colorless oil (524 mg, 42%).

^{1}H-NMR ($CDCl_3$, 400 MHz) δ (ppm) = 4.20 (4H, d, J = 2.4 Hz, OCH_2CCH), 3.72-3.67 (8H, m, OCH_2CH_2O), 2.42 (2H, t, J = 2.4 Hz, OCH$_2$CCH).

^{13}C-NMR ($CDCl_3$, 100 MHz) δ (ppm) = 79.8, 74.7, 70.6, 69.3, 58.6.

HRMS (ESI-TOF, positive): $[C_{10}H_{14}O_3Na]^+$ cal. 205.0835, found 205.0834.

(4) Dialkynyl OEG **21c**:

Triethylene glycol (1.12 g, 7.46 mmol), sodium hydride (627 mg, 15.7 mmol), propargyl bromide (1.69 mL, 15.7 mmol) and 20 mL anhydrous THF were used and the crude product was purified by column chromatography (hexane : AcOEt = 3 : 2) to give the dialkynyl OEG **21c** as a colorless oil (1.35 g, 80%).

^{1}H-NMR ($CDCl_3$, 400 MHz) δ (ppm) = 4.21 (4H, d, J = 2.3 Hz, OCH_2CCH), 3.72-3.67 (12H, m, OCH_2CH_2O), 2.44 (2H, t, J = 2.4 Hz, OCH$_2$CCH).

^{13}C-NMR ($CDCl_3$, 100 MHz) δ (ppm) = 79.8, 74.7, 70.7, 70.6, 69.2, 58.5.

HRMS (ESI-TOF, positive): $[C_{12}H_{18}O_4Na]^+$ cal. 249.1097, found 249.1112.

(5) Dialkynyl OEG **21d**:

Tetraethylene glycol (1.12 g, 5.74 mmol), sodium hydride (482 mg, 12.1 mmol), propargyl bromide (1.30 mL, 12.1 mmol) and 40 mL anhydrous THF were used and the crude product was purified by column chromatography (hexane : AcOEt = 1 : 1) to give the dialkynyl OEG **21d** as a colorless oil (1.55 g, 99%).

^{1}H-NMR ($CDCl_3$, 400 MHz) δ (ppm) = 4.21 (4H, d, J = 2.4 Hz, OCH_2CCH), 3.71-3.66 (16H, m, OCH_2CH_2O), 2.44 (2H, t, J = 2.3 Hz, OCH$_2$CCH).

^{13}C-NMR ($CDCl_3$, 100 MHz) δ (ppm) = 79.8, 74.7, 70.8, 70.7, 70.6, 69.3, 58.6.

HRMS (ESI-TOF, positive): $[C_{14}H_{22}O_5Na]^+$ cal. 293.1359, found 293.1377.

(6) Dialkynyl OEG **21e**:

Pentaethylene glycol (759 mg, 3.19 mmol), sodium hydride (268 mg, 6.69 mmol), propargyl bromide (721 μL, 6.69 mmol) and 60 mL anhydrous THF were used and the crude product was purified by column chromatography (chloroform : MeOH = 20 : 1) to give the dialkynyl OEG **21e** as a colorless oil (538 mg, 54%).

^{1}H-NMR ($CDCl_3$, 400 MHz) δ (ppm) = 4.21 (4H, d, J = 2.3 Hz, OCH_2CCH), 3.71-3.67 (8H, m, OCH_2CH_2O), 3.67-3.66 (12H, m, OCH_2CH_2O), 2.44 (2H, t, J = 2.4 Hz, OCH$_2$CCH).

^{13}C-NMR ($CDCl_3$, 100 MHz) δ (ppm) = 79.9, 74.7, 70.8, 70.6, 69.3, 58.6.

HRMS (ESI-TOF, positive): $[C_{16}H_{26}O_6Na]^+$ cal. 337.1622, found 337.1626; $[C_{16}H_{26}O_6K]^+$ cal. 353.1361, found 353.1366.

(7) Dialkynyl OEG **21f**:

Hexaethylene glycol (769 mg, 2.64 mmol), sodium hydride (222 mg, 5.55 mmol), propargyl bromide (598 μL, 5.55 mmol) and 50 mL anhydrous THF were used and the crude product was purified by column chromatography (chloroform : MeOH = 20 : 1) to give the dialkynyl OEG **21f** as a colorless oil (882 mg, 93%).

^{1}H-NMR ($CDCl_3$, 400 MHz) δ (ppm) = 4.21 (4H, d, J = 2.4 Hz, OCH_2CCH), 3.71-3.67 (8H, m, OCH_2CH_2O), 3.66-3.65 (16H, m, OCH_2CH_2O), 2.44 (2H, t, J = 2.3 Hz, OCH$_2$CCH).

^{13}C-NMR ($CDCl_3$, 100 MHz) δ (ppm) = 79.8, 74.7, 70.8, 70.6, 69.3, 58.6.

HRMS (ESI-TOF, positive): $[C_{18}H_{30}O_7Na]^+$ cal. 381.1884, found 381.1889; $[C_{18}H_{30}O_7K]^+$ cal. 397.1623, found 397.1631.

(8) Dialkynyl OEG **21g**:

The OEG diol **5a** (130 mg, 0.400 mmol), sodium hydride (35.1 mg, 0.880 mmol), propargyl bromide (94.0 μL, 0.880 mmol) and 20 mL anhydrous THF were used and the crude product was purified by column chromatography (chloroform : MeOH = 20 : 1) to give the dialkynyl OEG **21g** as a colorless oil (132 mg, 82%).

^{1}H-NMR ($CDCl_3$, 400 MHz) δ (ppm) = 4.21 (4H, d, J = 2.3 Hz, OCH_2CCH), 3.71-3.65 (28H, m, OCH_2CH_2O), 2.44 (2H, t, J = 2.4 Hz, OCH$_2$CCH).

^{13}C-NMR ($CDCl_3$, 100 MHz) δ (ppm) = 79.9, 74.7, 70.8, 70.6, 69.3, 58.6.

HRMS (ESI-TOF, positive): $[C_{20}H_{34}O_8Na]^+$ cal. 425.2146, found 425.2189; $[C_{20}H_{34}O_8K]^+$ cal. 441.1885, found 441.1929.

(9) Dialkynyl OEG **21h**:

The OEG diol **5b** (126 mg, 0.340 mmol), sodium hydride (29.9 mg, 0.750 mmol), propargyl bromide (81.0 μL, 0.750 mmol) and 15 mL anhydrous THF were used and the crude product was purified by column chromatography (chloroform : MeOH = 20 : 1) to give the dialkynyl OEG **21h** as a colorless oil (58.2 mg, 38 %).

^{1}H-NMR ($CDCl_3$, 400 MHz) δ (ppm) = 4.20 (4H, d, J = 2.4 Hz, OCH_2CCH), 3.71-3.64 (32H, m, OCH_2CH_2O), 2.43 (2H, t, J = 2.4 Hz, OCH$_2$CCH).

^{13}C-NMR ($CDCl_3$, 100 MHz) δ (ppm) = 79.9, 74.7, 70.8, 70.6, 69.3, 58.6.

HRMS (ESI-TOF, positive): $[C_{22}H_{38}O_9Na]^+$ cal. 469.2408, found 469.2435; $[C_{22}H_{38}O_9K]^+$ cal. 485.2147, found 485.2180.

(10) Dialkynyl OEG **21i**:

The OEG diol **5c** (126 mg, 0.300 mmol), sodium hydride (27.0 mg, 0.670 mmol), propargyl bromide (72.0 μL, 0.670 mmol) and 15 mL anhydrous THF were used and the crude product was purified by column chromatography (chloroform : MeOH = 20 : 1) to give the dialkynyl OEG **21i** as a colorless oil (100 mg, 68%).

^{1}H-NMR ($CDCl_3$, 400 MHz) δ (ppm) = 4.20 (4H, d, J = 2.3 Hz, OCH_2CCH), 3.71-3.64 (36H, m, OCH_2CH_2O), 2.43 (2H, t, J = 2.3 Hz, OCH$_2$CCH).

^{13}C-NMR ($CDCl_3$, 100 MHz) δ (ppm) = 79.9, 74.7, 70.8, 70.6, 69.3, 58.6.

HRMS (ESI-TOF, positive): $[C_{24}H_{42}O_{10}Na]^+$ cal. 513.2670, found 513.2690; $[C_{24}H_{42}O_{10}K]^+$ cal. 529.2410, found 529.2429.

(11) Dialkynyl OEG **21j**:

The OEG diol **5d** (134 mg, 0.290 mmol), sodium hydride (25.7 mg, 0.640 mmol), propargyl bromide (69.0 μL, 0.640 mmol) and 15 mL anhydrous THF were used and the crude product was purified by column chromatography (chloroform : MeOH = 40 : 1) to give the dialkynyl OEG **21j** as a colorless oil (93.9 mg, 61%).

^{1}H-NMR ($CDCl_3$, 400 MHz) δ (ppm) = 4.19 (4H, d, J = 2.1 Hz, OCH_2CCH), 3.70-3.64 (40H, m, OCH_2CH_2O), 2.43 (2H, t, J = 2.1 Hz, OCH$_2$CCH).

^{13}C-NMR ($CDCl_3$, 100 MHz) δ (ppm) = 79.9, 74.7, 70.8, 70.6, 69.3, 58.6.

HRMS (ESI-TOF, positive): $[C_{26}H_{46}O_{11}Na]^+$ cal. 557.2932, found 557.2926; $[C_{26}H_{46}O_{11}K]^+$ cal. 573.2672, found 573.2663.

(12) Dialkynyl OEG **21k**:

The OEG diol **5e** (276 mg, 0.550 mmol), sodium hydride (48.4 mg, 1.21 mmol), propargyl bromide (130 μL, 1.21 mmol) and 20 mL anhydrous THF were used and the crude product was purified by column chromatography (chloroform : MeOH = 50 : 1) to give the dialkynyl OEG **21k** as a colorless oil (285 mg, 90%).

^{1}H-NMR ($CDCl_3$, 400 MHz) δ (ppm) = 4.19 (4H, d, J = 2.3 Hz, OCH_2CCH), 3.71-3.64 (44H, m, OCH_2CH_2O), 2.43 (2H, t, J = 2.3 Hz, OCH$_2$CCH).

^{13}C-NMR ($CDCl_3$, 100 MHz) δ (ppm) = 79.9, 74.7, 70.8, 70.6, 69.3, 58.6.

HRMS (ESI-TOF, positive): $[C_{28}H_{50}O_{12}Na]^+$ cal. 601.3195, found 601.3205; $[C_{28}H_{50}O_{12}K]^+$ cal. 617.2934, found 617.2941.

(13) Dialkynyl OEG **21l**:

The OEG diol **5e** (273 mg, 0.500 mmol), sodium hydride (43.9 mg, 1.10 mmol), propargyl bromide (118 μL, 1.10 mmol) and 20 mL anhydrous THF were used and the crude product was purified by column chromatography (chloroform : MeOH = 40 : 1) to give the dialkynyl OEG **21l** as a colorless oil (202 mg, 65%).

^{1}H-NMR ($CDCl_3$, 400 MHz) δ (ppm) = 4.20 (4H, d, J = 2.4 Hz, OCH_2CCH), 3.70-3.65 (48H, m, OCH_2CH_2O), 2.44 (2H, t, J = 2.3 Hz, OCH$_2$CCH).

^{13}C-NMR ($CDCl_3$, 100 MHz) δ (ppm) = 79.9, 74.7, 70.8, 70.6, 69.3, 58.6.

HRMS (ESI-TOF, positive): $[C_{30}H_{54}O_{13}Na]^+$ cal. 645.3457, found 645.3494; $[C_{30}H_{54}O_{13}K]^+$ cal. 661.3196, found 661.3232.

6.1.16. Chemical preparation of bis-*N*-methylamine OEG 22

(1) Bis-*N*-methylamine OEG **22a**:

To a solution of the dibromide OEG **23a** (101 mg, 0.314 mmol) in EtOH (10 mL), *N*-benzyl methylamine (125 μL, 0.942 mmol) was added and the reaction mixture was heated up to reflux for 24 h until TLC and ESI-TOF analysis indicated complete consumption of the dibromide. The solvent was removed in vacuo. Afterwards the residue was dissolved in MeOH (10 mL) followed by hydrogenation with 10% palladium hydroxide on carbon (21.8 mg, 0.155 mmol) and 1M HCl (3.1 mL) under 15 bar hydrogen pressure for 10 h. Then the mixture was filtered over Celite and the filter cake was washed with MeOH three times. This solution was concentrated in vacuo and the crude product was purified by column chromatography (MeOH : NH_4OH [25% in water] = 9 : 1 to 5:1) to give the bis-*N*-methylamine **22a** as a yellow solid (29.6 mg, 43%).

^{1}H-NMR (DCM-d2, 400 MHz) δ (ppm) = 3.61-3.56 (12H, m, OCH_2CH_2O and CH_3HNCH$_2$CH_2O), 3.00 (4H, br s, CH_3HNCH_2CH$_2$O), 2.77 (2H, br s, CH_3HNCH$_2$CH$_2$O), 2.43 (6H, s, CH_3NHCH$_2$).

^{13}C-NMR (DCM-d2, 100 MHz) δ (ppm) = 70.7, 70.5, 69.7, 51.1, 35.7.

HRMS (ESI-TOF, positive): $[C_{10}H_{25}N_2O_3]^+$ cal. 221.1860, found 221.1866.

(2) Bis-*N*-methylamine OEG **22b**:

To a solution of the ditosylate OEG **12b** (196 mg, 0.358 mmol) in EtOH (10 mL), *N*-benzyl

methylamine (143 µL, 1.07 mmol) was added and the reaction mixture was heated up to reflux for 48 h until TLC analysis indicated complete consumption of the ditosylate. The solvent was removed in vacuo. Afterwards the residue was dissolved in MeOH (10 mL) followed by hydrogenation with 10% palladium hydroxide on carbon (26.3 mg, 0.0374 mmol) and 1M HCl (0.96 mL) under 15 bar hydrogen pressure for 20 h. Then the mixture was filtered over Celite and the filter cake was washed with MeOH three times. This solution was concentrated in vacuo and the crude product was washed with triethylamine to give the bis-*N*-methylamine **22b** as colorless oil (28.5 mg, 30%).

^{1}H-NMR (DCM-d2, 400 MHz) δ (ppm) = 3.89 (4H, t, J = 4.6 Hz, $CH_3HNCH_2CH_2O$), 3.72-3.59 (14H, m, OCH_2CH_2O and $CH_3HNCH_2CH_2O$), 3.15 (4H, t, J = 4.6 Hz, $CH_3HNCH_2CH_2O$), 2.71 (6H, s, CH_3NHCH_2).

^{13}C-NMR (DCM-d2, 100 MHz) δ (ppm) = 70.2, 70.1, 70.0, 66.1, 48.7, 33.7.

HRMS (ESI-TOF, positive): $[C_{12}H_{28}N_2O_4Na]^+$ cal. 287.1941, found 287.1947.

(3) Bis-*N*-methylamine OEG **22c**

To a solution of hexaethylene glycol 1,20-diazide[124] (170 mg, 0.511 mmol) in anhydrous THF, triphenylphosphine (295 mg, 1.13 mmol) was added at room temperature and the reaction mixture was stirred at room temperature until TLC and ESI-TOF analysis indicated complete consumption of the azide. To this iminophosphorane intermediate, iodomethane (70.7 µL, 1.13 mmol) were added and a white participation appeared. After 24 h, ESI-TOF analysis indicated the complete consumption of this intermediate and the solvent including the excess of iodomethane was removed in vacuum. Afterward, 1% KOH in MeOH (5.7 mL) was added to hydrolyze aminophosphonium salt. The solvent was removed in vacuo and the residue was absorbed on the silica gel and further purified by column chromatography (MeOH : NH_4OH [25% in water] = 9 : 1 to 5:1) to obtain the pure bis-*N*-methylamine OEG **22c** as a colorless oil (34.4 mg, 22%).

^{1}H-NMR (DCM-d2, 400 MHz) δ (ppm) = 3.64-3.44 (24H, m, OCH_2CH_2O and $CH_3HNCH_2CH_2O$), 2.70 (4H, br s, $CH_3HNCH_2CH_2O$), 2.39 (6H, s, CH_3NHCH_2), 1.75 (2H, br s, $CH_3HNCH_2CH_2O$).

^{13}C-NMR (DCM-d2, 100 MHz) δ (ppm) = 70.9, 70.7, 70.6, 51.7, 36.4.

HRMS (ESI-TOF, positive): $[C_{14}H_{32}N_2O_5Na]^+$ cal. 331.2203, found 331.2207.

(4) Bis-*N*-methylamine OEG **22d**:

To a solution of the dibromide OEG **23c** (109 mg, 0.219 mmol) in EtOH (2 mL), *N*-benzyl

methylamine (175 µL, 1.32 mmol) was added and the reaction mixture was heated up to 78°C for 20 h until TLC and ESI-TOF analysis indicated complete consumption of the dibromide. The solvent was removed in vacuo. Afterwards the residue was dissolved in MeOH (2.5 mL) followed by hydrogenation with 10% palladium hydroxide on carbon (30.8 mg, 0.0438 mmol) and palladium on carbon (46.7 mg, 0.0438 mmol) under 15 bar hydrogen pressure for 20 h. Then the mixture was filtered over Celite and the filter cake was washed with MeOH three times. This solution was concentrated in vacuo and the crude product was purified by column chromatography (MeOH : NH_4OH [25% in water] = 9 : 1) to give the bis-*N*-methylamine dibromide salt **22d** as a colorless solid (110 mg, 90%).

^{1}H-NMR (DCM-d2, 400 MHz) δ (ppm) = 3.94 (4H, t, J = 5.0 Hz, $CH_3HNCH_2CH_2O$), 3.74-3.62 (26H, m, OCH_2CH_2O and $CH_3HNCH_2CH_2O$), 3.41 (2H, s, $CH_3HNCH_2CH_2O$), 3.22 (4H, t, J = 5.1 Hz, $CH_3HNCH_2CH_2O$), 2.74 (6H, s, CH_3NHCH_2).

^{13}C-NMR (DCM-d2, 100 MHz) δ (ppm) = 70.7, 70.5, 70.3, 70.2, 66.2, 50.7, 49.0, 33.9.

HRMS (ESI-TOF, positive): $[C_{18}H_{41}N_2O_7]^+$ cal. 397.2908, found 397.2897; $[C_{18}H_{42}N_2O_9]^{2+}$ cal. 199.1491, found 199.1481; $[C_{18}H_{40}N_2O_7Na]^+$ cal. 419.2728, found 419.2715.

(5) Bis-*N*-methylamine OEG **22e**:

To a solution of the dibromide OEG **23d** (81.8 mg, 0.140 mmol) in EtOH (2 mL), *N*-benzyl methylamine (112 µL, 0.840 mmol) was added and the reaction mixture was heated up to 78°C for 20 h until TLC and ESI-TOF analysis indicated complete consumption of the dibromide. The solvent was removed in vacuo. Afterwards the residue was dissolved in MeOH (2.0 mL) followed by hydrogenation with 10% palladium hydroxide on carbon (19.7 mg, 0.0280 mmol) and palladium on carbon (29.8 mg, 0.0280 mmol) under 15 bar hydrogen pressure for 20 h. Then the mixture was filtered over Celite and the filter cake was washed with MeOH three times. This solution was concentrated in vacuo and the crude product was purified by column chromatography (MeOH : NH_4OH [25% in water] = 9 : 1) to give the bis-*N*-methylamine dibromide salt **22e** as a colorless solid (80.7 mg, 89%).

^{1}H-NMR (DCM-d2, 400 MHz) δ (ppm) = 3.92 (4H, t, J = 5.0 Hz, $CH_3HNCH_2CH_2O$), 3.74-3.58 (32H, m, OCH_2CH_2O), 3.41 (4H, s, $CH_3HNCH_2CH_2O$), 3.20 (4H, t, J = 5.2 Hz, $CH_3HNCH_2CH_2O$), 2.72 (6H, s, CH_3NHCH_2).

^{13}C-NMR (DCM-d2, 100 MHz) δ (ppm) = 70.7, 70.6, 70.5, 70.4, 70.2, 66.2, 50.7, 49.0, 33.8.

HRMS (ESI-TOF, positive): $[C_{22}H_{49}N_2O_9]^+$ cal. 485.3433, found 485.3596; $[C_{22}H_{50}N_2O_9]^{2+}$ cal. 243.1753, found 243.1851; $[C_{22}H_{48}N_2O_9Na]^+$ cal. 507.3252, found 507.3420.

(6) Bis-*N*-methylamine OEG **22f**:

To a solution of the dibromide OEG **23f** (80.0 mg, 0.118 mmol) in EtOH (3 mL), *N*-benzyl methylamine (47.5 µL, 0.357 mmol) was added and the reaction mixture was heated up to 78°C for 20 h until TLC and ESI-TOF analysis indicated complete consumption of the dibromide. The solvent was removed in vacuo. Afterwards the residue was dissolved in MeOH (2.0 mL) followed by hydrogenation with 10% palladium hydroxide on carbon (16.8 mg, 0.0238 mmol) and 1M HCl (1.18 mL) under 15 bar hydrogen pressure for 20 h. Then the mixture was filtered over Celite and the filter cake was washed with MeOH three times. This solution was concentrated in vacuo and the crude product was purified by column chromatography (MeOH : NH_4OH [25% in water] = 9 : 1) to give to give the bis-*N*-methylamine **22f** as a colorless oil (39.2 mg, 57%)

^{1}H-NMR (DCM-d2, 400 MHz) δ (ppm) = 3.61-3.51 (44H, m, $CH_3HNCH_2CH_2O$, OCH_2CH_2O, and $CH_3HNCH_2CH_2O$), 2.70 (4H, t, J = 5.2 Hz, $CH_3HNCH_2CH_2O$), 2.39 (6H, s, CH_3NHCH_2).

^{13}C-NMR (DCM-d2, 100 MHz) δ (ppm) = 70.9, 70.6, 51.7, 36.4.

HRMS (ESI-TOF, positive): $[C_{26}H_{57}N_2O_{11}]^+$ cal. 573.3957, found 573.4009; $[C_{26}H_{58}N_2O_{11}]^{2+}$ cal. 287.2015, found 287.2003; $[C_{26}H_{56}N_2O_{11}Na]^+$ cal. 595.3776, found 595.3752.

6.1.17. Chemical preparation of dibromide OEG 23

(1) General procedure for preparation of dibromide OEG **23a-g**

To a solution of ditosylate OEG **12** (1.0 equivalent) in acetone, lithium bromide (4.0 equivalents) was added at room temperature and the reaction mixture was stirred and heated up to reflux until TLC analysis indicated complete consumption of the ditosylate. The reaction mixture was concentrated in vacuo and the crude product was absorbed on the silica gel and further purified by column chromatography to obtain the pure dibromide OEG **23**.

(2) Dibromide OEG **23a**:

The ditosylate OEG **1a** (342 mg, 0.680 mmol), lithium bromide (179 mg, 2.04 mmol) and 20 mL acetone were used and the crude product was purified by column chromatography (chloroform : MeOH = 40 : 1) to give the ditosylate **23a** as a light yellow oil (188 mg, 87%).

^{1}H-NMR ($CDCl_3$, 400 MHz) δ (ppm) = 3.82 (4H, t, J = 6.2 Hz, $BrCH_2CH_2O$), 3.68 (8H, s,

OCH_2CH_2O), 3.48 (4H, t, J = 6.3 Hz, BrCH_2CH$_2$O).

^{13}C-NMR ($CDCl_3$, 100 MHz) δ (ppm) = 71.4, 70.9, 70.8, 30.6.

HRMS (ESI-TOF, positive): $[C_8H_{16}Br_2O_3Na]^+$ cal. 340.9358, 342.9338, 344.9318, found 340.9354, 342.9335, 344.9315.

(3) Dibromide OEG **23b**:

The ditosylate OEG **1b** (464 mg, 0.850 mmol), lithium bromide (224 mg, 2.54 mmol) and 20 mL acetone were used and the crude product was purified by column chromatography (chloroform : MeOH = 40 : 1) to give the ditosylate **23b** as a light yellow oil (261 mg, 84%).

^{1}H-NMR ($CDCl_3$, 400 MHz) δ (ppm) = 3.81 (4H, t, J = 6.4 Hz, BrCH$_2$CH_2O), 3.71-3.65 (12H, m, OCH_2CH_2O), 3.47 (4H, t, J = 6.3 Hz, BrCH_2CH$_2$O).

^{13}C-NMR ($CDCl_3$, 100 MHz) δ (ppm) = 71.4, 70.9, 70.8, 30.5.

HRMS (ESI-TOF, positive): $[C_{10}H_{20}Br_2O_4Na]^+$ cal. 384.9621, 386.9600, 388.9580, found 384.9644, 386.9624, 388.9602.

(4) Dibromide OEG **23c**:

The ditosylate OEG **12a** (165 mg, 0.242 mmol), lithium bromide (84.2 mg, 0.969 mmol) and 10 mL acetone were used and the crude product was purified by column chromatography (chloroform : MeOH = 40 : 1) to give the ditosylate **23c** as a light yellow oil (110 mg, 92%).

^{1}H-NMR ($CDCl_3$, 400 MHz) δ (ppm) = 3.79 (4H, t, J = 6.4 Hz, BrCH$_2$CH_2O), 3.68-3.60 (24H, m, OCH_2CH_2O), 3.45 (4H, t, J = 6.3 Hz, BrCH_2CH$_2$O).

^{13}C-NMR ($CDCl_3$, 100 MHz) δ (ppm) = 71.4, 70.9, 70.8, 30.6.

HRMS (ESI-TOF, positive): $[C_{16}H_{32}Br_2O_7Na]^+$ cal. 517.0407, 519.0387, 521.0369, found 517.0815, 519.0367, 521.0348.

(5) Dibromide OEG **23d**:

The ditosylate OEG **12b** (108 mg, 0.141 mmol), lithium bromide (49.6 mg, 0.565 mmol) and 5 mL acetone were used and the crude product was purified by column chromatography (chloroform : MeOH = 20 : 1) to give the ditosylate **23d** as a light yellow oil (82.3 mg, 99%).

^{1}H-NMR ($CDCl_3$, 400 MHz) δ (ppm) = 3.79 (4H, t, J = 6.3 Hz, BrCH$_2$CH_2O), 3.71-3.52 (32H, m, OCH_2CH_2O), 3.46 (4H, t, J = 6.3 Hz, BrCH_2CH$_2$O).

^{13}C-NMR ($CDCl_3$, 100 MHz) δ (ppm) = 71.4, 70.9, 70.8, 30.6.

HRMS (ESI-TOF, positive): $[C_{20}H_{40}Br_2O_9Na]^+$ cal. 605.0931, 607.0912, 609.0894, found

605.0862, 607.0830, 609.0815; $[C_{20}H_{40}Br_2O_9K]^+$ cal. 621.0671, 623.0651, 625.0634, found 621.0588, 623.0568, 625.0552.

(6) Dibromide OEG **23e**:

The ditosylate OEG **12c** (146 mg, 0.180 mmol), lithium bromide (63.3 mg, 0.722 mmol) and 5 mL acetone were used and the crude product was purified by column chromatography (DCM : MeOH = 20 : 1) to give the ditosylate **23e** as a light yellow oil (116 mg, 99%).

^{1}H-NMR ($CDCl_3$, 400 MHz) δ (ppm) = 3.81 (4H, t, J = 6.4 Hz, $BrCH_2CH_2O$), 3.72-3.61 (36H, m, OCH_2CH_2O), 3.47 (4H, t, J = 6.4 Hz, $BrCH_2CH_2O$).

^{13}C-NMR ($CDCl_3$, 100 MHz) δ (ppm) = 71.4, 70.9, 70.8, 70.7, 30.5.

MS (FAB, positive): $[C_{22}H_{45}Br_2O_{10}]^+$ cal. 629.14 found 629.2; $[C_{22}H_{44}Br_2O_{10}Na]^+$ cal. 651.12 found 651.3.

(7) Dibromide OEG **23f**:

The ditosylate OEG **12d** (191 mg, 0.222 mmol), lithium bromide (78.2 mg, 0.891 mmol) and 5 mL acetone were used and the crude product was purified by column chromatography (DCM : MeOH = 20 : 1) to give the ditosylate **23f** as a light yellow oil (139 mg, 94%).

^{1}H-NMR ($CDCl_3$, 400 MHz) δ (ppm) = 3.79 (4H, t, J = 6.4 Hz, $BrCH_2CH_2O$), 3.69-3.54 (40H, m, OCH_2CH_2O), 3.45 (4H, t, J = 6.3 Hz, $BrCH_2CH_2O$).

^{13}C-NMR ($CDCl_3$, 100 MHz) δ (ppm) = 71.4, 70.7, 70.5, 70.4, 30.5.

HRMS (ESI-TOF, positive): $[C_{24}H_{48}Br_2O_{11}Na]^+$ cal. 693.1456, 695.1437, 697.1421, found 693.1487, 695.1457, 697.1440; $[C_{24}H_{48}Br_2O_{11}K]^+$ cal. 709.1195, 711.1176, 713.1160, found 709.1213, 711.1196, 713.1180.

(8) Dibromide OEG **23g**:

The ditosylate OEG **12e** (149 mg, 0.165 mmol), lithium bromide (58.0 mg, 0.661 mmol) and 20 mL acetone were used and the crude product was purified by column chromatography (DCM : MeOH = 20 : 1) to give the ditosylate **23g** as a light yellow oil (143 mg, 86%).

^{1}H-NMR ($CDCl_3$, 400 MHz) δ (ppm) = 3.84-3.51 (48H, m, $BrCH_2CH_2O$ and OCH_2CH_2O), 3.48 (4H, t, J = 6.3 Hz, $BrCH_2CH_2O$).

^{13}C-NMR ($CDCl_3$, 100 MHz) δ (ppm) = 71.4, 70.9, 70.8, 30.5.

HRMS (ESI-TOF, positive): $[C_{26}H_{52}Br_2O_{12}Na]^+$ cal. 739.1699, found 739.1679; $[C_{26}H_{52}Br_2O_{12}K]^+$ cal. 753.1457, 755.1439, 757.1423, found 753.1441, 755.1420, 757.1398.

6.1.18. Chemical preparation of OEG alcohol monomethyl ether 26

(1) Monotosylate OEG monomethyl ether **24a**:

To a solution of diethylene glycol monomethyl ether (2.01 g, 16.8 mmol) in 20 mL THF, 4-methylbenzene sulfonyl chloride (4.84 g, 25.2 mmol) was added at room temperature and then cooled to 0°C. To this mixture, potassium hydroxide (3.10 g, 55.3 mmol) in H_2O (0.9 g/mL) was added dropwise over 1 h. Then the reaction mixture was stirred at 0°C for 30 min and some white precipitation appeared. Afterwards this mixture was further stirred at room temperature until TLC analysis indicated complete consumption of the OEG alcohol. The reaction mixture was neutralized with a saturated ammonium chloride solution and concentrated in vacuo. The residue was absorbed on the silica gel and further purified by flash column chromatography (hexane : AcOEt = 5 : 1 to 2 :1) to obtain the pure monotosylate OEG monomethyl ether **24a** as a colorless solid (4.60 g, 99%).

^{1}H-NMR ($CDCl_3$, 400 MHz) δ (ppm) = 7.80 (2H, d, J = 8.6 Hz, Ar-*H*), 7.34 (2H, d, J = 8.7 Hz, Ar-*H*), 4.19-4.14 (2H, m, $OCH_2CH_2OSO_2$), 3.71-3.67 (2H, m, $OCH_2CH_2OSO_2$), 3.60-3.46 (4H, m, OCH_2CH_2O), 3.35 (3H, s, $CH_3OCH_2CH_2$), 2.45 (3H, s, CH_3).

^{13}C-NMR ($CDCl_3$, 100 MHz) δ (ppm) = 145, 133, 130, 128, 72.0, 70.9, 69.4, 68.9, 59.2, 21.8.

(2) Monobenzylate OEG monomethyl ether **25**:

To a solution of monobenzylate OEG alcohol **2a** (0.883 g, 3.67 mmol) in 20 mL anhydrous THF at 0°C, sodium hydride (220 mg, 5.51 mmol) was added portionwise and the reaction mixture was stirred at 0°C for an additional 30 min. Afterwards the mixture was heated up to reflux for 1 h and then cooled to 0°C again. To this mixture, the monotosylate OEG monomethyl ether **24a** (1.01 g, 3.67 mmol) in 20 mL anhydrous THF was added dropwise though a dropping funnel over 30 min. Then the mixture was heated up to reflux for 20 h. The mixture was cooled to 0°C and neutralized with a saturated ammonium chloride solution, brine, and concentrated in vacuo. The residue was absorbed on the silica gel and further purified by column chromatography (DCM : MeOH = 20 :1) to obtain pure monobenzylate OEG monomethyl ether **25** as a colorless oil (1.13 g, 90%).

^{1}H-NMR ($CDCl_3$, 400 MHz) δ (ppm) = 7.36-7.25 (5H, m, Ar-*H*), 4.55 (2H, s, $BnCH_2O$), 3.69-3.58 (18H, m, OCH_2CH_2O), 3.56-3.50 (2H, m, $CH_3OCH_2CH_2O$), 3.36 (3H, s, $CH_3OCH_2CH_2$).

^{13}C-NMR ($CDCl_3$, 100 MHz) δ (ppm) = 138, 129, 128, 73.4, 72.2, 70.9, 70.8, 70.7, 69.6 59.2.

(3) OEG alcohol monomethyl ether **26**:

To a solution of monobenzylate OEG monomethyl ether **25** (670 mg, 1.96 mmol) in 20 mL EtOH, palladium on carbon (208 mg, 0.196 mmol) was added and the reaction mixture was hydrogenated under 1.0 bar H_2 and stirred at room temperature until TLC analysis indicated complete consumption of the monobenzylate. Afterwards the mixture was filtered over Celite and the filter cake was washed with MeOH three times. This solution was concentrated in vacuo and pure OEG alcohol monomethyl ether **26** was obtained as a colorless oil without any further purification (454 mg, 92%).

^{1}H-NMR ($CDCl_3$, 400 MHz) δ (ppm) = 3.74-3.71 (2H, m, $HOCH_2CH_2O$), 3.70-3.60 (16H, m, OCH_2CH_2O), 3.57-3.53 (2H, m, $HOCH_2CH_2O$), 3.38 (3H, s, $CH_3OCH_2CH_2$), 2.68 (1H, br s, $HOCH_2CH_2O$).

^{13}C-NMR ($CDCl_3$, 100 MHz) δ (ppm) = 72.7, 72.1, 70.8, 70.7, 70.5, 61.9, 59.2.

6.1.19. Chemical preparation of monotosylate OEG monomethyl ether 24b

To a solution of OEG alcohol monomethyl ether **26** (318 mg, 1.26 mmol) in 20 mL THF, 4-methylbenzene sulfonyl chloride (364 mg, 1.89 mmol) was added at room temperature and the solution was then cooled to 0°C. To this mixture, potassium hydroxide (234 mg, 4.16 mmol) in H_2O (0.9 g/mL) was added dropwise over 15 min. Then the reaction mixture was stirred at 0°C for 30 min and some white precipitation appeared. Afterwards this mixture was further stirred at room temperature until TLC analysis indicated complete consumption of the OEG alcohol. The reaction mixture was neutralized with a saturated ammonium chloride solution and concentrated in vacuo. The residue was absorbed on the silica gel and further purified by flash column chromatography (DCM : MeOH = 20:1) to obtain the pure monotosylate OEG monomethyl ether **24b** as a colorless solid (194 mg, 38%).

^{1}H-NMR ($CDCl_3$, 400 MHz) δ (ppm) = 7.80 (2H, d, J = 8.3 Hz, Ar-*H*), 7.34 (2H, d, J = 8.1 Hz, Ar-*H*), 4.18-4.14 (2H, m, $OCH_2CH_2OSO_2$), 3.70-3.67 (2H, m, $OCH_2CH_2OSO_2$), 3.66-3.53 (20H, m, OCH_2CH_2O), 3.38 (3H, s, $CH_3OCH_2CH_2$), 2.45 (3H, s, CH_3).

^{13}C-NMR ($CDCl_3$, 100 MHz) δ (ppm) = 145, 133, 130, 128, 72.1, 70.9, 70.8, 70.7, 69.4, 68.9, 59.2, 21.8.

6.1.20. Chemical preparation of 1-bromo OEG monomethyl ether 27

To a solution of monotosylate OEG monomethyl ether **24b** (177 mg, 0.436 mmol) in 10 mL acetone, lithium bromide (153 mg, 1.74 mmol) was added at room temperature and the reaction mixture was stirred and heated up to reflux until TLC analysis indicated complete consumption of the monotosylate. The reaction mixture was concentrated in vacuo and the crude product was absorbed on the silica gel and further purified by column chromatography (chloroform : MeOH = 20:1) to obtain the pure dibromide OEG **27** (132 mg, 96%) as a light yellow oil.

^{1}H-NMR ($CDCl_3$, 400 MHz) δ (ppm) = 3.81 (2H, t, J = 6.4 Hz, $BrCH_2CH_2O$), 3.69-3.63 (14H, m, OCH_2CH_2O), 3.57-3.53 (2H, m, $CH_3OCH_2CH_2$), 3.48 (2H, t, J = 6.3 Hz, $BrCH_2CH_2O$), 3.38 (3H, s, CH_3).

^{13}C-NMR ($CDCl_3$, 100 MHz) δ (ppm) = 72.1, 71.4, 70.9, 70.8, 70.7, 59.2, 30.5, 27.6.

HRMS (ESI-TOF, positive): $[C_{11}H_{24}BrO_5]^+$ cal. 315.0802, 317.0781, found 315.0727, 317.0688; $[C_{11}H_{23}BrO_5Na]^+$ cal. 337.0621, 339.0601, found 337.0624, 339.0605; $[C_{11}H_{23}BrO_5K]^+$ cal. 353.0360, 355.0340, found 353.0356, 355.0341.

6.1.21. Chemical preparation of monoalkynyl OEG monomethyl ether 28

(1) General procedure for preparation of monoalkynyl OEG 2**8a-b**:

To a solution of the OEG alcohol monomethyl ether (1.0 equivalent) in anhydrous THF at 0°C, sodium hydride (1.2 equivalents) was added portionwise and the reaction mixture was stirred at 0°C for an additional 30 min. Afterwards the mixture was heated up to reflux for 1h and then cooled to 0°C again. To this mixture, propargyl bromide (1.1 equivalents) 80% in toluene was added dropwise though a dropping funnel over 30 min. Then the mixture was heated up to reflux for 20 h. The mixture was cooled to 0°C and neutralized with a saturated ammonium chloride solution and concentrated in vacuo. The residue was absorbed on the silica gel and further purified by column chromatography to obtain the pure monoalkynyl OEG **28**.

(2) Monoalkynyl OEG **28a**:

Triethylene glycol monomethyl ether (741 mg, 4.28 mmol), sodium hydride (206 mg, 5.14 mmol), propargyl bromide (485 µL, 4.50 mmol) and 35 mL anhydrous THF were used and the crude product was purified by column chromatography (hexane : AcOEt = 1 : 1) to give the monoalkynyl OEG **28a** as a colorless oil (301 mg, 35%).

^{1}H-NMR ($CDCl_3$, 400 MHz) δ (ppm) = 4.19 (2H, d, J = 2.4 Hz, OCH_2CCH), 3.71-3.62 (10H, m,

OCH_2CH_2O), 3.36 (3H, s, OCH_3), 2.41 (1H, t, J = 2.3 Hz, OCH$_2$CCH).

^{13}C-NMR ($CDCl_3$, 100 MHz) δ (ppm) = 79.8, 74.7, 72.1, 70.8, 70.7, 70.6, 69.3, 59.2, 58.6.

HRMS (ESI-TOF, positive): $[C_{10}H_{18}O_4Na]^+$ cal. 225.1097, found 225.1113.

(4) Monoalkynyl OEG **28b**:

Pentaethylene glycol monomethyl ether **26** (326 mg, 1.24 mmol), sodium hydride (59.4 mg, 1.49 mmol), propargyl bromide (140 μL, 1.30 mmol) and 45 mL anhydrous THF were used and the crude product was purified by column chromatography (chloroform : MeOH = 20 : 1) to give the monoalkynyl OEG **28b** as a colorless oil (334 mg, 93%).

^{1}H-NMR ($CDCl_3$, 400 MHz) δ (ppm) = 4.19 (2H, d, J = 2.3 Hz, OCH_2CCH), 3.70-3.62 (18H, m, OCH_2CH_2O), 3.36 (3H, s, OCH_3), 2.42 (1H, t, J = 2.3 Hz, OCH$_2$CCH).

^{13}C-NMR ($CDCl_3$, 100 MHz) δ (ppm) = 79.8, 74.7, 72.1, 70.8, 70.7, 70.6, 69.3, 59.2, 58.6.

HRMS (ESI-TOF, positive): $[C_{14}H_{26}O_6Na]^+$ cal. 313.1622, found 313.1665.

6.2. Bivalent *trans*-diethylstilbestrol (DES) ligand

6.2.1. Chemical preparation of bivalent DES ligands 29-34

(1) General procedure for chemical preparations of bivalent DES ligands **29**-**32** and **34**:

To a solution of (*E*)-3,4-bis-(4-hydroxyphenyl)-3-hexenoic acid **39** (85% of *trans*-isomer, 2.1 equivalents), diamine OEG (1.0 equivalent), and triethylamine (2.2 equivalents) in anhydrous DMF at 0°C, a solution of benzotriazol-1-yl-oxytripyrrolidinophosphonium hexafluorophosphate (PyBOP, 2.2 equivalents) in anhydrous DCM was added. The reaction mixture was further stirred at 0°C for 30 min and then at room temperature for 24 h. The organic solvent was evaporated in vacuo and the residue was purified by column chromatography to obtain the bivalent DES ligand. A separation with RP-HPLC was performed to separate the bivalent DES ligand into *cis*-*cis*, *cis*-*trans*, and *trans*-*trans* isomers.

(2) Bivalent DES ligand **29**:

(*E*)-3,4-bis-(4-hydroxyphenyl)-3-hexenoic acid **39** (85% of *trans*-isomer, 42.0 mg, 0.141 mmol), diamine OEG **18a** (33.6 mg, 0.0671 mmol), triethylamine (20.7 μL, 0.148 mmol), PyBOP (76.8 mg, 0.148 mmol), anhydrous DMF (4 mL), and anhydrous DCM (4 mL) were used and the crude product was purified by column chromatography (chloroform : MeOH = 20:1 to 5:1) to obtain

bivalent DES ligand **29** as a colorless oil (45.1 mg, 63%). *Cis-cis* (5%), *cis-trans* (34%), and *trans-trans* (61%) isomers were separated by RP-HPLC (70% MeOH/H_2O) and characterized with ^{1}H-NMR according to the chemical shift of **38** (84% *trans*-isomer).

Cis-cis isomer of **29** (First fraction):

^{1}H-NMR (Acetone-d6, 400 MHz) δ (ppm) = 6.90-6.83 (8H, d and d, J = 8.7 Hz, 8.6 Hz, Ar-*H*), 6.60 (4H, d, J = 8.6 Hz, Ar-*H*), 6.56 (4H, d, J = 8.6 Hz, Ar-*H*), 3.60-3.54 (32H, m, OH_2CH_2CO), 3.53-3.49 (4H, m, OH_2CH_2CO), 3.46-3.39 (8H, s and t, J = 5.4 Hz, HNH_2CH_2CO, and H_2CC=O), 3.31 (4H, t, J = 5.3 Hz, HNH_2CH_2CO), 2.58 (4H, q, J = 7.6 Hz, H_3CH_2C), 0.94 (6H, t, J = 7.6 Hz, H_3CH_2C).

^{13}C-NMR (Acetone-d6, 100 MHz) δ (ppm) = 171, 156, 143, 135, 132, 131, 115, 71.1, 45.0, 42.8, 39.8, 28.7, 13.2.

Cis-trans isomer of **29** (Second fraction):

^{1}H-NMR (Acetone-d6, 400 MHz) δ (ppm) = 7.23 (2H, d, J = 8.4 Hz, (*E*)-Ar-*H*), 7.14 (2H, d, J = 8.5 Hz, (*Z*)-Ar-*H*), 6.90-6.81 (8H, m, (*E*,*Z*)-Ar-*H*), 6.59 (2H, d, J = 8.6 Hz, (*Z*)-Ar-H), 6.55 (2H, d, J = 8.6 Hz, (*Z*)-Ar-*H*), 3.61-3.46 (32H, m, OH_2CH_2CO), 3.46-3.40 (4H, s and t, J = 5.3 Hz, H_2CC=O and OH_2CH_2CO), 3.37-3.29 (6H, t and m, J = 5.6 Hz, OH_2CH_2CO, HNH_2CH_2CO, and H_2CC=O), 3.21 (2H, t, J = 5.2 Hz, HNH_2CH_2CO), 2.58 (2H, q, J = 7.6 Hz, (*Z*)-H_3CH_2C), 2.24 (2H, q, J = 7.4 Hz, (*E*)-H_3CH_2C), 0.94 (3H, t, J = 7.4 Hz, (*Z*)-H_3CH_2C), 0.80 (3H, t, J = 7.4 Hz, (*E*)-H_3CH_2C).

^{13}C-NMR (Acetone-d6, 100 MHz) δ (ppm) = 171, 170, 156, 155, 143, 134, 133, 131, 130, 115, 70.4, 70.2, 69.7, 43.1, 42.0, 39.1, 28.0, 12.9, 12.4, 11.1.

Trans-trans isomer of **29** (Third fraction):

^{1}H-NMR (Acetone-d6, 400 MHz) δ (ppm) = 7.23 (4H, d, J = 8.5 Hz, Ar-*H*), 7.14 (4H, d, J = 8.4 Hz, Ar-*H*), 6.85 (8H, m, Ar-*H*), 3.58-3.52 (32H, m, OH_2CH_2CO), 3.50-3.46 (4H, m, OH_2CH_2CO), 3.35 (4H, t, J = 5.7 Hz, HNH_2CH_2CO), 3.22 (4H, t, J = 5.4 Hz, HNH_2CH_2CO), 3.11 (4H, s, H_2CC=O), 2.24 (4H, q, J = 7.4 Hz, H_3CH_2C), 0.80 (6H, t, J = 7.4 Hz, H_3CH_2C).

^{13}C-NMR (Acetone-d6, 100 MHz) δ (ppm) = 171, 157, 144, 134, 132, 131, 116, 71.2, 71.0, 70.4, 49.6, 43.9, 39.8, 13.7, 11.9.

HRMS (ESI-TOF, positive): $[C_{58}H_{80}N_2O_{16}Na]^+$ cal. 1083.5400, found 1083.5420; $[C_{58}H_{80}N_2O_{16}K]^+$ cal. 1099.5139, found 1099.5162.

(3) Bivalent DES ligand **30**:

(*E*)-3,4-bis-(4-hydroxyphenyl)-3-hexenoic acid **39** (85% of *trans*-isomer, 32.0 mg, 0.107 mmol), diamine OEG **18b** (27.8 mg, 0.0510 mmol), triethylamine (16.0 μL, 0.112 mmol), PyBOP (58.4 mg, 0.112 mmol), anhydrous DMF (5 mL), and anhydrous DCM (5 mL) were used and the crude product was purified by column chromatography (chloroform : MeOH = 20:1 to 10:1) to obtain bivalent DES ligand **30** as a colorless oil (27.4 mg, 49%). *Cis*-*cis* (4%), *cis*-*trans* (31%), and *trans*-*trans* (65%) isomers were separated by RP-HPLC (70% MeOH/H_2O) and characterized with ^{1}H-NMR according to the chemical shift of **38** (84% *trans*-isomer).

Cis-*cis* isomer of **30** (First fraction):

^{1}H-NMR (Acetone-d6, 400 MHz) δ (ppm) = 6.90-6.84 (8H, d and d, J = 8.7 Hz, 8.7 Hz, Ar-*H*), 6.60 (4H, d, J = 8.7 Hz, Ar-*H*), 6.56 (4H, d, J = 8.7 Hz, Ar-*H*), 3.62-3.54 (36H, m, OH_2CH_2CO), 3.53-3.49 (4H, m, OH_2CH_2CO), 3.45-3.40 (8H, s and t, J = 5.3 Hz, HNH_2CH_2CO, and H_2CC=O), 3.37-3.29 (4H, m, HNH_2CH_2CO), 2.58 (4H, q, J = 7.6 Hz, H_3CH_2C), 0.94 (6H, t, J = 7.4 Hz, H_3CH_2C).

Cis-*trans* isomer of **30** (Second fraction):

^{1}H-NMR (Acetone-d6, 400 MHz) δ (ppm) = 7.23 (2H, d, J = 8.6 Hz, (*E*)-Ar-*H*), 7.14 (2H, d, J = 8.7 Hz, (*Z*)-Ar-*H*), 6.90-6.82 (8H, m, (*E*,*Z*)-Ar-*H*), 6.60 (2H, d, J = 8.7 Hz, (*Z*)-Ar-H), 6.55 (2H, d, J = 8.7 Hz, (*Z*)-Ar-*H*), 3.60-3.46 (40H, m, OH_2CH_2CO), 3.45-3.40 (4H, s and t, J = 5.4 Hz, H_2CC=O and OH_2CH_2CO), 3.38-3.29 (4H, m, OH_2CH_2CO, HNH_2CH_2CO, and H_2CC=O), 3.25-3.20 (2H, m, HNH_2CH_2CO), 2.58 (2H, q, J = 7.4 Hz, (*Z*)-H_3CH_2C), 2.24 (2H, q, J = 7.5 Hz, (*E*)-H_3CH_2C), 0.94 (3H, t, J = 7.4 Hz, (*Z*)-H_3CH_2C), 0.80 (3H, t, J = 7.4 Hz, (*E*)-H_3CH_2C).

Trans-*trans* isomer of **30** (Third fraction):

^{1}H-NMR (Acetone-d6, 400 MHz) δ (ppm) = 7.23 (4H, d, J = 8.6 Hz, Ar-*H*), 7.14 (4H, d, J = 8.6 Hz, Ar-*H*), 6.86-6.81 (8H, m, Ar-*H*), 3.60-3.52 (40H, m, OH_2CH_2CO), 3.50-3.46 (4H, m, OH_2CH_2CO), 3.36 (4H, t, J = 5.6 Hz, HNH_2CH_2CO), 3.22 (4H, q, J = 5.6 Hz, HNH_2CH_2CO), 3.11 (4H, s, H_2CC=O), 2.25 (4H, q, J = 7.6 Hz, H_3CH_2C), 0.80 (6H, t, J = 7.4 Hz, H_3CH_2C).

^{13}C-NMR (Acetone-d6, 100 MHz) δ (ppm) = 171,157, 144, 134, 132, 131, 116, 115, 71.1, 71.0, 70.5, 44.0, 39.9, 29.2, 13.7.

HRMS (ESI-TOF, positive): $[C_{58}H_{80}N_2O_{16}Na]^+$ cal. 1083.5400, found 1083.5420; $[C_{58}H_{80}N_2O_{16}K]^+$ cal. 1099.5139, found 1099.5162.

(4) Bivalent DES ligand **31**:

(*E*)-3,4-bis-(4-hydroxyphenyl)-3-hexenoic acid **39** (85% of *trans*-isomer, 36.9 mg, 0.124 mmol), diamine OEG **18c** (34.7 mg, 0.0590 mmol), triethylamine (18.2 μL, 0.130 mmol), PyBOP (67.5 mg, 0.130 mmol), anhydrous DMF (5 mL), and anhydrous DCM (5 mL) were used and the crude product was purified by column chromatography (chloroform : MeOH = 20:1 to 10:1) to obtain bivalent DES ligand **31** as a colorless oil (39.5 mg, 58%). *Cis*-*cis* (4%), *cis*-*trans* (33%), and *trans*-*trans* (62%) isomers were separated by RP-HPLC (70% MeOH/H_2O) and characterized with ^{1}H-NMR according to the chemical shift of **38** (84% *trans*-isomer).

Cis-*cis* isomer of **31** (First fraction):

^{1}H-NMR (Acetone-d6, 400 MHz) δ (ppm) = 6.90-6.84 (8H, d and d, J = 8.7 Hz, 8.6 Hz, Ar-*H*), 6.60 (4H, d, J = 8.7 Hz, Ar-*H*), 6.56 (4H, d, J = 8.7 Hz, Ar-*H*), 3.62-3.54 (40H, m, OH_2CH_2CO), 3.54-3.50 (4H, m, OH_2CH_2CO), 3.46-3.40 (8H, s and t, J = 5.3 Hz, HNH$_2$CH_2CO, and H_2CC=O), 3.35-3.29 (4H, m, HNH_2CH_2CO), 2.58 (4H, q, J = 7.6 Hz, H$_3$CH_2C), 0.94 (6H, t, J = 7.4 Hz, H_3CH_2C).

Cis-*trans* isomer of **31** (Second fraction):

^{1}H-NMR (Acetone-d6, 400 MHz) δ (ppm) = 7.23 (2H, d, J = 8.6 Hz, (*E*)-Ar-*H*), 7.14 (2H, d, J = 8.6 Hz, (*Z*)-Ar-*H*), 6.90-6.82 (8H, m, (*E*,*Z*)-Ar-*H*), 6.59 (2H, d, J = 8.6 Hz, (*Z*)-Ar-H), 6.55 (2H, d, J = 8.7 Hz, (*Z*)-Ar-*H*), 3.60-3.47 (44H, m, OH_2CH_2CO), 3.45-3.40 (4H, s and t, J = 5.3 Hz, H_2CC=O and OH_2CH_2CO), 3.38-3.28 (4H, m, OH_2CH_2CO, HNH$_2$CH_2CO, and H_2CC=O), 3.25-3.19 (2H, m, HNH_2CH_2CO), 2.58 (2H, q, J = 7.4 Hz, (*Z*)-H$_3$CH_2C), 2.24 (2H, q, J = 7.4 Hz, (*E*)-H$_3$CH_2C), 0.94 (3H, t, J = 7.4 Hz, (*Z*)-H_3CH_2C), 0.80 (3H, t, J = 7.4 Hz, (*E*)-H_3CH_2C).

^{13}C-NMR (Acetone-d6, 100 MHz) δ (ppm) = 170, 156, 155, 143, 134, 133, 131, 130, 115, 114, 70.3, 70.1, 69.6, 50.7, 50.4, 43.1, 42.0, 40.7, 39.1, 28.2, 27.9, 12.9, 12.3.

Trans-*trans* isomer of **31** (Third fraction):

^{1}H-NMR (Acetone-d6, 400 MHz) δ (ppm) = 7.23 (4H, d, J = 8.6 Hz, Ar-*H*), 7.14 (4H, d, J = 8.6 Hz, Ar-*H*), 6.86-6.81 (8H, m, Ar-*H*), 3.60-3.51 (40H, m, OH_2CH_2CO), 3.50-3.46 (4H, m, OH_2CH_2CO), 3.36 (4H, t, J = 5.6 Hz, HNH$_2$CH_2CO), 3.22 (4H, q, J = 5.5 Hz, HNH_2CH_2CO), 3.11 (4H, s, H_2CC=O), 2.25 (4H, q, J = 7.4 Hz, H$_3$CH_2C), 0.80 (6H, t, J = 7.4 Hz, H_3CH_2C).

^{13}C-NMR (Acetone-d6, 100 MHz) δ (ppm) = 171, 157, 144, 134, 132, 131, 116, 71.2, 70.9, 70.4, 43.9, 39.9, 29.1, 13.6, 11.8.

HRMS (ESI-TOF, positive): $[C_{62}H_{89}N_2O_{18}]^+$ cal. 1149.6105, found 1149.6143; $[C_{62}H_{88}N_2O_{18}Na]^+$ cal. 1171.5924, found 1171.5961; $[C_{62}H_{88}N_2O_{18}K]^+$ cal. 1187.5664, found 1187.5701.

(5) Bivalent DES ligand **32**:

(*E*)-3,4-bis-(4-hydroxyphenyl)-3-hexenoic acid **39** (85% of *trans*-isomer, 43.7 mg, 0.146 mmol), diamine OEG **19a** (30.7 mg, 0.0695 mmol), triethylamine (22.0 μL, 0.153 mmol), PyBOP (77.0 mg, 0.153 mmol), anhydrous DMF (5 mL), and anhydrous DCM (5 mL) were used and the crude product was purified by column chromatography (chloroform : MeOH = 20:1 to 10:1) to obtain bivalent DES ligand **32** as a colorless oil (35.4 mg, 51%). *Cis*-*cis* (2%), *cis*-*trans* (23%), and *trans*-*trans* (75%) isomers were separated by RP-HPLC (75% MeOH/H_2O) and characterized with ^{1}H-NMR according to the chemical shift of **38** (84% *trans*-isomer).

Cis-*cis* isomer of **32** (First fraction):

^{1}H-NMR (Acetone-d6, 400 MHz) δ (ppm) = 6.91-6.83 (8H, m, Ar-*H*), 6.59 (4H, d, J = 8.6 Hz, Ar-*H*), 6.55 (4H, d, J = 8.6 Hz, Ar-*H*), 3.59-3.49 (24H, m, OH_2CH_2CO), 3.46-3.39 (12H, m, HNH$_2$CH_2CO, H_2CC=O, and OCH_2CH$_2$), 3.34-3.27 (4H, q, J = 5.4 Hz, HNH_2CH$_2$CO), 2.57 (4H, q, J = 7.6 Hz, H$_3$CH_2C), 1.59 (4H, p, J = 3.3 Hz, OCH$_2$CH_2), 0.94 (6H, t, J = 7.4 Hz, H_3CH$_2$C).

Cis-*trans* isomer of **32** (Second fraction):

^{1}H-NMR (Acetone-d6, 400 MHz) δ (ppm) = 7.23 (2H, d, J = 8.6 Hz, (*E*)-Ar-*H*), 7.13 (2H, d, J = 8.5 Hz, (*Z*)-Ar-*H*), 6.91-6.81 (8H, m, (*E*,*Z*)-Ar-*H*), 6.59 (2H, d, J = 8.6 Hz, (*Z*)-Ar-H), 6.55 (2H, d, J = 8.6 Hz, (*Z*)-Ar-*H*), 3.60-3.46 (22H, m, OH_2CH_2CO), 3.46-3.39 (8H, m, OH_2CH$_2$CO, H_2CC=O and OCH_2CH$_2$), 3.38-3.28 (8H, m, HNH$_2$CH_2CO and HNH_2CH$_2$CO), 3.10 (2H, s, H_2CC=O), 2.58 (2H, q, J = 7.6 Hz, (*Z*)-H$_3$CH_2C), 2.24 (2H, q, J = 7.6 Hz, (*E*)-H$_3$CH_2C), 1.58 (4H, p, J = 3.3 Hz, OCH$_2$CH_2), 0.94 (3H, t, J = 7.4 Hz, (*Z*)-H_3CH$_2$C), 0.80 (3H, t, J = 7.4 Hz, (*E*)-H_3CH$_2$C).

^{13}C-NMR (Acetone-d6, 100 MHz) δ (ppm) = 171, 157, 156, 144, 143, 135, 134, 132, 131, 116, 115, 71.5, 71.2, 71.0, 70.8, 70.4, 39.9, 28.7, 27.2, 13.7, 13.2, 11.9.

Trans-*trans* isomer of **32** (Third fraction):

^{1}H-NMR (Acetone-d6, 400 MHz) δ (ppm) = 7.23 (4H, d, J = 8.6 Hz, Ar-*H*), 7.14 (4H, d, J = 8.6 Hz, Ar-*H*), 6.88-6.80 (8H, m, Ar-*H*), 3.58-3.46 (22H, m, OH_2CH_2CO), 3.45-3.39 (4H, m, OH_2CH$_2$CO), 3.38-3.28 (9H, t and m, J = 5.6 Hz, HNH$_2$CH_2CO), 3.22 (4H, q, J = 5.4 Hz, HNH_2CH$_2$CO), 3.11 (4H, s, H_2CC=O), 2.25 (4H, q, J = 7.4 Hz, H$_3$CH_2C), 1.57 (4H, p, J = 3.2 Hz, OCH$_2$CH_2), 0.80 (6H, t, J = 7.4 Hz, H_3CH$_2$C).

^{13}C-NMR (Acetone-d6, 100 MHz) δ (ppm) = 171, 157, 144, 134, 132, 131, 116, 71.5, 71.3, 71.2, 71.0, 70.8, 70.4, 47.0, 44.0, 39.9, 27.2, 13.7, 11.9.

HRMS (ESI-TOF, positive): $[C_{56}H_{77}N_2O_{14}]^+$ cal. 1001.5369, found 1001.5390; $[C_{56}H_{76}N_2O_{14}Na]^+$ cal. 1023.5189, found 1023.5212; $[C_{56}H_{76}N_2O_{14}K]^+$ cal. 1039.4928, found 1039.4955.

(6) Bivalent DES ligand **33**:

To a solution of (*E*)-3,4-bis-(4-hydroxyphenyl)-3-hexenoic acid **39** (85% of *trans*-isomer, 43.1 mg, 0.144 mmol), 1H-benzotriazole (HOBT·H2O, 24.2 mg, 0.179 mmol), 1-(3-dimethylaminopropyl) -3-ethylcarbodimide hydrocholorid (EDCl, 34.3 mg, 0.179 mmol), and diisopropyl amine (51.0 μL, 0.289 mmol) in THF (5 mL), diamine OEG **19b** (34.2 mg, 0.0688 mmol) in THF (1 mL) was added at room temperature and the reaction mixture was stirred at 56°C for 24 h. The reaction mixture was adjusted to pH = 7~8 with 5% $NaHCO_3$ and washed with ether, dried over $MgSO_4$ and concentrated in vacuo. The crude product was purified by column chromatography (chloroform : MeOH = 10:1) to obtain bivalent DES ligand **33** as a colorless oil (18.1 mg, 25%). *Cis-cis* (2%), *cis-trans* (34%), and *trans-trans* (64%) isomers were separated by RP-HPLC (80% MeOH/H_2O) and characterized with ^{1}H-NMR according to the chemical shift of **38** (84% *trans*-isomer).

Cis-trans isomer of **33** (Second fraction):

^{1}H-NMR (Acetone-d6, 400 MHz) δ (ppm) = 7.24 (2H, d, J = 8.4 Hz, (*E*)-Ar-*H*), 7.14 (2H, d, J = 8.6 Hz, (*Z*)-Ar-*H*), 6.90-6.81 (8H, m, (*E*,*Z*)-Ar-*H*), 6.60 (2H, d, J = 8.6 Hz, (*Z*)-Ar-H), 6.55 (2H, d, J = 8.6 Hz, (*Z*)-Ar-*H*), 3.59-3.46 (24H, m, OH_2CH_2CO), 3.45-3.39 (8H, m, OCH_2CH$_2$ and HNH$_2$CH_2CO), 3.37-3.28 (4H, m, HNH_2CH$_2$CO and H_2CC=O), 3.21 (2H, q, J = 5.2, HNH_2CH$_2$CO), 3.10 (2H, s, H_2CC=O), 2.58 (2H, q, J = 7.5 Hz, (*Z*)-H$_3$CH_2C), 2.24 (2H, q, J = 7.6 Hz, (*E*)-H$_3$CH_2C), 1.58-1.45 (4H, m, OCH$_2$CH_2 CH$_2$CH$_2$), 1.33-1.27 (8H, m, OCH$_2$CH$_2$ CH_2CH_2), 0.94 (3H, t, J = 7.4 Hz, (*Z*)-H_3CH$_2$C), 0.80 (3H, t, J = 7.4 Hz, (*E*)-H_3CH$_2$C).

Trans-trans isomer of **33** (Third fraction):

^{1}H-NMR (Acetone-d6, 400 MHz) δ (ppm) = 7.23 (4H, d, J = 8.5 Hz, Ar-*H*), 7.14 (4H, d, J = 8.4 Hz, Ar-*H*), 6.87-6.81 (8H, m, Ar-*H*), 3.59-3.44 (24H, m, OH_2CH_2CO), 3.41 (4H, t, J = 6.6 Hz, OH_2CH$_2$CH$_2$CH$_2$), 3.35 (4H, t, J = 5.6 Hz, HNH$_2$CH_2CO), 3.22 (4H, q, J = 4.9 Hz, HNH_2CH$_2$CO), 3.10 (4H, s, H_2CC=O), 2.25 (4H, q, J = 7.5 Hz, H$_3$CH_2C), 1.50 (4H, p, J = 6.8 Hz, OCH$_2$CH_2CH$_2$CH$_2$), 1.37-1.26 (8H, m, OCH$_2$CH$_2$CH_2CH_2), 0.80 (6H, t, J = 7.4 Hz, H_3CH$_2$C).

^{13}C-NMR (Acetone-d6, 100 MHz) δ (ppm) = 171, 157, 144, 134, 132, 131, 116, 115, 71.7, 71.2, 71.0, 70.8, 70.5, 44.0, 39.9, 30.5, 30.2, 26.9, 13.7, 11.9.

HRMS (ESI-TOF, positive): $[C_{60}H_{84}N_2O_{14}Na]^+$ cal. 1079.5815, found 1079.5729; $[C_{60}H_{84}N_2O_{14}Na_2]^{2+}$ cal. 551.2854, found 551.2805.

(7) Bivalent DES ligand **34**:

(*E*)-3,4-bis-(4-hydroxyphenyl)-3-hexenoic acid **39** (85% of *trans*-isomer, 39.6 mg, 0.133 mmol), diamine OEG **20** (35.7 mg, 0.0633 mmol), triethylamine (19.5 μL, 0.139 mmol), PyBOP (72.4 mg, 0.139 mmol), anhydrous DMF (5 mL), and anhydrous DCM (5 mL) were used and the crude product was purified by column chromatography (chloroform : MeOH = 20:1 to 10:1) to obtain bivalent DES ligand **34** as a colorless oil (48.4 mg, 68%). *Cis*-*cis* (6%), *cis*-*trans* (31%), and *trans*-*trans* (63%) isomers were separated by RP-HPLC (75% MeOH/H_2O) and characterized with ^{1}H-NMR according to the chemical shift of **38** (84% *trans*-isomer).

Cis-*cis* isomer of **34** (First fraction):

^{1}H-NMR (Acetone-d6, 400 MHz) δ (ppm) = 7.63 (4H, d, J = 8.2 Hz, biphenyl-*H*), 7.44 (4H, d, J = 8.1 Hz, biphenyl-*H*), 6.89-6.83 (8H, m, Ar-*H*), 6.59 (4H, d, J = 8.6 Hz, Ar-*H*), 6.55 (4H, d, J = 8.6 Hz, Ar-*H*), 4.60 (4H, s, OCH_2Ar), 3.67-3.55 (20H, m, OH_2CH_2CO), 3.53-3.49 (4H, m, OH_2CH_2CO) 3.44-3.38 (8H, s and t, J = 5.5 Hz, H_2CC=O and HNH$_2$CH_2CO), 3.29 (4H, q, J = 5.7 Hz, HNH_2CH$_2$CO), 2.56 (4H, q, J = 7.5 Hz, H$_3$CH_2C), 0.92 (6H, t, J = 7.6 Hz, H_3CH$_2$C).

Cis-*trans* isomer of **34** (Second fraction):

^{1}H-NMR (Acetone-d6, 400 MHz) δ (ppm) = 7.63 (4H, d, J = 8.1 Hz, biphenyl-*H*), 7.44 (4H, dd, J = 3.5 Hz, 8.2 Hz, biphenyl-*H*), 7.23 (2H, d, J = 8.6 Hz, (*E*)-Ar-*H*), 7.13 (2H, d, J = 8.6 Hz, (*Z*)-Ar-*H*), 6.89-6.81 (8H, m, (*E*,*Z*)-Ar-*H*), 6.59 (2H, d, J = 8.7 Hz, (*Z*)-Ar-H), 6.55 (2H, d, J = 8.6 Hz, (*Z*)-Ar-*H*), 4.59-4.58 (4H, s and s, OCH_2Ar), 3.67-3.53 (22H, m, OH_2CH_2CO), 3.53-3.46 (4H, m, OH_2CH$_2$CO) 3.44-3.39 (4H, s and t, J = 5.4 Hz, CH_2C=O and HNH$_2$CH_2CO), 3.36-3.32 (2H, m, HNH_2CH$_2$CO), 3.22-3.16 (2H, q, J = 5.4 Hz, HNH_2CH$_2$CO), 3.09 (2H, s, CH_2C=O) 2.56 (2H, q, J = 7.5 Hz, (*Z*)-H$_3$CH_2C), 2.23 (2H, q, J = 7.6 Hz, (*E*)-H$_3$CH_2C), 0.92 (3H, t, J = 7.6 Hz, (*Z*)-H_3CH$_2$C), 0.79 (3H, t, J = 7.4 Hz, (*E*)-H_3CH$_2$C).

Trans-*trans* isomer of **34** (Third fraction):

^{1}H-NMR (Acetone-d6, 400 MHz) δ (ppm) = 7.62 (4H, d, J = 8.2 Hz, biphenyl-*H*), 7.44 (4H, d, J = 8.1 Hz, biphenyl-*H*), 7.22 (4H, d, J = 8.6 Hz, Ar-*H*), 7.13 (4H, d, J = 8.6 Hz, Ar-*H*), 6.87-6.80 (8H,

m, Ar-*H*), 4.58 (4H, s, OC*H*$_2$Ar), 3.67-3.53 (20H, m, O*H*$_2$C*H*$_2$CO), 3.50-3.46 (4H, m, O*H*$_2$CH$_2$CO), 3.34 (4H, t, *J* = 5.4 Hz, HNH$_2$C*H*$_2$CO), 3.19 (4H, q, *J* = 5.5 Hz, HN*H*$_2$CH$_2$CO), 3.09 (4H, s, *H*$_2$CC=O), 2.23 (4H, q, *J* = 7.4 Hz, H$_3$C*H*$_2$C), 0.79 (6H, t, *J* = 7.4 Hz, *H*$_3$CH$_2$C).

HRMS (ESI-TOF, positive): $[C_{66}H_{81}N_2O_{14}]^+$ cal. 1125.5682, found 1125.5694; $[C_{66}H_{80}N_2O_{14}Na]^+$ cal. 1147.5502, found 1147.5514; $[C_{66}H_{80}N_2O_{14}K]^+$ cal. 1163.5241, found 1163.5261.

6.2.2. Chemical preparation of (d,l)-1,2-bis-(4-methoxyphenyl)-l-butane 35

To a soultion of sodium hydride (2.47 g, 61.8 mmol) in anhydrous THF (50 mL), a soultion of desoxyanisoin (10.6 g, 41.2 mmol) in anhydrous THF (80 mL) was added dropwise at 0 °C, then the reaction mixture was allowed to warm up to room temperature and stirred for 1 h. This mixture was added slowly to a solution of iodoethane (3.36 mL, 41.2 mmol) in anhydrous THF (20 mL) at 0°C. The reaction mixture was allowed to warm up to room temperature and stirred for 12 h. Afterwards the reaction was quenched with water at 0°C. The solvent was removed in vacuo and the residue was washed with DCM, brine, and dried over $MgSO_4$. The organic solvent was evaporated in vacuo and the residue was purified by column chromatography (hexane: AcOEt = 5:1) to obtain (d,l)-α-ethyl deoxyanisoin **35** as a yellow oil (7.87 g, 67%).

^{1}H-NMR ($CDCl_3$, 400 MHz) δ (ppm) = 7.95 (2H, d, *J* = 8.9 Hz, Ar-*H*), 7.21 (2H, d, *J* = 8.7 Hz, Ar-*H*), 6.86 (2H, d, *J* = 9.0 Hz, Ar-*H*), 6.81 (2H, d, *J* = 8.8 Hz, Ar-*H*), 4.34 (1H, t, *J* = 7.3 Hz, *H*CC=O), 3.81 (3H, s, C*H*$_3$OAr), 3.74 (3H, s, C*H*$_3$OAr), 2.15 (1H, septet, *J* = 7.3 Hz, H$_3$C*H*$_2$CHC), 1.81 (1H, septet, *J* = 7.5 Hz, H$_3$C*H*$_2$CHC), 0.88 (3H, t, *J* = 7.4 Hz, *H*$_3$CH$_2$CHC).

^{13}C-NMR ($CDCl_3$, 100 MHz) δ (ppm) = 199, 163, 159, 132, 131, 130, 129, 114, 55.6, 55.4, 54.3, 27.3, 12.5.

HRMS (ESI-TOF, positive): $[C_{18}H_{20}O_3Na]^+$ cal. 307.1305, found 307.1325; $[C_{18}H_{20}O_3K]^+$ cal. 323.1044, found 323.1065.

6.2.3. Chemical preparation of ethyl 3-hydroxy-3,4-bis-(4-methoxyphenyl)hexanoate 36

Zinc powder (10 um) was washed with dilute hydrochloric acid, twice with water, and once each with ethanol and diethyl ether and finally dried in vacuum. To this washed zinc (3.37 g, 50.6 mmol), 50% of a soultion of d,l-α-ethyldeoxyanisoin **35** (3.42 g, 12.0 mmol) and ethyl bromoacetate (5.72 mL, 50.6 mmol) in dry benzene (20 mL) was added and the reaction mixture

was heated briefly to reflux, initiating the reaction. The remainder of the reagent solution was then added dropwise, and the mixture was heated to reflux for 2 h. The organozinc intermediate was hydrolyzed by the gradual addition of 5% aqueous sulfuric acid, and this mixture was washed with ether, water, 5% sodium hydrogen carbonate, and again with water, dried over $MgSO_4$. The organic solution was filtered over silica gel and concentrated in vacuo. The residue, i.e., a mixture of diastereomers of ethyl 3-hydroxy-3,4-bis-(4-methoxyphenyl)hexanoate, was purifed with HPLC (DCM) to obtain three factions: (1) Starting materials **35** and ethyl bromoacetate; (2) More mobile diastereomer of **36** and (3) less mobile diastereomer of **36** as a colorless oil (3.68 g, 82%).

More mobile diastereomer of **36**:

^{1}H-NMR ($CDCl_3$, 400 MHz) δ (ppm) = 7.33 (2H, d, J = 8.7 Hz, Ar-*H*), 7.22 (2H, d, J = 7.9 Hz, Ar-*H*), 6.89-6.81 (4H, m, Ar-*H*), 4.35 (1H, br s, *H*O), 3.87-3.78 (8H, q and s, J = 7.2 Hz, H_3CH_2COC=O and H_3COAr), 2.75 (1H, d, J = 16 Hz, CH_2CC=O), 2.56 (1H, dd, J = 2.1 Hz, 12 Hz, H_3CH_2CHC), 2.36 (1H, d, J = 16 Hz, CH_2CC=O), 1.78-1.65 (1H, m, H_3CH_2CHC), 1.51-1.41 (1H, m, H_3CH_2CHC), 0.96 (3H, t, J = 7.2 Hz, H_3CH_2COC=O), 0.52 (3H, t, J = 7.3 Hz, H_3CH_2CHC).

^{13}C-NMR ($CDCl_3$, 100 MHz) δ (ppm) = 174, 159, 158, 138, 133, 131, 127, 114, 113, 104, 60.7, 58.8, 55.4, 45.1, 22.2, 14.1, 12.8.

Less mobile diastereomer of **36**:

^{1}H-NMR ($CDCl_3$, 400 MHz) δ (ppm) = 7.09 (2H, d, J = 8.8 Hz, Ar-*H*), 6.80-6.72 (6H, m, Ar-*H*), 4.52 (1H, br s, *H*O), 3.97 (2H, q, J = 6.7 Hz, H_3CH_2COC=O) 3.79 and 3.78 (6H, s, H_3COAr), 2.92 (1H, d, J = 16 Hz, CH_2CC=O), 2.78-2.72 (2H, dd and d, J = 3.1 Hz, 12 Hz, and 16 Hz, H_3CH_2CHC and CH_2CC=O), 2.08-1.98 (1H, m, H_3CH_2CHC), 1.42-1.28 (1H, m, H_3CH_2CHC), 1.07 (3H, t, J = 7.2 Hz, H_3CH_2COC=O), 0.62 (3H, t, J = 7.3 Hz, H_3CH_2CHC).

^{13}C-NMR ($CDCl_3$, 100 MHz) δ (ppm) = 174, 159, 158, 136, 132, 131, 128, 113, 104, 77.2, 60.8, 58.5, 55.3, 43.5, 21.8, 14.2, 12.5.

6.2.4. Chemical preparation of (*E*,*Z*)-ethyl 3,4-bis-(4-methoxyphenyl)-2-hexenoate 37

To a solution of both diastereomers of ethyl 3-hydroxy-3,4-bis(4-methoxyphenyl)hexanoate 36 (3.26 g, 8.76 mmol) in dry pyridine (20 mL), thionyl chloride (1.27 mL, 17.5 mmol) were added dropwise at room temperature and then the reaction mixture was stirred at room temperature for 3

h. Benzene (10 mL) was added to precipitate the pyridine hydrochloride, and the solvent was removed in vacuo. The residue was dissolved in ether, washed with two times water, dried over $MgSO_4$. The black crude product was purified by column chromatography (hexane : AcOEt = 10:1) to obtain *cis*- and *trans*- isomers of ethyl 3,4-bis-(4-methoxyphenyl)-2-hexenoate **37** as a yellow oil (3.03 g, 98%).

Cis-isomer of **37** (the first fraction):

^{1}H-NMR ($CDCl_3$, 400 MHz) δ (ppm) = 7.18 (2H, d, J = 8.4 Hz, Ar-*H*), 6.82 (2H, d, J = 8.7 Hz, Ar-*H*), 6.79 (2H, d, J = 8.9 Hz, Ar-*H*), 6.69 (2H, d, J = 8.8 Hz, Ar-*H*), 5.91 (1H, s, C=C*H*C=O), 5.36 (1H, dd, J = 6.1 Hz, 9.2 Hz, H_3CH_2CHCC), 4.25 (2H, q, J = 7.1 Hz, H_3CH_2COC=O) 3.80 (3H, s, H_3COAr), 3.76 (3H, s, H_3COAr), 1.88 (1H, septet, J = 7.3 Hz, H_3CH_2CHC), 1.72-1.61 (1H, m, H_3CH_2CHC), 1.33 (3H, t, J = 7.2 Hz, H_3CH_2COC=O), 0.92 (3H, t, J = 7.3 Hz, H_3CH_2CHC).

^{13}C-NMR ($CDCl_3$, 100 MHz) δ (ppm) = 167, 163, 160, 158, 134, 133, 130, 129, 120, 114, 113, 60.2, 55.4, 45.0, 24.4, 14.5, 12.3.

Trans-isomer of **37** (the second fraction):

^{1}H-NMR ($CDCl_3$, 400 MHz) δ (ppm) = 6.99 (2H, d, J = 8.7 Hz, Ar-*H*), 6.82-6.73 (6H, m, Ar-*H*), 5.91 (1H, d, J = 0.68 Hz, C=C*H*C=O), 3.97 (2H, q, J = 7.1 Hz, H_3CH_2COC=O), 3.78 (3H, s, H_3COAr), 3.77 (3H, s, H_3COAr), 3.42 (1H, t, J = 7.8 Hz, H_3CH_2CHCC), 1.93-1.68 (2H, m, H_3CH_2CHC), 1.07 (3H, t, J = 7.2 Hz, H_3CH_2COC=O), 0.89 (3H, t, J = 7.2 Hz, H_3CH_2CHC).

^{13}C-NMR ($CDCl_3$, 100 MHz) δ (ppm) = 167, 162, 159, 158, 133, 132, 130, 129, 117, 114, 113, 60.0, 56.4, 55.4, 55.3, 26.5, 14.2, 12.7.

6.2.5. Chemical preparation of (*E*,*Z*)-ethyl 3,4-bis-(4-hydroxyphenyl)-3-hexenoate 38

(1) By using precursor **37**:

To a solution of (*E*,*Z*)-ethyl 3,4-bis-(4-methoxyphenyl)-2-hexenoate **37** (160 mg, 0.450 mmol) in anhydrous DCM (8 mL) which was cooled in a dry ice/2-propanol bath, boron tribromide (170 µL, 1.80 mmol) were added dropwise and this reaction mixture was further stirred under the cooling for 1 h. Afterwards, the reaction mixture was warmed up to 0°C and stirred for 4 h. The reaction mixture was again cooled to -78°C followed by the addition of absolute EtOH (2 mL) to quench the reaction. The solvent was removed under a stream of dry argon and the residue was absorbed on the silica gel and further purified by column chromatography (chloroform : MeOH = 20:1) to

obtain a mixture of *cis*- and *trans*- isomers (*trans*-isomer: 84%) of ethyl 3,4-bis-(4-hydroxyphenyl)-3-hexenoate **38** as a red oil (38.9 mg, 27%) and a styrene byproduct (105 mg, 72%).

(2) By using precursor (*E*/*Z*)-ethyl 3,4-bis(4-methoxyphenyl)hex-4-enoate **41a**:

To a solution of **41a** (1.59 g, 4.47 mmol) in anhydrous DCM (30 mL), which was cooled in a dry ice/2-propanol bath, boron tribromide (1.69 mL, 17.9 mmol) was added dropwise and this reaction mixture was further stirred under the cooling for 1 h. Afterwards, the reaction mixture was warmed up to 0°C and stirred for 4 h. The reaction mixture was again cooled to -78°C followed by the addition of absolute EtOH (5 mL) to quench the reaction. The solvent was removed under a stream of dry argon and the residue was absorbed on the silica gel and further purified by column chromatography (chloroform : MeOH = 40:1) to obtain a mixture of *cis*- and *trans*- isomers (*trans*-isomer: 84%) of ethyl 3,4-bis- (4-hydroxyphenyl)-3-hexenoate **38** as a red oil (560 mg, 38%).

Since the facile isomerization of the stilbene structure takes place in organic solvent of low dielectric constant, both stereoisomers were applied for the next step without any further separation and a geometrical isomer separation by HPLC (2%MeOH/DCM) was only performed for the characterization of *trans*-isomer of **38**. The chemical shift of *trans*-isomer of **38** was consistent with previous report[143] and further characterized by ROESY spectra.

Trans-isomer of **38**:

^{1}H-NMR ($CDCl_3$, 400 MHz) δ (ppm) = 7.08-7.03 (4H, m, Ar-*H*), 6.78-6.72 (4H, m, Ar-*H*), 3.94 (2H, q, J = 7.1 Hz, H_3CH_2COC=O), 3.14 (2H, s, H_2CC=O), 2.19 (2H, q, J = 7.4 Hz, H_3CH_2CHC), 1.08 (3H, t, J = 7.2 Hz, H_3CH_2COC=O), 0.78 (3H, t, J = 7.4 Hz, H_3CH_2CHC).

^{13}C-NMR ($CDCl_3$, 100 MHz) δ (ppm) = 173, 156, 144, 133, 130, 129, 115, 114, 50.7, 40.9, 28.1, 12.2.

HRMS (ESI-TOF, positive): $[C_{20}H_{22}O_4Na]^+$ cal. 349.1410, found 349.1402; $[C_{40}H_{44}O_8Na]^+$ cal. 675.2928, found 675.2888.

6.2.6. Chemical preparation of (*E*,*Z*)-3,4-bis-(4-hydroxyphenyl)-3-hexenoic acid 39

To a solution of (*E*,*Z*)-ethyl 3,4-bis- (4-hydroxyphenyl)-3-hexenoate **38** (354 mg, 1.09 mmol) in THF (10 mL), 2.5 mL of 5 N NaOH solution was added. This mixture was heated tup to reflux for

2 h. To this cold reaction mixture, 0.5 mL 1 N NaOH solution was added and the aqueous layer was washed with ether and concentrated in vacuo. The aqueous layer was acidified with 6 N HCl, and the precipitate was collected. The crude product was purified by column chromatography (chloroform : MeOH = 10:1) to obtain a mixture of *cis*- and *trans*- isomers (*trans*-isomer: 85%) of 3,4-bis-(4-hydroxyphenyl)-3-hexenoic acid **39** as a colorless solid (408 mg, 99%).

Trans-isomer of **39**:

^{1}H-NMR (MeOD, 400 MHz) δ (ppm) = 7.08-7.03 (4H, d, J = 8.6 Hz, Ar-*H*), 6.81-6.75 (4H, m, Ar-*H*), 3.15 (2H, s, H_2CC=O), 2.22 (2H, q, J = 7.4 Hz, H_3CH_2CHC), 0.80 (3H, t, J = 7.4 Hz, H_3CH_2CHC).

^{13}C-NMR (MeOD, 100 MHz) δ (ppm) = 176, 157, 145, 135, 134, 132, 131, 116, 115, 62.1, 42.6, 29.6, 13.7.

HRMS (ESI-TOF, positive): $[C_{18}H_{18}O_4Na]^+$ cal. 321.1097, found 321.1103; $[C_{36}H_{36}O_8Na]^+$ cal. 619.2302, found 619.2312.

6.2.7. Chemical preparation of (d,l)- ethyl 3,4-bis(4-methoxyphenyl)-4-oxobutanoate 40a

To a soultion of sodium hydride (1.43 g, 35.8 mmol) in anhydrous THF (40 mL), a soultion of desoxyanisoin (8.34 g, 31.9 mmol) in anhydrous THF (60 mL) was added dropwise at 0 °C, then the reaction mixture was heated up to reflux and stirred for 1 h. To this mixture, a solution of ethyl bromoacetate (5.52 mL, 48.8 mmol) in anhydrous THF (20 mL) was added slowly to at 0°C. The reaction mixture was heated uo to reflux and stirred for 5 h. Afterwards the reaction was quenched with water at 0°C. The solvent was removed in vacuo and the residue was washed with ether, brine, and dried over $MgSO_4$. The organic solvent was evaporated in vacuo and the residue was purified by column chromatography (hexane: AcOEt = 5:1) to obtain (d,l)-ethyl 3,4-bis(4-methoxyphenyl)-4-oxobutanoate **40a** as a yellow oil (10.4 g, 96%).

^{1}H-NMR ($CDCl_3$, 400 MHz) δ (ppm) = 7.95 (2H, d, J = 8.9 Hz, Ar-*H*), 7.21 (2H, d, J = 8.8 Hz, Ar-*H*), 6.85 (2H, d, J = 8.8 Hz, Ar-*H*), 6.81 (2H, d, J = 8.7 Hz, Ar-*H*), 5.00 and 4.98 (1H, 2×d, J = 5.3 Hz, O=CCH$_2$C*H*C=O), 4.08 (2H, q, J = 7.1 Hz, OCH_2CH$_3$), 3.81 (3H, s, H_3COAr), 3.74 (3H, s, H_3COAr), 3.30 (1H, dd, J = 9.5 Hz, 16.8 Hz, O=CCH_2CHC=O), 2.67 (1H, dd, J = 5.3 Hz, 16.8 Hz, O=CCH_2CHC=O), 1.19 (3H, t, J = 7.0 Hz, OCH$_2$CH_3).

^{13}C-NMR ($CDCl_3$, 100 MHz) δ (ppm) = 197, 172, 164, 159, 131, 129, 115, 114, 104, 60.8, 55.6,

55.4, 48.5, 38.9, 29.9, 27.6, 14.3.

6.2.8. Chemical preparation of (d,l)-ethyl 7,8-bis(4-methoxyphenyl)-8-oxooctanoate 40b

To a solution of desoxyanisoin (11.0 g, 42.8 mmol) in anhydrous THF (110 mL) at 0°C, sodium hydride (2.02 g, 50.5 mmol) was added portionwise over 10 min. The reaction mixture was further stirred for 30 min and then heated up to reflux for 1h. Ethyl 6-bromohexanoate (11.5 mL, 63.1 mmol) was added dropwise at 0°C and then the reaction mixture was refluxed for 20 h. The reaction mixture was quenched and adjusted to pH = 7~8 with 5% $NaHCO_3$ and washed with water, ether, dried over $MgSO_4$ and concentrated in vacuo. The crude product was purified by column chromatography (hexane : AcOEt = 10:1) to obtain (d,l)-ethyl 7,8-bis(4-methoxyphenyl)-8-oxooctanoate **40b** as a light yellow solid (12.1 g, 72%).

^{1}H-NMR ($CDCl_3$, 400 MHz) δ (ppm) = 7.94 (2H, d, J = 8.9 Hz, Ar-*H*), 7.20 (2H, d, J = 8.7 Hz, Ar-*H*), 6.86 (2H, d, J = 8.9 Hz, Ar-*H*), 6.81 (2H, d, J = 8.8 Hz, Ar-*H*), 4.43 (1H, t, J = 7.3 Hz, O=C*H*$CH_2CH_2CH_2CH_2CC$=O), 4.12 (2H, q, J = 7.2 Hz, OC*H*$_2CH_3$), 3.82 (3H, s, *H*$_3$COAr), 3.75 (3H, s, *H*$_3$COAr), 2.23 (2H, t, J = 7.5 Hz, O=CHC*H*$_2CH_2$C H$_2CH_2$C*H*$_2$CC=O), 2.18-2.07 (1H, m, O=CHC*H*$_2CH_2CH_2CH_2CH_2CC$=O), 1.84-1.72 (1H, m, O=CHC*H*$_2CH_2CH_2CH_2CH_2CC$=O), 1.59 (2H, p, J = 7.4 Hz, O=CHC*H*$_2CH_2CH_2CH_2CH_2CC$=O), 1.43-1.18 (7H, m and t, J = 7.2 Hz, O=CHCH$_2$C*H*$_2$C*H*$_2$CH$_2$CH$_2$CC=O and OCH$_2$C*H*$_3$).

^{13}C-NMR ($CDCl_3$, 100 MHz) δ (ppm) = 199, 174, 163, 159, 132, 131, 130, 129, 114, 60.4, 55.6, 55.4, 52.5, 34.5, 34.0, 29.3, 27.5, 25.0, 14.4.

6.2.9. Chemical preparation of (*E*/*Z*)-ethyl 3,4-bis(4-methoxyphenyl)hex-4-enoate 41a

To a suspension of (ethyl)triphenylphosphonium bromide (2.57 g, 6.86 mmol) in anhydrous diethyl ether (30 mL), *n*-buthyl lithium (2.5 M in hexane, 2.23 mL, 5.57 mmol) was added dropwise at 0°C and the reaction mixture was stirred at room temperature for 1 h. Afterwards the reation mixture was chilled to 0°C and a solution of (d,l)-ethyl 3,4-bis(4-methoxyphenyl)-4-oxobutanoate **40a** (1.47 g, 4.29 mmol) in diethylether (30 mL) was added dropwise over 15 min. Then the mixture was stirred at room temperature for 12 h. The reaction was quenched with 3% aqueous NH_4Cl solution and the mixture was washed with diethyl ether, brine, dried over $MgSO_4$, and concentrated in vacuo. The crude product was purified by column

chromatography (hexane : AcOEt = 5:1) to obtain (*E*/*Z*)-ethyl 3,4-bis(4-methoxy-phenyl)hex-4-enoate **41a** as a colorless oil (805 mg, 53%).

^{1}H-NMR ($CDCl_3$, 400 MHz) δ (ppm) = 7.07 (1H, d, J = 8.6 Hz, Ar-*H*), 7.02 (1H, d, J = 8.7 Hz, Ar-*H*), 6.85-6.60 (5H, m, Ar-*H*), 6.68 (1H, d, J = 8.8 Hz, Ar-*H*), 5.59 (1H, q, J = 7.0 Hz, *Z*-C*H*CH_3), 4.71 (1H, dd, J = 6.7 Hz, 8.8 Hz, *E*-C*H*CH_3), 4.15-4.02 (3H, m, O=CCH_2C*H*C and OC*H*$_2CH_3$), 3.81-3.73 (6H, 4×s, *H*$_3$COAr), 2.83-2.75 and 2.68-2.60 (2H, m, O=CC*H*$_2$CHC), 1.92 and 1.47 (3H, d and d, J = 6.8 Hz and 6.3 Hz, CHC*H*$_3$), 1.28-1.15 (3H, m, OCH_2C*H*$_3$).

^{13}C-NMR ($CDCl_3$, 100 MHz) δ (ppm) = 173, 158, 143, 135, 134, 132, 130, 129, 125, 122, 114, 113, 104, 60.6, 60.5, 55.4, 49.2, 40.3, 39.7, 37.7, 14.9, 14.4, 14.3.

6.2.10. Chemical preparation of (*E*,*Z*)-ethyl 7,8-bis(4-methoxyphenyl)dec-8-enoate 41b

To a solution of both diastereomers of ethyl 8-hydroxy-7,8-bis(4-methoxyphenyl)decanoate **44** (201 mg, 0.469 mmol) in anhydrous pyridine (8 mL), thionyl chloride (68.4 µL, 0.938 mmol) was added dropwise at room temperature and then the reaction mixture was stirred at room temperature for 3 h. Benzene (2 mL) was added to precipitate the pyridine hydrochloride, and the solvent was removed in vacuo. The residue was dissolved in ether, washed with two times water, dried over $MgSO_4$, and concentrated in vacuo. The black crude product was purified by column chromatography (hexane : AcOEt = 10:1) to obtain (*E*,*Z*)-ethyl 7,8-bis(4-methoxyphenyl) dec-8-enoate **41b** as a yellow oil (108 mg, 55%).

^{1}H-NMR ($CDCl_3$, 400 MHz) δ (ppm) = 6.98 (2H, d, J = 8.7 Hz, Ar-*H*), 6.80-6.69 (6H, m, Ar-*H*), 5.58 (1H, s, C=C*H*), 4.10 (2H, q, J = 7.2 Hz, OC*H*$_2CH_3$), 3.78 (3H, s, *H*$_3$COAr), 3.77 (3H, s, *H*$_3$COAr), 3.39 (1H, t, J = 7.4 Hz, CC*H*$CH_2CH_2CH_2CH_2CC$=O), 2.24 (2H, t, J = 7.4 Hz, $CCHCH_2CH_2CH_2CH_2$C*H*$_2$CC=O), 1.70-1.52 (4H, m, CCHC*H*$_2CH_2CH_2$C*H*$_2CH_2$CC=O), 1.47 (3H, d, J = 6.6 Hz, CC*H*$_3$), 1.35-1.19 (7H, m and t, J = 7.2 Hz, $CCHCH_2$C*H*$_2$C*H*$_2CH_2CH_2$CC=O and OCH_2C*H*$_3$).

^{13}C-NMR ($CDCl_3$, 100 MHz) δ (ppm) = 174, 158, 145, 136, 133, 130, 129, 121, 114, 113, 60.3, 55.4, 55.3, 53.3, 34.6, 29.4, 27.8, 25.1, 14.9, 14.4.

6.2.11. Chemical preparation of (*E*)-N-ethyl-3,4-bis(4-hydroxyphenyl)hex-3-enamide 42

To a solution of (*E*)-3,4-bis-(4-hydroxyphenyl)-3-hexenoic acid **39** (85% of *trans*-isomer, 109 mg,

0.367 mmol), 1H-benzotriazole (HOBT·H_2O, 59.5 mg, 0.440 mmol), 1-(3-dimethylaminopropyl) -3-ethylcarbodimide hydrocholorid (EDCl, 84.4 mg, 0.440 mmol), and diisopropyl amine (128 µL, 0.733 mmol) in THF (15 mL), 2.0 M ethylamine in THF (367 µL, 0.733 mmol) was added at room temperature and the reaction mixture was stirred at room temperature for 24 h. The reaction mixture was adjusted to pH = 7~8 with 1 M HCl and washed with ethyl acetate, dried over $MgSO_4$ and concentrated in vacuo. The crude product was purified by column chromatography (chloroform : MeOH = 10:1) to obtain a mixture of *cis*- and *trans*- isomers (*trans*-isomer: 80%) of **42** as a white solid (19.7 mg, 16%). *Trans*-isomer was characterized with ^{1}H-NMR according to the chemical shift of **38** (84% *trans*-isomer).

Trans-isomer of **42**:

^{1}H-NMR (MeOD, 400 MHz) δ (ppm) = 7.15 (2H, d, J = 8.6 Hz, Ar-*H*), 6.08 (2H, d, J = 8.6 Hz, Ar-*H*), 6.80-6.74 (4H, m, Ar-*H*), 3.06 (2H, s, H_2CC=O), 3.01 (2H, q, J = 7.2 Hz, HNCH_2CH$_3$), 2.23 (2H, q, J = 7.4 Hz, H$_3$CH_2C), 0.91 (3H, t, J = 7.2 Hz, HNCH$_2$CH_3), 0.79 (3H, t, J = 7.4 Hz, H_3CH$_2$CHC).

^{13}C-NMR (MeOD, 100 MHz) δ (ppm) = 157, 134, 132, 131, 116, 115, 44.1, 35.3, 29.7, 14.9, 13.7.

HRMS (ESI-TOF, positive): $[C_{20}H_{24}NO_3]^+$ cal. 326.1751, found 326.1761; $[C_{20}H_{23}NO_3Na]^+$ cal. 348.1570, found 348.1586; $[C_{40}H_{46}N_2O_6Na]^+$ cal. 673.3248, found 673.3272.

6.2.12. Chemical preparation of bivalent DES ligand 43

To a solution of (*E*)-3,4-bis-(4-hydroxyphenyl)-3-hexenoic acid **39** (85% of *trans*-isomer, 105 mg, 0.353 mmol), 1H-benzotriazole (HOBT·H_2O, 59.0 mg, 0.437 mmol), 1-(3-dimethylaminopropyl) -3-ethylcarbodimide hydrocholorid (EDCl, 83.7 mg, 0.437 mmol), and diisopropyl amine (124 µL, 0.706 mmol) in THF (15 mL), 2,2'-(ethylenedioxy)-bis-(ethylamine) (25.1 µL, 0.168 mmol) was added at room temperature and the reaction mixture was stirred at room temperature for 24 h. The reaction mixture was adjusted to pH = 7~8 with 5% $NaHCO_3$ and washed with ethyl acetate, dried over $MgSO_4$ and concentrated in vacuo. The crude product was purified by column chromatography (chloroform : MeOH = 10:1) to obtain a mixture of *cis*- and *trans*- isomers (*trans*-isomer: 80%) of bivalent DES ligand **43** as a colorless oil (27.2 mg, 23%). *Trans*-isomer was characterized with ^{1}H-NMR according to the chemical shift of **38** (84% *trans*-isomer).

Trans-isomer of **43**:

^{1}H-NMR (Acetone-d6, 400 MHz) δ (ppm) = 7.21 (2H, d, J = 8.5 Hz, Ar-*H*), 6.08 (2H, d, J = 8.6 Hz, Ar-*H*), 6.85-6.80 (4H, m, Ar-*H*), 3.45-3.42 (4H, m, OCH_2CH_2O) 3.33 (4H, q, J = 5.7 Hz, HNCH_2CH_2O), 2.22 (4H, q, J = 5.4 Hz, HNCH_2CH$_2$O), 3.14 (2H, s, H_2CC=O), 2.25 (4H, q, J = 7.4 Hz, H$_3$CH_2C), 0.80 (6H, t, J = 7.4 Hz, H_3CH$_2$CHC).

^{13}C-NMR (Acetone-d6, 100 MHz) δ (ppm) = 172, 157, 144, 135, 134, 132, 131, 116, 115, 71.0, 70.4, 44.1, 40.0, 39.9, 13.7.

HRMS (ESI-TOF, positive): $[C_{42}H_{48}N_2O_8Na]^+$ cal. 731.3303, found 731.3294.

6.2.13. Chemical preparation of ethyl 8-hydroxy-7,8-bis(4-methoxyphenyl)decanoate 44

To a solution of (d,l)-ethyl 7,8-bis(4-methoxyphenyl)-8-oxooctanoate **40b** (1.03 g, 2.59 mmol) in anhydrous THF (30 mL) at 0°C, 1.0 M ethyl magnesium bromide in anhydrous THF (3.89 mL, 3.89 mmol) was added dropwise over 30 min. The reaction mixture was further stirred at room temperature for 2 h. The reaction mixture was quenched with 5% NH_4Cl and washed with water, ether, dried over $MgSO_4$ and concentrated in vacuo. The crude product was purified by column chromatography (DCM) and HPLC (C-18, 1%AcOEt/$CHCl_3$) to obtain three factions: (1) Starting materials **40b** (92.2 mg); (2) More mobile diastereomer of **44** (17%) and (3) less mobile diastereomer of **44** (83%) as a light yellow solid (527 mg, 48%).

More mobile diastereomer of **44**:

^{1}H-NMR ($CDCl_3$, 400 MHz) δ (ppm) = 7.26 (2H, d, J = 8.7 Hz, Ar-*H*), 7.11 (2H, d, J = 8.6 Hz, Ar-*H*), 6.91-6.82 (4H, m, Ar-*H*), 4.06 (2H, q, J = 7.2 Hz, OCH_2CH$_3$), 3.83 (3H, s, H_3COAr), 3.81 (3H, s, H_3COAr), 2.81 (1H, dd, J = 2.9 Hz, 12 Hz, HOC*H*CH$_2$CH$_2$CH$_2$CH$_2$C H$_2$CC=O), 2.12 (2H, t, J = 7.6 Hz, HOCHCH$_2$CH$_2$CH$_2$CH$_2$CH_2CC=O), 1.80-1.61 (2H, m, H$_3$CH_2C), 1.48-1.28 (4H, m, HOCHCH_2CH$_2$CH$_2$CH_2CH$_2$CC=O), 1.24-0.82 (8H, t and m, J = 7.2 Hz, OCH$_2$CH_3 and *H*OCHCH$_2$CH_2CH_2CH$_2$CH$_2$CC=O), 0.53 (3H, t, J = 7.4 Hz, H_3CH$_2$C).

^{13}C-NMR ($CDCl_3$, 100 MHz) δ (ppm) = 174, 158, 137, 133, 127, 114, 113, 79.4, 60.3, 56.1, 55.4, 34.5, 29.5, 29.1, 27.7, 25.0, 14.4, 7.90.

Less mobile diastereomer of **44**:

^{1}H-NMR ($CDCl_3$, 400 MHz) δ (ppm) = 7.08 (2H, d, J = 8.6 Hz, Ar-*H*), 6.86-6.74 (4H, m, Ar-*H*), 6.72 (2H, d, J = 8.1 Hz, Ar-*H*), 4.08 (2H, q, J = 7.2 Hz, OCH_2CH$_3$), 3.80 (3H, s, H_3COAr), 3.77 (3H, s, H_3COAr), 2.81 (1H, dd, J = 2.8 Hz, 12 Hz, HOC*H*CH$_2$CH$_2$CH$_2$CH$_2$C H$_2$CC=O), 2.17 (2H,

t, J = 7.6 Hz, HOCHCH$_2$CH$_2$CH$_2$CH$_2$CH_2CC=O), 1.98-1.74 (3H, m, H$_3$CH_2C and HOCHCH$_2$CH$_2$CH$_2$CH$_2$CH$_2$CC=O), 1.56-1.39 (3H, m, HOCHCH_2CH_2CH$_2$C H$_2$CH$_2$CC=O), 1.31-1.10 (5H, t and m, J = 7.1 Hz, HOCHCH$_2$CH_2CH_2CH$_2$CH$_2$CC=O and OCH$_2$CH_3), 1.03-0.91 (2H, m, HOCHCH$_2$CH$_2$CH$_2$CH_2CH$_2$CC=O), 0.71 (3H, t, J = 7.3 Hz, H_3CH$_2$C).

^{13}C-NMR (CDCl$_3$, 100 MHz) δ (ppm) = 174, 158, 136, 132, 131, 128, 113, 79.1, 60.3, 57.0, 55.4, 55.3, 53.6, 34.5, 31.2, 29.4, 28.7, 27.7, 25.0, 14.4, 7.98.

HRMS (ESI-TOF, positive): $[C_{26}H_{36}O_5Na]^+$ cal. 451.2455, found 451.2467; $[C_{26}H_{36}O_5K]^+$ cal. 467.2194, found 467.2202; $[C_{52}H_{72}O_{10}Na]^+$ cal. 879.5018, found 879.5020.

6.3. Bivalent raloxifene (RAL) ligand

6.3.1. Chemical preparation of bivalent RAL ligands 46-58

(1) General procedure for chemical preparations of bivalent RAL ligands **46-58**

The raloxifen azide **45** (2.1 equivalents) and dipropargyl ether OEG **21** (1.0 equivalent) were suspended in a 1:1 mixture of water and *tert*-butyl alcohol (1 mL). Sodium ascorbate (0.2 equivalent, freshly prepared 1M solution in water) was added, followed by the addition of copper (II) sulfate pentahydrate (0.02 equivalent, 0.3 M solution in water). The heterogeneous mixture was stirred vigorously until TLC analysis indicated complete consumption of the reactants. A saturated EDTA solution (2 mL) was added to quench the reaction. Then the solvent was removed in vacuo and the residue was absorbed on the silica gel and further purified by column chromatography.

(2) Bivalent RAL ligand **46**:

The raloxifen azide **45** (38.9 mg, 0.0902 mmol) and propargyl ether (4.49 μL, 0.0429 mmol) were used and the crude product was purified by column chromatography (DCM : MeOH = 20 : 1 to 10 : 1) to give **46** as a yellow solid (17.2 mg, 42 %).

^{1}H-NMR (DMSO-d6, 400 MHz) δ (ppm) = 8.14 (2H, s, triazol-H), 7.64 (4H, d, J = 8.9 Hz, Ar-H), 7.33 (2H, d, J = 2.3 Hz, Ar-H), 7.22 (2H, d, J = 8.8 Hz, Ar-H), 7.15 (4H, d, J = 8.7 Hz, Ar-H), 6.90 (4H, d, J = 9.0 Hz, Ar-H), 6.84 (2H, dd, J = 2.3 Hz, 8.8 Hz, Ar-H), 6.66 (4H, d, J = 8.7 Hz, Ar-H), 4.73 (4H, t, J = 4.9 Hz, OCH_2CH$_2$-triazol), 4.53 (4H, s, triazol-CH_2O), 4.42 (4H, t, J = 4.9 Hz, OCH$_2$CH_2-triazol).

^{13}C-NMR (DMSO-d6, 100 MHz) δ (ppm) = 193, 162, 158, 156, 144, 141, 139, 132, 130, 125, 124, 123, 116, 115, 107, 70.8, 68.5, 62.6.

HRMS (ESI-TOF, positive): $[C_{52}H_{40}N_6O_9S_2Na]^+$ cal. 979.2190, found 979.2184.

(3) Bivalent RAL ligand **47**:

The raloxifen azide **45** (29.5 mg, 0.0684 mmol) and dipropargyl ether **21a** (4.5 mg, 0.0326 mmol) were used and the crude product was purified by column chromatography (DCM : MeOH = 20 : 1 to 10 : 1) to give **47** as a yellow solid (30.2 mg, 91%).

^{1}H-NMR (DMSO-d6, 400 MHz) δ (ppm) = 8.12 (2H, s, triazol-*H*), 7.64 (4H, d, *J* = 8.9 Hz, Ar-*H*), 7.34 (2H, d, *J* = 2.2 Hz, Ar-*H*), 7.22 (2H, d, *J* = 8.8 Hz, Ar-*H*), 7.15 (4H, d, *J* = 8.7 Hz, Ar-*H*), 6.89 (4H, d, *J* = 9.0 Hz, Ar-*H*), 6.84 (2H, dd, *J* = 2.3 Hz, 8.8 Hz, Ar-*H*), 6.66 (4H, d, *J* = 8.7 Hz, Ar-*H*), 4.72 (4H, t, *J* = 4.9 Hz, OCH_2CH$_2$-triazol), 4.48 (4H, s, triazol-CH_2O), 4.41 (4H, t, *J* = 4.9 Hz, OCH$_2$CH_2-triazol), 3.53 (4H, s, OCH_2OCH_2O).

^{13}C-NMR (DMSO-d6, 100 MHz) δ (ppm) = 193, 162, 158, 156, 144, 141, 139, 132, 131, 130, 124, 123, 116, 115, 107, 68.8, 66.4, 63.5.

HRMS (ESI-TOF, positive): $[C_{54}H_{44}N_6O_{10}S_2Na]^+$ cal. 1023.2453, found 1023.2455.

(4) Bivalent RAL ligand **48**:

The raloxifen azide **45** (46.7 mg, 0.108 mmol) and dipropargyl ether **21b** (9.4 mg, 0.0515 mmol) were used and the crude product was purified by column chromatography (DCM : MeOH = 20 : 1) to give **48** as a yellow solid (35.1 mg, 65%).

^{1}H-NMR (DMSO-d6, 400 MHz) δ (ppm) = 8.12 (2H, s, triazol-*H*), 7.64 (4H, d, *J* = 8.9 Hz, Ar-*H*), 7.33 (2H, d, *J* = 2.2 Hz, Ar-*H*), 7.22 (2H, d, *J* = 8.7 Hz, Ar-*H*), 7.15 (4H, d, *J* = 8.7 Hz, Ar-*H*), 6.89 (4H, d, *J* = 9.0 Hz, Ar-*H*), 6.84 (2H, dd, *J* = 2.3 Hz, 8.8 Hz, Ar-*H*), 6.66 (4H, d, *J* = 8.7 Hz, Ar-*H*), 4.72 (4H, t, *J* = 5.0 Hz, OCH_2CH$_2$-triazol), 4.48 (4H, s, triazol-CH_2O), 4.41 (4H, t, *J* = 5.0 Hz, OCH$_2$CH_2-triazol), 3.52-3.49 (4H, m, OCH_2CH_2), 3.48-3.46 (4H, m, OCH_2CH_2).

^{13}C-NMR (DMSO-d6, 100 MHz) δ (ppm) = 193, 163, 158, 156, 145, 141, 140, 133, 132, 131, 130, 125, 124, 116, 115, 108, 70.2, 69.4, 66.9, 63.9.

HRMS (ESI-TOF, positive): $[C_{56}H_{49}N_6O_{11}S_2]^+$ cal. 1045.2895, found 1145.2890, $[C_{56}H_{48}N_6O_{11}S_2Na]^+$ cal. 1067.2715, found 1067.2728.

(5) Bivalent RAL ligand **49**:

The raloxifen azide **45** (44.0 mg, 0.102 mmol) and dipropargyl ether **21c** (11.0 mg, 0.0486 mmol)

were used and the crude product was purified by column chromatography (DCM : MeOH = 20 : 1 to 10 :1) to give **49** as a yellow solid (12.2 mg, 32%).

^{1}H-NMR (DMSO-d6, 400 MHz) δ (ppm) = 8.11 (2H, s, triazol-*H*), 7.64 (4H, d, *J* = 8.9 Hz, Ar-*H*), 7.33 (2H, d, *J* = 2.2 Hz, Ar-*H*), 7.22 (2H, d, *J* = 8.7 Hz, Ar-*H*), 7.15 (4H, d, *J* = 9.0 Hz, Ar-*H*), 6.89 (4H, d, *J* = 9.0 Hz, Ar-*H*), 6.84 (2H, dd, *J* = 2.3 Hz, 8.8 Hz, Ar-*H*), 6.66 (4H, d, *J* = 8.7 Hz, Ar-*H*), 4.73 (4H, t, *J* = 5.0 Hz, OCH_2CH$_2$-triazol), 4.48 (4H, s, triazol-CH_2O), 4.41 (4H, t, *J* = 5.0 Hz, OCH$_2$CH_2-triazol), 3.52-3.44 (12H, m, OCH_2CH_2).

^{13}C-NMR (DMSO-d6, 100 MHz) δ (ppm) = 193, 162, 158, 156, 144, 141, 139, 132, 130, 124, 123, 116, 115, 107, 69.7, 69.6, 68.9, 63.4.

HRMS (ESI-TOF, positive): $[C_{58}H_{52}N_6O_{12}S_2Na]^+$ cal. 1111.2977, found 1111.2998.

(6) Bivalent RAL ligand **50**:

The raloxifen azide **45** (38.2 mg, 0.0885 mmol) and dipropargyl ether **21d** (11.4 mg, 0.0422 mmol) were used and the crude product was purified by column chromatography (DCM : MeOH = 20 : 1 to 10 :1) to give **50** as a yellow solid (19.5 mg, 41%).

^{1}H-NMR (DMSO-d6, 400 MHz) δ (ppm) = 8.12 (2H, s, triazol-*H*), 7.64 (4H, d, *J* = 8.9 Hz, Ar-*H*), 7.34 (2H, d, *J* = 2.2 Hz, Ar-*H*), 7.22 (2H, d, *J* = 8.7 Hz, Ar-*H*), 7.15 (4H, d, *J* = 8.7 Hz, Ar-*H*), 6.90 (4H, d, *J* = 9.0 Hz, Ar-*H*), 6.84 (2H, dd, *J* = 2.3 Hz, 8.8 Hz, Ar-*H*), 6.67 (4H, d, *J* = 8.7 Hz, Ar-*H*), 4.73 (4H, t, *J* = 4.9 Hz, OCH_2CH$_2$-triazol), 4.49 (4H, s, triazol-CH_2O), 4.42 (4H, t, *J* = 4.9 Hz, OCH$_2$CH_2-triazol), 3.52-3.46 (10H, m, OCH_2CH_2), 3.45 (6H, br s, OCH_2CH_2).

^{13}C-NMR (DMSO-d6, 100 MHz) δ (ppm) = 193, 162, 158, 156, 144, 141, 139, 132, 130, 124, 123, 116, 115, 107, 69.7, 69.6, 68.9, 66.4, 63.4.

HRMS (ESI-TOF, positive): $[C_{60}H_{56}N_6O_{13}S_2Na]^+$ cal. 1155.3239, found 1155.3262.

(7) Bivalent RAL ligand **51**:

The raloxifen azide **45** (33.4 mg, 0.0774 mmol) and dipropargyl ether **21e** (11.6 mg, 0.0369 mmol) were used and the crude product was purified by column chromatography (DCM : MeOH = 20 : 1 to 10 :1) to give **51** as a yellow solid (11.2 mg, 22%).

^{1}H-NMR (DMSO-d6, 400 MHz) δ (ppm) = 8.11 (2H, s, triazol-*H*), 7.64 (4H, d, *J* = 8.9 Hz, Ar-*H*), 7.32 (2H, d, *J* = 2.2 Hz, Ar-*H*), 7.21 (2H, d, *J* = 8.8 Hz, Ar-*H*), 7.14 (4H, d, *J* = 8.7 Hz, Ar-*H*), 6.89 (4H, d, *J* = 9.0 Hz, Ar-*H*), 6.83 (2H, dd, *J* = 2.3 Hz, 8.8 Hz, Ar-*H*), 6.65 (4H, d, *J* = 8.6 Hz, Ar-*H*), 4.73 (4H, t, *J* = 5.0 Hz, OCH_2CH$_2$-triazol), 4.49 (4H, s, triazol-CH_2O), 4.42 (4H, t, *J* = 5.0 Hz,

OCH_2CH_2-triazol), 3.51-3.47 (10H, m, OCH_2CH_2), 3.44 (10H, br s, OCH_2CH_2).

^{13}C-NMR (DMSO-d6, 100 MHz) δ (ppm) = 193, 162, 158, 156, 144, 141, 139, 132, 130, 124, 123, 116, 115, 107, 69.7, 69.6, 68.9, 66.4, 63.4.

HRMS (ESI-TOF, positive): $[C_{62}H_{60}N_6O_{14}S_2Na]^+$ cal. 1199.3501, found 1199.3489.

(8) Bivalent RAL ligand **52**:

The raloxifen azide **45** (36.5 mg, 0.0846 mmol) and dipropargyl ether **21f** (13.8 mg, 0.0403 mmol) were used and the crude product was purified by column chromatography (DCM : MeOH = 20 : 1 to 10 :1) to give **52** as a yellow solid (18.4 mg, 39%).

^{1}H-NMR (DMSO-d6, 400 MHz) δ (ppm) = 8.12 (2H, s, triazol-*H*), 7.64 (4H, d, *J* = 8.9 Hz, Ar-*H*), 7.33 (2H, d, *J* = 2.2 Hz, Ar-*H*), 7.22 (2H, d, *J* = 8.8 Hz, Ar-*H*), 7.15 (4H, d, *J* = 8.7 Hz, Ar-*H*), 6.90 (4H, d, *J* = 9.0 Hz, Ar-*H*), 6.84 (2H, dd, *J* = 2.3 Hz, 8.8 Hz, Ar-*H*), 6.66 (4H, d, *J* = 8.7 Hz, Ar-*H*), 4.73 (4H, t, *J* = 4.9 Hz, OCH_2CH_2-triazol), 4.49 (4H, s, triazol-CH_2O), 4.42 (4H, t, *J* = 4.9 Hz, OCH_2CH_2-triazol), 3.52-3.47 (10H, m, OCH_2CH_2), 3.45 (14H, br s, OCH_2CH_2).

^{13}C-NMR (DMSO-d6, 100 MHz) δ (ppm) = 193, 162, 158, 156, 144, 141, 139, 132, 130, 124, 123, 116, 115, 107, 69.7, 68.9, 66.4, 63.5.

HRMS (ESI-TOF, positive): $[C_{64}H_{64}N_6O_{15}S_2Na]^+$ cal. 1243.3763, found 1243.3766.

(9) Bivalent RAL ligand **53**:

The raloxifen azide **45** (29.3 mg, 0.0679 mmol) and dipropargyl ether **21g** (13.0 mg, 0.0323 mmol) were used and the crude product was purified by column chromatography (DCM : MeOH = 20 : 1 to 10 :1) to give **53** as a yellow solid (30.4 mg, 75%).

^{1}H-NMR (DMSO-d6, 400 MHz) δ (ppm) = 8.12 (2H, s, triazol-*H*), 7.64 (4H, d, *J* = 9.0 Hz, Ar-*H*), 7.34 (2H, d, *J* = 2.0 Hz, Ar-*H*), 7.22 (2H, d, *J* = 8.7 Hz, Ar-*H*), 7.15 (4H, d, *J* = 8.7 Hz, Ar-*H*), 6.90 (4H, d, *J* = 9.0 Hz, Ar-*H*), 6.84 (2H, dd, *J* = 2.3 Hz, 8.8 Hz, Ar-*H*), 6.67 (4H, d, *J* = 8.7 Hz, Ar-*H*), 4.73 (4H, t, *J* = 5.0 Hz, OCH_2CH_2-triazol), 4.50 (4H, s, triazol-CH_2O), 4.42 (4H, t, *J* = 5.0 Hz, OCH_2CH_2-triazol), 3.52-3.46 (28H, m, OCH_2CH_2).

^{13}C-NMR (DMSO-d6, 100 MHz) δ (ppm) = 193, 162, 158, 156, 144, 141, 139, 132, 130, 124, 123, 116, 115, 107, 69.7, 68.9, 63.4.

HRMS (ESI-TOF, positive): $[C_{66}H_{67}N_6O_{16}S_2]^+$ cal. 1265.4206, found 11265.4187; $[C_{66}H_{66}N_6O_{16}S_2Na]^+$ cal. 1287.4025, found 1287.4003; $[C_{66}H_{66}N_6O_{16}S_2K]^+$, cal. 1303.3765, found 1303.3748.

(10) Bivalent RAL ligand **54**:

The raloxifen azide **45** (22.9 mg, 0.0531 mmol) and dipropargyl ether **21h** (11.3 mg, 0.0252 mmol) were used and the crude product was purified by column chromatography (DCM : MeOH = 20 : 1 to 10 :1) to give **54** as a yellow solid (15.0 mg, 46%).

^{1}H-NMR (DMSO-d6, 400 MHz) δ (ppm) = 8.12 (2H, s, triazol-*H*), 7.64 (4H, d, *J* = 8.9 Hz, Ar-*H*), 7.33 (2H, d, *J* = 2.2 Hz, Ar-*H*), 7.22 (2H, d, *J* = 8.7 Hz, Ar-*H*), 7.15 (4H, d, *J* = 8.7 Hz, Ar-*H*), 6.90 (4H, d, *J* = 9.0 Hz, Ar-*H*), 6.84 (2H, dd, *J* = 2.2 Hz, 8.8 Hz, Ar-*H*), 6.67 (4H, d, *J* = 8.7 Hz, Ar-*H*), 4.73 (4H, t, *J* = 4.9 Hz, OCH_2CH$_2$-triazol), 4.50 (4H, s, triazol-CH_2O), 4.42 (4H, t, *J* = 4.9 Hz, OCH$_2$CH_2-triazol), 3.51-3.46 (32H, m, OCH_2CH_2).

^{13}C-NMR (DMSO-d6, 100 MHz) δ (ppm) = 193, 162, 158, 156, 144, 141, 139, 132, 130, 124, 123, 116, 115, 107, 70.1, 69.7, 68.9, 66.4, 63.4.

HRMS (ESI-TOF, positive): $[C_{68}H_{72}N_6O_{17}S_2Na_2]^{2+}$ cal. 677.2090, found 677.2059, $[C_{68}H_{73}N_6O_{17}S_2]^+$ cal. 1309.4468, found 1309.4423; $[C_{68}H_{72}N_6O_{17}S_2Na]^+$ cal. 1331.4288, found 1331.4237; $[C_{68}H_{72}N_6O_{17}S_2K]^+$, cal. 1347.4027, found 1347.3978.

(11) Bivalent RAL ligand **55**:

The raloxifen azide **45** (25.9 mg, 0.0600 mmol) and dipropargyl ether **21i** (14.0 mg, 0.0286 mmol) were used and the crude product was purified by column chromatography (DCM : MeOH = 20 : 1 to 10 :1) to give **55** as a yellow solid (22.9 mg, 58%).

^{1}H-NMR (DMSO-d6, 400 MHz) δ (ppm) = 8.12 (2H, s, triazol-*H*), 7.65 (4H, d, *J* = 8.8 Hz, Ar-*H*), 7.33 (2H, d, *J* = 2.1 Hz, Ar-*H*), 7.22 (2H, d, *J* = 8.8 Hz, Ar-*H*), 7.15 (4H, d, *J* = 8.6 Hz, Ar-*H*), 6.90 (4H, d, *J* = 8.8 Hz, Ar-*H*), 6.84 (2H, dd, *J* = 2.1 Hz, 8.7 Hz, Ar-*H*), 6.67 (4H, d, *J* = 8.6 Hz, Ar-*H*), 4.73 (4H, t, *J* = 4.6 Hz, OCH_2CH$_2$-triazol), 4.50 (4H, s, triazol-CH_2O), 4.42 (4H, t, *J* = 4.6 Hz, OCH$_2$CH_2-triazol), 3.51-3.47 (36H, m, OCH_2CH_2).

^{13}C-NMR (DMSO-d6, 100 MHz) δ (ppm) = 193, 162, 158, 156, 144, 141, 139, 132, 130, 124, 123, 116, 115, 107, 69.7, 69.6, 69.1, 68.9, 66.4, 63.5.

HRMS (ESI-TOF, positive): $[C_{70}H_{76}N_6O_{18}Na_2]^{2+}$ cal. 699.2221, found 699.2251, $[C_{70}H_{77}N_6O_{18}]^+$ cal. 1353.4730, found 1353.4769; $[C_{70}H_{76}N_6O_{18}Na]^+$ cal. 1375.4550, found 1375.4595; $[C_{70}H_{76}N_6O_{18}K]^+$, cal. 1391.4289, found 1391.4341.

(12) Bivalent RAL ligand **56**:

The raloxifen azide **45** (29.1 mg, 0.0674 mmol) and dipropargyl ether **21j** (15.0 mg, 0.0321 mmol)

were used and the crude product was purified by column chromatography (DCM : MeOH = 20 : 1 to 10 :1) to give **56** as a yellow solid (22.9 mg, 59%).

^{1}H-NMR (DMSO-d6, 400 MHz) δ (ppm) = 8.12 (2H, s, triazol-*H*), 7.65 (4H, d, *J* = 8.8 Hz, Ar-*H*), 7.34 (2H, d, *J* = 2.1 Hz, Ar-*H*), 7.22 (2H, d, *J* = 8.7 Hz, Ar-*H*), 7.15 (4H, d, *J* = 8.7 Hz, Ar-*H*), 6.90 (4H, d, *J* = 8.8 Hz, Ar-*H*), 6.84 (2H, dd, *J* = 2.1 Hz, 8.8 Hz, Ar-*H*), 6.67 (4H, d, *J* = 8.6 Hz, Ar-*H*), 4.74 (4H, t, *J* = 4.8 Hz, OCH_2CH$_2$-triazol), 4.50 (4H, s, triazol-CH_2O), 4.42 (4H, t, *J* = 4.8 Hz, OCH$_2$CH_2-triazol), 3.52-3.47 (40H, m, OCH_2CH_2).

^{13}C-NMR (DMSO-d6, 100 MHz) δ (ppm) = 193, 162, 158, 156, 144, 141, 139, 132, 130, 124, 123, 116, 115, 107, 71.9, 69.8, 69.7, 69.1, 68.9, 66.4, 63.5.

HRMS (ESI-TOF, positive): $[C_{72}H_{80}N_6O_{19}S_2Na_2]^{2+}$ cal. 721.2352, found 721.2380; $[C_{72}H_{81}N_6O_{19}S_2]^+$ cal. 1397.4992, found 1397.5032; $[C_{72}H_{80}N_6O_{19}S_2Na]^+$ cal. 1419.4812, found 1419.4858; $[C_{72}H_{80}N_6O_{19}S_2K]^+$, cal. 1435.4551, found 1435.4601.

(13) Bivalent RAL ligand **57**:

The raloxifen azide **45** (25.7 mg, 0.0596 mmol) and dipropargyl ether **21k** (16.4 mg, 0.0284 mmol) were used and the crude product was purified by column chromatography (DCM : MeOH = 20 : 1 to 10 :1) to give **57** as a yellow solid (27.6 mg, 68%).

^{1}H-NMR (DMSO-d6, 400 MHz) δ (ppm) = 8.12 (2H, s, triazol-*H*), 7.64 (4H, d, *J* = 8.9 Hz, Ar-*H*), 7.34 (2H, d, *J* = 2.1 Hz, Ar-*H*), 7.22 (2H, d, *J* = 8.8 Hz, Ar-*H*), 7.15 (4H, d, *J* = 8.7 Hz, Ar-*H*), 6.90 (4H, d, *J* = 9.0 Hz, Ar-*H*), 6.84 (2H, dd, *J* = 2.2 Hz, 8.7 Hz, Ar-*H*), 6.67 (4H, d, *J* = 8.7 Hz, Ar-*H*), 4.73 (4H, t, *J* = 4.8 Hz, OCH_2CH$_2$-triazol), 4.50 (4H, s, triazol-CH_2O), 4.42 (4H, t, *J* = 4.8 Hz, OCH$_2$CH_2-triazol), 3.51-3.47 (44H, m, OCH_2CH_2).

^{13}C-NMR (DMSO-d6, 100 MHz) δ (ppm) = 193, 162, 158, 156, 144, 141, 140, 132, 130, 124, 123, 116, 115, 69.8, 68.9, 66.4, 63.5.

HRMS (ESI-TOF, positive): $[C_{74}H_{84}N_6O_{20}S_2Na_2]^{2+}$ cal. 743.2483, found 743.2487; $[C_{74}H_{85}N_6O_{20}S_2]^+$ cal. 1441.5255, found 1441.5263; $[C_{74}H_{84}N_6O_{20}S_2Na]^+$ cal. 1463.5074, found 1463.5081; $[C_{74}H_{84}N_6O_{20}S_2K]^+$, cal. 1479.4813, found 1479.4822.

(14) Bivalent RAL ligand **58**:

The raloxifen azide **45** (26.3 mg, 0.0610 mmol) and dipropargyl ether **21l** (18.1 mg, 0.0290 mmol) were used and the crude product was purified by column chromatography (DCM : MeOH = 20 : 1 to 10 :1) to give **58** as a yellow solid (32.4 mg, 75%).

^{1}H-NMR (DMSO-d6, 400 MHz) δ (ppm) = 8.12 (2H, s, triazol-*H*), 7.65 (4H, d, *J* = 8.9 Hz, Ar-*H*), 7.34 (2H, d, *J* = 2.2 Hz, Ar-*H*), 7.22 (2H, d, *J* = 8.7 Hz, Ar-*H*), 7.15 (4H, d, *J* = 8.7 Hz, Ar-*H*), 6.90 (4H, d, *J* = 9.0 Hz, Ar-*H*), 6.84 (2H, dd, *J* = 2.3 Hz, 8.8 Hz, Ar-*H*), 6.67 (4H, d, *J* = 8.6 Hz, Ar-*H*), 4.74 (4H, t, *J* = 4.9 Hz, OC*H*$_2$CH$_2$-triazol), 4.50 (4H, s, triazol-C*H*$_2$O), 4.43 (4H, t, *J* = 4.9 Hz, OCH$_2$C*H*$_2$-triazol), 3.52-3.47 (48H, m, OC*H*$_2$C*H*$_2$).

^{13}C-NMR (DMSO-d6, 100 MHz) δ (ppm) = 193, 162, 158, 156, 144, 141, 139, 132, 130, 124, 123, 116, 115, 107, 69.7, 68.9, 63.5.

HRMS (ESI-TOF, positive): $[C_{76}H_{88}N_6O_{21}S_2Na_2]^{2+}$ cal. 765.2614, found 765.2564, $[C_{76}H_{88}N_6O_{21}S_2Na]^{+}$ cal. 1507.5336, found 1507.5276; $[C_{76}H_{88}N_6O_{21}S_2K]^{+}$, cal. 1529.5075, found 1529.5105.

6.3.2. Chemical preparation of monovalent RAL ligands 59-61

(1) General procedure for chemical preparations of monovalent RAL ligands **59-61**

The raloxifen azide **45** (1.0 equivalent) and propargyl ether **28** (1.0 equivalent) were suspended in a 1:1 mixture of water and *tert*-butyl alcohol (1 mL). Sodium ascorbate (0.1 equivalent, freshly prepared 1M solution in water) was added, followed by the addition of copper(II) sulfate pentahydrate (0.01 equivalent, 0.3 M solution in water). The heterogeneous mixture was stirred vigorously until TLC analysis indicated complete consumption of the reactants. A saturated EDTA solution (2 mL) was added to quench the reaction. Then the solvent was removed in vacuo and the residue was absorbed on the silica gel and further purified by column chromatography.

(2) Monovalent RAL ligand **59**:

The raloxifen azide **45** (26.5 mg, 0.0614 mmol) and methyl propargyl ether (16.0 μL, 0.184 mmol) were used and the crude product was purified by column chromatography (DCM : MeOH = 20 : 1 to 15 :1) to give a yellow solid (25.3 mg, 83%).

^{1}H-NMR (DMSO-d6, 400 MHz) δ (ppm) = 9.86 (2H, br s, PhO*H*), 8.13 (1H, s, triazol-*H*), 7.65 (2H, d, *J* = 8.9 Hz, Ar-*H*), 7.34 (1H, d, *J* = 2.2 Hz, Ar-*H*), 7.23 (1H, d, *J* = 8.7 Hz, Ar-*H*), 7.15 (2H, d, *J* = 8.7 Hz, Ar-*H*), 6.90 (2H, d, *J* = 9.0 Hz, Ar-*H*), 6.85 (1H, dd, *J* = 2.3 Hz, 8.8 Hz, Ar-*H*), 6.67 (2H, d, *J* = 8.7 Hz, Ar-*H*), 4.74 (2H, t, *J* = 5.0 Hz, OC*H*$_2$CH$_2$-triazol), 4.44-4.42 (4H, m, triazol-C*H*$_2$OMe, OCH$_2$C*H*$_2$-triazol).

^{13}C-NMR (DMSO-d6, 100 MHz) δ (ppm) = 193, 162, 158, 144, 141, 139, 132, 130, 124, 123, 116,

115, 107, 66.4, 64.9, 57.3, 48.8.

HRMS (ESI-TOF, positive): $[C_{27}H_{23}N_3O_5SNa]^+$ cal. 524.1251, found 524.1269.

(3) Monovalent RAL ligand **60**:

The raloxifen azide **45** (29.5 mg, 0.0684 mmol) and propargyl ether **28a** (13.0 mg, 0.0684 mmol) were used and the crude product was purified by column chromatography (DCM : MeOH = 20 : 1) to give **60** as a yellow solid (32.2 mg, 79%).

^{1}H-NMR (MeOD, 400 MHz) δ (ppm) = 7.99 (1H, s, triazol-*H*), 7.66 (2H, d, *J* = 8.9 Hz, Ar-*H*), 7.38 (1H, d, *J* = 8.8 Hz, Ar-*H*), 7.25 (1H, d, *J* = 2.3 Hz, Ar-*H*), 7.16 (2H, d, *J* = 8.8 Hz, Ar-*H*), 6.85 (1H, dd, *J* = 2.3 Hz, 8.8 Hz, Ar-*H*), 6.78 (2H, d, *J* = 8.9 Hz, Ar-*H*), 6.61 (2H, d, *J* = 8.7 Hz, Ar-*H*), 4.76 (2H, t, *J* = 4.8 Hz, OCH_2CH$_2$-triazol), 4.60 (2H, s, triazol-CH_2O), 4.37 (2H, t, *J* = 4.7 Hz, OCH$_2$CH_2-triazol), 3.64-3.46 (15H, m, OCH_2CH_2, OCH_3).

^{13}C-NMR (MeOD, 100 MHz) δ (ppm) = 196, 164, 157, 146, 144, 142, 134, 132, 131, 126, 125, 117, 116, 108, 73.0, 71.6, 71.4, 70.8, 67.8, 65.1, 59.2.

HRMS (ESI-TOF, positive): $[C_{33}H_{35}N_3O_8SNa]^+$ cal. 656.2037, found 656.2038.

(4) Monovalent RAL ligand **61**:

The raloxifen azide **45** (17.8 mg, 0.0413 mmol) and propargyl ether **28b** (13.2 mg, 0.0450 mmol) were used and the crude product was purified by column chromatography (DCM : MeOH = 30 : 1 to 15 : 1) to give **61** as a yellow solid (24.2 mg, 69%).

^{1}H-NMR (MeOD, 400 MHz) δ (ppm) = 8.01 (1H, s, triazol-*H*), 7.67 (2H, d, *J* = 8.9 Hz, Ar-*H*), 7.38 (1H, d, *J* = 8.8 Hz, Ar-*H*), 7.25 (1H, d, *J* = 2.0 Hz, Ar-*H*), 7.17 (2H, d, *J* = 8.7 Hz, Ar-*H*), 6.85 (1H, dd, *J* = 2.3 Hz, 8.8 Hz, Ar-*H*), 6.81 (2H, d, *J* = 8.8 Hz, Ar-*H*), 6.62 (2H, d, *J* = 8.7 Hz, Ar-*H*), 4.77 (2H, t, *J* = 4.7 Hz, OCH_2CH$_2$-triazol), 4.62 (2H, s, triazol-CH_2O), 4.40 (2H, t, *J* = 4.7 Hz, OCH$_2$CH_2-triazol), 3.65-3.47 (23H, m, OCH_2CH_2, OCH_3).

^{13}C-NMR (MeOD, 100 MHz) δ (ppm) = 196, 164, 159, 157, 146, 144, 142, 134, 132, 131, 126, 125, 117, 116, 108, 72.9, 71.4, 71.3, 70.7, 67.9, 65.0, 59.2.

HRMS (ESI-TOF, positive): $[C_{37}H_{43}N_3O_{10}SNa]^+$ cal. 744.2561, found 744.2580.

6.4. Bivalent *cis*-4-OH tamoxifen (OHT) ligand

6.4.1. Chemical preparation of bivalent OHT ligands 62-70

(1) General procedure for chemical preparations of bivalent OHT ligands **62**-**68** and **70**:

To a solution of bis(*N*-methylamine) OEG spacer **22** (1.0 equivalent) and sodium triacetoxyborohydride (3.0 equivalents) in anhydrous THF, (*E*,*Z*)-2-(4-(1-(4-hydroxyphenyl)-2-phenyl-but-1-enyl) phenoxy)acetaldehyde **77** (2.2 equivalents) were added at room temperature and the reaction mixture was stirred at room temperature until TLC analysis indicated complete consumption of the aldehyde **77**. The reaction mixture was neutralized with a saturated $NaHCO_3$ solution and concentrated in vacuo. The residue was absorbed on the silica gel and further purified by column chromatography to obtain the pure product. Three pure isomers was obtained by a separation with RP-HPLC and characterized by ^{1}H-NMR according to the chemical shift of **76**.

(2) Bivalent OHT ligand **62**:

1,5-bis(methylamino)-3-oxapentane (6.00 mg, 0.0445 mmol), (*E*,*Z*)-isomer of **77** (40.7 mg, 0.111 mmol), sodium triacetoxyborohydride (28.9 mg, 0.133 mmol) and 10 mL anhydrous THF were used and the crude product was purified by column chromatography (chloroform : MeOH = 10:1 to 5:1 + 3% triethylamine) and by RP-HPLC (80% MeOH/H_2O + 0.4% diethylamine) to obtain **62** (33.1 mg, 81%) as three pure isomers: *cis*-*cis* (29%), *cis*-*trans* (47%), and *trans*-*trans* (24%) isomer.

Cis-*cis* isomer of **62** (the first fraction):

^{1}H-NMR (Acetone-d6, 400 MHz) δ (ppm) = 7.19-7.11 (8H, m, Ar-*H*), 7.11-7.04 (6H, m, Ar-*H*), 6.84 (4H, d, *J* = 8.6 Hz, Ar-*H*), 6.77 (4H, d, *J* = 8.8 Hz, Ar-*H*), 6.55 (4H, d, *J* = 8.8 Hz, Ar-*H*), 3.92 (4H, t, *J* = 6.0 Hz, ArOCH_2CH_2N), 3.49 (8H, t, *J* = 5.9 Hz, CH_2OCH_2), 2.74 (4H, t, *J* = 6.0 Hz, ArOCH$_2$CH_2N), 2.60 (4H, t, *J* = 5.9 Hz, NCH_2CH$_2$O), 2.49 (4H, q, *J* = 7.4 Hz, CH_2CH$_3$), 2.29 (6H, s, NCH_3), 0.90 (6H, t, *J* = 7.4 Hz, CH$_2$CH_3).

Cis-*trans* isomer of **62** (the second fraction):

^{1}H-NMR (Acetone-d6, 400 MHz) δ (ppm) = 7.03 (14H, m, Ar-*H*), 6.92 (2H, d, *J* = 8.7 Hz, (*E*)-Ar-*H*), 6.84 (2H, d, *J* = 8.7 Hz, (*Z*)-Ar-*H*), 6.78 (2H, d, *J* = 8.8 Hz, (*Z*)-Ar-*H*), 6.69 (2H, d, *J* = 8.8 Hz, (*E*)-Ar-*H*), 6.57 (2H, d, *J* = 8.8 Hz, (*Z*)-Ar-*H*), 6.48 (2H, d, *J* = 8.7 Hz, (*E*)-Ar-*H*), 4.09 (2H, t, *J* = 5.9 Hz, (*E*)-ArOCH_2CH$_2$N), 3.94 (2H, t, *J* = 6.0 Hz, (*Z*)-ArOCH_2CH$_2$N), 3.57-3.51 (4H, m, CH_2OCH_2), 2.84 (2H, t, *J* = 6.0 Hz, (*Z*)-ArOCH$_2$CH_2N), 2.76 (2H, t, *J* = 5.9 Hz, (*E*)-NCH_2CH$_2$O), 2.66 (2H, t, *J* = 5.8 Hz, (*Z*)-ArOCH$_2$CH_2N), 2.63 (2H, t, *J* = 5.8 Hz, (*E*)-ArOCH$_2$CH_2N), 2.51-2.44 (4H, 2×q, *J* = 7.4 Hz, 7.4 Hz, CH_2CH$_3$), 2.36 (3H, s, (*Z*)-NCH_3),

2.31 (3H, s, (*E*)-NCH_3), 0.90 (6H, t, *J* = 7.4 Hz, CH_2CH_3).

Trans-trans isomer of **62** (the third fraction):

^{1}H-NMR (Acetone-d6, 400 MHz) δ (ppm) = 7.20-7.05 (14H, m, Ar-*H*), 6.94 (4H, d, *J* = 8.7 Hz, Ar-*H*), 6.69 (4H, d, *J* = 8.7 Hz, Ar-*H*), 6.48 (4H, d, *J* = 8.7 Hz, Ar-*H*), 4.14 (4H, t, *J* = 5.9 Hz, ArOCH_2CH$_2$N), 3.61 (4H, *J* = 5.7 Hz, CH_2OCH_2), 2.92 (4H, t, *J* = 5.7 Hz, ArOCH$_2$CH_2N), 2.75 (4H, t, *J* = 5.6 Hz, ArOCH$_2$CH_2N), 2.47 (4H, q, *J* = 7.4 Hz, CH_2CH$_3$), 2.42 (6H, s, NCH_3), 0.90 (6H, t, *J* = 7.4 Hz, CH$_2$CH_3).

HRMS (ESI-TOF, positive): $[C_{54}H_{62}O_5N_2]^{2+}$ cal. 409.2324, found 409.2333; $[C_{54}H_{61}O_5N_2]^{+}$ cal. 817.4575, found 817.4581; $[C_{54}H_{60}O_5N_2Na]^{+}$ cal. 839.4394, found 839.4406.

(3) Bivalent OHT ligand **63**:

1,8-bis(methylamino)-3,6-dioxaoctane (10.0 mg, 0.0556 mmol), (*E*,*Z*)-isomer of **77** (46.8 mg, 0.128 mmol), sodium triacetoxyborohydride (37.2 mg, 0.167 mmol) and 15 mL anhydrous THF were used and the crude product was purified by column chromatography (chloroform : MeOH = 20:1 to 10:1 + 3% triethylamine) and by RP-HPLC (82% MeOH/H_2O + 0.4% diethylamine) to obtain **63** (27.5 mg, 53%) as three pure isomers: *cis-cis* (31%), *cis-trans* (47%), and *trans-trans* (22%) isomer.

Cis-cis isomer of **63** (the first fraction):

^{1}H-NMR (Acetone-d6, 400 MHz) δ (ppm) = 7.18-7.11 (8H, m, Ar-*H*), 7.10-7.05 (6H, m, Ar-*H*), 6.84 (4H, d, *J* = 8.5 Hz, Ar-*H*), 6.77 (4H, d, *J* = 8.7 Hz, Ar-*H*), 6.56 (4H, d, *J* = 8.8 Hz, Ar-*H*), 3.91 (4H, t, *J* = 6.0 Hz, ArOCH_2CH$_2$N), 3.53-3.47 (8H, m, CH_2OCH_2), 2.72 (4H, t, *J* = 6.0 Hz, ArOCH$_2$CH_2N), 2.58 (4H, t, *J* = 5.9 Hz, NCH_2CH$_2$O), 2.48 (4H, q, *J* = 7.4 Hz, CH_2CH$_3$), 2.28 (6H, s, NCH_3), 0.90 (6H, t, *J* = 7.4 Hz, CH$_2$CH_3).

Cis-trans isomer of **63** (the second fraction):

^{1}H-NMR (Acetone-d6, 400 MHz) δ (ppm) = 7.18-7.12 (10H, m, Ar-*H*), 7.10-7.05 (4H, m, Ar-*H*), 6.92 (2H, d, *J* = 8.8 Hz, (*E*)-Ar-*H*), 6.84 (2H, d, *J* = 8.7 Hz, (*Z*)-Ar-*H*), 6.78 (2H, d, *J* = 8.8 Hz, (*Z*)-Ar-*H*), 6.69 (2H, d, *J* = 8.7 Hz, (*E*)-Ar-*H*), 6.57 (2H, d, *J* = 8.8 Hz, (*Z*)-Ar-*H*), 6.48 (2H, d, *J* = 8.7 Hz, (*E*)-Ar-*H*), 4.08 (2H, t, *J* = 6.0 Hz, (*E*)-ArOCH_2CH$_2$N), 3.93 (2H, t, *J* = 6.0 Hz, (*Z*)-ArOCH_2CH$_2$N), 3.59-3.48 (8H, m, CH_2OCH_2), 2.83 (2H, t, *J* = 6.0 Hz, (*Z*)-ArOCH$_2$CH_2N), 2.74 (2H, t, *J* = 6.0 Hz, (*E*)-NCH_2CH$_2$O), 2.65 (2H, t, *J* = 5.9 Hz, (*Z*)-ArOCH$_2$CH_2N), 2.60 (2H, t, *J* = 6.0 Hz, (*E*)-ArOCH$_2$CH_2N), 2.53-2.43 (4H, 2×q, *J* = 7.4 Hz, 7.4 Hz, CH_2CH$_3$), 2.35 (3H, s,

(*Z*)-NC*H*$_3$), 2.29 (3H, s, (*E*)-NC*H*$_3$), 0.90 (6H, t, *J* = 7.4 Hz, CH$_2$C*H*$_3$).

Trans-trans isomer of **63** (the third fraction):

^{1}H-NMR (Acetone-d6, 400 MHz) δ (ppm) = 7.18-7.07 (14H, m, Ar-*H*), 6.93 (4H, d, *J* = 8.8 Hz, Ar-*H*), 6.69 (4H, d, *J* = 8.7 Hz, Ar-*H*), 6.48 (4H, d, *J* = 8.7 Hz, Ar-*H*), 4.10 (4H, t, *J* = 6.0 Hz, ArOC*H*$_2$CH$_2$N), 3.61-3.51 (8H, m, C*H*$_2$OC*H*$_2$), 2.85 (4H, t, *J* = 6.0 Hz, ArOCH$_2$C*H*$_2$N), 2.67 (4H, t, *J* = 5.9 Hz, ArOCH$_2$C*H*$_2$N), 2.47 (4H, q, *J* = 7.4 Hz, C*H*$_2$CH$_3$), 2.36 (6H, s, NC*H*$_3$), 0.90 (6H, t, *J* = 7.3 Hz, CH$_2$C*H*$_3$).

HRMS (ESI-TOF, positive): $[C_{56}H_{66}O_6N_2]^{2+}$ cal. 431.2455, found 431.2470; $[C_{56}H_{65}O_6N_2]^{+}$ cal. 861.4837, found 861.4854; $[C_{56}H_{64}O_6N_2Na]^{+}$ cal. 883.4657, found 883.4676.

(4) Bivalent OHT ligand **64**:

The bis(*N*-methylamino) OEG spacer **22a** (12.0 mg, 0.0545 mmol), (*E*,*Z*)-isomer of **77** (44.9 mg, 0.125 mmol), sodium triacetoxyborohydride (35.7 mg, 0.163 mmol) and 5 mL anhydrous THF were used and the crude product was purified by column chromatography (chloroform : MeOH = 20:1 to 10:1 + 3% triethylamine) and by RP-HPLC (80% MeOH/H$_2$O + 0.4% diethylamine) to obtain **64** (13.3 mg, 29%) as three pure isomers: *cis-cis* (26%), *cis-trans* (49%), and *trans-trans* (25%) isomer.

Cis-cis isomer of **64** (the first fraction):

^{1}H-NMR (Acetone-d6, 400 MHz) δ (ppm) = 7.18-7.12 (8H, m, Ar-*H*), 7.11-7.05 (6H, m, Ar-*H*), 6.84 (4H, d, *J* = 8.6 Hz, Ar-*H*), 6.77 (4H, d, *J* = 8.8 Hz, Ar-*H*), 6.57 (4H, d, *J* = 8.8 Hz, Ar-*H*), 3.93 (4H, t, *J* = 6.0 Hz, ArOC*H*$_2$CH$_2$N), 3.54-3.48 (12H, m, C*H*$_2$OC*H*$_2$), 2.74 (4H, t, *J* = 6.0 Hz, ArOCH$_2$C*H*$_2$N), 2.60 (4H, t, *J* = 5.9 Hz, NC*H*$_2$CH$_2$O), 2.48 (4H, q, *J* = 7.4 Hz, C*H*$_2$CH$_3$), 2.29 (6H, s, NC*H*$_3$), 0.90 (6H, t, *J* = 7.3 Hz, CH$_2$C*H*$_3$).

Cis-trans isomer of **64** (the second fraction):

^{1}H-NMR (Acetone-d6, 400 MHz) δ (ppm) = 7.18-7.10 (10H, m, Ar-*H*), 7.10-7.05 (4H, m, Ar-*H*), 6.93 (2H, d, *J* = 8.7 Hz, (*E*)-Ar-*H*), 6.84 (2H, d, *J* = 8.4 Hz, (*Z*)-Ar-*H*), 6.78 (2H, d, *J* = 8.7 Hz, (*Z*)-Ar-*H*), 6.69 (2H, d, *J* = 8.7 Hz, (*E*)-Ar-*H*), 6.57 (2H, d, *J* = 8.8 Hz, (*Z*)-Ar-*H*), 6.48 (2H, d, *J* = 8.7 Hz, (*E*)-Ar-*H*), 4.11 (2H, t, *J* = 5.9 Hz, (*E*)-ArOC*H*$_2$CH$_2$N), 3.95 (2H, t, *J* = 5.9 Hz, (*Z*)-ArOC*H*$_2$CH$_2$N), 3.59-3.51 (12H, m, C*H*$_2$OC*H*$_2$), 2.87 (2H, t, *J* = 5.8 Hz, (*Z*)-ArOCH$_2$C*H*$_2$N), 2.77 (2H, t, *J* = 5.9 Hz, (*E*)-NC*H*$_2$CH$_2$O), 2.69 (2H, t, *J* = 5.8 Hz, (*Z*)-ArOCH$_2$C*H*$_2$N), 2.63 (2H, t, *J* = 5.7 Hz, (*E*)-ArOCH$_2$C*H*$_2$N), 2.53-2.44 (4H, 2×q, *J* = 7.4 Hz, 7.4 Hz, C*H*$_2$CH$_3$), 2.38 (3H, s,

(*Z*)-NC*H*$_3$), 2.32 (3H, s, (*E*)-NC*H*$_3$), 0.90 (6H, t, *J* = 7.4 Hz, CH$_2$C*H*$_3$).

Trans-trans isomer of **64** (the third fraction):

^{1}H-NMR (Acetone-d6, 400 MHz) δ (ppm) = 7.18-7.06 (14H, m, Ar-*H*), 6.94 (4H, d, *J* = 8.7 Hz, Ar-*H*), 6.69 (4H, d, *J* = 8.7 Hz, Ar-*H*), 6.49 (4H, d, *J* = 8.6 Hz, Ar-*H*), 4.11 (4H, t, *J* = 5.9 Hz, ArOC*H*$_2$CH$_2$N), 3.60-3.54 (12H, m, C*H*$_2$OC*H*$_2$), 2.86 (4H, t, *J* = 5.8 Hz, ArOCH$_2$C*H*$_2$N), 2.68 (4H, t, *J* = 5.8 Hz, ArOCH$_2$C*H*$_2$N), 2.47 (4H, q, *J* = 7.4 Hz, C*H*$_2$CH$_3$), 2.38 (6H, s, NC*H*$_3$), 0.90 (6H, t, *J* = 7.4 Hz, CH$_2$C*H*$_3$).

HRMS (ESI-TOF, positive): $[C_{58}H_{70}O_7N_2]^{2+}$ cal. 453.2586, found 453.2583; $[C_{58}H_{69}O_7N_2]^{+}$ cal. 905.5099, found 905.5093; $[C_{58}H_{68}O_7N_2Na]^{+}$ cal. 927.4919, found 927.4913.

(5) Bivalent OHT ligand **65**:

The bis(*N*-methylamino) OEG spacer **22b** (12.6 mg, 0.0477 mmol), (*E*,*Z*)-isomer of **77** (39.3 mg, 0.110 mmol), sodium triacetoxyborohydride (31.2 mg, 0.143 mmol) and 5 mL anhydrous THF were used and the crude product was purified by column chromatography (chloroform : MeOH = 20:1 to 10:1 + 3% triethylamine) and by RP-HPLC (82% MeOH/H$_2$O + 0.4% diethylamine) to obtain **65** (18.4 mg, 39%) as three pure isomers: *cis-cis* (27%), *cis-trans* (49%), and *trans-trans* (24%) isomer.

Cis-cis isomer of **65** (the first fraction):

^{1}H-NMR (Acetone-d6, 400 MHz) δ (ppm) = 7.18-7.11 (8H, m, Ar-*H*), 7.10-7.04 (6H, m, Ar-*H*), 6.84 (4H, d, *J* = 8.6 Hz, Ar-*H*), 6.77 (4H, d, *J* = 9.0 Hz, Ar-*H*), 6.57 (4H, d, *J* = 8.8 Hz, Ar-*H*), 3.93 (4H, t, *J* = 6.0 Hz, ArOC*H*$_2$CH$_2$N), 3.61-3.52 (16H, m, C*H*$_2$OC*H*$_2$), 2.74 (4H, t, *J* = 6.0 Hz, ArOCH$_2$C*H*$_2$N), 2.60 (4H, t, *J* = 5.9 Hz, NC*H*$_2$CH$_2$O), 2.48 (4H, q, *J* = 7.4 Hz, C*H*$_2$CH$_3$), 2.30 (6H, s, NC*H*$_3$), 0.90 (6H, t, *J* = 7.4 Hz, CH$_2$C*H*$_3$).

Cis-trans isomer of **65** (the second fraction):

^{1}H-NMR (Acetone-d6, 400 MHz) δ (ppm) = 7.18-7.12 (10H, m, Ar-*H*), 7.10-7.05 (4H, m, Ar-*H*), 6.93 (2H, d, *J* = 8.8 Hz, (*E*)-Ar-*H*), 6.84 (2H, d, *J* = 8.7 Hz, (*Z*)-Ar-*H*), 6.78 (2H, d, *J* = 8.8 Hz, (*Z*)-Ar-*H*), 6.69 (2H, d, *J* = 8.8 Hz, (*E*)-Ar-*H*), 6.57 (2H, d, *J* = 8.8 Hz, (*Z*)-Ar-*H*), 6.48 (2H, d, *J* = 8.8 Hz, (*E*)-Ar-*H*), 4.10 (2H, t, *J* = 5.9 Hz, (*E*)-ArOC*H*$_2$CH$_2$N), 3.93 (2H, t, *J* = 6.0 Hz, (*Z*)-ArOC*H*$_2$CH$_2$N), 3.59-3.50 (16H, m, C*H*$_2$OC*H*$_2$), 2.84 (2H, t, *J* = 6.0 Hz, (*Z*)-ArOCH$_2$C*H*$_2$N), 2.74 (2H, t, *J* = 6.0 Hz, (*E*)-NC*H*$_2$CH$_2$O), 2.67 (2H, t, *J* = 5.9 Hz, (*Z*)-ArOCH$_2$C*H*$_2$N), 2.60 (2H, t, *J* = 5.9 Hz, (*E*)-ArOCH$_2$C*H*$_2$N), 2.52-2.44 (4H, 2×q, *J* = 7.4 Hz, 7.4 Hz, C*H*$_2$CH$_3$), 2.36 (3H, s,

(*Z*)-NCH_3), 2.30 (3H, s, (*E*)-NCH_3), 0.90 (6H, t, *J* = 7.4 Hz, CH_2CH_3).

Trans-trans isomer of **65** (the third fraction):

^{1}H-NMR (Acetone-d6, 400 MHz) δ (ppm) = 7.18-7.06 (14H, m, Ar-*H*), 6.94 (4H, d, *J* = 8.8 Hz, Ar-*H*), 6.69 (4H, d, *J* = 8.7 Hz, Ar-*H*), 6.48 (4H, d, *J* = 8.7 Hz, Ar-*H*), 4.10 (4H, t, *J* = 6.0 Hz, ArOCH_2CH$_2$N), 3.60-3.53 (16H, m, CH_2OCH_2), 2.85 (4H, t, *J* = 6.0 Hz, ArOCH$_2$CH_2N), 2.67 (4H, t, *J* = 5.9 Hz, ArOCH$_2$CH_2N), 2.47 (4H, q, *J* = 7.3 Hz, CH_2CH$_3$), 2.37 (6H, s, NCH_3), 0.90 (6H, t, *J* = 7.4 Hz, CH_2CH_3).

HRMS (ESI-TOF, positive): $[C_{60}H_{74}O_8N_2]^{2+}$ cal. 475.2717, found 475.2721; $[C_{60}H_{73}O_8N_2]^{+}$ cal. 949.5361, found 949.5367; $[C_{60}H_{72}O_8N_2Na]^{+}$ cal. 971.5181, found 971.5187.

(6) Bivalent OHT ligand **66**:

The bis(*N*-methylamino) OEG spacer **22c** (15.5 mg, 0.0503 mmol), (*E*,*Z*)-isomer of **77** (39.6 mg, 0.111 mmol), sodium triacetoxyborohydride (32.9 mg, 0.151 mmol) and 10 mL anhydrous THF were used and the crude product was purified by column chromatography (chloroform : MeOH = 20:1 to 10:1 + 3% triethylamine) and by RP-HPLC (82% MeOH/H_2O + 0.4% diethylamine) to obtain **66** (32.6 mg, 66%) as three pure isomers: *cis-cis* (28%), *cis-trans* (48%), and *trans-trans* (24%) isomer.

Cis-cis isomer of **66** (the first fraction):

^{1}H-NMR (Acetone-d6, 400 MHz) δ (ppm) = 7.20-7.12 (8H, m, Ar-*H*), 7.12-7.05 (6H, m, Ar-*H*), 6.84 (4H, d, *J* = 8.7 Hz, Ar-*H*), 6.78 (4H, d, *J* = 8.7 Hz, Ar-*H*), 6.58 (4H, d, *J* = 8.8 Hz, Ar-*H*), 4.00 (4H, t, *J* = 5.8 Hz, ArOCH_2CH$_2$N), 3.61-3.52 (20H, t and m, *J* = 5.8 Hz, CH_2OCH_2), 2.90 (4H, t, *J* = 5.6 Hz, ArOCH$_2$CH_2N), 2.75 (4H, t, *J* = 5.6 Hz, NCH_2CH$_2$O), 2.48 (4H, q, *J* = 7.3 Hz, CH_2CH$_3$), 2.42 (6H, s, NCH_3), 0.90 (6H, t, *J* = 7.4 Hz, CH_2CH_3).

Cis-trans isomer of **66** (the second fraction):

^{1}H-NMR (Acetone-d6, 400 MHz) δ (ppm) = 7.19-7.11 (10H, m, Ar-*H*), 7.10-7.05 (4H, m, Ar-*H*), 6.94 (2H, d, *J* = 8.7 Hz, (*E*)-Ar-*H*), 6.84 (2H, d, *J* = 8.6 Hz, (*Z*)-Ar-*H*), 6.78 (2H, d, *J* = 8.8 Hz, (*Z*)-Ar-*H*), 6.69 (2H, d, *J* = 8.6 Hz, (*E*)-Ar-*H*), 6.58 (2H, d, *J* = 8.8 Hz, (*Z*)-Ar-*H*), 6.48 (2H, d, *J* = 8.7 Hz, (*E*)-Ar-*H*), 4.14 (2H, t, *J* = 5.9 Hz, (*E*)-ArOCH_2CH$_2$N), 3.97 (2H, t, *J* = 5.8 Hz, (*Z*)-ArOCH_2CH$_2$N), 3.64-3.52 (20H, t and m, *J* = 5.8 Hz, CH_2OCH_2), 2.93 (2H, t, *J* = 6.0 Hz, (*Z*)-ArOCH$_2$CH_2N), 2.83 (2H, t, *J* = 5.8 Hz, (*E*)-NCH_2CH$_2$O), 2.75 (2H, t, *J* = 5.8 Hz, (*Z*)-ArOCH$_2$CH_2N), 2.69 (2H, t, *J* = 5.8 Hz, (*E*)-ArOCH$_2$CH_2N), 2.51-2.45 (4H, 2×q, *J* = 7.4 Hz,

7.4 Hz, CH_2CH$_3$), 2.43 (3H, s, (*Z*)-NCH_3), 2.37 (3H, s, (*E*)-NCH_3), 0.90 (6H, t, *J* = 7.3 Hz, CH$_2$CH_3).

Trans-trans isomer of **66** (the third fraction):

^{1}H-NMR (Acetone-d6, 400 MHz) δ (ppm) = 7.18-7.05 (14H, m, Ar-*H*), 6.94 (4H, d, *J* = 8.7 Hz, Ar-*H*), 6.69 (4H, d, *J* = 8.8 Hz, Ar-*H*), 6.49 (4H, d, *J* = 8.7 Hz, Ar-*H*), 4.15 (4H, t, *J* = 5.8 Hz, ArOCH_2CH$_2$N), 3.65-3.54 (20H, t and m, *J* = 5.8 Hz, CH_2OCH_2), 2.94 (4H, t, *J* = 5.9 Hz, ArOCH$_2$CH_2N), 2.76 (4H, t, *J* = 5.8 Hz, ArOCH$_2$CH_2N), 2.52-2.41 (10H, q and s, *J* = 7.5 Hz, CH_2CH$_3$ and NCH_3), 0.90 (6H, t, *J* = 7.4 Hz, CH$_2$CH_3).

HRMS (ESI-TOF, positive): $[C_{62}H_{78}O_9N_2]^{2+}$ cal. 497.2848, found 497.2839; $[C_{62}H_{77}O_9N_2]^{+}$ cal. 993.5624, found 993.5627; $[C_{62}H_{76}O_9N_2Na]^{+}$ cal. 1015.5443, found 1015.5442; $[C_{62}H_{76}O_9N_2K]^{+}$ cal. 1031.5182, found 1031.5192.

(7) Bivalent OHT ligand **67**:

The bis(*N*-methylamino) OEG spacer **22d** (21.8 mg, 0.0390 mmol), (*E*,*Z*)-isomer of **77** (30.8 mg, 0.0859 mmol), sodium triacetoxyborohydride (25.6 mg, 0.117 mmol) and 5 mL anhydrous THF/DCM (3:2) were used and the crude product was purified by column chromatography (chloroform : MeOH = 20:1 to 10:1 + 3% triethylamine) and by RP-HPLC (82% MeOH/H_2O + 0.4% diethylamine) to obtain **67** (12.0 mg, 28%) as three pure isomers: *cis-cis* (28%), *cis-trans* (48%), and *trans-trans* (24%) isomer.

Cis-cis isomer of **67** (the first fraction):

^{1}H-NMR (Acetone-d6, 400 MHz) δ (ppm) = 7.18-7.11 (8H, m, Ar-*H*), 7.10-7.04 (6H, m, Ar-*H*), 6.84 (4H, d, *J* = 8.6 Hz, Ar-*H*), 6.78 (4H, d, *J* = 8.7 Hz, Ar-*H*), 6.57 (4H, d, *J* = 8.8 Hz, Ar-*H*), 3.94 (4H, t, *J* = 6.0 Hz, ArOCH_2CH$_2$N), 3.57-3.49 (28H, m, CH_2OCH_2), 2.74 (4H, t, *J* = 6.0 Hz, ArOCH$_2$CH_2N), 2.61 (4H, t, *J* = 5.9 Hz, NCH_2CH$_2$O), 2.49 (4H, q, *J* = 7.4 Hz, CH_2CH$_3$), 2.30 (6H, s, NCH_3), 0.90 (6H, t, *J* = 7.4 Hz, CH$_2$CH_3).

Cis-trans isomer of **67** (the second fraction):

^{1}H-NMR (Acetone-d6, 400 MHz) δ (ppm) = 7.20-7.12 (10H, m, Ar-*H*), 7.12-7.05 (4H, m, Ar-*H*), 6.94 (2H, d, *J* = 8.7 Hz, (*E*)-Ar-*H*), 6.84 (2H, d, *J* = 8.6 Hz, (*Z*)-Ar-*H*), 6.78 (2H, d, *J* = 8.8 Hz, (*Z*)-Ar-*H*), 6.69 (2H, d, *J* = 8.6 Hz, (*E*)-Ar-*H*), 6.57 (2H, d, *J* = 8.8 Hz, (*Z*)-Ar-*H*), 6.48 (2H, d, *J* = 8.7 Hz, (*E*)-Ar-*H*), 4.10 (2H, t, *J* = 6.0 Hz, (*E*)-ArOCH_2CH$_2$N), 3.94 (2H, t, *J* = 6.0 Hz, (*Z*)-ArOCH_2CH$_2$N), 3.62-3.45 (28H, m, CH_2OCH_2), 2.85 (2H, t, *J* = 6.0 Hz, (*Z*)-ArOCH$_2$CH_2N),

2.74 (2H, t, J = 6.0 Hz, (*E*)-NCH_2CH$_2$O), 2.67 (2H, t, J = 5.9 Hz, (*Z*)-ArOCH$_2$CH_2N), 2.61 (2H, t, J = 5.9 Hz, (*E*)-ArOCH$_2$CH_2N), 2.53-2.44 (4H, 2×q, J = 7.4 Hz, 7.4 Hz, CH_2CH$_3$), 2.37 (3H, s, (*Z*)-NCH_3), 2.30 (3H, s, (*E*)-NCH_3), 0.90 (6H, t, J = 7.4 Hz, CH$_2$CH_3).

Trans-trans isomer of **67** (the third fraction):

^{1}H-NMR (Acetone-d6, 400 MHz) δ (ppm) = 7.18-7.05 (14H, m, Ar-*H*), 6.94 (4H, d, J = 8.7 Hz, Ar-*H*), 6.70 (4H, d, J = 8.7 Hz, Ar-*H*), 6.48 (4H, d, J = 8.7 Hz, Ar-*H*), 4.11 (4H, t, J = 6.0 Hz, ArOCH_2CH$_2$N), 3.61-3.52 (28H, m, CH_2OCH_2), 2.85 (4H, t, J = 6.0 Hz, ArOCH$_2$CH_2N), 2.67 (4H, t, J = 6.0 Hz, ArOCH$_2$CH_2N), 2.47 (4H, q, J = 7.4 Hz, CH_2CH$_3$), 2.37 (6H, s, NCH_3), 0.91 (6H, t, J = 7.4 Hz, CH$_2$CH_3).

HRMS (ESI-TOF, positive): $[C_{66}H_{86}O_{11}N_2]^{2+}$ cal. 541.3110, found 541.3070; $[C_{66}H_{85}O_{11}N_2]^{+}$ cal. 1081.6148, found 1081.6095; $[C_{66}H_{84}O_{11}N_2Na]^{+}$ cal. 1103.5967, found 1103.5915; $[C_{66}H_{84}O_{11}N_2K]^{+}$ cal. 1119.5707, found 1119.5663.

(8) Bivalent OHT ligand **68**:

The bis(*N*-methylamino) OEG spacer **22e** (21.7 mg, 0.0336 mmol), (*E*,*Z*)-isomer of **77** (36.1 mg, 0.101 mmol), sodium triacetoxyborohydride (29.3 mg, 0.134 mmol) and 4 mL anhydrous THF/DCM (1:1) were used and the crude product was purified by column chromatography (chloroform : MeOH = 20:1 to 10:1 + 3% triethylamine) and by RP-HPLC (80% MeOH/H_2O + 0.4% diethylamine) to obtain **68** (9.30 mg, 24%) as three pure isomers: *cis-cis* (30%), *cis-trans* (45%), and *trans-trans* (25%) isomer.

Cis-cis isomer of **68** (the first fraction):

^{1}H-NMR (Acetone-d6, 400 MHz) δ (ppm) = 7.19-7.11 (8H, m, Ar-*H*), 7.10-7.04 (6H, m, Ar-*H*), 6.85 (4H, d, J = 8.6 Hz, Ar-*H*), 6.78 (4H, d, J = 8.8 Hz, Ar-*H*), 6.58 (4H, d, J = 8.8 Hz, Ar-*H*), 3.94 (4H, t, J = 6.0 Hz, ArOCH_2CH$_2$N), 3.58-3.49 (36H, m, CH_2OCH_2), 2.75 (4H, t, J = 6.0 Hz, ArOCH$_2$CH_2N), 2.61 (4H, t, J = 5.9 Hz, NCH_2CH$_2$O), 2.48 (4H, q, J = 7.4 Hz, CH_2CH$_3$), 2.31 (6H, s, NCH_3), 0.90 (6H, t, J = 7.4 Hz, CH$_2$CH_3).

Cis-trans isomer of **68** (the second fraction):

^{1}H-NMR (Acetone-d6, 400 MHz) δ (ppm) = 7.20-7.11 (10H, m, Ar-*H*), 7.10-7.05 (4H, m, Ar-*H*), 6.94 (2H, d, J = 8.8 Hz, (*E*)-Ar-*H*), 6.84 (2H, d, J = 8.6 Hz, (*Z*)-Ar-*H*), 6.78 (2H, d, J = 8.8 Hz, (*Z*)-Ar-*H*), 6.69 (2H, d, J = 8.7 Hz, (*E*)-Ar-*H*), 6.57 (2H, d, J = 8.8 Hz, (*Z*)-Ar-*H*), 6.48 (2H, d, J = 8.7 Hz, (*E*)-Ar-*H*), 4.11 (2H, t, J = 6.0 Hz, (*E*)-ArOCH_2CH$_2$N), 3.94 (2H, t, J = 6.0 Hz,

(*Z*)-ArOC*H*$_2$CH$_2$N), 3.60-3.44 (36H, m, C*H*$_2$OC*H*$_2$), 2.85 (2H, t, *J* = 6.0 Hz, (*Z*)-ArOCH$_2$C*H*$_2$N), 2.74 (2H, t, *J* = 6.0 Hz, (*E*)-NC*H*$_2$CH$_2$O), 2.67 (2H, t, *J* = 5.9 Hz, (*Z*)-ArOCH$_2$C*H*$_2$N), 2.61 (2H, t, *J* = 5.9 Hz, (*E*)-ArOCH$_2$C*H*$_2$N), 2.53-2.44 (4H, 2×q, *J* = 7.4 Hz, 7.4 Hz, C*H*$_2$CH$_3$), 2.37 (3H, s, (*Z*)-NC*H*$_3$), 2.30 (3H, s, (*E*)-NC*H*$_3$), 0.90 (6H, t, *J* = 7.3 Hz, CH$_2$C*H*$_3$).

Trans-trans isomer of **68** (the third fraction):

^{1}H-NMR (Acetone-d6, 400 MHz) δ (ppm) = 7.18-7.06 (14H, m, Ar-*H*), 6.94 (4H, d, *J* = 8.7 Hz, Ar-*H*), 6.70 (4H, d, *J* = 8.7 Hz, Ar-*H*), 6.48 (4H, d, *J* = 8.7 Hz, Ar-*H*), 4.11 (4H, t, *J* = 6.0 Hz, ArOC*H*$_2$CH$_2$N), 3.61-3.52 (36H, m, C*H*$_2$OC*H*$_2$), 2.85 (4H, t, *J* = 5.8 Hz, ArOCH$_2$C*H*$_2$N), 2.68 (4H, t, *J* = 5.9 Hz, ArOCH$_2$C*H*$_2$N), 2.47 (4H, q, *J* = 7.6 Hz, C*H*$_2$CH$_3$), 2.37 (6H, s, NC*H*$_3$), 0.91 (6H, t, *J* = 7.3 Hz, CH$_2$C*H*$_3$).

HRMS (ESI-TOF, positive): $[C_{70}H_{94}O_{13}N_2]^{2+}$ cal. 585.3373, found 585.3386; $[C_{70}H_{93}O_{13}N_2]^{+}$ cal. 1169.6672, found 1169.6694.

(9) Bivalent OHT ligand **70**:

The bis(*N*-methylamino) OEG spacer **22f** (23.9 mg, 0.0417 mmol), (*E*,*Z*)-isomer of **77** (32.9 mg, 0.0918 mmol), sodium triacetoxyborohydride (27.4 mg, 0.125 mmol) and 5 mL anhydrous THF were used and the crude product was purified by column chromatography (chloroform : MeOH = 20:1 to 10:1 + 3% triethylamine) and by RP-HPLC (82% MeOH/H$_2$O + 0.4% diethylamine) to obtain **70** (30.9 mg, 61%) as three pure isomers: *cis-cis* (28%), *cis-trans* (48%), and *trans-trans* (24%) isomer.

Cis-cis isomer of **70** (the first fraction):

^{1}H-NMR (Acetone-d6, 400 MHz) δ (ppm) = 7.20-7.12 (8H, m, Ar-*H*), 7.12-7.04 (6H, m, Ar-*H*), 6.85 (4H, d, *J* = 8.6 Hz, Ar-*H*), 6.78 (4H, d, *J* = 8.8 Hz, Ar-*H*), 6.58 (4H, d, *J* = 9.0 Hz, Ar-*H*), 3.94 (4H, t, *J* = 6.0 Hz, ArOC*H*$_2$CH$_2$N), 3.59-3.51 (44H, m, C*H*$_2$OC*H*$_2$), 2.75 (4H, t, *J* = 6.0 Hz, ArOCH$_2$C*H*$_2$N), 2.61 (4H, t, *J* = 5.9 Hz, NC*H*$_2$CH$_2$O), 2.49 (4H, q, *J* = 7.4 Hz, C*H*$_2$CH$_3$), 2.30 (6H, s, NC*H*$_3$), 0.90 (6H, t, *J* = 7.3 Hz, CH$_2$C*H*$_3$).

Cis-trans isomer of **70** (the second fraction):

^{1}H-NMR (Acetone-d6, 400 MHz) δ (ppm) = 7.20-7.12 (10H, m, Ar-*H*), 7.11-7.05 (4H, m, Ar-*H*), 6.94 (2H, d, *J* = 8.7 Hz, (*E*)-Ar-*H*), 6.85 (2H, d, *J* = 8.6 Hz, (*Z*)-Ar-*H*), 6.78 (2H, d, *J* = 8.8 Hz, (*Z*)-Ar-*H*), 6.69 (2H, d, *J* = 8.7 Hz, (*E*)-Ar-*H*), 6.57 (2H, d, *J* = 8.8 Hz, (*Z*)-Ar-*H*), 6.49 (2H, d, *J* = 8.7 Hz, (*E*)-Ar-*H*), 4.11 (2H, t, *J* = 6.0 Hz, (*E*)-ArOC*H*$_2$CH$_2$N), 3.94 (2H, t, *J* = 6.0 Hz,

(*Z*)-ArOC*H*$_2$CH$_2$N), 3.62-3.47 (44H, m, C*H*$_2$OC*H*$_2$), 2.85 (2H, t, *J* = 5.9 Hz, (*Z*)-ArOCH$_2$C*H*$_2$N), 2.75 (2H, t, *J* = 6.0 Hz, (*E*)-NC*H*$_2$CH$_2$O), 2.68 (2H, t, *J* = 5.9 Hz, (*Z*)-ArOCH$_2$C*H*$_2$N), 2.61 (2H, t, *J* = 5.9 Hz, (*E*)-ArOCH$_2$C*H*$_2$N), 2.53-2.44 (4H, 2×q, *J* = 7.4 Hz, 7.4 Hz, C*H*$_2$CH$_3$), 2.37 (3H, s, (*Z*)-NC*H*$_3$), 2.30 (3H, s, (*E*)-NC*H*$_3$), 0.91 (6H, t, *J* = 7.3 Hz, CH$_2$C*H*$_3$).

Trans-trans isomer of **70** (the third fraction):

^{1}H-NMR (Acetone-d6, 400 MHz) δ (ppm) = 7.18-7.06 (14H, m, Ar-*H*), 6.94 (4H, d, *J* = 8.7 Hz, Ar-*H*), 6.70 (4H, d, *J* = 8.7 Hz, Ar-*H*), 6.49 (4H, d, *J* = 8.6 Hz, Ar-*H*), 4.11 (4H, t, *J* = 6.0 Hz, ArOC*H*$_2$CH$_2$N), 3.61-3.53 (44H, m, C*H*$_2$OC*H*$_2$), 2.85 (4H, t, *J* = 6.0 Hz, ArOCH$_2$C*H*$_2$N), 2.67 (4H, t, *J* = 5.9 Hz, ArOCH$_2$C*H*$_2$N), 2.47 (4H, q, *J* = 7.6 Hz, C*H*$_2$CH$_3$), 2.37 (6H, s, NC*H*$_3$), 0.91 (6H, t, *J* = 7.4 Hz, CH$_2$C*H*$_3$).

HRMS (ESI-TOF, positive): $[C_{74}H_{102}O_{15}N_2]^{2+}$ cal. 629.3635, found 629.3608; $[C_{74}H_{101}O_{15}N_2]^{+}$ cal. 1257.7197, found 1257.7149; $[C_{74}H_{100}O_{15}N_2Na]^{+}$ cal. 1279.7016, found 1279.6968; $[C_{74}H_{100}O_{15}N_2K]^{+}$ cal. 1295.6755, found 1295.6736.

(10) General procedure for chemical preparations of bivalent OHT ligand **69** an **70**:

To a solution of (*E*,*Z*)-endoxifen **74** (4.0 equivalents), dibromide OEG spacer **23** (1.0 equivalent) in anhydrous THF, diisopropylethylamine (4.0 equivalents) was added and the reaction mixture was stirred and gradually heated up to 60° C until TLC analysis indicated complete consumption of **23**. The reaction mixture was diluted in ethyl acetate followed by washing the organic phase with a pH = 10 Na_2CO_3/$NaHCO_3$ aqueous buffer. The combined organic layers were dried over $MgSO_4$ and concentrated in vacuo. The residue was absorbed on the silica gel and further purified by column chromatography to obtain the pure product.

(11) Bivalent OHT ligand **69**:

The dibromide OEG spacer **23f** (26.2 mg, 0.0417 mmol), the endoxifen **74** (34.2 mg, 0.0917 mmol), diisopropylethylamine (22.0 μL, 0.125 mmol), and 3 mL anhydrous THF were used. The crude product was purified by column chromatography (Chloroform : MeOH = 10:1 to 10:1 + 3% triethylamine) to give **69** (18.0 mg, 37%) as a mixture of *cis-cis*, *cis-trans*, and *trans-trans* isomers.

^{1}H-NMR (DCM-d2, 400 MHz) δ (ppm) = 7.20-7.02 (14H, m, Ar-*H*), 6.84-6.66 (8H, m, Ar-*H*), 6.49-6.42 (4H, m, Ar-*H*), 4.11-4.03 (2H, m, ArOC*H*$_2$CH$_2$N), 3.95-6.87 (2H, m, ArOC*H*$_2$CH$_2$N), 3.61-3.49 (40H, m, C*H*$_2$OC*H*$_2$), 2.90-2.84 (2H, m, ArOCH$_2$C*H*$_2$N), 2.80-2.74 (2H, m,

NCH_2CH$_2$O), 2.74-2.68 (2H, m, ArOCH$_2$CH_2N), 2.68-2.62 (2H, m, ArOCH$_2$CH_2N), 2.50-2.42 (4H, m, CH_2CH$_3$), 2.39, 2.37, 2.32, and 2.30 (6H, 4×s, NCH_3), 0.90 (6H, t, J = 7.4 Hz, CH$_2$CH_3).

^{13}C-NMR (DCM-d2, 100 MHz) δ (ppm) = 158, 157, 156, 155, 143, 141, 138, 137, 136, 136, 132, 131, 130, 128, 126, 123, 116, 115, 114, 70.8, 69.4, 69.3, 66.2, 57.5, 57.4, 56.8, 43.3, 43.2, 31.0, 29.4, 29.3, 13.7.

HRMS (ESI-TOF, positive): $[C_{72}H_{98}O_{14}N_2]^{2+}$ cal. 607.3504, found 607.3511; $[C_{72}H_{97}O_{14}N_2]^{+}$ cal. 1213.6934, found 1213.6772; $[C_{72}H_{96}O_{14}N_2Na]^{+}$ cal. 1235.6754, found 1235.6892; $[C_{72}H_{96}O_{14}N_2K]^{+}$ cal. 1251.6493, found 1251.6490.

(12) Bivalent OHT ligand **70** (the second procedure):

The dibromide OEG spacer **23g** (30.8 mg, 0.0458 mmol), the endoxifen **74** (43.5 mg, 0.115 mmol), diisopropylethylamine (24.1 μL, 0.137 mmol), and 4 mL anhydrous THF were used. The crude product was purified by column chromatography (Chloroform : MeOH = 10:1 + 3% triethylamine) to give **70** (18.9 mg, 33%) as a mixture of *cis*-*cis*, *cis*-*trans*, and *trans*-*trans* isomers.

6.4.2. Chemical preparation of 1,1-bis(4-hydroxyphenyl)-2-phenylbut-1-ene 71

To a stirred suspension of zinc powder (6.40 g, 98.0 mmol) in anhydrous THF (20 mL), titanium tetrachloride (4.88 mL, 44.2 mol) was added dropwise under argon at 0°C. When the addition was complete, the mixture was warmed to room temperature and then refluxed for 2 h. To the cooled dark suspension of the titanium reagent, a solution of 4,4'-hydroxybenzophenone (1.60 g, 7.25 mmol) and propiophenone (3.14 g, 23.2 mmol) in anhydrous THF (40 mL) was added dropwise at 0°C, and the mixture was refluxed in the dark for 2 h. After being cooled to room temperature, the reaction mixture was quenched with 10% aqueous potassium carbonate (30 mL) and extracted with ethyl acetate. The organic layer was washed with brine, dried over $MgSO_4$, and concentrated in vacuo. The rosy residue was dissolved in the *n*-hexane and the insoluble solid was filtered. The rosy crude product was purified by column chromatography ($CHCl_3$: AcOEt = 5:1) to obtain 1,1-bis(4-hydroxyphenyl)-2-phenylbut-1-ene **71** as a white solid (2.27 g, 99%).

^{1}H-NMR ($CDCl_3$, 400 MHz) δ (ppm) = 7.17-7.11 (2H, m, Ar-*H*), 7.10-7.05 (3H, m, Ar-*H*), 7.04-6.99 (2H, d, J = 8.6 Hz, Ar-*H*), 6.76 (2H, d, J = 8.7 Hz, Ar-*H*), 6.65 (2H, d, J = 8.7 Hz, Ar-*H*), 6.39 (2H, d, J = 8.7 Hz, Ar-*H*), 2.47 (2H, d, J = 7.4 Hz, CCH_2CH$_3$), 0.90 (3H, t, J = 7.3 Hz, CCH$_2$CH_3).

^{13}C-NMR ($CDCl_3$, 100 MHz) δ (ppm) = 157, 156, 144, 142, 140, 137, 136, 133, 131, 129, 127, 116, 115, 30.0, 14.1.

HRMS (ESI-TOF, negative): $[C_{22}H_{19}O_2]^-$ cal. 315.1391, found 315.1418; $[C_{44}H_{39}O_4]^-$ cal. 631.2854, found 631.2893.

6.4.3. Chemical preparation of 2-[(*N*-benzyloxycarbonyl)methylamino]ethanol 72

To a solution of 2-(methylamino) ethanol (2.95 g, 39.3 mmol) and triethyl amine (7.11 mL, 51.1 mmol) in anhydrous DCM (100 mL), benzyl chloroformate (6.13 mL, 41.3 mmol) in anhydrous DCM (40 mL) was added dropwise at 0°C over 30 min and the reaction mixture was further stirred at room temperature for 24 h. The reaction mixture was washed with 10% citric acid (120 mL), 10% $KHCO_3$, water, dried over $MgSO_4$ and concentrated in vacuo. The crude product was purified by column chromatography (hexane : AcOEt = 3:2) to obtain 2-[(*N*-benzyloxycarbonyl) methylamino] ethanol **72** as colorless oil (5.78 g, 70%).

^{1}H-NMR ($CDCl_3$, 400 MHz) δ (ppm) = 7.39-7.28 (5H, m, Ar-*H*), 5.12 (2H, s, ArCH_2O), 3.75 (2H, br s, CH_2CH_2OH), 3.44 (2H, t, *J* = 4.5 Hz, CH_2CH_2OH), 2.99 (3H, s, NCH_3), 2.60 (1H, s, O*H*).

^{13}C-NMR ($CDCl_3$, 100 MHz) δ (ppm) = 158, 137, 129, 128, 67.4, 61.3, 61.1, 52.1, 51.2, 35.5.

6.4.4. Chemical preparation of (*E*,*Z*)-benzyl 2-(4-(1-(4-hydroxyphenyl)-2-phenylbut-1-enyl) phenoxy)ethyl(methyl)carbamate 73

To a solution of 2-[(*N*-benzyloxycarbonyl)methylamino]ethanol **72** (206 mg, 0.983 mmol), triphenylphosphine (391 mg, 1.47 mmol), and 1,1-bis(4-hydroxyphenyl)-2-phenylbut-1-ene **71** (311 mg, 0.983 mmol) in anhydrous THF (10 mL), a solution of diethyl azodicarbonylate (DEAD, 236 μL, 1.47 mmol) in anhydrous THF (10 mL) was added at 0°C over 30 min. This reaction mixture was further stirred at room temperature for 24 h. The solvent was removed in vacuo and the residue was dissolved in diethyl ether, washed with saturated $NaHCO_3$, brine, dried over $MgSO_4$, and concentrated in vacuo. The crude product was further purified by two times column chromatography (chloroform : MeOH = 20:1, hexane : AcOEt = 3:2) to obtain a mixutrue of *cis*- and *trans*- isomers (*cis* : *trans* = 1:1) of benzyl 2-(4-(1-(4-hydroxyphenyl)-2-phenylbut-1-enyl) phenoxy)ethyl(methyl)carbamate **73** as a light yellow solid (200 mg, 40%). Due to the facile isomerization of the triarylethylene structure, a

geometrical isomer separation was not performed for **73**.

^{1}H-NMR ($CDCl_3$, 400 MHz) δ (ppm) = 7.38-7.28 (10H, m, Ar-*H*), 7.18-7.06 (14H, m, Ar-*H*), 6.88-6.78 (4H, m, Ar-*H*), 6.73-6.69 (4H, m, Ar-*H*), 6.54-6.43 (4H, m, Ar-*H*), 5.15 (2H, s, ArCH_2O), 5.11 (2H, s, ArCH_2O), 4.14 (1H, t, J = 4.8 Hz, OCH_2CH$_2$N), 4.08 (1H, t, J = 5.0 Hz, OCH_2CH$_2$N), 3.98 (1H, t, J = 5.0 Hz, OCH_2CH$_2$N), 3.92 (1H, t, J = 5.2 Hz, OCH_2CH$_2$N), 3.72-3.64 (2H, m, OCH$_2$CH_2N), 3.61-3.54 (2H, m, OCH$_2$CH_2N), 3.09 (3H, s, NCH_3), 3.00 (3H, s, NCH_3), 2.52-2.43 (4H, 2 × d, J = 7.4 Hz, 7.4 Hz, CCH_2CH$_3$), 0.92 (6H, t, J = 7.4 Hz, CCH$_2$CH_3).

^{13}C-NMR ($CDCl_3$, 100 MHz) δ (ppm) = 155, 154, 143, 141, 138, 137, 136, 132, 131, 130, 129, 128, 126, 115, 114, 113, 67.6, 67.5, 49.5, 49.2, 36.3, 29.3, 29.2, 13.8.

6.4.5. Chemical preparation of (*E*,*Z*)-4-(1-(4-(2-(methylamino)ethoxy)phenyl)-2-phenylbut-1-enyl)phenol 74

To a solution of (*E*,*Z*)-benzyl 2-(4-(1-(4-hydroxyphenyl)-2-phenylbut-1-enyl)phenoxy)ethyl (methyl)carbamate **73** (352 mg, 0.694 mmol) in ethyl acetate (50 mL), palladium on barium sulfate (5%, 148 mg, 0.0694 mmol) was added and the mixture was hydrogenated for 96 h until TLC analysis indicated complete consumption of **73**. The mixture was filtered over Celite and the filter cake was washed with ethyl acetate. The crude product was concentrated in vacuo and further purified by column chromatography (chloroform : MeOH = 10:1, + 3% triethylamine) to obtain a mixutrue of *cis*- and *trans*- isomers (*cis* : *trans* = 1:1) of 4-(1-(4-(2-(methylamino) ethoxy)phenyl)-2-phenylbut- 1-enyl)phenol **74** as a colorless oil. *Cis*- and *trans*- isomers were separated by RP-HPLC (75% MeOH/H_2O + 0.05% triethylamine) and characterized with ^{1}H-NMR according to the reference 176.

Cis-isomer of **74** (the first fraction):

^{1}H-NMR (MeOD, 400 MHz) δ (ppm) = 7.17-7.05 (7H, m, Ar-*H*), 6.93 (2H, d, J = 8.8 Hz, Ar-*H*), 6.64 (2H, d, J = 8.8 Hz, Ar-*H*), 6.39 (2H, d, J = 8.7 Hz, Ar-*H*), 4.11 (2H, t, J = 5.2 Hz, OCH_2CH$_2$N), 2.96 (2H, t, J = 5.2 Hz, OCH$_2$CH_2N), 2.47 (5H, s and q, J = 7.4 Hz, NCH_3 and CCH_2CH$_3$), 0.90 (3H, t, J = 7.4 Hz, CCH$_2$CH_3).

Trans-isomer of **74** (the second fraction):

^{1}H-NMR (MeOD, 400 MHz) δ (ppm) = 7.18-7.04 (5H, m, Ar-*H*), 7.01 (2H, d, J = 8.6 Hz, Ar-*H*), 6.93 (4H, 2 × d, J = 8.6 Hz, 8.7 Hz, Ar-*H*), 6.57 (2H, d, J = 8.8 Hz, Ar-*H*), 3.95 (2H, t, J = 5.1 Hz,

OCH_2CH$_2$N), 2.87 (2H, t, J = 5.3 Hz, OCH$_2$CH_2N), 2.48 (2H, q, J = 7.4 Hz, CCH_2CH$_3$), 2.41 (3H, s, NCH_3), 0.90 (3H, t, J = 7.4 Hz, CCH$_2$CH_3).

HRMS (ESI-TOF, positive): $[C_{25}H_{28}NO_2]^+$ cal. 374.2115, found 374.2142; $[C_{25}H_{27}NO_2Na]^+$ cal. 396.1934, found 396.1866.

6.4.6. Chemical preparation of monovalent OHT ligand 75

The monomethyl bromide OEG ether **27** (17.5 mg, 0.0555 mmol), the endoxifen **74** (21.8 mg, 0.583 mmol), diisopropylethylamine (38.9 µL, 0.222 mmol), and 3 mL anhydrous THF were used. The crude product was purified by column chromatography (DCM : MeOH = 10:1 to 5:1 to 100% MeOH) and RP-HPLC (75%MeOH/H_2O + 50mM NH_4OH) to give **75** (11.9 mg, 35%) as two pure isomers: *cis*-isomer (34%) and *trans*-isomer (66%).

Cis-isomer of **75** (the first fraction):

^{1}H-NMR (MeOD, 400 MHz) δ (ppm) = 7.17-7.12 (2H, m, Ar-*H*), 7.11-7.05 (3H, m, Ar-*H*), 7.01 (2H, d, J = 8.6 Hz, Ar-*H*), 6.78-6.83 (4H, m, Ar-*H*), 6.56 (2H, d, J = 8.8 Hz, Ar-*H*), 3.97 (2H, t, J = 5.6 Hz, ArOCH_2CH$_2$N), 3.62-3.54 (14H, m, CH_2OCH_2), 3.53-3.49 (2H, m, NCH$_2$CH_2O), 3.34 (3H, s, OCH_3), 2.82 (2H, t, J = 5.6 Hz, ArOCH$_2$CH_2N), 2.69 (2H, t, J = 5.6 Hz, NCH_2CH$_2$O), 2.48 (2H, q, J = 7.4 Hz, CH_2CH$_3$), 2.35 (3H, s, NCH_3), 0.91 (3H, t, J = 7.4 Hz, CH$_2$CH_3).

Trans-isomer of **75** (the second fraction):

^{1}H-NMR (MeOD, 400 MHz) δ (ppm) = 7.16-7.12 (2H, m, Ar-*H*), 7.12-7.05 (5H, m, Ar-*H*), 6.92 (2H, d, J = 8.7 Hz, Ar-*H*), 6.64 (2H, d, J = 8.7 Hz, Ar-*H*), 6.39 (2H, d, J = 8.6 Hz, Ar-*H*), 4.14 (2H, t, J = 5.4 Hz, ArOCH_2CH$_2$N), 3.67-3.57 (14H, m, CH_2OCH_2), 3.53-3.50 (2H, m, NCH$_2$CH_2O), 3.34 (3H, s, OCH_3), 2.93 (2H, t, J = 5.6 Hz, ArOCH$_2$CH_2N), 2.76 (2H, t, J = 5.7 Hz, NCH_2CH$_2$O), 2.51-2.39 (5H, q and s, J = 7.3 Hz, CH_2CH$_3$ and NCH_3), 0.91 (3H, t, J = 7.4 Hz, CH$_2$CH_3).

HRMS (ESI-TOF, positive): $[C_{36}H_{50}O_7N]^+$ cal. 608.3582, found 608.3575; $[C_{36}H_{49}O_7NNa]^+$ cal. 630.3401, found 630.3392.

6.4.7. Chemical preparation of (*E*,*Z*)-4-(1-(4-(2,2-diethoxyethoxy)phenyl)-2-phenylbut-1-enyl)phenol 76

To a solution of 1,1-bis(4-hydroxyphenyl)-2-phenylbut-1-ene **71** (1.07 g, 3.39 mmol) in anhydrous DMF (20 mL), a solution of sodium ethoxide (21% in EtOH, 1.27 mL, 3.39 mmol) in anhydrous

DMF (10 mL) was added dropwise over 30 min at 70°C and the reaction mixture was stirred and heated up to 120°C for 30 min. After the mixture was cooled to room temperature, a solution of bromoacetal diethylacetal (526 µL, 3.39 mmol) in anhydrous DMF (20 mL) was added dropwise and the mixture was stirred at 120°C for 3 h. The solvent was removed in vacuo. The residue was washed with ethyl acetate, brine, dried over $MgSO_4$, and concentrated in vacuo. The crude product was further purified by 2 times column chromatography (chloroform : MeOH = 40:1, hexane : AcOEt = 5:1) to a mixture of *cis*- and *trans*- isomers of 4-(1-(4-(2,2-diethoxyethoxy)phenyl)-2-phenylbut-1-enyl)phenol **76** as a yellow oil (627 mg, 43%). Due to the facile isomerization of the triarylethylene structure, a geometrical isomer separation by RP-HPLC (85%MeOH/H_2O) was only performed for the characterization of *cis*- and *trans*-isomers of **76** with the NOE spectra method.

Cis-isomer of **76** (the first fraction):

^{1}H-NMR (Acetone-d6, 250 MHz) δ (ppm) = 8.38 (1H, s, Ar-O*H*), 7.24-7.02 (7H, m, Ar-*H*), 6.90-6.74 (4H, 2 × d, J = 8.8 Hz, 8.8 Hz, Ar-*H*), 6.59 (2H, d, J = 8.1 Hz, Ar-*H*), 4.74 (1H, t, J = 5.2 Hz, OCH_2CH), 3.84 (2H, d, J = 5.9 Hz, OCH_2CH), 3.77-3.48 (4H, m, OCH_2CH_3), 2.50 (2H, q, J = 7.4 Hz, CCH_2CH_3), 1.14 (6H, t, J = 6.6 Hz, OCH_2CH_3), 0.91 (3H, t, J = 7.4 Hz, CCH_2CH_3).

^{13}C-NMR (Acetone-d6, 62.5 MHz) δ (ppm) =157, 143, 141, 139, 137, 136, 133, 131, 130, 129, 127, 116, 114, 101, 69.1, 62.8, 29.5, 15.7, 13.8.

Trans-isomer of **76** (the second fraction):

^{1}H-NMR (Acetone-d6, 250 MHz) δ (ppm) = 8.13 (1H, s, Ar-O*H*), 7.23-7.07 (7H, m, Ar-*H*), 6.96 (2H, d, J = 8.1 Hz, Ar-*H*), 6.70 (2H, d, J = 8.8 Hz, Ar-*H*), 6.49 (2H, d, J = 8.8 Hz, Ar-*H*), 4.85 (1H, t, J = 5.1 Hz, OCH_2CH), 4.00 (2H, d, J = 5.2 Hz, OCH_2CH), 3.80-3.58 (4H, m, OCH_2CH_3), 2.48 (2H, q, J = 7.4 Hz, CCH_2CH_3), 1.19 (6H, t, J = 7.4 Hz, OCH_2CH_3), 0.91 (3H, t, J = 7.4 Hz, CCH_2CH_3).

^{13}C-NMR (Acetone-d6, 62.5 MHz) δ (ppm) = 158, 156, 144, 141, 139, 137, 133, 131, 129, 127, 116, 115, 114, 101, 69.4, 69.2, 62.9, 29.5, 15.7, 13.9.

HRMS (ESI-TOF, positive): $[C_{28}H_{32}O_4Na]^+$ cal. 455.2193, found 455.2170; $[C_{28}H_{32}O_4K]^+$ cal. 471.1932, found 471.1908; $[C_{56}H_{64}O_8Na]^+$ cal. 887.4493, found 887.4453.

6.4.8. Chemical preparation of (*E*,*Z*)-2-(4-(1-(4-hydroxyphenyl)-2-phenylbut-1-enyl)

phenoxy)acetaldehyde 77

To a solution of (*E*,*Z*)-4-(1-(4-(2,2-diethoxyethoxy)phenyl)-2-phenylbut- 1-enyl)phenol **76** (467 mg, 1.08 mmol) in THF (4.7 mL), 3 M HCl (4.7 mL) was added and the reaction mixture was stirred at 50°C for 20 h until TLC analysis indicated complete consumption of **76**. The organic solvent was removed in vacuo and the residue was neutralized with saturated NaHCO3, washed with diethyl ether, brine, dried over $MgSO_4$, and concentrated in vacuo. The crude product was further purified by column chromatography (hexane : AcOEt = 5:1 to 1:1) to obtain a mixture of *cis*- and *trans*-isomers (*cis* : *trans* = 1:1) of 2-(4-(1-(4-hydroxyphenyl)-2-phenylbut-1-enyl) phenoxy)acetaldehyde **77** as a white solid (318 mg, 82%). Since the aldehyde forms a stabile hemiacetal with alcohol, a geometrical isomer separation by HPLC was not performed and the product was characterized according to the chemical shift of **76**.

^{1}H-NMR (Acetone-d6, 400 MHz) δ (ppm) = 9.83 (1H, s, aldehyde-*H*), 9.72 (1H, s, aldehyde-*H*), 8.37 (1H, s, Ar-O*H* of *cis*-isomer), 8.13 (1H, s, Ar-O*H* of *trans*-isomer), 7.20-7.06 (14H, m, Ar-*H*), 7.07 (4H, d, J = 8.6 Hz, Ar-H of *cis*-isomer), 6.96 (2H, d, J = 8.8 Hz, Ar-*H* of *trans*-isomer), 6.84 (2H, d, J = 8.7 Hz, Ar-H of *cis*-isomer), 6.81 (2H, d, J = 8.9 Hz, Ar-*H* of *cis*-isomer), 6.70 (2H, d, J = 8.7 Hz, Ar-*H* of *trans*-isomer), 6.60 (2H, d, J = 9.0 Hz, Ar-H of *cis*-isomer), 6.49 (2H, d, J = 8.7 Hz, Ar-*H* of *trans*-isomer), 4.80 (2H, s, OCH_2C=O), 4.61 (2H, s, OCH_2C=O), 2.53-2.43 (4H, 2 × q, J = 7.5 Hz, 7.4 Hz, CCH_2CH$_3$), 0.90 (3H, t, J = 7.4 Hz, CCH$_2$CH_3).

^{13}C-NMR (Acetone-d6, 100 MHz) δ (ppm) = 199, 158, 157, 156, 144, 142, 139, 138, 136, 135, 133, 131, 129, 127, 116, 115, 114, 73.7, 73.4, 13.9.

HRMS (ESI-TOF, negative): $[C_{24}H_{21}O_3]^-$ cal. 357.1496, found 357.1505; $[C_{48}H_{43}O_6]^-$ cal. 715.3065, found 715.3075.

7. References

[1] M. Mammen, S. Choi, G. M. Whitesides, *Angew. Chem. Int. Ed.* **1998**, *37*, 2754-2794.

[2] F. Marin, G. Luquet, B. Marie, D. Medakovic, *Current Topics in Developmental Biology* **2007**, *80*, 209-276.

[3] W. J. Lees, A. Spaltenstein, J. E. Kingery-Wood, G. M. Whitesides, *J. Med. Chem.* **1994**, *37*, 3419-3433.

[4] M. Mammen, G. Dahmann, G. M. Whitesides, *J. Med. Chem.* **1995**, *38*, 4179-4190.

[5] Y. C. Lee, R. T. Lee, *Acc. Chem. Res.* **1995**, *28*, 321-327.

[6] T. Dam, R. Roy, S. Das, S. Oscarson, C. Brewer, *J. Biol. Chem.* **2000**, *275*, 14223-14230.

[7] P. I. Kitov, J. M. Sadowska, G. Mulvey, G. D. Armstrogn, H. Ling, N. S. Pannu, R. J. Read, D. R. Bundle, *Nature* **2000**, *403*, 669-672.

[8] D. Schwefel, C. Maierhofer, J. G. Beck, S. Seeberger, K. Diederichs, H. M. Möller, W. Welte, V. Wittmann, *J. Am. Chem. Soc.* **2010**, *132*, 8704–8719.

[9] B. Bilgicer, D. T. Moustakas, G. M. Whitesides, *J. Am. Chem. Soc.* **2007**, *129*, 3722-3728.

[10] A. Perl, A. Gomez-Casado, D. Thompson, H. H. Dam, P. Jonkheijm, D. N. Reinhoudt, J. Huskens, *Nature Chemistry* **2011**, *3*, 317-322.

[11] E. T. Mack, P. W. Snyder, R. Perez-Castillejos, G. M. Whitesides, *J. Am. Chem. Soc.* **2011**, *133*, 11701-11715.

[12] W. Spevak, J. O. Nagy, D. H. Charych, M. E. Schaefer, J. H. Gilbert, M. D. Bednarski, *J. Am. Chem. Soc.* **1993**, *115*, 1146-1147.

[13] I. Papp, J. Dernedde, S. Enders, R. Haag, *Chem. Commun.* **2008**, 5851-5853.

[14] V. Wittmann, S. Takayama, K. W. Gong, G. Weitz-Schmidt, C. Wong, *J. Org. Chem.* **1998**, *63*, 5137-5143.

[15] C. Maierhofer, K. Rohmer, V. Wittmann, *Bioorg. Med. Chem.* **2007**, *15*, 7661-7676.

[16] S. Choi, *Synthetic Mutilvalent Molecules*, John Wiley & Sons, Hoboken, New Jersey, **2004**.

[17] J. S. Roman, A. Gallardo, B. Levenfeld, *Adv. Mater.* **1995**, *7*, 203-208.

[18] V. M. Krishnamurthy, V. Semetey, p. J. Bracher, N. Shen, G. M. Whitesides, *J. Am. Chem. Soc.* **2007**, *129*, 1312-1320.

[19] V. M. Krishnamurthy, L. A. Estroff, G. M. Whitesides, *Fragment-based Approaches in Drug Discovery: Multivalency in Ligand Design*, WILEY-VCH Verlag GmbH & Co. KGaA, Weinheim, **2006**.

[20] M. Mammen, E. I. Shakhnovich, G. M. Whitesides, *J. Org. Chem.* **1998**, *63*, 3168-3175.

[21] E. K. Fan, Z. S. Zhang, W. E. Minke, Z. Hou, C. Verlinde, W. G. J. Hol, *J. Am. Chem. Soc.* **2000**, *122*, 2663-2664.

[22] A. Jain, G. M. Whitesides, R. S. Alexander, D. W. Christianson, *J. Med. Chem.* **1994**, *37*, 2100-2105.

[23] G. J. Wang, A. D. Hamilton, *Chem. Eur. J.* **2002**, *8*, 1954-1961.

[24] W. H. Chapman, R. Breslow, *J. Am. Chem. Soc.* **1995**, *117*, 5462-5469.

[25] R. Schweitzerstenner, A. Licht, I. Luscher, I. Pecht, *Biochemistry* **1987**, *26*, 3602-3612.

[26] B. Schuler, E. A. Lipman, P. J. Steinbach, M. Kumke, W. A. Eaton, *Proc. Natl. Acad. Sci. USA* **2005**, *102*, 2754-2759.

[27] J. M. Paar, N. T. Harris, D. Holowka, B. Baird, *J. Immunol.* **2002**, *169*, 856-864.

[28] V. Semetey, D. Moustakas, G. M. Whitesides, *Angew. Chem. Int. Ed.* **2006**, *45*, 588-591.

[29] A. Bujotzek, M. Shan, R. Haag, M. Weber, *J. Comput. Aided. Mol. Des.* **2011**, *25*, 253-262.

[30] M. Shan, A. Bujotzek, F. Abendroth, A. Wellner, R. Gust, O. Seitz, M. Weber, R. Haag, *ChemBioChem* **2011**, *12*, 2587-2598.

[31] E. K. Woller, E. D. Walter, J. R. Morgan, D. J. Singel, M. J. Cloninger, *J. Am. Chem. Soc.* **2003**, *125*, 8820-8826.

[32] S. Stiriba, H. Frey, R. Haag, *Angew. Chem. In. Ed.* **2002**, *41*, 1329-1334.

[33] R. Haag, J. Stumbé, A. Sunder, H. Frey, A. Hebel, *Macromolecules* **2000**, *33*, 8158-8166.

[34] A. Sunder, R. Mülhaupt, R. Haag, H. Frey, *Adv. Mater.* **2000**, *12*, 235-239.

[35] C. R. Bertozzi, L. L. Kiessling, *Science* **2001**, *291*, 2357-2364.

[36] J. E. Gestwicki, C. W. Cairo, L. E. Strong, K. A. Oetjen, L. L. Kiessling, *J. Am. Chem. Soc.* **2002**, *124*, 14922-14933.

[37] L. L. Kiessling, J. E. Gestwicki, L. E. Strong, *Angew. Chem. Int. Ed.* **2006**, *45*, 2348-2368.

[38] M. Weinhart, D. Groeger, S. Enders, J. Dernedde, R. Haag, *Biomaromolecules* **2011**, *12*, 2502-2511.

[39] M. Weinhart, D. Gröger, S. Enders, S. B. Riese, J. Dernedde, R. K. Kainthan, D. E. Brooks, R. Haag, *Macromolecular Bioscience* **2011**, *11*, 1088-1098.

[40] G. K. Ackers, M. L. Doyle, D. Myers, M. A. Daugherty, *Science* **1992**, *255*, 54-63.

[41] A. Schön, E. Freire, *Biochemistry* **1989**, *28*, 5019-5024.

[42] D. H. Williams, E. Stephens, D. P. O'Brien, M. Zhou, *Angew. Chem. Int. Ed.* **2004**, *43*, 6596-6616.

[43] J. J. Lundquist, E. J. Toone, *Chem. Rev.* **2002**, *102*, 555-578.

[44] D. R. Bundle, R. Alibes, S. Nilar, A. Otter, M. Warwas, P. Zhang, *J. Am. Chem. Soc.* **1998**,

120, 5317-5318.

[45] N. NavTre, N. Amiot, A. van Oijen, A. Imberty, A. Poveda, J. Jimenez-Barbero, A. Cooper, M. A. Nutley, G. J. Boons, *Chem. Eur. J.* **1999**, *5*, 2281-2294.

[46] T. Christensen, D. M. Gooden, J. E. Kung, E. J. Toone, *J. Am. Chem. Soc.* **2003**, *125*, 7357-7366.

[47] M. Akke, N. J. Skelton, J. Koerdel, A. G. Palmer, W. J. Chazin, *Biochemistry* **1993**, *32*, 9832-9844.

[48] L. Spyracopoulos, S. M. Gagne, M. X. Li, B. D. Sykes, *Biochemistry* **1998**, *37*, 18032-18044.

[49] V. M. Krishnamurthy, B. R. Bohall, V. Semetey, G. M. Whitesides, *J. Am. Chem. Soc.* **2006**, *128*, 5802-5812.

[50] R. H. Kramer, J. W. Karpen, *Nature* **1998**, *395*, 710-713.

[51] A. Mulder, T. Auletta, A. Sartori, S. D. Ciotto, A. Casnati, R. Ungaro, J. Huskens, D. N. Reinhoudt, *J. Am. Chem. Soc.* **2004**, *126*, 6627-6636.

[52] P. I. Kitov, H. Shimizu, S. W. Homans, D. R. Bundle, *J. Am. Chem. Soc.* **2003**, *125*, 3284-3294.

[53] P. I. Kitov, D. R. Bundle, *J. Am. Chem. Soc.* **2003**, *125*, 16271-16284.

[54] A. Mulder, J. Huskens, D. N. Reinhoudt, *Org. Biomol. Chem.* **2004**, *2*, 3409-3424.

[55] C. A. Hunter, H. L. Anderson, *Angew. Chem. Int. Ed.* **2009**, *48*, 7488-7499.

[56] G. Ercolani, L. Schiaffino, *Angew. Chem. Int. Ed.* **2011**, *50*, 1762-1768.

[57] J. J. Lundquist, S. D. Debenham, E. J. Toone, *J. Org. Chem.* **2000**, *65*, 8245-8250.

[58] J. E. Gestwicki, L. E. Strong, C. W. Cairo, F. J. Boehm, L. L. Kiessling, *Chem. Biol.* **2002**, *9*, 163-169.

[59] Z. Zhang, E. A. Merritt, M. Ahn, C. Roach, Z. Hou, C. L. M. J. Verlinde, W. G. J. Hol, E. Fan, *J. Am. Chem. Soc.* **2002**, *124*, 12991-12998

[60] W. Blokzijl, J. B. F. N. Engberts, *Angew. Chem. Int. Ed.* **1993**, *32*, 1545-1579.

[61] J. Rao, J. Lahiri, R. M. Weis, G. M. Whitesides, *J. Am. Chem. Soc.* **2000**, *122*, 2698-2710.

[62] J. Rao, J. Lahiri, L. Isaacs, R. M. Weis, G. M. Whitesides, *Science* **1998**, *280*, 708-711.

[63] D. H. Williams, J. P. L. Cox, A. J. Doig, M. Gardner, U. Gerhard, P. T. Kaye, A. R. Lai, I. A. Nicholls, C. J. Salter, R. C. Mitchell, *J. Am. Chem. Soc.* **1991**, *113*, 7020-7030.

[64] N. J. de Mol, M. I. Catalina, F. J. Dekker, M. J. E. Fischer, A. J. R. Heck, R. M. Liskamp, *ChemBioChem* **2005**, *6*, 2261-2270.

[65] F. J. Dekker, N. J. de Mol, M. J. E. Fischer, R. M. J. Liskamp, *Bioorg. Med. Chem. Lett.* **2003**, *13*, 1241-1244.

[66] C. A. Hunter, S. Tomas, *Chem. Biol.* **2003**, *10*, 1023-1032.

[67] M. R. Perutz, *Q. Rev. Biophys.* **1989**, *22*, 139-236.

[68] G. Ercolani, *J. Am. Chem. Soc.* **2003**, *125*, 16097-10103.

[69] T. K. Dam, R. Roy, D. Page, C. F. Brewer, *Biochemistry* **2002**, *41*, 1351-1358.

[70] T. K. Dam, H. Gabius, S. Andre, H. Kaltner, M. Lensch, C. Fred Brewer, *Biochemistry* **2005**, *44*, 12564-12571.

[71] T. K. Dam, C. F. Brewer, *Biochemistry* **2008**, *47*, 8470-8476.

[72] T. K. Dam, T. A. Gerken, C. F. Brewer, *Biochemistry* **2009**, *48*, 3822-3827.

[73] J. M. Gargano, T. Ngo, J. Y. Kim, D. W. K. Acheson, W. J. Lees, *J. Am. Chem. Soc.* **2001**, *123*, 12909-12910.

[74] J. Huskens, A. Mulder, T. Auletta, C. A. Nijhuis, M. J. W. Ludden, D. N. Reinhoudt, *J. Am. Chem. Soc.* **2004**, *126*, 6784-6797.

[75] J. D. Badjic, S. J. Cantrill, J. F. Stoddart, *J. Am. Chem. Soc.* **2004**, *126*, 2288-2289.

[76] S. Lata, A. Reichel, R. Brock, R. Tampe, J. Piehler, *J. Am. Chem. Soc.* **2005**, *127*, 10205-10215.

[77] W. Jiang, *PhD Thesis: Supramolecular Synthesis via Integrative Self-Sorting*, Freie Universität Berlin, Berlin, **2010**.

[78] V. C. Jordan, *J. Med. Chem.* **2003**, *46*, 883-908.

[79] C. Avendano, J. C. Menendez, *Medicinal Chemistry of Anticancer Drugs: Anticancer Drugs That Inhibit Hormone Action*, Elsevier, Amsterdam, **2008**.

[80] E. Ottow, H. Weinmann, *Nuclear Receptors as Drug Targets*, Wiley-VCH, Weinheim, **2008**.

[81] V. C. Jordan, B. J. A. Furr, *Hormone Therapy in Breast and Prostate Cancer*, Humana Press, Totowa, **2002**.

[82] S. Green, P. Walter, V. Kumar, A. Krust, J. Bornert, P. Argos, P. Chambon, *Nature* **1986**, *320*, 134-139.

[83] G. L. Greene, P. Gilna, M. Waterfield, A. Baker, Y. Hort, J. Shine, *Science* **1986**, *231*, 1150-1154.

[84] G. G. J. M. Kuiper, E. Enmark, M. P. Huikko, S. Nilsson, J. Gustafsson, *Proc. Natl. Acad. Sci. USA* **1996**, *93*, 5925-5930.

[85] J. F. Couse, J. Lindzey, K. Grandien, J. Gustafsson, K. S. Korach, *Endocrinology* **1997**, *138*, 4613-4621.

[86] H. Gronemeyer, J. Gustafsson, V. Laudet, *Nature Review Drug Discovery* **2004**, *3*, 950-964.

[87] D. J. Mangeisdorf, C. Thummei, Miguei Beato, P. Herrlich, G. Schuetz, K. Umesono, B. Blumberg, P. Kastner, M. Mark, P. Chambon, R. M. Evans, *Cell* **1995**, *83*, 835-839.

[88] F. Minutolo, M. Macchia, B. S. Katzenellenbogen, J. A. Katzenellenbogen, *Med. Research. Rev.* **2011**, *31*, 364-442.

[89] S. Bertini, A. D. Cupertinis, C. Granchi, B. Bargagli, T. Tuccinardi, A. Martinelli, M. Macchia, J. R. Gunther, K. E. Carlson, J. A. Katzenellenbogen, F. Minutolo, *Eur. J. Med. Chem.* **2011**, *46*, 2453-2462.

[90] A. Fahrnow, U. Egner, *Current Opinion in Biotechnology* **1999**, *10*, 550-556.

[91] K. S. Korach, *Science* **1994**, *266*, 1524-1527.

[92] V. Kumar, P. Chambon, *Cell* **1988**, *55*, 145-156.

[93] J. W. R. Schwabe, L. Chapman, J. T. Finch, D. Rhodes, *Cell* **1993**, *75*, 567-578.

[94] A. C. Gee, J. A. Katzenellenbogen, *Mol. Endocrinology* **2001**, *15*, 421-428.

[95] A. Tamrazi, K. E. Carlson, J. A. Katzenellenbogen, *Mol. Endocrinology* **2003**, *17*, 2593-2602.

[96] A. Shiau, D. Barstad, P. M. Loria, L. Cheng, P. J. Kushner, D. A. Agard, G. L. Greene, *Cell* **1998**, *95*, 927-937.

[97] M. E. Lieberman, J. Gorski, V. C. Jordan, *J. Biol. Chem.* **1983**, *258*, 4741-4745.

[98] K. Ekena, K. E. Weis, J. A. Katzenellenbogen, B. S. Katzenellenbogen, *J. Biol. Chem.* **1997**, *272*, 5069-5075.

[99] A. C. W. Pike, A. M. Brzozowski, R. E. Hubbard, T. Bonn, A. Thorsell, O. Engstroem, J. Ljunggren, J. Gustafsson, M. Carlquist, *The EMBO Journal* **1999**, *18*, 4608-4618.

[100] H. Gao, J. A. Katzenellenbogen, R. Garg, C. Hansch, *Chem. Rev.* **1999**, *99*, 723-744.

[101] B. M. Weichman, A. C. Notides, *J. Biol. Chem.* **1977**, *252*, 8856-8862.

[102] M. Salomonsson, J. Haeggblad, B. W. O'Malley, G. M. Sitbon, *J. Steroid Biochem. Molec. Biol.* **1994**, *48*, 447-452.

[103] A. M. Brzozowski, A. C. W. Pike, Z. Dauter, R. E. Hubbard, T. Bonn, O. Engstroem, L. Oehman, G. L. Greene, J. Gustafsson, M. Carlquist, *Nature* **1997**, *389*, 753-758.

[104] M. E. Brandt, L. E. Vickery, *J. Biol. Chem.* **1997**, *272*, 4843-4849.

[105] H. Wang, G. A. Peters, X. Zeng, M. Tang, W. Ip, S. A. Khan, *J. Biol. Chem.* **1995**, *270*, 23322-23329.

[106] A. Tamrazi, K. E. Carlson, J. R. Daniels, K. M. Hurth, J. A. Katzenellenbogen, Mol. *Endocrinology* **2002**, *16*, 2706-2719.

[107] J. A. Katzenellenbogen, H. J. Johnson, H. N., Myers, *Biochemistry* **1973**, *12*, 4085-4092.

[108] K. E. Carlson, I. Choi, A. Gee, B. S. Katzenellenbogen, J. A. Katzenellenbogen, *Biochemistry* **1997**, *36*, 14897-14905.

[109] A. L. LaFrate, *PhD Thesis: Synthesis and Biological Evaluation of Coactivator Binding*

Inhibitors and Bivalent Ligands for the Estrogen Receptor, University of Illinois at Urbana-Champaign, **2008**.

[110] R. M. Eglen, *ASSAY and Drug Development Technologies* **2002**, *1*, 97-104.

[111] R. M. Eglen, R. Singh, *Comb. Chem. High Throughput Screen* **2003**, *6*, 381-387.

[112] M. Weber, M. Ferrer, W. Zhang, J. Inglese, B. Strulovici, P. Kunapuli, *Assay Drug Dev Technol.* **2004**, *2*, 39-49.

[113] R. M. Eglen, *Comb. Chem. High Throughput Screen* **2005**, *8*, 311-318.

[114] S. Kim, J. A. Katzenellenbogen, *Bioorg. Med. Chem.* **2000**, *8*, 785-793.

[115] F. Hafner, E. Holler, E. von Angerer, *J. Steroid Biochem. Molec. Biol.* **1996**, *58*, 385-393.

[116] V. Lubczyk, H. Bachmann, R. Gust, *J. Med. Chem.* **2002**, *45*, 5358-5364.

[117] K. E. Bergmann, C. H. Wooge, K. E. Carlson, B. S. Katzenellenbogen, J. A. Katztenellenbogen, *J. Steroid Biochem. Molec. Biol.* **1994**, *49*, 139-152.

[118] D. Osella, G. Dutto, C. Nervi, M. J. McGlinchey, A. Vessieres, G. Jaouen, *J. Organomet. Chem.* **1997**, *533*, 97-102.

[119] S. Groleau, J. Nault, M. Lepage, M. Couture, N. Dallaire, G. Berube, R. G. Gaudreault, *Bioorg. Chem.* **1999**, *27*, 383-394.

[120] D. Rabouin, V. Perron, B. N'Zemba, R. C. Gaudreault, G. Berube, Bioorg. *Med. Chem. Lett.* **2003**, *13*, 557-560.

[121] G. Berube, D. Rabouin, V. Perron, B. N'Zemba, R. C. Gaudreault, S. Parent, E. Asselin, *Steroids* **2006**, *71*, 911-921.

[122] K. W. Nettles, J. B. Bruning, G. Gil, E. E. O'Neill, J. Nowak, A. Hughs, Y. Kim, E. R. DeSombre, R. Dilis, R. N. Hanson, A. Joachimiak, G. L. Greene, *EMBO Rep.* **2007**, *8*, 563-568.

[123] M. Li, H. M. Greenblatt, O. Dym, S. Albeck, A. Pais, C. Gunanathan, D. Milstein, H. Degani, J. L. Sussman, *J. Med. Chem.* **2011**, *54*, 3575-3580.

[124] A. L. LaFrate, K. E. Carlson, J. A. Katzenellenbogen, *Bioorg. Med. Chem.* **2009**, *17*, 3528-3535.

[125] A. E. Wendlandt, S. M. Yelton, D. Lou, D. S. Watt, D. J. Noonan, *Steroids* **2010**, *75*, 825-833.

[126] A. M. Scutaru, M. Wenzel, R. Gust, *Eur. J. Med. Chem.* **2011**, *46*, 1604-1615.

[127] E. L. Rickert, J. P. Trebley, A. C. Peterson, M. M. Morrell, R. V. Weatherman, *Biomacromolecules* **2007**, *8*, 3608-3612.

[128] J. M. Holub, M. J. Garabedian, K. Kirshenbaum, *Mol. BioSyst.* **2011**, *7*, 337-345.

[129] K. J. Ho, J. K. Liao, *Arterioscler Thromb. Vasc. Biol*. **2002**, *22*, 1951-1961.

[130] H. P. Kim, J. Y. Lee, J. K. Jeong, S. W. Bae, H. K. Lee, I. Jo, *Biochem. Biophys. Res. Commun.* **1999**, *263*, 257-262.

[131] E. R. Levin, *J. Appl. Physiol* **2001**, *91*, 1860-1867.

[132] E. R. Levin, *Steroids* **2002**, *67*, 471-475.

[133] M. Razandi, G. Alton, A. Pedram, S. Ghonshani, P. Webb, E. R. Levin, *Mol. Cell Biol.* **2003**, *23*, 1633-1646.

[134] M. Razandi, A. Pedram, I. Merchenthaler, G. L. Greene, E. R. Levin, *Mol. Endocrinol* **2004**, *18*, 2854-2856.

[135] W. R. Harrington, S. H. Kim, C. C. Funk, Z. Erdogan, R. Schiff, J. A. Katzenellenbogen, B. S. Katzenellenbogen, *Mol. Endocrinology* **2006**, *20*, 491-502.

[136] S. H. Kim, J. A. Katzenellenbogen, *Angew. Chem. Int. Ed.* **2006**, *45*, 7243-7248.

[137] F. M. Veronese, G. Pasut, *Drug Discovery Today* **2005**, *10*, 1451-1458.

[138] M. S. Thompson, T. P. Vadala, M. L. Vadala, Y. Lin, J. S. Riffle, *Polymer* **2008**, *49*, 345-373.

[139] G. Coudert, M. Mpassi, G. Guillaumet, C. Selve, *Synthetic Communications* **1986**, *16*, 19–26.

[140] E. M. D. Keegstra, J. W. Zwikker, M. R. Roest, L. W. Jenneskens, *J. Org. Chem.* **1992**, *57*, 6678-6680.

[141] Y. Chen, G. L. Baker, *J. Org. Chem.* **1999,** *64*, 6870-6873.

[142] M. B. Andrus, T. M. Turner, E. P. Updegraff, Z. E. Sauna, S. V. Ambudkar, *Tetrahedron Letters* **2001**, *42*, 3819-3822.

[143] S. Svedhem, C. Hollander, J. Shi, P. Konradsson, B. Liedberg, S. C. T. Svensson, *J. Org. Chem.* **2001**, *66*, 4494-4503.

[144] P. G. M. Wuts, T. W. Greene, *Greene's Protective Groups in Organic Synthesis*, John Wiley & Sons, **2007**.

[145] S. Wolfe, *Acc. Chem. Res.* **1972**, *5*, 102-111.

[146] F. A. Carey, R. J. Sundberg, *Advanced Organic Chemistry (Part A)*, Springer, New York, **2007**.

[147] I. V. Alabugin, T. A. Zeidan, *J. Am. Chem. Soc.* **2002**, *124*, 3175-3185.

[148] R. Kjellander, E. Florin, *J. Chem. Soc., Faraday Trans. 1* **1981**, *77*, 2053-2077.

[149] M. Sundaralingam, *Nature* **1968**, *217*, 35-37.

[150] K. B. Wiberg, M. A. Murcko, K. E. Laidig, P. J. MacDougall, *J. Phys. Chem.* **1990**, *94*, 6956-6959.

[151] H. J. Kreuzer, R. L. C. Wang, M. Grunze, *New J. Phys.* **1999**, *1*, 21.1-21.16.

[152] R. Begum, H. Matsuura, *J. Chem. Soc., Faraday Trans.* **1997**, *93*, 3839-3848.

[153] H. Staudinger, J. Meyer, *Helv. Chim. Acta* **1919**, *2*, 635.

[154] M. Lange, A. L. Pettersen, K. Undheim, *Tetrahedron* **1998**, *54*, 5745-5752.

[155] C. R. Bertozzi, M. D. Bednarski, *J. Org. Chem.* **1991**, *56*, 4326-4329.

[156] R. Huisgen, *Angew. Chem. Int. Ed.* **1963**, *2*, 633-645.

[157] H. C. Kolb, M. G. Finn, K. B. Sharpless, *Angew. Chem. Int. Ed.* **2001**, *40*, 2004-2021.

[158] V. V. Rostovtsev, L. G. Green, V. V. Fokin, K. B. Sharpless, *Angew. Chem. Int. Ed.* **2002**, *41*, 2596-2599.

[159] P. Wothers, N. Greeves, S. Warren, J. Clayden, *Organic Chemistry*, Oxford, New York, **2001**.

[160] F. A. Carey, R. J. Sundberg, *Advanced Organic Chemistry (Part B)*, Springer, New York, **2007.**

[161] A. F. Magid, C. A. Maryanoff, K. G. Carson, *Tetrahedron letters* **1990**, *31*, 5595-5598.

[162] A. F. Magid, K. G. Carson, B. D. Harris, C. A. Maryanoff, R. D. Shah, *J. Org. Chem.* **1996**, *61*, 3849-3862.

[163] E. C. Knuf, J. Jiang, M. S. Gin, *J. Org. Chem.* **2003**, *68*, 9166-9169.

[164] R. N. Salvatore, C. H. Yoon, K. W. Jung, *Tetrahedron* **2001**, *57*, 7785-7811.

[165] W. Eschweiler, *Chem. Ber.* **1905**, *38*, 880.

[166] H. T. Clarke, H. B. Gillespie, S. Z. Weisshaus, *J. Am. Chem. Soc.* **1933**, *55*, 4571-4587.

[167] K. Hemming, M. J. Bevan, C. Loukou, S. D. Patel, D. Renaudeau, *Synlett* **2000**, *11*, 1565-1568.

[168] F. P. Cossio, C. Alonso, B. Lecea, M. Ayerbe, G. Rubiales, F. Palacios, *J. Org. Chem.* **2006**, *71*, 2839-2847.

[169] J. W. Lee, S. C. Han, J. H. Kim, K. Lee, *Bull. Korean Chem. Soc.* **2006**, *27*, 1667-1670.

[170] F. Palacios, C. Alonso, D. Aparicio, G. Rubiales, J. M. Santos, *Tetrahedron* **2007**, *63*, 523-575.

[171] H. J. Cristau, C. Garcia, J. Kadoura, E. Torreilles, *Phosphorous, Sulfur Silicon Relat. Elem.* **1990**, *49*, 151-154.

[172] S. Ayesa, B. Samuelsson, B. Classon, *Synlett* **2008**, *1*, 97-99.

[173] A. N. Hulme, E. M. Rosser, *Org. Lett.* **2002**, *4*, 265-267.

[174] A. L. Wilds, W. R. Biggerstaff, *J. Am. Chem. Soc.* **1945**, *67*, 789-793.

[175] R. W. Hartmann, A. Heindl, M. R. Schneider, H. Schönenberger, *J. Med. Chem.* **1986**, *29*, 322-328.

[176] R. Goswami, S. G. Harsy, D. F. Heiman, J. A. Katzenellenbogen, *J. Med. Chem.* **1980**, *23*, 1002-1008.

[177] G. Walter, R. Liebl, E. Von Angerer, *Arch. Pharm. Pharm. Med. Chem.* **2004**, *337*, 634-644.

[178] K. A. Hill, D. M. Peterson, K. M. Damodaran, P. N. Rao, *Steroids* **1981**, *37*, 327-343.

[179] J. A. Katzenellenbogen, R. J. McGorrin, T. Tatee, *J. Med. Chem.* **1981**, *24*, 435-450.

[180] V. W. Winkler, M. A. Nyman, R. S. Egan, *Steroids* **1971**, *17*, 197-207.

[181] M. Schneider, E. von Angerer, G. Kranzfelder, H. Schoenenberger, *Arch. Pharm.* **1980**, *313*, 919-925.

[182] B. Castro, J. R. Dormoy, G. Evin, C. Selve, *Tetrahedron Letters* **1975**, *16*, 1219-1222.

[183] D. S. Kemp, M. Trangle, K. Trangle, *Tetrahedon Letters* **1974**, *15*, 2695-2696.

[184] E. Walton, G. Brownlee, *Nature* **1943**, *151*, 305-306.

[185] J. A. Katzenellenbogen, K. E. Carlson, B. S. Katzenellenbogen, *J. Steroid Biochem.* **1985**, *22*, 589-596.

[186] M. Waibel, M. D. Angelis, F. Stossi, K. J. Kieser, K. E. Carlson, B. S. Katzenellenbogen, J. A. Katzenellenbogen, *Eur. J. Med. Chem.* **2009**, *44*, 3412-3424.

[187] J. A. Katzenellenbogen, *J. Med. Chem.* **2011**, *54*, 5271-5282.

[188] V. V. Tyulmenkov, C. M. Klinge, *Arch. Biochem. Biophys.* **2000**, *381*, 135-142.

[189] W. P. van Hoorn, *J. Med. Chem.* **2002**, *45*, 584-589.

[190] K. Krohn, K. Kulikowski, G. Leclercq, *J. Med. Chem.* **1989**, *32*, 1532-1538.

[191] G. Walter, R. Liebl, E. von Angerer, *Bioorg. Med. Chem. Lett.* **2004**, *14*, 4659-4663.

[192] S. Y. Dai, M. J. Chalmers, J. Bruning, K. S. Bramlett, H. E. Osborne, C. Rafizadeh, R. J. Barr, Y. Wang, M. Wang, T. P. Burris, J. A. Dodge, P. R. Griffin, *Proc. Natl. Acad. Sci. USA* **2008**, *105*, 7171-7176.

[193] C. R. Schmid, J. P. Sluka, K. M. Duke, *Tetrahedron Letter* **1999**, *40*, 675-678.

[194] C. W. Tornoe, C. Christensen, M., Meldal, *J. Org. Chem.* **2002**, *67*, 3057-3064.

[195] W. B. Panko, J. H. Clark, *J. Steroid Bichem.* **1981**, *15*, 383-386.

[196] Y. Wang, N. Y. Chirgadze, S. L. Briggs, S. Khan, E. V. Jensen, T. P. Burris, *Proc. Natl. Acad, Sci. USA* **2006**, *103*, 9908-9911.

[197] D. J. Kojetin, T. P. Burris, E. V. Jensen, S. A. Khan, *Endocr. Relat. Cancer* **2008**, *15*, 851-870.

[198] F. Abendroth, A. Bujotzek, M. Shan, R. Haag, M. Weber, O. Seitz, *Angew. Chem. Int. Ed.* **2011**, *50*, 5892-5896.

[199] D. Han, F. H. Foersterling, X. Li, J. R. Deschamps, H. Cao, J. M. Cool, *Bioorg. Med. Chem. Lett.* **2004**, *14*, 1465-1469.

[200] B. Testa, P. Jenner, G. J. Kilpatrick, N. E. Tayar, H. V. D. Waterbeemd, C. D. Marsden, *Biochemical Pharmacology* **1987**, *36*, 4041-4046.

[201] V. C. Jordan, S. Mittal, B. Gosden, R. Koch, M. E. Lieberman, *Environmental Health Perspectives* **1985**, *61*, 97-110.

[202] D. W. Robertson, J. A. Katzenellenbogen, D. J. Long, E. A. Rorke, B. S. Katzenellenbogen, *J. Steroid Biochemistry* **1982**, *16*, 1-13.

[203] D. W. Robertson, J. A. Katzenellenbogen, *J. Org. Chem.* **1982**, *47*, 2387-2393.

[204] I. R. Hardcastle, M. G. Rowlands, R. M. Grimshaw, J. Houghton, M. Jarman, *J. Med. Chem.* **1996**, *39*, 999-1004.

[205] P. Y. Maximov, C. B. Myers, R. F. Curpan, J. S. Wambi, V. C. Jordan, *J. Med. Chem.* **2010**, *53*, 3273-3283.

[206] R. Gust, V. Lubczyk, *J. Steroid Biochem. Mol. Biology* **2003**, *86*, 57-70.

[207] V. Lubczyk, H. Bachmann, R. Gust, *J. Med. Chem.* **2003**, *46*, 1484-1491.

[208] S. Gauthier, J. Mailhot, F. Labrie, *J. Org. Chem.* **1996**, *61*, 3890-3893.

[209] S. Gauthier, J. Sanceau, J. Mailhot, B. Caron, J. Cloutier, *Tetrahedron* **2000**, *56*, 703-709.

[210] A. Detsi, M. Koufaki, T. Calogeropoulou, *J. Org. Chem.* **2002**, *67*, 4608-4611.

[211] D. D. Yu, B. M. Forman, *J. Org. Chem.* **2003**, *68*, 9489-9491.

[212] D. L. Mohler, G. Shen, *Org. Biomol. Chem.* **2006**, *4*, 2082-2087.

[213] K. Ogawa, Y. Matsushita, I. Yamawaki, M. Kaneda, J. Shibata, T. Toko, T. Asao, *Chem. Pharm. Bull.* **1991**, *39*, 911-916.

[214] P. J. Burke, T. H. Koch, *J. Med. Chem.* **2004**, *47*, 1193-1206.

[215] A. F. Abdel-Magid, C. A. Maryanoff, K. G. Carson, *Tetrahedron Letters* **1990**, *31*, 5595-5598.

[216] A. F. Abdel-Magid, K. G. Carson, B. D. Harris, C. A. Maryanoff, R. D. Shah, *J. Org. Chem.* **1996**, *61*, 3849-3862.

[217] B. T. Cho, S. K. Kang, *Tetrahedron* **2005**, *61*, 5725-5734.

[218] V. C. Jordan, B. W. O'Malley, *J. Clinical Oncology* **2007**, *25*, 5815-5824.

[219] A. A. Parent, J. R. Gunther, J. A. Katzenellenbogen, *J. Med. Chem.* **2008**, *51*, 6512-6530.

[220] J. R. Gunther, I. W. Moore, M. L. Collins, J. A. Katzenellenbogen, *ACS Chem. Biol.* **2008**, *3*, 282-286.

[221] J. R. Gunther, A. A. Parent, J. A. Katzenellenbogen, *ACS Chem. Biol.* **2009**, *4*, 435-440.

[222] T. W. Corson, N. Aberle, C. M. Crews, *ACS Chem. Biol.* **2008**, *3*, 677-692.

[223] K. M. Bonger, S. Hoogendoorn, C. J. van Koppen, C. M. Timmers, G. A. van der Marel, H. S. Overkleeft, *ACS Med. Chem. Lett.* **2011**, *2*, 85-89.

[224] V. Semetey, D. Moustakas, G. M. Whitesides, *Angew. Chem. Int. Ed.* **2006**, *45*, 588-591.

8. Zusammenfassung

Diese Arbeit beschäftigt sich mit der Synthese von drei verschiedenen Serien von bivalenten Estrogenrezeptor(ER)-Liganden, die abhängig von der Struktur des jeweiligen Liganden (Diethylstilbestrol, Raloxifen, und 4-Hydroxy Tamoxifen) durch variable Abstandhalter miteinander verbunden sind. Die bivalenten Liganden wurden sowohl bezüglich ihrer biologischen Aktivität, als auch ihrer Bindungsaffinität und -fähigkeit zum Estrogenrezeptor hin untersucht.

Im ersten Teil dieser Arbeit wurden bivalente *trans*-Diethylstilbestrolanaloga (DES) über variable Abstandshalter aus Oligoethylenglycolstrukturen oder Oligoethylenglycol-Konjugaten (die, z.B. eine starre Biphenoleinheit enthalten) miteinander verbrückt. In vitro Studien zeigten, dass eine polare Amid-Verknüpfung am bivalenten Liganden die Bindungsaffinität zum Rezeptor, im Vergleich zum monovalenten Liganden, dramatisch verringert. Als Folge wurden nur sehr schwache Bindungsaffinitäten beobachtet, wobei die kurzkettigen (10.8 Å), bivalenten Diethylstilbestrolanaloga höhere Bindungsaffinitäten als die Langkettigen (34.8 und 46.7 Å) zeigten. Unter den langkettigen Analogien zeigte, der bivalente Ligand die höchste Affinität, der über eine 43.1 Å lange Oligoethylenglycoleinheit verbrückt ist. Die Differenz der Bindungsaffinitäten vom mono- zum bivalenten Analogon lässt vermuten, dass es zu einer unerwarteten Wechselwirkung zwischen der zweiten Diethylstilbestrol Komponente und der Rezeptoroberfläche kommt. Darüber hinaus konnte eine Computer Simulation zeigen, dass zum einen der Abstand zwischen den beiden Diethylstilbestrolanaloga durch Faltung verkürzt ist, und zum Anderen, dass es zu einer hydrophoben Wechselwirkung zwischen den beiden Diethylstilbestrol-Komponenten und den starren Oligoethylenglycol-Konjugaten kommt.[29]

Um die Struktur-Aktivitäts-Beziehung (SAB) der bivalenten Estrogenrezeptoren besser verstehen zu können, wurden im zweiten Teil dieser Arbeit bivalente Raloxifene (RAL), die durch flexible Oligoethylenglycolstrukturen unterschiedlicher Länge (4.7-47.7 Å) verbrückt wurden, synthetisiert und untersucht. Um deren unterschiedliche Bindungsaffinitäten erklären zu können, wurden zwei verschiedene Bindungsmodi, entweder intra- oder intermolekularer Art vermutet (Abbildung 1a). Es zeigte sich, dass 22.7 Å der kritische Mindestabstand ist, bei dem die intra- und intermolekulare Ligandenbindungsdomäne vom ERα-Dimer gerade noch unterschieden

werden können. Die maximal intermolekulare, bivalente Bindungsaffinität (10% Relative Bindungsaffinität (RBA, bezogen auf Estradiol (E_2)) wurde bei einem Abstand von 26.7 Å erreicht. Bemerkenswerterweise wurde experimentell bestätigt, dass bivalente Liganden, die über einen langen Abstandshalter miteinander verknüpft sind, schwächere Bindungsaffinitäten aufgrund von Liganden-Abschirmung und Faltung der Oligoethylenglycolstrukturen aufweisen. Im Gegensatz dazu können bivalente Liganden, verbunden über kürzere Abstandshalter, leichter an den Rezeptor binden. Als Konsequenz zeigen solche Liganden stärkere Bindungsaffinitäten zum Estrogenrezeptor (Abbildung 1b). So hat der Unterschied in Entropie (die Faltung der Kette) und Enthalpie (intramolekulare Wechselwirkungen) zwischen der ursprünglichen und finalen Konformation der bivalenten Raloxifenanaloga einen großen Einfluss auf die Protein-Ligand Wechselwirkung. Darüber hinaus haben die bivalenten Raloxifenanaloga durch den Mangel an Wasserstoffbrückenbindungen zwischen Proteinrest (ASP351) und den 1,2,3-Triazolgruppen einen unerwünschten enthalpischen Einfluss auf die Ligand-Rezeptor Wechselwirkung.[30]

Um die unerwünschte Verminderung der Bindungsaffinität des Estrogenrezeptors, bedingt durch strukturelle Modifizierung der bivalenten Raloxifenanaloga, zu vermeiden, wurde ein neuer bivalenter Ligand basierend auf einem monovalenten Estrogenrezeptor konzipiert. Im dritten Teil dieser Arbeit wurden bivalente *cis*-4-Hydroxytamoxifen (OHT)-Derivate, basierend auf monovalenten *cis*-OHT Liganden, verbrückt über Oligoethylenglykolketten im Längenbereich von 7.2-43.1 Å, untersucht. Diese Derivate wurden bezüglich ihrer Bindungsaffinität zu den Estrogenrezeptor-Subtypen α und β (ERα und ERβ) untersucht. Obwohl ihre ER-Bindungsmöglichkeiten durch die unerwünschte Konformation in wässriger Umgebung vermindert ist,[30] finden sich zwei Affinitätsmaxima bei den Abstandslängen 14.4 und 28.8 Å (bis zu 37% und 31% RBA von E_2, Abbildung 1c), welche mit intra- bzw. intermolekularen bivalenten Bindungsmodi korrespondieren. Diese Ergebnisse stimmen nicht nur mit unserer ursprünglichen Hypothese überein, sondern liefern auch ein intuitives und präzises Verständnis der SAB von bivalenten Estrogenliganden beider ER- Subtypen, insbesondere für ERβ.

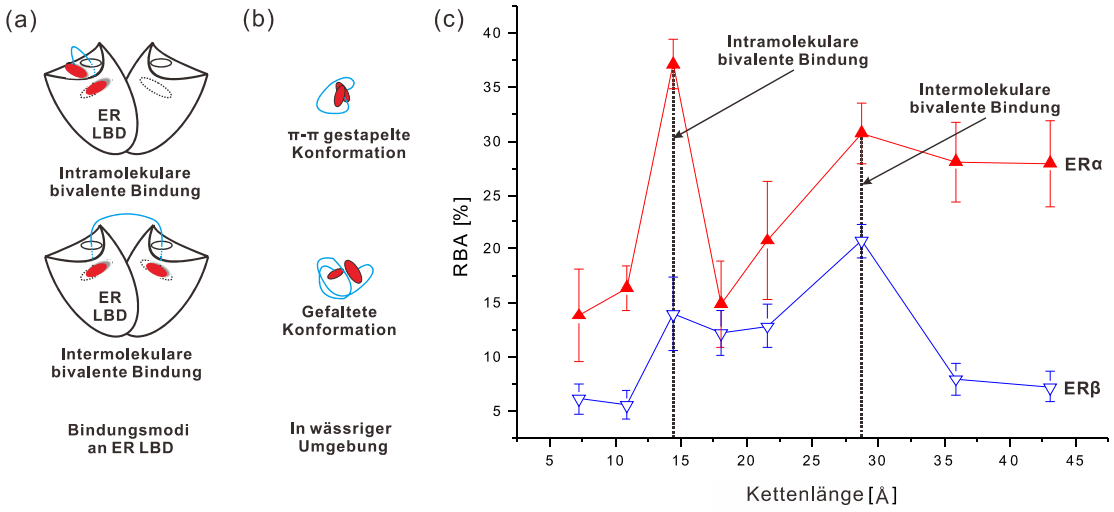

Abb.1. (a) Vereinfachte Darstellung der zwei möglichen Bindungsmodi der Ligandenbindungsdomäne des Estrogenrezeptors (ER LBD). (b) Verschiedene Konformationsmöglichkeiten der bivalenten Estrogenliganden in wässriger Umgebung. (c) Affinitätsmaxima an beide ER-Bindungsmodi (intra- und intermolekularer Art).

Basierend auf den unterschiedlichen ER-Bindungsaffinitäten der hier vorgestellten, bivalenten Estrogenliganden wurde hinreichend gezeigt, dass zahlreiche Faktoren, wie z.B. Estrogen-agonistische- oder Estrogen-antagonistische Eigenschaften, für das bivalente Estrogen-Liganden-Design berücksichtigt werden müssen.

Erstens, Antagonisten, wie Raloxifen und 4-Hydroxytamoxifen besitzen durch ihre jeweilige Seitenkette einen leichteren Zugang zu der antagonistischen Bindungsstelle des Estrogenrezeptors. Im Gegensatz dazu, können Agonisten nur durch Modifikation der steroidalen Struktur in der Position 17 α so einen Zugang erhalten. Diese Änderung hätte jedoch eine Abnahme der ER-Bindungsaffinität zur Folge. Im Vergleich, wiesen bivalente Ethinylestradiol (EE_2)-Liganden von LaFrate[124] sehr viel höhere Bindungsaffinitäten auf, als bivalente E_2-Liganden,[120,121] da sie an der besagten Position keine entsprechende Modifikation besitzen. Zweitens, die Bindungsposition und die Abstandshalter sollten konsistent mit der Umgebung des jeweilig gebundenen Estrogenliganden sein. Im Falle des bivalenten *trans*-DES-Liganden wurde die Estrogenrezeptor-Bindungsaffinität durch die Einführung einer hydrophilen Amidgruppe dramatisch reduziert. Im Umkehrschluss kann die tertiäre Amingruppe von 4-Hydroxytamoxifen die hydrophile Wechselwirkung zu Proteinresten aufrecht erhalten und schlussendlich weisen bivalente *cis*-OHT Liganden eine höhere ER-Bindungsaffinität als ihre Raloxifenanaloga auf. Drittens, die Verwendung einer rigiden Einheit, die ursprünglich von Whitesides postuliert wurde,

kann den entropischen Verlust der Konformation minimieren und die Bindungsaffinität erhöhen, solange keine intramolekularen Wechselwirkungen zwischen dieser starren Einheit und dem gebundenen Liganden auftritt. Ein gutes Beispiel ist gegeben durch bivalente Estrogenliganden, die über rigide DNA Abstandshalter verbrückt sind.[198] Im Gegensatz dazu, wurde im Fall von flexiblen Abstandshaltern entdeckt, dass intramolekulare, hydrophobe Wechselwirkungen zwischen Bisphenylsegmenten des Abstandshalters und verbrückten *trans*-DES-Liganden eine signifikante Reduktion der ER-Bindungsaffinität hervorrufen.[29] Letztendlich können durch den Einsatz von flexiblen Abstandshaltern verschiedene strukturelle Anforderungen, wie z.B. der Winkel zwischen den Liganden und/oder die Abstandshalterlänge erbracht werden. Die Möglichkeit besteht nicht bei Verwendung von rigiden Abstandshaltern. Die Flexibilität von Polyether-Abstandhaltern erhöht dennoch die strukturelle Unbestimmtheit der Liganden aufgrund der Konformationsfaltung und hydrophoben-hydrophoben Wechselwirkung der verbrückten Estrogenanaloga.[30]

Schlussfolgernd lässt sich feststellen, dass das Erreichen einer hohen Affinität bivalenter Verbindungen zu dimeren ER-Ligandenbindungsdomäne eine große Herausforderung darstellt. In dieser Arbeit wurde die Struktur-Aktivitäts-Beziehung von bivalenten Estrogenliganden, die durch variable Abstandshalter unterschiedlicher Länge verbrückt sind, etabliert. Zwei bivalente ER-Bindungsmodi, intra- und intermolekular, die essentiell für das Design von hochaffinen, bivalenten Estrogenliganden sind, wurden vorgestellt und bestätigt. Die Ergebnisse verdeutlichen, dass das Erreichen von bivalenter Bindung zu dimeren Estrogenrezeptoren nicht einfach nur durch Struktur-Aktivität-Bestimmung, wie z.B. Wahl eines geeigneten Abstandshalters um zwei Liganden miteinander zu verbrücken, erreicht wird, sondern, dass ein systemisches Verständnis über das Bindungsverhalten vom bivalenten Liganden an den Estrogenrezeptor und die intramolekularen hydrophilen, bzw. hydrophoben Wechselwirkung in der wässrigen Umgebung berücksichtigt werden müssen. Darüber hinaus muß eine weitere Untersuchung der intramolekularen, bivalenten Bindung am Estrogenrezeptor gewährleistet werden. Bivalente Liganden, die über kurze Oligoethylenglykoleinheiten (Kettenlänge ca. 10 - 14 Å) verbrückt sind, bieten eine neue Möglichkeit für die Synthese von hochaffinen Inhibitoren, um eine Estrogenrezeptor-Coaktivator-Wechselwirkung zu verhindern.

9. Publications and Presentations

9.1. Publications

[1] "Towards A Rational Spacer Design for Bivalent Inhibition of Estrogen Receptor" by A. Bujotzek, **M. Shan**, R. Haag, M. Weber, *J. Comput. Aided. Mol. Des.* **2011**, *25*, 253-262.

[2] "DNA-Controlled Bivalent Presentation of Ligands for the Estrogen Receptor" by F. Abendroth, A. Bujotzek, **M. Shan**, R. Haag, M. Weber, O. Seitz, *Angew. Chem. Int. Ed.* **2011**, *50*, 8592-8596.

[3] "Conformational Analysis of Bivalent Estrogen Receptor-Ligands: From Intramolecular to Intermolecular Binding" by **M. Shan**, A. Bujotzek, F. Abendroth, A. Wellner, R. Gust, O. Seitz, M. Weber, R. Haag, *ChemBioChem* **2011**, *12*, 2587-2598.

[4] "Design, Synthesis and Evaluation of High-affinity Bivalent Estrogen ligands" by **M. Shan**, A. Bujotzek, M. Weber, K. Carlson, J. A. Katzenellenbogen, R. Haag, manuscript in preparation.

9.2. Presentations

[1] ORCHEM 2008 – 16. Vortragstagung Liebig-Vereinigung für Organische Chemie, Weimar, Germany, September 01-03, 2008.
Poster: "Synthesis of Spacer-linked Bivalent Estrogen Analogs" by **M. Shan** and R. Haag.

[2] 4th Fabisch- Symposium for Cancer Research and Molecular Cell Biology (2nd Targeted Tumor Therapies), Berlin, Germany, April 01-04, 2009.
Poster: "Novel Spacer-linked Bivalent Estrogen Analogs" by **M. Shan**, A. Wellner, R. Gust, and R. Haag.

[3] 3rd European Conference on Chemistry for Life Sciences, Frankfurt am Main, Germany, September 02-05, 2009.
Poster and oral presentation: "Design, Synthesis and Evaluation of Spacer-linked Bivalent Estrogen Analogs" by **M. Shan**, A. Wellner, R. Gust, and R. Haag.

[4] Frontiers in Medicinal Chemistry, Münster, Germany, March 14-17, 2010.

Poster: “Design, Synthesis, and Evaluation of Spacer-linked Bivalent Estrogen Analogs” by **M. Shan**, K. Carlson, A. Wellner, J. A. Katzenellenbogen, R. Gust, and R. Haag.

[5] Frontiers in Medicinal Chemistry, Saarbrücken, Germany, March 20-23, 2011.

Post: “Design, Synthesis, and Evaluation of Spacer-linked Bivalent Estrogen Analogs” by **M. Shan**, K. E. Carlson, F. Abendroth, A. Bujotzek, M. Weber, O. Seitz, J. A. Katzenellenbogen, and R. Haag.

10. Curriculum Vitae

For reasons of data protection, the Curriculum vitae is not published in the online version.